JAN 14 1988

C 13.58:87-3632

NBSIR 87-3632

The Influence of Cement Pore Solution on Alkali-Silica Reaction

L. J. Struble

U.S. DEPARTMENT OF COMMERCE
National Bureau of Standards
National Engineering Laboratory
Center for Building Technology
Gaithersburg, MD 20899

May 1987

Issued September 1987

Prepared for
Purdue University
West Lafayette, IN 47904

COMPLETED

NBSIR 87-3632

THE INFLUENCE OF CEMENT PORE SOLUTION ON ALKALI-SILICA REACTION

L. J. Struble

U.S. DEPARTMENT OF COMMERCE
National Bureau of Standards
National Engineering Laboratory
Center for Building Technology
Gaithersburg, MD 20899

May 1987

Issued September 1987

Prepared for
Purdue University
West Lafayette, IN 47904

U.S. DEPARTMENT OF COMMERCE, Clarence J. Brown, *Acting Secretary*
NATIONAL BUREAU OF STANDARDS, Ernest Ambler, *Director*

PREFACE

This document formed the basis for a thesis submitted to the faculty of Purdue University in partial fulfillment of the requirements for the degree of Doctor of Philosophy.

The guidance and support provided by Professor S. Diamond throughout this study is sincerely appreciated. The author also wishes to thank the other members of her advisory committee, Drs. W.L. Dolch, D. Winslow, and T. West, for their support.

These studies were carried out both at Martin Marietta Laboratories and at the National Bureau of Standards; support and assistance provided by many colleagues in both laboratories is gratefully acknowledged. In particular, the author thanks Drs. J. Mills, J. Skalny, J. Clifton, and G. Frohnsdorff for their support. Discussion and counsel regarding these studies provided by Dr. P. Brown and by Professor H.F.W. Taylor, and technical assistance provided by B. Roe, K. Galuk, and C. Spring are gratefully acknowledged.

Finally, the author wishes to express special appreciation to her husband and son for their unfailing support and patience throughout this study.

These studies were supported in part by the National Science Foundation, Grant No. CEE 82-10791, and in part by the National Bureau of Standards.

A number of trade names and company products are identified throughout this document to specify adequately the experimental procedures. In no case does such identification imply recommendation or endorsement by the national Bureau of Standards, nor does it imply that the products are necessarily the best available for the purpose.

TABLE OF CONTENTS

Page

LIST OF TABLES . . . vi

LIST OF FIGURES . . . ix

ABSTRACT . . . xvii

CHAPTER 1 - INTRODUCTION . . . 1

- Alkali-Silica Reaction Mechanism . . . 2
    - Gel Formation . . . 3
    - Swelling of Gel . . . 5
    - Pessimum Proportion . . . 6
    - Aggregate Parameters . . . 10
- Influence of Cement Alkali Distribut . . . 16
- Cement Pore Solution . . . 19

CHAPTER 2 - EXPERIMENTAL METHODS . . . 24

- Materials . . . 24
    - Cements . . . 25
    - Aggregates . . . 26
- Methods Used To Analyze Materials . . . 28
    - Chemical Composition . . . 28
    - Phase Composition . . . 28
    - Alkali Distribution . . . 30
    - Quick Chemical Test . . . 32
- Mortar Preparation . . . 34
- Aggregate Reactions in Model Pore Solutions . . . 38
- Pore Solution Expression . . . 40
- Methods Used To Analyze Solutions . . . 46
    - Determination of pH . . . 46
    - Hydroxide . . . 48
    - Potassium, Sodium, Calcium, and Sulfate . . . 48
    - Silica . . . 49

CHAPTER 3 - RESULTS AND DISCUSSION . . . 52

- Composition of Materials . . . 52

(Table of Contents, continued)

Page

- Cements 52
- Aggregates. 65
- Quick Chemical Test for Aggregate Reactivity 69
- Mortar Bar Expansion 75
- Reaction of Aggregates in Model Pore Solutions . . 104
- Pore Solutions Expressed from Limestone Mortars. . 108
  - Expression. 108
  - Chemical Compositions 109
    - pH 110
    - Hydroxide 115
    - Sodium 118
    - Potassium. 118
    - Calcium. 123
    - Silica 123
    - Sulfate. 127
    - Lithium. 131

CHAPTER 4 - IMPLICATIONS CONCERNING REACTION MECHANISMS. 133

- Mortar Bar Expansion 133
- Cement Alkali Levels and Mortar Bar Expansion. . . 139
- Pore Solution Composition. 143
  - Pore Solution Composition and Alkali Distribution. 150
  - Pore Solution Composition and Mortar Bar Expansion 163
- Aggregate Reactions in Model Pore Solutions. . . . 176
  - Dissolution Curve 177
  - Reduction in pH 179
  - Implications of Pore Solution Composition . . . 179
  - Correlation with Expansion. 183

CHAPTER 5 - SUMMARY AND CONCLUSIONS 190

- Experimental Findings. 190
- Conclusions. 194

REFERENCES. 196

APPENDICES

- Appendix A. Analytical Procedures 208
  - pH. 208
  - Hydroxide. 213
  - Calcium, Potassium, Sodium, and Sulfate Ions. 215

(Table of Contents, continued)

Page
Silica. 216
Appendix B. Bags for Storage of Pore Solutions. . 224
Appendix C. X-ray Diffraction Patterns of Cements. 224
Appendix D. Expansion Results 226
Appendix E. Calculations of Alkali Levels in Pore Solutions 260

VITA. 265

LIST OF TABLES

Table	Page
1. Typical compositions of gels in reacted concretes	4
2. Summary of mortar bar tests for various aggregate materials	11
3. Rate of dissolution of various forms of silica at pH 8.5	15
4. Summary of pore solution studies	21
5. Aggregate grading for use in mortars	35
6. Compositions of model pore solutions	39
7. Proportion of each aggregate added to model pore solutions	41
8. Chemical compositions of cements (percent)	53
9. Phase compositions and other parameters, calculated from chemical compositions of the cements (percent)	54
10. Principal alkali phases determined by XRD	57
11. Levels of alkali dissolved during water extraction of various durations (percent)	59
12. Results of sodium distributions among various cement phases (percent)	60
13. Results of potassium distributions among various cement phases (percent)	61
14. Chemical compositions of aggregate materials (percent)	66
15. Results of quick chemical test for aggregate reactivity	73
16. Results of mortar bar expansion measurements	93

(List of Tables, continued)

Table Page
17. Concentrations of silica produced by reaction of aggregates in model pore solutions (mM) 105

18. Level of pH produced by reaction of aggregates in model pore solutions. 106

19. Measured ionic concentration levels in pore solutions of limestone mortars 111

20. Measured pH levels in pore solutions of limestone mortars. 113

21. Measured hydroxide levels in pore solutions of limestone mortars (mM) 116

22. Measured sodium levels in pore solutions of limestone mortars (mM) 119

23. Measured potassium levels in pore solutions of limestone mortars (mM) 121

24. Measured calcium levels in pore solutions of limestone mortars (mM) 124

25. Measured silica levels in pore solutions of limestone mortars (mM) 126

26. Measured sulfate levels in pore solutions of limestone mortars (mM) 129

27. Measured lithium levels in pore solutions of limestone mortars (mM) 132

28. Functions used to describe expansion levels. . . . 140

Appendix
Table

29. Replicate pH measurements. 211

30. Calculated and measured pH levels. 212

31. Hydroxide ion titrations to assess accuracy and precision. 214

32. Changes in mass of water-filled, sealed, plastic bags used to store pore solution 225

33. XRD peaks used to identify alkali phases 243

(List of Tables, continued)

Table Page
34. Average measured expansion for each mortar 244
35. Bound water (estimated using data reported by Dalzeil and Gutteridge, 1986). 261
36. Degree of hydration of cement phases for Model 1 (estimated from curves reported by Pratt and Ghose, 1983) 262
37. Hydration rates of cement phases for Model 2 (estimated from data reported by Dalzeil and Gutteridge, 1986). 263
38. Hydration rates of cement phases for Model 3 . . . 264

LIST OF FIGURES

Figure Page

1. Level of dissolution of amorphous silica versus pH of solution (Iler, 1979) 12

2. Rate of dissolution of amorphous silica versus pH of solution (Iler, 1979) 13

3. X-ray diffraction pattern of the residue of Cement A after 10-min water extraction, with weak peaks highlighted that are attributed to ettringite (top) based on the JCPDS data (Card No. 9-414, bottom), as reported by Struble (1985) 33

4. Container and rack used for mortar bar expansion studies 37

5. Diagram of apparatus for expressing and collecting pore solution from hardened mortar 42

6. Set-up for expressing and collecting pore solution from hardened mortar 43

7. Results of sodium distributions determined by chemical analysis of cements after various chemical extractions 62

8. Results of potassium distributions determined by chemical analysis of cements after various chemical extractions 63

9. XRD pattern of limestone Piece K, rich in dolomite 67

10. XRD pattern of limestone Piece M, with little dolomite 68

11. XRD pattern of opal. 70

12. XRD pattern of quartzite 71

13. XRD pattern of granite 72

(List of Figures, continued)

Figure Page

14. Results of quick chemical test, showing the curve that separates the innocuous and the deleterious regions according to ASTM C 289. 74

15. Expansion of mortar bars prepared with Cement A and various levels of opal 76

16. Expansion of mortar bars prepared with Cement A and various levels of quartzite. 77

17. Expansion of mortar bars prepared with Cement A, with and without gneissic granite 78

18. Expansion of mortar bars prepared with Cement B and various levels of opal 79

19. Expansion of mortar bars prepared with Cement B and various levels of quartzite. 80

20. Expansion of mortar bars prepared with Cement B, with and without gneissic granite 81

21. Expansion of mortar bars prepared with Cement C and various levels of opal 82

22. Expansion of mortar bars prepared with Cement C and various levels of quartzite. 83

23. Expansion of mortar bars prepared with Cement C, with and without gneissic granite 84

24. Expansion of mortar bars prepared with Cement D and various levels of opal 85

25. Expansion of mortar bars prepared with Cement D and various levels of quartzite. 86

26. Expansion of mortar bars prepared with Cement D, with and without gneissic granite 87

27. Expansion of mortar bars prepared with Cement E and various levels of opal 88

28. Expansion of mortar bars prepared with Cement F and various levels of opal 89

(List of Figures, continued)

Figure Page

29. Expansion of mortar bars prepared with Cement G and various levels of opal 90

30. Expansion of mortar bars prepared with Cement H and various levels of opal 91

31. Expansion of mortar bars prepared with Cement H and various levels of opal, using an expanded scale for expansion. 92

32. Expansion of mortar bars prepared with opal, at the level determined to be its pessimum for each cement (2% for all except A, which is 4%) 100

33. Expansion of mortar bars prepared with quartzite, at the level determined to be its pessimum for each cement (20% for Cements A through C, 10% for Cement D). 101

34. Expansion of mortar bars prepared with 100% gneissic granite 102

35. Expansion of mortar bars prepared with 100% limestone. 103

36. Levels of pH in pore solutions of limestone mortars. 114

37. Levels of hydroxide ion in pore solutions of limestone mortars. 117

38. Levels of sodium ion in pore solutions of limestone mortars. 120

39. Levels of potassium ion in pore solutions of limestone mortars. 122

40. Levels of calcium ion in pore solutions of limestone mortars. 125

41. Levels of silica in pore solutions of limestone mortars. 128

42. Levels of sulfate ion in pore solutions of limestone mortars. 130

(List of Figures, continued)

Figure Page

43. Expansion levels of mortar bars prepared with Cement A and 4% opal, shown on a log time scale and a square root time scale. 134

44. Expansion levels of mortar bars prepared with Cement A and 20% quartzite, shown on a log time scale and a square root time scale 135

45. Expansion levels of mortar bars prepared with Cement A and granite, shown on a log time scale and a square root time scale. 136

46. Expansion levels of mortar bars prepared with Cement A and limestone, shown on a log time scale and a square root time scale. 137

47. Final mortar bar expansion versus the total alkali level of each cement 142

48. Calculated pH levels, from the measured hydroxide ion levels and an activity coefficient of unity, versus the measured pH levels in pore solutions of limestone mortars. 145

49. Measured sulfate levels versus measured pH levels in pore solutions of limestone mortars 146

50. Measured silica levels versus measured pH levels in pore solutions of limestone mortars 149

51. Measured calcium levels versus measured pH levels in pore solutions of limestone mortars 151

52. Alkali concentration levels in pore solutions of limestone mortars prepared using Cement A, measured and calculated according to various models. 155

53. Alkali concentration levels in pore solutions of limestone mortars prepared using Cement B, measured and calculated according to various models 156

54. Alkali concentration levels in pore solutions of limestone mortars prepared using Cement C, measured and calculated according to various models 157

(List of Figures, continued)

Figure Page
55. Alkali concentration levels in pore solutions of limestone mortars prepared using Cement D, measured and calculated according to various models 158

56. Alkali concentration levels in pore solutions of limestone mortars prepared using Cement E, measured and calculated according to various models 159

57. Alkali concentration levels in pore solutions of limestone mortars prepared using Cement F, measured and calculated according to various models 160

58. Alkali concentration levels in pore solutions of limestone mortars prepared using Cement G, measured and calculated according to various models 161

59. Alkali concentration levels in pore solutions of limestone mortars prepared using Cement H, measured and calculated according to various models 162

60. Final mortar bar expansion with various reactive aggregates versus pH levels of the pore solutions in limestone mortars. 165

61. Final mortar bar expansion with various reactive aggregates versus sodium concentrations of the pore solutions in limestone mortars. 166

62. Final mortar bar expansion with various reactive aggregates versus potassium concentrations of the pore solutions in limestone mortars. 168

63. Final mortar bar expansion with various reactive aggregates versus total alkali (sodium plus potassium) concentrations of the pore solutions in limestone mortars. 169

64. Final mortar bar expansion with various reactive aggregates versus calcium concentrations of the pore solutions in limestone mortars. 170

65. Final mortar bar expansion with various reactive aggregates versus lithium concentrations of the pore solutions in limestone mortars. 171

(List of Figures, continued)

Figure Page

66. Final mortar bar expansion with various reactive aggregates versus the sodium concentration of the pore solutions in limestone mortars of the high-alkali cements. 173

67. Final mortar bar expansion with various reactive aggregates versus the potassium concentration of the pore solutions in limestone mortars of the high-alkali cements. 174

68. Final mortar bar expansion with various reactive aggregates versus the sodium plus potassium concentrations of the pore solutions in limestone mortars of the high-alkali cements. 175

69. Silica and pH levels in alkali hydroxide solutions produced by reactions of various aggregates from the present study, and by dissolution of silica gel (Dent Glasser and Kataoka, 1981), showing the curve reported by Dent Glasser and Kataoka that separates stable and unstable silica solutions 178

70. Reduction in hydroxide ion level produced by reaction of various aggregates in model pore solutions versus initial pH level of each solution. 180

71. Silica level produced by reaction of various aggregates in model pore solutions versus initial pH level of each solution. 182

72. Measured mortar bar expansion versus estimated reduction in hydroxide ion concentration for each aggregate-pore solution reaction 185

73. Measured mortar bar expansion versus estimated silica concentration for each aggregate-pore solution reaction. 186

Appendix
Figure

74. Measured pH level at various times showing precision of pH determination. 210

75. Calibration curve for calcium. 217

76. Calibration curve for sodium 218

(List of Figures, continued)

Figure Page
77. Calibration curve for potassium 219

78. Calibration curve for sulfate 220

79. Typical UV absorbance spectra for silica specimens, showing reagent blank (bottom-most curve), 1.0 μM silica standard (second curve), 2.0 μM silica standard (third curve), and an unknown specimen (topmost curve) 221

80. Calibration curve for silica 222

81. XRD pattern of Cement A ignited at 500°C and extracted in salicylic acid/methanol solution 227

82. XRD pattern of Cement A ignited at 500°C and extracted in aqueous KOH-sugar solution 228

83. XRD pattern of Cement B ignited at 500°C and extracted in salicylic acid/methanol solution 229

84. XRD pattern of Cement B ignited at 500°C and extracted in aqueous KOH-sugar solution 230

85. XRD pattern of Cement C ignited at 500°C and extracted in salicylic acid/methanol solution 231

86. XRD pattern of Cement C ignited at 500°C and extracted in aqueous KOH-sugar solution 232

87. XRD pattern of Cement D ignited at 500°C and extracted in salicylic acid/methanol solution 233

88. XRD pattern of Cement D ignited at 500°C and extracted in aqueous KOH-sugar solution 234

89. XRD pattern of Cement E ignited at 500°C and extracted in salicylic acid/methanol solution 235

90. XRD pattern of Cement E ignited at 500°C and extracted in aqueous KOH-sugar solution 236

91. XRD pattern of Cement F ignited at 500°C and extracted in salicylic acid/methanol solution 237

92. XRD pattern of Cement F ignited at 500°C and extracted in aqueous KOH-sugar solution 238

(List of Figures, continued)

Figure Page
93. XRD pattern of Cement G ignited at 500°C and extracted in salicylic acid/methanol solution. 239

94. XRD pattern of Cement G ignited at 500°C and extracted in aqueous KOH-sugar solution. 240

95. XRD pattern of Cement H ignited at 500°C and extracted in salicylic acid/methanol solution 241

96. XRD pattern of Cement H ignited at 500°C and extracted in aqueous KOH-sugar solution. 242

ABSTRACT

Struble, Leslie Jeanne. Ph.D., Purdue University, May 1987.
The Influence of Cement Pore Solution on Alkali-Silica
Reaction. Major Professor: Sidney Diamond.

The alkali-silica reaction, which may cause expansion and sometimes cracking of concrete, takes place between alkali (sodium and potassium), usually derived from the cement, and certain forms of silica that may occur in the aggregate. The goal of the study described here, which concerns the influence of the composition of the aqueous solution present in the pores of hydrating mortar, is to improve our understanding of certain details of alkali-silica reaction mechanisms.

Compositions of the pore solutions were varied through the selection of cements with various alkali contents and distributions. Expansion studies were carried out using these cements and certain reactive aggregates. The expansion studies indicated an influence of the cement alkali distribution on expansion due to alkali-silica reaction.

Effects of the chemical composition of pore solutions on expansion were studied directly. Pore solutions were expressed from limestone (control) mortars prepared from the same cements, and concentration levels of various ionic species were measured. The solutions were shown to consist primarily of hydroxide and alkali ions, with pH levels ranging from 13.4 to 14.0. When composition results were compared with the expansion results of mortars containing opal, the levels of hydroxide and alkali ions were shown to influence the expansion. A threshold in pH was observed, between 13.65 and 13.83, below which there was little or no expansion, and above which there was significant expansion. In addition, a direct correlation was observed between expansion and the level of either sodium or sodium plus potassium.

Reactions of the aggregates in model pore solutions were studied and compared with expansion levels produced by the aggregates in mortars. The reactions were shown to produce various levels of dissolved silica and reduction in pH, and the levels of silica correlate directly with the mortar-bar expansion levels produced by each aggregate and proportion. Thus expansion appears to be a function of the extent of the reaction of aggregate in pore solution, which depends on the material, its proportion, and the solution pH level, and is further influenced by the amount of sodium or sodium plus potassium in the pore solution.

CHAPTER 1

INTRODUCTION

A major concern in the production of durable concrete is to avoid degradation due to alkali-silica reaction, a chemical reaction that sometimes takes place between cement and aggregate. The reaction occurs between alkali (sodium and potassium) hydroxides, usually derived from the cement, and certain forms of silica that may occur in the aggregate. The reaction produces expansion, which often causes the concrete to crack, and may ultimately cause failure of the structure.

Although there have been a substantial number of descriptions of alkali-silica reaction in concrete since the first reports in 1940 by Stanton (1940), it appears from a recent review (Diamond, 1975) that only the general aspects of the mechanisms involved in alkali-silica reaction and its resulting expansion are understood. Many details of the mechanisms are still being investigated and some are the subject of controversy. The goal of the study described here is to improve our understanding of certain details of alkali-silica reaction mechanisms.

This study is focused on the influence of the composition of the aqueous solution present in the pores of hydrating mortar on alkali-silica reaction. The study was carried out in three parts. The objective of the first part was to determine how pore solution composition influences expansion of mortars containing reactive aggregate. This first part involved mortar-bar expansion studies using cements with various distributions of alkalies among the cement compounds, so as to provide variations in compositions of the pore solutions. From these studies, an apparent influence of the cement alkali distribution on expansion due to alkali-silica reaction was detected. The objective of the second part was to study directly the compositions of the pore solutions, both the influence of alkali distribution on the pore solution composition and the influence of pore solution composition on mortar bar expansion. The objective of the third part was to study the influence of pore solution composition on its reaction with the several aggregates used in the expansion studies. Finally, the results of the three studies were integrated so as to explore the relationships between pore solution composition and alkali-silica reaction.

The introductory chapter provides a review of the various chemical and physico-chemical mechanisms of the alkali-silica reaction and its resulting expansion. Of the many papers describing alkali-silica reaction, only those concerned with reaction mechanisms are included. This first chapter also provides a review of certain relevant aspects of cement chemistry, specifically concerning the distribution of alkalies among the various phases in portland cement, and the composition of the pore solution in hydrating portland cement pastes and mortars.

Alkali-Silica Reaction Mechanism

As noted previously, while the mechanisms of the alkali-silica reaction are understood in general terms, the details are often the subject of controversy. The general aspects, as reviewed by Diamond (1975, 1976), may be summarized as follows:

1. The reaction does not directly involve alkali, but occurs between silica in the aggregate and hydroxide ions in the pore solution.

2. The concentration of hydroxide ions is controlled predominantly by the concentrations of sodium and potassium ions in the pore solution.

3. The product of the reaction is a gel, an amorphous semi-solid or solid material consisting principally of silica, alkali, calcium, and water, as summarized in Table 1.

4. This gel may imbibe water and swell, producing expansion and possibly cracking of the mortar or concrete.

Gel Formation

Although there have been many descriptions published of gels formed during alkali-silica reaction, comparatively little is known about the process by which these gels form. The formation of silica gels by processes of polymerization from a concentrated solution and of coagulation of a colloidal silica sol have been described (Iler, 1979), but these processes seem unlikely in concrete. An alternative hypothesis is that alkali-silica gels form by incomplete dissolution of silica in an alkali hydroxide solution. Dent Glasser and Kataoka (1981) and later Figg (1983) suggested that dissolution of well-crystallized or dense silica produces monomeric silicate ions in solution; but poorly ordered silicates dissolve only partially so as to produce a gel, i.e. a network of polymeric silicate ions and associated alkali ions.

It has not been clear whether calcium plays any fundamental role in alkali-silica gel formation. Powers and Steinour (1955) suggested that calcium plays a very important role, that at high concentrations of alkali, the calcium concentrations in the pore solution would be low, and a gel low in calcium would form. Likewise, at low

Table 1. Typical compositions of gels in reacted concretes[a].

	Level	Percent (%)
SiO_2	high	50
Na_2O	moderate	10
K_2O	moderate	5 to 10
CaO	low	0 to 5
H_2O	moderate	10 to 20

[a] Summarized from analyses of gels from reacted concrete (Hester and Smith, 1953, Idorn, 1961, and Thaulow and Knudsen. 1975).

concentrations of alkali the calcium concentrations would be high, and a gel high in calcium would form. Significant, though variable, levels of calcium have been determined from chemical analyses of gels in reacted concrete (Table 1), but it is not known whether the calcium is an integral component of the gel or is derived from associated $Ca(OH)_2$ or $CaCO_3$.

Quite different conclusions regarding calcium were reported by Dent Glasser and Kataoka (1982) from studies of the reaction between silica gel and sodium hydroxide solution or mixed calcium and sodium hydroxide solutions. As expected, reaction between silica gel and sodium hydroxide solution was shown to produce a sodium-silica gel. However, the reaction between silica gel and a mixed calcium and sodium hydroxide solution produced C-S-H[1] gel, possibly containing some sodium. Only when the calcium ion concentration was reduced to a very low value did a sodium-silica gel form, after which the system behaved the same way as the system containing no calcium.

Swelling of Gel

The mechanism by which gels imbibe water and expand is usually described as osmosis. Osmotic imbibition can generate pressure, although strictly speaking the term "osmotic pressure" in physical chemistry refers to the applied pressure necessary to prevent such imbibition, rather than that exerted by the system due to the imbibition. The specific details concerning how such pressure might be generated in concrete have been somewhat controversial. Hansen (1944) suggested that the alkali-silica product dissociates into complex ions that cannot diffuse through cement paste, so pressure is generated by the transfer of water through the paste, acting as a semipermeable membrane, into the alkali-silica sol or solution. Powers and Steinour (1955), on the other hand, suggested that the primary cause of damage is simple swelling of solid gel as it imbibes water, and no semipermeable membrane is necessary; they described this swelling as osmosis by analogy to swelling of clays, in which the solute is chemically bound to the crystal. The swelling process was discussed in similar terms by Dent Glasser (1979) and by Calleja (1980), each of whom argued that the swell pressure generated by alkali-silica gel is osmotic in origin; that the silica framework of the gel is the osmotic membrane, allowing passage of water in, but not allowing transport of the soluble species out. The soluble species are the alkali ions, which are prevented from migrating out by electrochemical attraction to the silica framework.

---

[1] The following abbreviations, commonly used in chemical formulae of cement phases, are used: C for CaO, S for SiO_2, A for Al_2O_3, F for Fe_2O_3, H for H_2O, N for Na_2O, and K for K_2O.

Pessimum Proportion

Evidence suggesting that the gel composition is a critical factor in expansion due to alkali-silica reaction is provided by the well-established pessimum proportion effect, i.e. the occurrence of a maximum in expansion at some intermediate proportion of reactive silica (for example, see Mindess and Young, 1981). A less well-known effect, perhaps related, involves the particle size of the reactive silica. It appears that most aggregate components that cause expansion due to alkali-silica reaction have a particle size that is pessimum with regards to expansion, i.e. that very coarse or very fine particles of reactive aggregate produce less expansion than particles of intermediate sizes (Vivian, 1951). Fly ash and other pozzolanic materials are used to prevent expansion due to alkali-silica reaction (Mindess and Young, 1981), although these materials contain amorphous silica and are expected to be reactive;

this apparent anomaly is presumably an example of the pessimum particle-size effect.

Hansen (1944) and later Pike et al (1955) attributed the pessimum proportion effect specifically to variation in the ratio of alkali to silica in the reaction product. They argued that a gel of some particular ratio of alkali to silica would generate a maximum swell pressure. At lower ratios, a lower osmotic pressure would be generated; at higher alkali levels, the gel would become sufficiently fluid to flow out through the paste before generating much pressure.

Aspects of this mechanism were supported in studies of synthetic sodium silica gels reported by Struble and Diamond (1981a, 1981b). Swell pressure was measured while synthetic sodium-silica gels were allowed to sorb water. The measured swell pressure appeared to depend on gel composition, with the maximum pressure observed for gels with intermediate sodium contents. However, reduced swell pressures in gels of higher sodium contents did not appear to be caused by the gel flowing through the restraining material, as had been suggested by Hansen (1944). From these studies, a concept was developed (Struble, 1979), consistent with discussions by Dent Glasser (1979) and by Calleja (1980), to explain the observed swelling behavior. The concept involved consideration of the degree of polymerization and the extent of bonding between individual polymeric silica units in the gel. It was suggested that for high swell pressure to be generated, a pessimum nanostructure[2], rather than pessimum proportion, is required. The structure was thought to be affected by such factors as age, degree of carbonation, and temperature, as well as by gel composition.

---

[2] The term nanostructure is used to refer to the structure of a material at a nanometer scale.

Dent Glasser and Kataoka (1981), on the other hand, suggested that the pessimum effect is a result of the nature of silica dissolution in alkali hydroxide solution. They showed a solubility curve for silica in a high pH solution and the paths by which individual systems approached equilibrium. In each case, dissolution of SiO_2 was accompanied by reduction in hydroxide ion concentration. Dissolution proceeded until all solid was used up or until the limiting curve was reached. The reduction in hydroxide ion concentration indicated that SiO_2 dissolution may be self-limiting. Furthermore, when the amount of dissolved silica was plotted against the total SiO_2/Na_2O ratio, a maximum level of dissolved silica was observed at an intermediate SiO_2/Na_2O ratio. This maximum in dissolved silica was considered to provide an explanation for the pessimum effect.

Still another hypothesis concerning the pessimum effect involves the influence of calcium concentration on swelling properties. As discussed previously, Powers and Steinour (1955) suggested that the calcium level of the gel causes the pessimum effect due to the expected inverse relationship between calcium and alkali concentrations in solution. They suggested that a gel low in calcium would tend to swell, but a gel high in calcium would be nonswelling. They further suggested that as the concentration of alkali decreased through reaction with silica, the calcium concentration should increase, such that subsequent reaction with additional silica would produce a relatively nonswelling calcium-alkali-silica gel. They attributed the decrease in expansion at higher proportions of reactive aggregate to this effect, i.e. that addition of a greater proportion of reactive aggregate than the pessimum amount would produce a nonswelling gel, reducing the overall expansion from that generated with the pessimum proportion of aggregate. Recent determinations of the composition of pore solutions expressed from hardened paste or mortar, discussed below, demonstrate that the pore solutions are predominantly aqueous solutions of potassium and sodium hydroxide, and contain very little calcium, and thus do not support the hypothesis of Powers and Steinour.

A final explanation for the pessimum proportion effect was discussed by both Ozol (1975) and Hobbs (1978). At low proportions of reactive silica, it was considered that the amount of gel is limited by the low amount of reactive silica; at proportions higher than the pessimum, the amount of gel is thought to be limited by the amount of alkali ion in solution. This explanation implies that the gel forms with a constant composition, and that expansion is a function of the amount of gel.

Any mechanism for alkali-silica reaction must be consistent with the effect of some fly ashes and other pozzolans in reducing expansion. Pozzolans may reduce expansion through the pessimum proportion effect, since pozzolans serve to decrease the ratio of alkali to total reactive silica in the system. An alternative explanation was suggested by Chatterji (1979), who observed that solid $Ca(OH)_2$ is a necessary component for expansion and suggested that the beneficial effects of pozzolans might occur because they deplete the solid $Ca(OH)_2$, a suggestion supported by others (Tang et al, 1983, and van Aardt and Visser, 1982). Another explanation for the effect of pozzolans was provided by results of Bhatty and Greening (1978), supported later by Glasser and Marr (1984), showing that the amount of alkali bound by C-S-H gel increases for gels of lower Ca/Si ratio. Since hydration of a mixture of cement and fly ash, compared to cement alone, produces gel of lower Ca/Si ratio, the mixture is expected to bind more alkali.

Aggregate Parameters

The principal aggregates susceptible to alkali-silica reaction, as reviewed by Diamond (1976), are glassy silica, opal, chert, flint, and strained quartz. It appears that both the degree and rate of expansion vary considerably for these materials. Two studies, by McConnell et al (1947) and by Gaskin et al (1955), include expansion data for a large number of reactive aggregates. The expansion characteristics of these aggregates (the degree and rate of expansion, and the proportion of each constituent in the total aggregate that produces maximum expansion) are summarized in Table 2. It must be noted with regards to Table 2 that the terminology used to describe aggregates is not entirely consistent between the two references. However, the data in Table 2 illustrate that expansion characteristics vary considerably among the different aggregate types. The degree of expansion ranged from 0.04 to 2.2%, with the highest expansion produced by opal and pyrex glass, and the lowest by some of the quartz, chert, and flint materials. Rates of expansion measured during the initial expansion period ranged from 0.001% to 0.88% per month. The most rapid expansions were produced by opal and chalcedony (both porous materials), and the slowest by quartz, chert, and flint. Observed pessimum proportions ranged from 5% to 100%, with the higher pessimum levels characteristic of pyrex glass, quartz, and chalcedony, and the lowest pessimum provided by opal.

The degree and rate of expansion produced by a particular aggregate may relate to its rate of dissolution in alkaline solution. Though only sparingly soluble in a neutral solution, silica is quite soluble in an alkaline solution (Iler, 1979). Both the rate of dissolution and the level reached increase substantially as pH levels increase, as shown in Figs. 1 and 2 for pH levels up to 10. Iler (1979) described the effect as follows:

Table 2. Summary of mortar bar tests for various aggregate materials.

Aggregate	Pessimum Proportion (%)	Expansion Level (%)	Expansion Rate (% per week)	Reference[a]
Chalcedony	20	0.3	0.05	(1)
Chalcedony	100	0.9	0.08	(1)
Chalcedony	20	>0.9	0.11	(1)
Chert	10	>>0.2	0.05	(1)
Chert	50	>0.3	0.09	(1)
Chert	20	>0.5	0.002[b]	(2)
Flint	20	>>0.1	0.02	(1)
Flint	50	>0.4	0.01	(1)
Flint	10	0.8	0.007	(2)
Microcrystalline Quartz	20	>0.04	0.0002	(2)
Microcrystalline Quartz	50-100	0.5	0.02	(1)
Opal	5	>2.2	0.21	(1)
Opal	5	>>1.5	0.06	(2)
Pyrex glass	50-100	>1.4	0.02	(2)

[a] References: (1) McConnell et al (1947), and (2) Gaskin et al (1955).

[b] Expansion began after a delay of ~3 years.

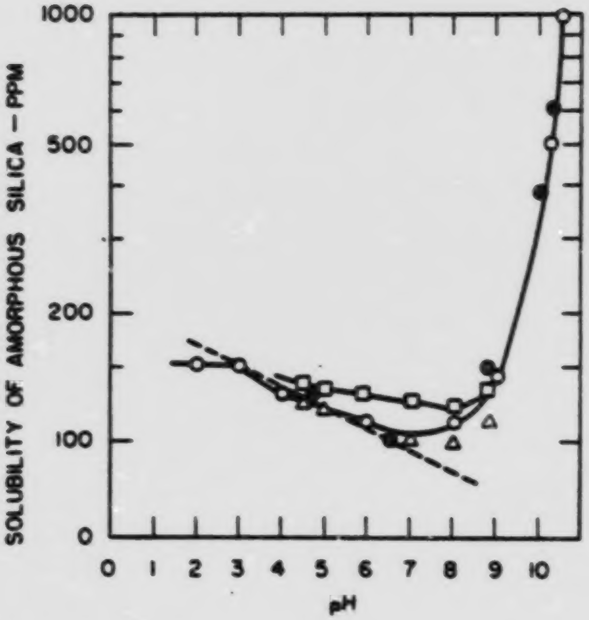

Figure 1. Level of dissolution of amorphous silica versus pH of solution (Iler, 1979).

BEST COPY AVAILABLE

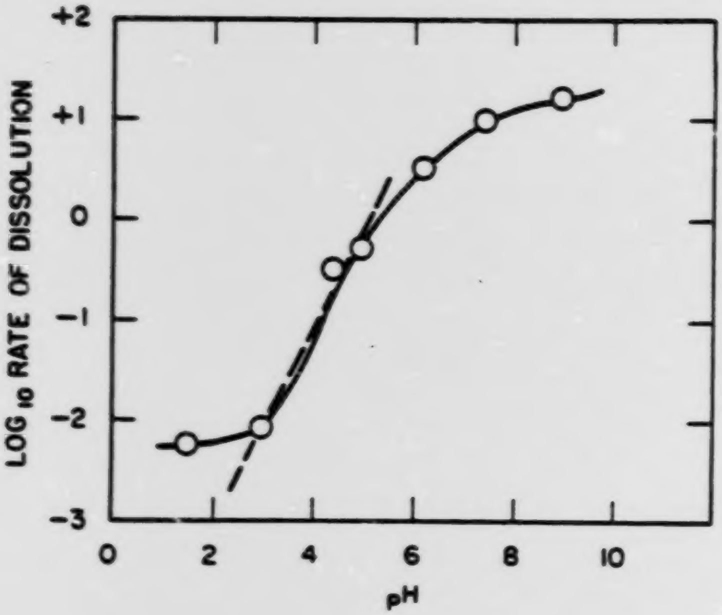

Figure 2. Rate of dissolution of amorphous silica versus pH of solution (Iler, 1979).

BEST COPY AVAILABLE

> "The hydroxyl ion is the unique catalyst in alkaline solutions . . . The first step is the adsorption of OH^- ion, after which a silicon atom goes into solution as a silicate ion. If the pH is much below 11, the silicate ion hydrolyzes to soluble silica, $Si(OH)_4$, and OH^- ions and the process is repeated . . . Above pH 11 the hydroxyl ions act in the same way, converting $Si(OH)_4$ to silicate ions, thus keeping the solution unsaturated so that silica continues to dissolve. But below pH 11, even down to pH 3, the OH^- ion is only the catalyst that controls the rate at which silica dissolves until the solution reaches saturation."

Although aggregates are known to vary with respect to the characteristic degree and rate of expansion produced, only a few studies have addressed the causes of such variation. Iler (1979) noted a substantial variation in rate of dissolution for various forms of silica (Table 3), with glass > tridymite > cristobalite > quartz. Since this order of dissolution rates is generally similar to the order of expansion produced by these materials when used as aggregate, it may be that differences in expansion characteristics of various forms of silica are associated with differences in therate of silica dissolution. An alternative explanation was suggested by Grattan-Bellew (1978), that the rate of expansion during the main expansion phase is directly related to the content of microcrystalline material in the aggregate. The dissolution rate was suggested by Dent Glasser and Kataoka (1981) to depend on microstructure, specifically the permeability to the alkali hydroxide solution. They noted that for a well crystallized, dense silica, dissolution would occur slowly at the surface, whereas for poorly crystalline aggregates, channels allow reactants to penetrate into the interior and dissolution would proceed much more rapidly.

Dissolution may also be a function of the nanostructure, in particular the degree of local disorder in the structure.

Table 3. Rate of dissolution of various forms of silica at pH 8.5[a].

Form of Silica	Rate of Dissolution ($\mu g\ ml^{-1}\ day^{-1}$)
Fused glass	39.0
Quartz	2.8
Cristobalite	6.0
Tridymite	4.5

[a] Reported by Iler (1979).

In summary, the principal features of the alkali-silica reaction are the gel formation and gel swelling. Gel formation appears to be the result of a dissolution-type process, with the rate of dissolution depending on the concentration of hydroxide ion in the pore solution and on microstructural and other features of the specific form of silica. Once formed, the tendency of the gel reaction product to imbibe water and swell appears to depend on its chemical composition. The gel composition is undoubtedly influenced by the composition of the pore solution, in particular the levels of sodium and potassium ions. Therefore, both the reaction to form gel and the tendency of the gel to cause expansion are certainly influenced by and may be controlled by the composition of the pore solution.

Influence of Cement Alkali Distribution

It has been understood in a general way for some time that expansion due to alkali-silica reaction depends both on the amount and nature of the reactive aggregate, and on the amount of alkali in the mortar or concrete (Vivian, 1950). In most cases, the alkali in mortar or concrete is derived from the portland cement, where it may occur in a number of specific phases. Because these phases vary in their rate of dissolution during cement hydration, it is likely that the precise distribution of alkali among the various cement components will also influence expansion. How the alkalies (i.e. sodium and potassium) occur in cement was reviewed by Jawed and Skalny (1977, 1978) and subsequently by Skalny and Klemm (1981). The following discussion is based largely on these reviews.

Alkalies occur in clinker either in various alkali sulfate phases, or substituted in the calcium silicate, calcium aluminate, and calcium aluminoferrite clinker phases. If sulfate is present in the kiln, alkalies tend to form alkali sulfates, K_2SO_4 and $(K,Na)_2SO_4$, and calcium potassium sulfate, also called calcium langbeinite, $K_2Ca_2(SO_4)_3$. The double alkali sulfate forms a solid solution, with proportions of potassium and sodium ranging from a molar ratio of 3:1 to a ratio of 1:3. If the potassium content is sufficiently greater than the sodium content, the alkali sulfate formed is the potassium end member of this solution, and any excess potassium forms K_2SO_4. If there is more than enough sulfate to react with all alkali present, $CaSO_4$ is formed, which subsequently reacts with K_2SO_4 in the kiln to form the double sulfate $K_2Ca_2(SO_4)_3$.

The alkali sulfate phases frequently appear as deposits of fine crystals on the surfaces of calcium silicate crystals. There are two reasons for this occurrence. The first is that the alkali sulfate melt is insoluble in the liquid phase of the clinker, so on cooling the clinker, the alkali sulfate remains liquid below the temperature at which the clinker liquid solidifies. The second is that alkali sulfate vapor may deposit onto cooling clinker surfaces.

If the sulfate level is not sufficient to combine with all the available alkalies, alkalies will enter the major clinker phases. Of the four major phases, C_3A and C_2S can incorporate particularly high levels of alkali (Strunge et al, 1985), and their crystal structures may be modified by this substitution. Pure C_3A is cubic, but sufficiently sodium-rich C_3A becomes orthorhombic, the end member of a continuous solid-solution series having the approximate composition NC_8A_3 (Skalny and Klemm, 1981). Clinker C_3A may also contain potassium, and there have been reports of tetragonal C_3A containing potassium (KC_8A_3) (Gebhardt, 1986) or both sodium and potassium (Regourd and Mortureux, 1977). The other principal alkali-containing clinker phase is C_2S, typically occurring in clinker as the β-C_2S polymorph. At high levels of potassium, the α'-C_2S polymorph is stabilized, with a composition approximating $KC_{23}S_{12}$ (Jawed and

Skalny, 1977). At high levels of sodium and a very rapid rate of cooling, the α-C_2S polymorph may also be stabilized, but these conditions are rarely met in practice (Gies and Knöfel, 1986).

It is not clear from the literature to what extent sodium and potassium are partitioned between the calcium silicates and the interstitial phases, and what specific parameters control this partitioning. Possible factors include the rate and temperature of burning and the rate of cooling.

It thus appears that the principal cause of variation in alkali distribution is the degree sulfate is available to combine with alkali. Extensive alkali substitution in the calcium silicate and calcium aluminate phases occurs only when there is very little sulfate in the kiln. Since the clinker sulfate is most often derived from sulfur in the fuel, clinkers low in sulfate are produced only using natural gas or other fuel very low in sulfur.

The influence of the alkali distribution among cement phases on the alkali concentrations in the pore solutions of hydrated cement systems particularly depends on what proportion of alkali occurs in sulfate phases. When cement is mixed with water, the alkali sulfates and calcium potassium sulfate appear to dissolve quite rapidly (Jawed and Skalny, 1978). In contrast, alkalies combined in the calcium silicate and calcium aluminate clinker phases are not expected to dissolve until these phases hydrate. It was demonstrated experimentally by both Jawed et al (1983) and Shin and Glasser (1983) that Na combined in Na-rich (orthorhombic) C_3A goes into solution only as the C_3A phase hydrates, and it is reasonable to expect that alkalies combined in the other three major clinker phases would behave in a similar manner. The hydration of each of these phases proceeds at a different rate, with C_3A hydrating most rapidly, C_3S at a moderate rate, and C_2S and C_4AF relatively slowly (Pratt and Ghose, 1983, and Dalziel and Gutteridge, 1986). Differences in the alkali distribution among cement phases may thus influence the rate at which alkali concentrations increase in the pore solution, and thereby may influence the levels of expansion due to alkali-silica reaction.

Despite this expectation, there is no agreement concerning any specific influence of the distribution of alkalies in the cement on expansion. Comparing correlations between expansion and water-soluble alkali or total alkali, two studies demonstrated closer correlations with water-soluble alkali (Hobbs, 1980, and Brandt and Oberholster, 1983), but a third study showed no difference (Gilliland and Bartley, 1950). Davis (1951) compared mortars prepared from two cements with clinkers of the same composition but cooled at different rates in order to modify the distribution of alkalies in the clinkers. The mortars prepared from cement with the rapidly cooled clinker expanded more slowly than mortars from cement with the slowly cooled clinker, but the ultimate expansions of mortars from the two cements were similar. The evidence is thus inconclusive concerning any influence of the cement alkali distribution on expansion.

Cement Pore Solution

When cement and water are mixed together, a series of chemical reactions is begun, which includes dissolution of cement phases and formation of new hydrated phases. Dissolution rapidly converts the water to a concentrated solution of sodium, potassium, hydroxide, and sulfate ions, with lesser amounts of calcium and silicate ions. As hydration proceeds, some of the solvent water combines in hydrated phases and thus is removed from the solution, which thereby becomes more highly concentrated in dissolved species. However, not all the water is used in the hydration reactions, and the remaining solution may persist in the pores of the hardened paste.

A method to express pore solution from hardened paste or mortar was first reported in 1973 by Longuet et al (1973). Prior to this report, pore solutions could be obtained for analysis only by filtration or centrifuging, often using a water/cement ratio much higher than would be found in concrete, and only at very early ages (e.g. up to 5 hours). For example, the aqueous phase studies of Lawrence (1966), which have been influential in our understanding of cement hydration, were carried out using filtration of cement pastes at early ages. Longuet et al (1973) described a device for expressing pore solution from paste or mortar at late ages (up to 1 year) without limits on the water/cement ratio. A similar device, subsequently used at Purdue University, was described by Barneyback and Diamond (1981). Since then, an increasing number of laboratories have used these devices in pore solution studies.

The composition of the pore solution is important in understanding any concrete reaction, i.e. alkali-silica reaction, corrosion of steel, stability of glass in concrete, interaction of concrete with constituents of radioactive nuclear waste, and cement hydration. Studies utilizing pore solution composition are summarized in Table 4 for all these areas of research.

Taken together, these studies (Table 4) indicate that the pore solution in portland cement paste or mortar after the first day or so of hydration consists predominantly of potassium, sodium, and hydroxide ions in water. Typical potassium concentration levels fall between 200 mM and 600 mM, and typical sodium concentration levels between 50 mM and 300 mM. The only other cation reported is calcium, typically at concentration levels below 4 mM. Typical hydroxide concentration levels fall between 200 and 1000 mM,

Table 4. Summary of pore solution studies.

Area of Study	Reference
Cement Hydration	Lawrence (1966) Lashchenko and Loganina (1972) Diamond (1975) Penko (1983) Luke and Glasser (1986)
Nuclear Waste Containment	Glasser, Angus, McCulloch, MacPhee, and Rahman (1984)
Corrosion	Longuet, Burglen, and Zelwer (1973) Page and Vennesland (1983) Lambert, Page, and Short (1985) Roy, Malek, Rattanussorn and Grutzeck (1985)
Stability of Glass	Xue, Xu, and Ye (1983)
Effect of Mineral Additives	Diamond (1981) Glasser and Marr (1984) Glasser and Marr (1985) Silsbee, Malek, and Roy, (1986)
Alkali-Silica Reaction	Diamond and Barneyback (1976) Marr and Glasser (1983) Diamond (1983) Barneyback (1983) Kollek, Varma, and Zaris (1986)

with pH levels between 13.2 and 13.8. Typical concentration levels for both sulfate and silica are below 20 mM.

A number of studies have discussed the influence of pozzolanic materials on the composition of pore solution, in particular on levels of alkali and hydroxide. Diamond reported reduction in alkali concentration with incorporation of two low-calcium flyashes, but only to the extent that cement was replaced by fly ash (Diamond, 1981). He subsequently reported major reduction in hydroxide ion concentrations with incorporation of silica fume, modest reduction with one fly ash, and no reduction with another fly ash (Diamond, 1983). Page and Vennesland found similar reductions with silica fume (1983), as did Glasser and Marr (1984, and 1985).

The principal treatment of the pore solution composition as it relates to alkali-silica reaction was provided by Barneyback (1983). He reported pore solution compositions from many mortars containing reactive and nonreactive aggregate, and concluded that high levels of alkali and hydroxide ions in the pore solution are the primary cause of alkali-aggregate reaction. As had been indicated earlier by Barneyback and Diamond (1976), concentrations of alkali in mortars containing reactive aggregate were seen to decrease progressively, indicating transfer of alkali ions to alkali-silica reaction product. Reactive aggregate and pozzolanic material were each shown to reduce the amount of alkali in solution and to increase the amount of residual unbound water in the pore solution, though the magnitude of these effects was seen to vary substantially from material to material (Barneyback, 1983).

Diamond (1983) suggested that there may be a threshold concentration of hydroxide ion required for triggering alkali-silica expansion, probably on the order of 0.25 M. Kolleck et al (1986) similarly suggested that the hydroxide ion concentration must be reduced below approximately 0.3 M by fly ash in order for expansion to be prevented.

In summary, studies of pore solution composition have provided considerable information about alkali-silica reaction mechanisms. However, there are at present a number of aspects of this reaction that are not well understood or agreed upon. Furthermore, additional studies involving pore solution composition may add to our understanding of the reaction mechanisms. The present studies have been carried out with these considerations in mind.

CHAPTER 2

EXPERIMENTAL METHODS

The materials and procedures used for the various experimental studies are described in this second chapter, including mortar-bar expansion studies, pore solution studies, and aggregate reactivity studies. Some of the materials and procedures used in this work have already been described by Struble and Diamond (1986).

In general, the methods used, especially those for determining chemical compositions, were standard and widely-used procedures that need not be described in great detail. However, procedures for analysis of pore solution composition were daveloped or modified specifically for these studies and are not widely used. Therefore, these procedures are discussed in considerable detail. Because it is important in discussing results to understand the accuracy and precision of each analytical procedure, all analytical procedures and estimations of precision are described in detail in Appendix A.

Materials

The materials used to prepare mortars for measurement of expansion and for expression of pore solutions were portland cement, sand-sized aggregate, and water. Several different cements and aggregates were used, as described below.

Cements

Eight cements with various distributions of alkali among cement phases were selected for use in the study, designed to determine if the alkali distribution of the cement influences mortar expansion due to alkali-silica reaction. High alkali cements[3] were sought whose alkalies were concentrated either in one of the alkali sulfate phases, K_2SO_4, $(K,Na)_2SO_4$, and $K_2Ca_2(SO_4)_3$, or in one of the principal alkali-containing clinker phases, C_3A and C_2S. In order to find such cements, many cement companies were contacted, and a number of candidate cements were obtained and evaluated using the chemical analyses provided by the manufacturers and using qualitative X-ray diffraction (XRD) analyses. Nevertheless, it proved difficult to obtain high alkali cements with the desired variations in alkali distribution. Based on the evaluations, eight cements (designated A through H) were selected for these experiments. Four of the cements (E through H) are relatively low in alkali, used in spite of their low alkali levels to provide the targeted distributions of alkali among the cement phases.

No special procedures were followed in collecting the cements. Six of the cements were collected by cement company personnel, either at the mill or the silo. Two of the cements were obtained from other laboratory programs: Cement C is Cement 67 in the collection of the Cement and Concrete Reference Laboratory (CCRL) at the National Bureau of Standards (Pielert et al, 1985), and Cement D is LTS 41 from a collection at the Construction Technology Laboratories of the Portland Cement Association (Lerch and Ford, 1948).

---

[3] Following the designation in ASTM Standard Specification for Portland Cement (C 150-81), high alkali cements are those whose total alkali, expressed as equivalent percent of Na_2O, is greater than 0.60 percent.

Each cement was sealed in a polyethylene bag immediately on receipt for storage throughout this study. In this way, it was hoped to avoid unwanted hydration due to atmospheric water vapor.

Aggregates

As has been discussed previously, aggregates vary significantly in potential degree and rate of expansion. Therefore, four different aggregate materials were selected for the present study to provide a range of expansion characteristics.

A limestone[4] that had been used in previous, unrelated studies (Struble and Mindess, 1983) was selected as a nonreactive aggregate, to serve as a control and for diluting the reactive components. The usual nonreactive aggregate used in alkali-silica studies has been Ottawa sand, a quartz sand specified in the ASTM Test for Compressive Strength of Hydraulic Cement Mortars (C 109-80). However, it now appears that any form of silica may have some potential to participate in alkali-silica reaction, albeit quite slowly for well-crystallized quartz. For this reason it was decided to use limestone as the nonreactive aggregate. While some limestones also undergo an expansive reaction with alkalies (the alkali-carbonate reaction), reactive limestones are typically coarse-grained, argillaceous and rich in dolomite (Ramachandran et al, 1981). The limestone used here was selected from a quarry with no known history of alkali-carbonate reaction and thought to contain only minimal levels of dolomite, although subsequent results (discussed in the next chapter) showed that rock from certain regions of the quarry contained appreciable levels of dolomite.

---

[4] Obtained from Martin Marietta Aggregates Company, Pinesburg MD.

Beltane opal was selected as the aggregate with potential for a high degree and rapid rate of expansion. This rock was first used as a standard reactive aggregate in alkali-silica studies by Barneyback (1983), and since then has been used as a reactive aggregate in a number of alkali-silica studies (Diamond and Barneyback, 1976; Brotschi and Mehta, 1978; Diamond, 1978; Gutteridge and Hobbs, 1980; Figg, 1981; and Diamond et al, 1981). The opal is a hydrothermally altered rhyolite, collected from an abandoned open-pit mine in California (Barneyback, 1983). Gutteridge and Hobbs (1980) determined that its reactive constituents include both an opaline material amorphous to X-rays, and α-cristobalite, whose reactivity was shown to vary with temperature. Novaculite[5], a very fine-grained orthoquartzite, was selected for its potential to cause moderate expansion. Novaculite is a metamorphosed chert composed of microgranular quartz, uniform in grain size (Frondel, 1962). McConnell et al (1947) used novaculite as a reactive aggregate in their alkali-silica studies, but did not discuss what constituent of the rock is reactive. The novaculite used in the present studies has an average grain size of approximately 10 μm (Mindess and Struble, 1982).

A gneissic granite[6] was selected to provide potential for a low level of expansion, which develops slowly. This aggregate is known to be reactive in concrete bridges (Mather, 1983), and was reported by Buck (1983) to be slightly reactive in laboratory studies. Petrographic examination of one thin section indicated that strained quartz, which had been considered by Buck to be the reactive material, is a major constituent.

---

[5] Obtained from Ward's Natural Science Establishment Inc., Rochester, NY.

[6] Obtained from Martin Marietta Aggregate Company, Camak GA.

Each of the four aggregates was collected with the intent of providing a sufficient amount of homogeneous, well-characterized sample for these studies. One or more large (0.1 to 1 m^3) piece of the limestone, quartzite, and gneissic granite was obtained and individually crushed for use throughout the present studies. The opal had been sampled in a similar manner by Diamond and Barneyback (1976). Sufficiently large samples were initially collected and crushed to complete the present studies for all but the limestone. Two large limestone pieces, designated A/B and C, were collected at the start of the project. Unexpectedly, Piece C was found to contain considerable dolomite, as described in the next chapter; Piece C was not used for these studies, and the portion of the quarry found to be rich in dolomite was avoided. Additional pieces, designated K and M, were collected later in the study, and Piece K was also found to contain dolomite.

Methods Used To Analyze Materials

Chemical Composition

Bulk chemical compositions of all cements and aggregates were determined using an X-ray fluorescence spectrophotometer (XRF)[7]. Samples were ground, pressed into pellets, and analyzed according to standard analytical procedures.

Phase Composition

The phase compositions of cements and aggregates were determined qualitatively by powder XRD[8]. Speci-mens were first ground in a mortar and pestle until they would pass a

---

[7] Applied Research Laboratories 72000 X-ray fluorescence spectrophotometer.

[8] Philips APD 3600 X-ray diffractometer.

38 μm (No. 400) sieve, then pressed lightly into sample holders using a back-filling technique. The copper X-ray tube was operated at 45 KVP and 40 mA. Specimens were scanned using a step size of 0.02° (2θ) and count time of 1.0 sec. Diffracted radiation was monochromated using a graphite crystal, and measured using a scintillation-type detector. The crystalline phases present were identified by interpreting the XRD patterns with the aid of a standard XRD data file[9].

The XRD analyses of cements were repeated after selective extractions of certain cement phases to facilitate identification of phases in the extraction residues. Samples were first ignited for 30 minutes at 500°C, to convert calcium sulfate dihydrate (gypsum) and calcium sulfate hemihydrate to anhydrite, and thus remove interfering XRD peaks. One portion of each sample was extracted using a salicylic acid and methanol extraction procedure, and another portion sample using a hot, aqueous potassium hydroxide and sugar extraction procedure, both described below.

The salicylic acid-methanol extraction, first reported by Takashima (1958), selectively dissolves the calcium silicates and any free calcium oxide, facilitating identification of C_3A, C_4AF, and other remaining phases. In particular, the extraction allows identification of the C_3A polymorph and of alkali sulfate phases. The procedure followed for these studies (Struble, 1985) was to stir 2 g sample into a solution of 18 g salicylic acid in 70 ml methanol, mix the slurry for 30 min, filter the solid residue, wash the residue with methanol, and allow it to dry. As described by Struble (1985), an important aspect is that there be no contamination of the solution by water, since even small amounts of water were shown to cause partial dissolution of calcium alkali sulfate, so methanol was dried immediately prior to each extraction using a molecular sieve[10]. The similar extraction in a solution of maleic acid and methanol, which is commonly used for this type of analysis, was found to be inappropriate for determining the distribution of alkalies in cement (Struble, 1985).

---

[9] Joint Committee on Powder Diffraction Standards (JCPDS) powder diffraction file.

The KOH-sugar extraction, described by Gutteridge (1979), involves partial dissolution of cement in a hot, aqueous solution of potassium hydroxide and sugar. The treatment removes C_3A, C_4AF, alkali sulfate, calcium langbeinite, and calcium sulfate phases. The extraction is necessary in order to identify α- or α'-C_2S, whose diagnostic XRD peaks are interfered with by the principal peak from C_3A. A solution of 50 ml H_2O, 5 g KOH, and 5 g sucrose was mixed and heated to 85°C; an ~1.5-g sample was added, and the resulting slurry was stirred for 1.0 min while maintaining the temperature between 80° and 85°C. The resulting suspension often clogs a filter paper and cannot be filtered, so the sample was recovered by centrifuging, decanting most liquid, then filtering the solid residue using Whatman No. 50 paper. The residue was washed with hot water, washed again with methanol, and then allowed to dry.

Alkali Distribution

A number of chemical analyses were carried out in an attempt to determine the quantitative distributions of alkalies among the various identified phases in the cements. Two selective extraction procedures were used for these determinations, the salicylic acid-methanol extraction described previously, and a water extraction. The former procedure was invoked to determine alkali combined in the calcium silicate phases (C_3S and C_2S); the latter, to determine alkali present as alkali sulfate and calcium potassium sulfate (calcium langbeinite). Alkalies combined in the calcium aluminate phases (C_3A and C_4AF) were calculated as the difference between the total alkali and the alkali soluble in the two extractions.

---

[10] Linde 3A, obtained from Matheson Scientific Corp.

Maintaining appropriate selectivity of the salicylic acid-methanol extraction required particular care, as hydration of the cement prior to extraction was expected to modify the apparent alkali distribution indicated using the extraction. All extractions were carried out on samples that had been freshly ignited at 500°C for 30 min to prevent error due to prior hydration. Hydration during the salicylic acid-methanol extraction is also possible (Struble, 1985), so contamination of the solution by water was rigorously avoided.

The water extraction procedure was modified from that described in Section 17.2 of the ASTM Methods for Chemical Analysis of Hydraulic Cement (C 114-83b). The following procedure was used: cement and water were mixed, using 25 ml water per g cement (2.5 times higher than the ratio specified in the ASTM method); this slurry was agitated for a specified period of time (as described below), then filtered and the extract analyzed using an atomic absorption spectrophotometer[11] (AA) to determine the sodium and potassium concentrations. Standard methods recommended by the manufacturer were used in the AA analysis, both in preparation of specimens within the recommended concentration ranges, and in preparation of calibration specimens.

These water extractions were initially carried out for 10 min, as specified in the ASTM method. However, XRD analysis of many residues from the 10-min extraction indicated that weak peaks attributed to ettringite were present (Fig. 3). Ettringite formation implies that some C_3A is dissolving during the extraction. Depending on the alkali content of the C_3A, its partial dissolution during water extraction could be a source of error when using water-soluble alkali to calculate the proportions of alkali sulfate phases. Therefore, the water extractions were repeated using much shorter extraction times (5 s and 1 min) to minimize dissolution of C_3A.

---

[11] Perkin-Elmer Atomic Absorption Spectrophotometer Model 303.

It was initially intended that the solutions obtained from extraction in salicylic acid and methanol be analyzed directly by AA. However, analysis of these solutions was difficult or impossible due to precipitation (apparently of salicylic acid) when water was added to dilute the solutions. Therefore, alkali contents were determined indirectly using the solid residues. The total alkali contents were determined for the unextracted cement and then for the residue from extraction in salicylic acid and methanol, and the alkalies dissolved in the salicylic acid-methanol solution were calculated by difference. The analytical procedure specified in Section 17.1 of ASTM Method C 114 was used for these analyses. In this procedure, the samples are dissolved in hydrochloric acid, and the concentrations of sodium and potassium in solution were measured by AA.

Quick Chemical Test

Each aggregate was tested for alkali-silica reactivity according to the ASTM Test for Potential Reactivity of Aggregates (C 289-81) (the quick chemical test). A single specimen of each aggregate was stored in a sodium hydroxide solution (1 mole/l) at 80°C for 24 h, filtered, and the solutions then analyzed for hydroxide ion concentration by titration and for silica concentration by AA. The source of limestone used for the quick chemical test was Piece A/B.

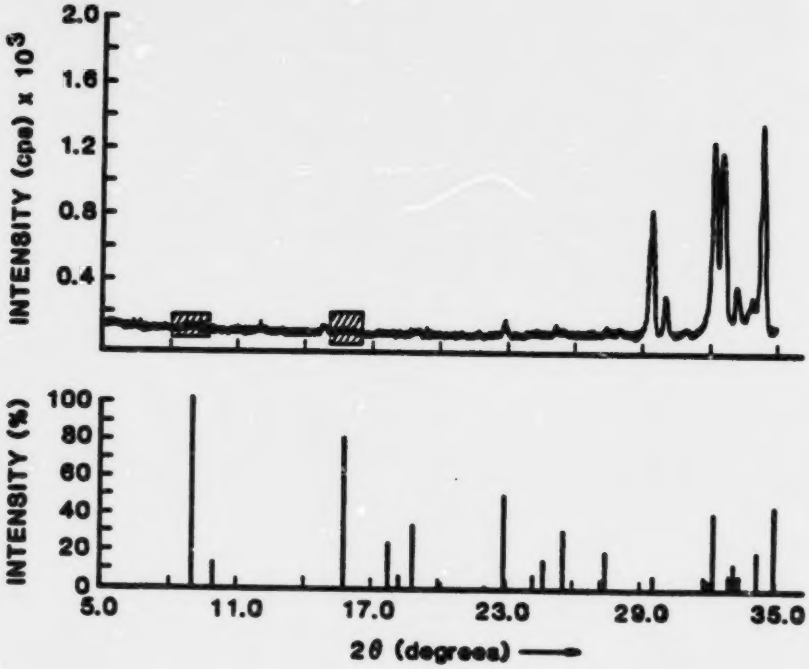

Figure 3. X-ray diffraction pattern of the residue of Cement A after 10-min water extraction, with weak peaks highlighted that are attributed to ettringite (top) based on the JCPDS data (Card No. 9-414, bottom), as reported by Struble (1985).

BEST COPY AVAILABLE

Mortar Preparation

Aggregates for mortar were crushed, sieved, then reconstituted in the grading (Table 5) specified in ASTM Test for Potential Alkali Reactivity of Cement-Aggregate Combinations (C 227-81). The limestone served as base aggregate. Most of the mortars were prepared using limestone Piece A/B, though a few mortars containing reactive aggregate may have been prepared using limestone Piece K or Piece M. In the reactive mortar mixes, each reactive aggregate material was substituted for the same portion by weight of limestone. Several replacement levels were selected for each aggregate in order to bracket the pessimum proportion. The pessimum proportion of Beltane opal was expected to be approximately 6 percent, based on results of Barneyback (1983); for novaculite, the pessimum proportion was expected to be near 50 percent (McConnell et al, 1947), and for the gneissic granite near 100 percent (Buck, 1983). Replacement levels used for opal were therefore 1, 2, 4, 8, and 12 percent by weight of the total aggregate. For quartzite they were 20, 30, and 50 percent, and the granite was tested only at 100 percent replacement, i.e. with no limestone.

With one exception, mortar bars were prepared according to ASTM Method C 227. The method specifies a flow level rather than water content, and requires one to use whatever water content results in the specified flow level. However, the principal objectives of the present study were to explore the effect of cement phase composition on pore solution composition, and to explore the effect of pore solution composition on expansion. Thus it was decided not to vary the water content. Instead, a single water-to-cement ratio of 0.485, as specified in the ASTM Method C 109, was used in all mortars.

Each mortar batch consisted of 300 g cement, 675 g sand, and 145.5 ml water, and was mixed in an electric mixer

Table 5. Aggregate grading for use in mortars[a].

Sieve Size		Weight
Passing	Retained	(%)
No. 4 (4.75 mm)	No. 8 (2.36 mm)	10
No. 8 (2.36 mm)	No. 16 (1.18 mm)	25
No. 16 (1.18 mm)	No. 30 (600 μm)	25
No. 30 (600 μm)	No. 50 (300 μm)	25
No. 50 (300 μm)	No. 100 (150 μm)	15

[a] From ASTM C 227.

according to the ASTM Standard Method for Mechanical Mixing of Hydraulic Cement Pastes and Mortars of Plastic Consistency (C 305-80). That procedure prescribes the order in which to add the components and the times of mixing; it specifies a rest period of 30 s between initial and final mixing, and a total mixing and standing time of 4 min.

Bars for expansion measurements were prepared from each batch of mortar according to ASTM Method C 227. The specimens were cast in a bar mold by filling the mold with mortar in two layers, tamping to compact each layer and to work mortar around the gage studs. The molds were stored for 24 h over water in a sealed container at room temperature (~22°C). The bars were then demolded, their lengths measured as described below, and stored for expansion studies.

Expansion measurements were made using a length comparator, as described in ASTM Standard Specification for Apparatus for Use in Measurement of Length Change of Hardened Cement Paste, Mortar, and Concrete (C 490-83a). The dial gauge mounted on a stand allows comparison of length to the nearest 0.0001 inch to a reference bar of Tygon-covered invar metal. Two bars were tested for each mortar.

Bars were stored vertically over water using the container[12] and rack (Fig. 4) presently under consideration for ASTM Method C 227 by ASTM Subcommittee C09.02.02. For convenience, all bars were stored at room temperature (~22°C), rather than the 37.8°C temperature specified in ASTM Method C 227 (37.8°C). The inside circumference and lid of each container were lined with blotting paper. On the bottom of the container was placed a layer of rocks (~10

---

[12] Obtained from United States Plastic Corporation, Lima Ohio.

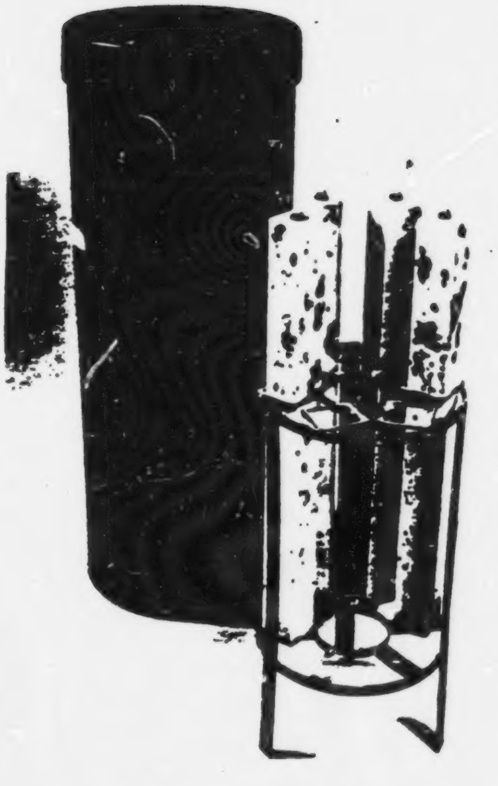

Figure 4. Container and rack used for mortar-bar expansion studies.

BEST COPY AVAILABLE

mm cross section), which was covered with water. The lid was sealed using vinyl tape.

Mortars for expressing pore solutions were prepared in a similar manner, then cast in plastic cylinders[13], 2 in diameter, the lids of which were sealed with vinyl tape. It is important that the specimens for expressing pore solution not be allowed to bleed, and thus cause local variation in water-to-cement ratio, so these specimens were not tamped. The sealed specimens were stored at room temperature until squeezed.

Aggregate Reactions in Model Pore Solutions

The effects of exposing aggregates to model pore solutions were studied to explore the effects of solution alkalinity and of the ratio of aggregate to solution. Aggregate samples were allowed to react in solutions of designated concentrations of potassium and sodium hydroxide. After the specified reaction time, each solution was filtered and analyzed for pH and dissolved silica. The various experimental parameters were selected to duplicate the parameters in the mortar bars, so that the reaction rates observed could be correlated with the observed mortar-bar expansion data. The solution compositions were selected to model the compositions determined for pore solutions expressed from mortars containing only limestone aggregate, prepared using Piece K. Solutions were prepared from reagent-grade potassium hydroxide and sodium hydroxide, using water that had been distilled, deionized, and freshly boiled to prevent unwanted carbonation. The molar ratio of potassium to sodium in all solutions was 3:1, while concentrations of potassium and sodium hydroxide were chosen so as to vary the pH between 13.2 and 14.0 (Table 6).

---

[13] Nalgene vial, 160 ml capacity.

Table 6. Compositions of model pore solutions.

Solution No.	Nominal pH	KOH (mM)	NaOH (mM)
1	13.1	117	39
2	13.4	237	78
3	13.7	473	159
4	13.9	750	250

The aggregates were those used in the mortar-bar expansion tests, limestone (Piece K), opal, quartzite, and gneissic granite, in the same sand-sized grading used for mortar bars. Details of the mixtures are provided in Table 7. The ratios between aggregate and pore solution were selected so as to approximate the ratio in mortar bars between pore solution and the reactive constituent. Various aggregate/solution ratios were studied, corresponding to the various proportions of reactive aggregate in the mortars, as indicated in Table 7.

Specimens were prepared in the following manner. A 5-ml aliquot of solution was added to the aggregate, using the amount listed in Table 7. These were mixed in a polyethylene vial inside a glove box in a nitrogen atmosphere. Vials were stoppered, shaken briefly to wet the aggregate, sealed using vinyl tape, and allowed to react for the desired length of time. After 1, 2,or 3 weeks the samples were filtered using 0.2 μm filters[14], while minimizing the contact of solution with air. The filtered solutions were immediately analyzed for both pH and dissolved silica, using the analytical procedures described below.

Pore Solution Expression

Pore solutions were expressed from hardened mortars using a steel die similar to that employed by Barneyback (1983), which in turn was based on the device used by Longuet et al (1973). The die (Figs. 5 and 6) consists of a cylindrical body, a base plate, and a piston. It is designed so that when the paste or mortar specimen in the cylinder is loaded, some portion of solution in the pores of the hardened cement paste is squeezed out to the cylinder wall, where it moves down to the base plate and out through

---

[14] Millipore.

Table 7. Proportion of each aggregate added to model pore solutions.

Material	Proportion (%)	Amount added to 5 ml solution[a] (g)
Limestone	100	23.19
Opal	2	0.46
	4	0.93
	8	1.86
Quartzite	20	4.64
	30	6.96
	50	12.60
Gneissic granite	100	23.19

[a] Calculated from proportions of aggregate and mixing water in mortar.

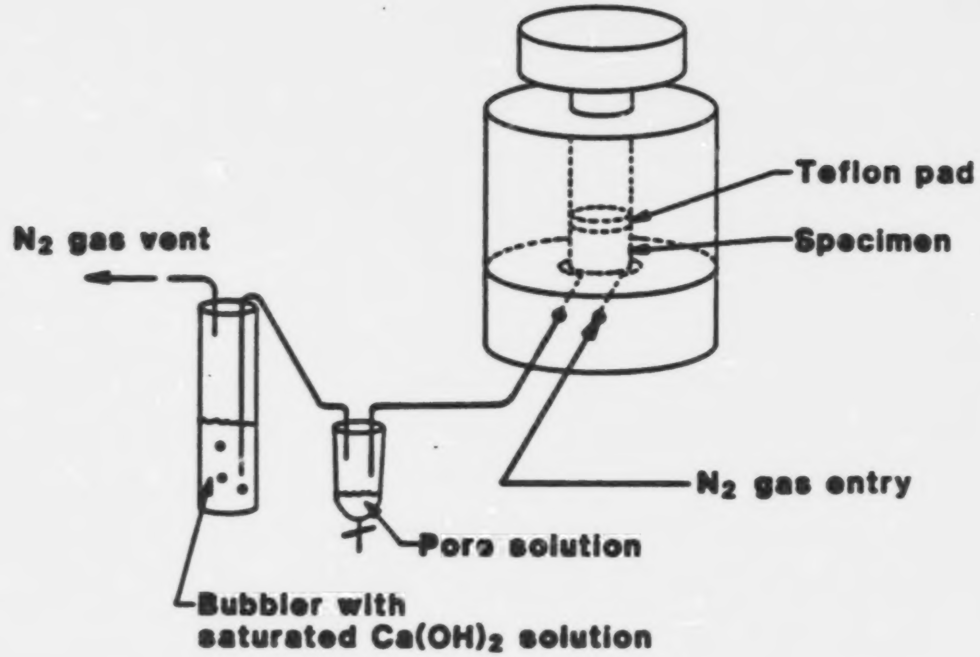
Teflon pad
Specimen
N_2 gas vent
N_2 gas entry
Pore solution
Bubbler with
saturated $Ca(OH)_2$ solution

Figure 5. Diagram of apparatus for expressing and collecting pore solution from hardened mortar.

BEST COPY AVAILABLE

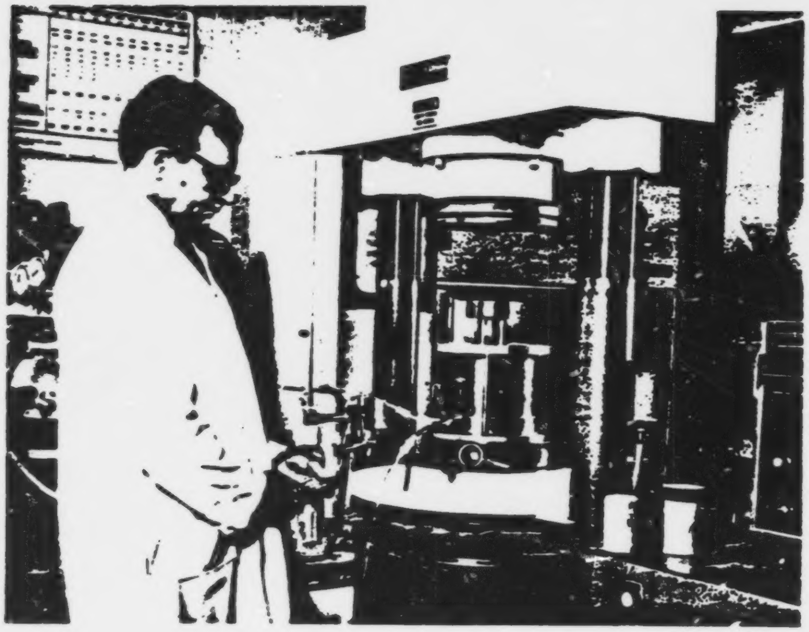

Figure 6. Set-up for expressing and collecting pore solution from hardened mortar.

BEST COPY AVAILABLE

the groove to the collection system. To prevent corrosion of the die by the pore solution, all inside surfaces were sprayed with a mold-release spray[15] prior to placing the specimen in the die. Similarly, a cylindrical Teflon pad (shown in Fig. 5) was inserted above the specimen to protect the bottom of the piston from damage during loading by the mortar and to prevent solution from leaking out the top of the die.

Once assembled, the collection system (including the groove in the base plate) was flushed continuously with nitrogen gas. The gas flow serves to aid in expelling solution out of the die into the collection system and to avoid contamination of the solution by atmospheric carbon dioxide. After passing through the base plate and the collection apparatus, the nitrogen gas was bubbled through a saturated $Ca(OH)_2$ solution, which served to monitor gas flow and to prevent backflow.

Pore solution was expressed by loading the die in compression, using a 1.3 MN capacity testing machine. Expression appeared to be most efficient when the pressure was cycled between an upper pressure of 500 MPa and a lower pressure of 350 MPa, at a rate of approximately 50 MPa per sec. For each specimen, this loading cycle was repeated until no further pore solution was obtained, typically 5 to 10 cycles.

The expressed pore solution was collected in a 10-ml capacity plastic syringe (shown in Fig. 5). The syringe was equipped with tubing in place of the needle, and the tubing was closed using a hemostat clamp. The top of the syringe was sealed with a neoprene stopper through which two tubes were inserted, one an inlet for solution and nitrogen gas from the die and the other an outlet for nitrogen gas to the bubbler. This collection apparatus is considered to improve the system used by Barneyback (1983) in two respects: first, it requires no manipulation of the collection apparatus during expression, freeing the operator to maintain control of the testing machine; and second, the syringe allows convenient estimation of the volume of solution expressed during each loading or unloading cycle.

---

[15] Crown 6075 Dry Film Lubricant and Mold Release Agent, a 20% dispersion of a white, waxy, tetrafluoroethylene polymer in a liquid, freon TF solvent.

As soon as a loading cycle was finished, the pore solution was transferred to a storage container, a 3 ml capacity plastic bag[16] selected to allow transfer of solution without exposure to air (after preliminary tests described in Appendix B). The tubing at the bottom of the syringe was inserted into the bag and unclamped, and the pore solution, aided by the gas flow, would pass from the syringe into the bag. The small plastic bag was quickly squeezed to remove excess air and heat-sealed to close. Later, solution was removed from the sealed bag for analysis, while the bag and syringe were maintained in a nitrogen atmosphere, by puncturing with a syringe needle.

After each expression the pressed mortar was removed and the die cleaned. First, the cylinder of the die was placed on a supporting ring on the platen of the testing machine. The head of the piston was removed, and the piston loaded until both mortar and piston were expelled. The entire die could then be cleaned with tap water, or with 2M HNO_3[17] if necessary. It was then rinsed with ethanol, allowed to dry, and lastly sprayed with the mold release to prevent corrosion during storage.

---

[16] Nalgene Filmware Scintillation System with Heat Sealer.

[17] Nitric acid was selected because it is relatively noncorrosive to electrodeposited chromium (Uhlig, 1948).

Methods Used to Analyze Solutions

The expressed pore solutions, sealed in plastic bags, were stored in a nitrogen atmosphere for later analysis. Within a few days, each solution was sampled and diluted for the various chemical analyses. Two aliquots were secured, one diluted ~1:100 for hydroxide ion titration and for analysis by ion chromatograph (IC), and the other used for silica determination. The dilution procedure (Appendix A) allowed precise determination of the volume of pore solution used without exposure to, and possible contamination by, atmospheric carbon dioxide or by silica glass. Finally, the remaining solution in its plastic bag (and still in the nitrogen atmosphere) was used for pH measurement.

Determination of pH

In order to determine pH or hydroxide ion concentration, a method was required that is precise and accurate over the expected pH range of 13.2 to 13.9. A pH electrode was preferred, because it provides a rapid, convenient method for analysis of a large number of solutions. Furthermore, a pH electrode provides a direct measure of hydroxide ion activity, a parameter considered more relevant to reactivity of the solution than hydroxide ion concentration.

On the other hand, the determination of pH level in pore solutions using a pH electrode has a number of possible sources of error. One concerns the pH response of a glass electrode in highly alkaline concentrated solutions. The response is not perfect; it may produce an error, termed an alkaline error, that depends on the pH, the concentration of each alkali ion, and the temperature. The error serves to reduce the apparent pH. The principal error is due to sodium, while the error due to potassium is smaller (Bates, 1973). Estimates of the expected errors of the particular electrode were provided by the manufacturer (Jackson, 1984) for alkaline solutions at 25°C as follows: the error of a solution whose sodium concentration is 200 mM and whose pH is 13 is less than 0.01 pH units; the error of a solution whose sodium concentration is 500 mM and whose pH is 13 is 0.05 pH units; and the error of a solution whose sodium concentration is 200 mM and whose pH is 14 is 0.5 pH units. As discussed previously, the pH levels of the pore solutions are expected to range between 13.2 and 13.9, the concentration levels of sodium ion are expected to be at or below 300 mM (Barneyback, 1983), and the solutions are expected to be much higher in potassium than sodium. The alkaline error, therefore, is expected to range from less than 0.1 pH unit to as high as 0.5 pH units.

Another possible source of error in the measurement of pH concerns standards for calibration. Accepted analytical procedures for pH determination require that calibration solutions bracket the specimens in pH. In this case bracketing was not possible, since no buffer solution with pH greater than 13 was available, and the highest commercial buffer solution was pH 11.

A third possible source of error in measuring pH is due to the small volumes of pore solution available for the determination. Standard practice for pH determination requires first rinsing the electrode with the unknown solution, so as to precondition the electrode, then immersing the electrode in the solution while it is being continuously stirred. Less than 1.0 ml solution was used for each pH determination. Such small volumes precluded either rinsing the electrode or stirring the solution while the electrode was immersed.

Therefore, preliminary studies were carried out to determine whether analysis of these solutions by pH electrode and calibrating with buffer solutions of pH 7 and 11 would be sufficiently accurate and precise for these experiments. These studies, described in Appendix A, indicated that pH of both the solutions for studying aggregate reaction rate and the pore solutions expressed from hardened mortar could be measured with adequate accuracy using the pH electrode and meter by the procedures described in Appendix A.

Hydroxide

The diluted solutions were analyzed for hydroxide ion concentration using titration. The titration method, described in Appendix A, involved titrating each basic pore solution with hydrochloric acid (HCl) and methyl orange, whose end point is pH ~3.8. The diluted solutions had been stored prior to the titration for a considerable length of time (up to 1 year in plastic, screw-top bottles), and they could no longer be considered free of dissolved carbon dioxide. In a basic solution, dissolved carbon dioxide tends to form HCO_3^- and decrease the apparent pH. By selecting the methyl orange indicator with its acidic end point (below the pK_a of 6.35), HCO_3^- is converted to H_2CO_3, and error due to dissolved carbon dioxide is prevented.

Replicate titrations (Appendix A) indicated that the precision for hydroxide determination of a solution whose hydroxide ion concentration was 8.6 mM, was 0.1 mM.

Potassium, Sodium, Calcium, and Sulfate

The diluted solutions were analyzed for potas-sium, sodium, calcium, and sulfate using an IC[18], a method selected because it provides convenient and rapid analysis. The method, described in more detail in Appendix A, utilized two ion exchange columns, the first a separator column and the second a suppressor column. The separator column captures the particular species (monovalent cation, divalent cation, or anion). The captured ions are then flushed from the separator column into the suppressor column by an eluent solution. The suppressor column removes the eluent species and converts each sample anion to its acid, which is not retarded by the suppressor resin and passes through the detector. Suppressor columns are regenerated automatically after each analysis, so the lifetime of the column is not a factor in the precision or the time allowed for analysis. The ions are detected quantitatively using a conductivity meter. Data are collected and intensities measured by computer[19]. The results include a spectrum (conductivity versus retention time) and the integrated intensity of each peak.

---

[18] Dionex System 12 Analyzer.

As described in Appendix A, preliminary calibrations demonstrated that the IC method provides adequate accuracy and sensitivity for determination of calcium, potassium, sodium, and sulfate. The calibrations demonstrated concentration ranges through which results were linear and indicated analytical precision levels (for specimens diluted 1:100) as follows: for calcium, linear to 0.25 mM with precision ±0.005 mM; for potassium, 13 mM and ±0.08 mM; for sodium, 22 mM and ±0.06 mM; and for sulfate, 1 mM and ±0.05 mM.

Silica

Both the solutions used to study reaction rate of aggregates and the solutions expressed from hardened mortar were analyzed for dissolved silica by a colorimetric determination using a silicate-molybdate-rhodamine B complex. The method is highly sensitive, allowing precise determination of silica in the pore solutions in which concentrations were expected to be very low. However, the sensitivity of the method required substantial dilutions of many of the solutions used to study reaction rate of aggregates, in which silica concentrations much greater than the linear range of the method are found.

---

[19] Nelson Analytical 760 Interface, Nelson 3000 Chromatography System software, and Epson Equity I, an IBM-compatible personal computer.

Determination of silica concentrations at the trace levels expected in the expressed pore solutions required care to avoid contamination. Solutions were prepared using reagent-grade chemicals, and water was freshly re-distilled, then stored in plastic bottles. Solutions (except the HNO_3) were prepared within one week of the analysis. A plastic micro-syringe and needle was used to remove the specified amount of unknown sample from its sealed plastic bag. Solutions for dilution were measured using automatic pipettes[20]. Pyrex glass volumetric flasks were used to prepare solutions of known concentration, but solutions were immediately transferred into polyethylene bottles or vials to avoid contamination by silica.

The procedure used in the present experiments, described in Appendix A, was modified slightly from that used by Taleb (1985), in turn based on the method described by Golkowska and Pszonicki (1973). Both references note the importance of controlling acidity for proper reaction between silica and molybdate and between the silico-molybdate complex and the Rhodamine B dye, and the modifications were selected to facilitate control of pH. Another important parameter is the reaction time, and reaction times for formation of both the silico-molybdate complex and its complex with Rhodamine B were carefully controlled.

As described in Appendix A, preliminary calibrations demonstrated that the colorimetric method provides adequate accuracy and precision for determination of silica in the concentration range up to 2 μM in the diluted specimen, or approximately 50 μM in the starting pore solution.

---

[20] Eppendorf Digital Pipette, 100 to 1000 μL capacity, with disposable, polypropylene tips.

CHAPTER 3

RESULTS AND DISCUSSION

In this third chapter, the various experimental results are presented and discussed. Additional discussions of results as they relate to alkali-silica reaction mechanisms are reserved for the following chapter.

Composition of Materials

Cements

The chemical compositions of the eight cements are listed in Table 8. Their nominal phase compositions, calculated from the chemical compositions using the Bogue equations as described in ASTM C 150, are listed in Table 9.

According to ASTM C 150, cements having alkali contents of less than 0.60 percent (equivalent Na_2O) are designated low alkali cements. Four of the cements used (Cements A through D) have alkali contents far in excess of the 0.60 percent value and are considered to be high-alkali cements. One (Cement F) is borderline in this respect, with a value of 0.62 percent; the other three (Cements E, G, and H) are low-alkali cements.

The relative amounts of K_2O and Na_2O vary, though all cements except Cement H contain more K_2O than Na_2O. Qualitative x-ray diffraction (XRD) analyses were carried out to provide a preliminary indication of whether the selected cements vary as intended in their alkali phases. The analyses, described in greater detail in Appendix C,

Table 8. Chemical compositions of cements (percent).

	A	B	C	D	E	F	G	H
Na_2O	0.36	0.23	0.25	0.30	0.27	0.20	0.20	0.36
MgO	2.41	1.53	3.93	2.27	2.65	1.69	1.10	2.72
Al_2O_3	6.02	6.01	4.91	4.24	3.79	2.80	4.40	4.60
SiO_2	19.60	20.29	20.54	20.29	21.8	22.53	20.54	21.76
SO_3	3.49	2.45	3.41	3.33	2.57	2.30	2.97	2.91
K_2O	1.25	1.05	1.02	0.80	0.44	0.61	0.31	0.26
CaO	62.90	64.83	62.13	64.20	62.9	64.03	65.81	64.43
Fe_2O_3	2.06	2.40	1.79	2.61	3.38	4.03	2.50	1.25
LOI	0.56	0.72	1.26	1.19	1.60	1.74	1.15	1.30
TOTAL	98.65	99.51	99.24	99.23	99.50	99.93	98.98	99.59

Table 9. Phase compositions and other parameters, calculated from chemical compositions of the cements (percent)[a].

	A	B	C	D	E	F	G	H
C_3S	54	59	52	65	52	58	70	56
C_2S	16	14	20	9	23	21	6	20
C_3A	12	12	10	7	4	1	7	10
C_4AF	6	7	5	8	10	12	8	4
$CaSO_4$	6	4	6	6	4	4	5	5
Total alkali (equivalent Na_2O)	1.22	0.95	0.95	0.85	0.57	0.62	0.41	0.54

[a] Calculated according to ASTM C 150.

allow identification of specific, alkali-containing phases. For example, the alkali sulfate phases, i.e. K_2SO_4, $(K,Na)_2SO_4$, and $K_2Ca_2(SO_4)_3$, are readily identifiable. Other possible alkali-containing phases are the various principal clinker phases, particularly C_3A and C_2S. When these clinker phases contain sufficient alkali levels, their crystal structures are modified. Crystal modifications that may be caused by alkali and that can be identified using XRD are the orthorhombic modification of C_3A, and α- or α'-C_2S.

C_3A typically occurs as a cubic or an orthorhombic phase. While cubic C_3A may contain some Na_2O or K_2O in its crystal structure, it is generally agreed that higher levels of alkali are associated with the orthorhombic structure (for example, see Regourd, 1983). One can readily distinguish between the cubic and orthorhombic phases, even if both are present in the same cement.

High levels of alkali may stabilize α- or α'-modifications of C_2S, though it is not clear whether these modifications necessarily indicate high concentrations of alkali. By XRD analysis, one can identify a phase that is either α- or α'-C_2S in a KOH-sugar extraction residue, but cannot differentiate between the two phases. It appears, however, that the presence of α-C_2S is highly unlikely in a production clinker, and that α'-C_2S is a much more common constituent (Gies and Knöfel, 1986).

The existence of specific alkali-bearing phases in the cements was determined by qualitative analysis of the XRD patterns of each cement. Patterns were collected of each unextracted cement, of the residue after extraction of each ignited cement in a salicylic acid-methanol solution, and of the residue after extraction of each cement in an aqueous KOH-sugar solution (Appendix C). These patterns were analyzed to identify the principal alkali-bearing phases in each cement.

Results of the XRD analysis (Table 10) indicate that the predominant alkali phases vary considerably among the eight cements. While each of the high-alkali cements (A through D) contains some form of alkali sulfate, the predominant alkali-bearing phase is orthorhombic C_3A in Cement B, $K_2Ca_2(SO_4)_3$ in Cement C, and K_2SO_4 in Cements A and D. Thus these cements vary somewhat in their distribution of alkali among the clinker phases, but none contains α'-C_2S as the predominant alkali-bearing phase. In order to include a cement whose principal alkali-bearing phase is α'-C_2S, it was necessary to include cements lower in alkali level, even though the mortars prepared from them may not expand appreciably. In Cement E, α'-C_2S is the predominant alkali-bearing phase. In the other low-alkali or borderline cements, the predominant alkali-bearing phases are orthorhombic C_3A (Cement H), $K_2Ca_2(SO_4)_3$ (Cement G), and K_2SO_4 (Cement F). Thus the eight cements selected for this study vary in their distribution of alkalies among the cement phases, but four low-alkali or borderline cements were needed to achieve this desired variation.

Alkali levels determined after various chemical extractions were used to provide a more quantitative indication of the distributions of alkali among the cement phases. However, some assumptions were necessary to relate results of the chemical analyses to the distributions of alkalies among cement phases. For example, the alkali soluble in the water extraction are expected to derive primarily from alkali sulfate phases, K_2SO_4, $(K,Na)_2SO_4$, and $K_2Ca_2(SO_4)_3$ (Pollitt and Brown, 1969, and Osbaeck, 1984). The alkalies found in residues after salicylic acid-methanol extraction derive both from alkali sulfates and from calcium aluminate and calcium aluminoferrite phases; of these, most is expected to be derived from C_3A (Jawed and Skalny, 1977). Finally, the alkalies in the residues after KOH-sugar

Table 10. Principal alkali phases determined by XRD.

Cement	Alkali phases
A	largely K_2SO_4 some $K_2Ca_2(SO_4)_3$ some orthorhombic C_3A some α'-C_2S
B	largely orthorhombic C_3A some K_2SO_4 some α'-C_2S
C	predominantly $K_2CA_2(SO_4)_3$
D	predominantly K_2SO_4
E	largely α'-C_2S some K_2SO_4 some $K_2Ca_2(SO_4)_3$
F	some K_2SO_4 some $K_2Ca_2(SO_4)_3$ some α'-C_2S
G	some $K_2Ca_2(SO_4)_3$ some orthorhombic C_3A some α'-C_2S
H	largely orthorhombic C_3A

extraction derive from the calcium silicate phases, of which most is probably derived from C_2S (Jawed and Skalny, 1977).

As discussed previously, identification of ettringite in extraction residues raised the concern that alkalies determined after a 10-min water extraction, as specified in ASTM C 114, were derived not only from the sulfate phases, but also in part from C_3A. Therefore, alkalies were determined after shorter extraction times to assure that measured "water-soluble" alkalies were derived more nearly from the alkali sulfate phases alone. Table 11 lists concentrations of alkalies determined after extraction in water for 5 s, 1 min, or 10 min. It appears from these results that the alkali dissolved during the 5-s extraction are generally equivalent to the alkali dissolved during the 1-min extraction, but not in all cases to the 10-min extraction. In particular, higher levels of alkali were determined from the 10-min extraction than from the 1-min extraction of Cement A, from which extra Na_2O was found in the longer extraction, and Cements B and H, from which extra K_2O was found. Similar results were reported by Osbaeck (1984), who noted discrepancies between water-soluble alkalies and the calculated levels of alkali present as sulfate phases, and attributed the discrepancies to partial dissolution of alkali-containing C_3A. In the present work, it was thus decided to estimate the levels of alkali derived from alkali sulfate and calcium langbeinite using the 1-min extraction results, rather than the 10-min extraction results specified in ASTM C 114.

The distributions of sodium and potassium among the cement phases are presented in Tables 12 and 13, and in Figs. 7 and 8. These results were used in conjunction with the qualitative XRD results to provide quantitative estimates of the specific alkali distributions present. By combining these results, it was concluded that the source of most alkali in Cements A and C is the alkali sulfate phases

Table 11. Levels of alkali dissolved during water extraction of various durations (percent)[a].

	K_2O			Na_2O		
Cement	5 sec	1 min	10 min	5 sec	1 min	10 min
A	1.26	1.21	1.26	0.24	0.22	0.39
B	0.54	0.55	0.61	0.07	0.02	0.08
C	0.87	0.96	0.96	0.16	0.13	0.14
D	0.58	0.63	0.65	0.05	0.01	0.06
E	0.14	0.15	0.16	0.04	0.03	0.08
F	0.26	0.30	0.28	0.05	0.00	-0.11
G	0.22	0.20	0.22	0.02	-0.02	0.03
H	0.06	0.08	0.15	0.00	0.06	0.07

[a] Negative results are attributed to analytical error.

Table 12. Results of sodium distributions among various cement phases (percent)[a].

Cement	Alkali Sulfates[b]	Calcium Aluminate and Aluminoferrite[c]	Calcium Silicates[d]
A	0.24	-0.02	0.14
B	0.07	-0.03	0.20
C	0.16	-0.10	0.19
D	0.05	0.00	0.06
E	0.04	0.00	0.17
F	0.05	-0.10	0.06
G	0.02	0.05	0.07
H	0.00	0.07	0.25

[a] Determined by AA analysis; negative results are attributed to analytical error.

[b] Soluble in a 1-min water extraction.

[c] Determined by difference between total alkali and alkali in the residue after salicylic acid/methanol extraction.

[d] Determined by difference between the alkali insoluble in salicylic acid/methanol and in water.

Table 13. Results of potassium distributions among various cement phases (percent)[a].

Cement	Alkali Sulfates[b]	Calcium Aluminate and Aluminoferrite[c]	Calcium Silicates[d]
A	1.26	-0.03	0.06
B	0.54	0.25	0.26
C	0.87	0.06	0.07
D	0.58	0.10	0.56
E	0.14	0.08	0.21
F	0.26	0.05	0.33
G	0.22	0.07	0.21
H	0.06	0.14	0.15

[a] Determined by AA analysis; negative results are attributed to analytical error.

[b] Soluble in a 1-min water extraction.

[c] Determined by difference between total alkali and alkali in the residue after salicylic acid/methanol extraction.

[d] Determined by difference between the alkali insoluble in salicylic acid/methanol and in water.

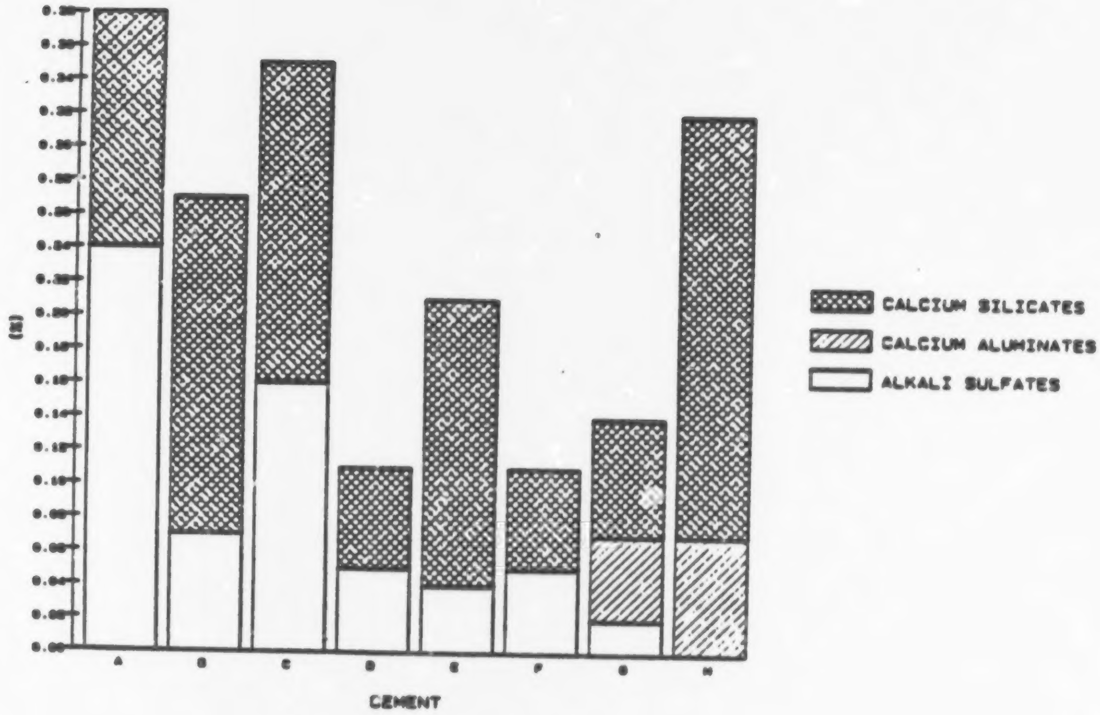

Figure 7. Results of sodium distributions determined by chemical analysis of cements after various chemical extractions.

BEST COPY AVAILABLE

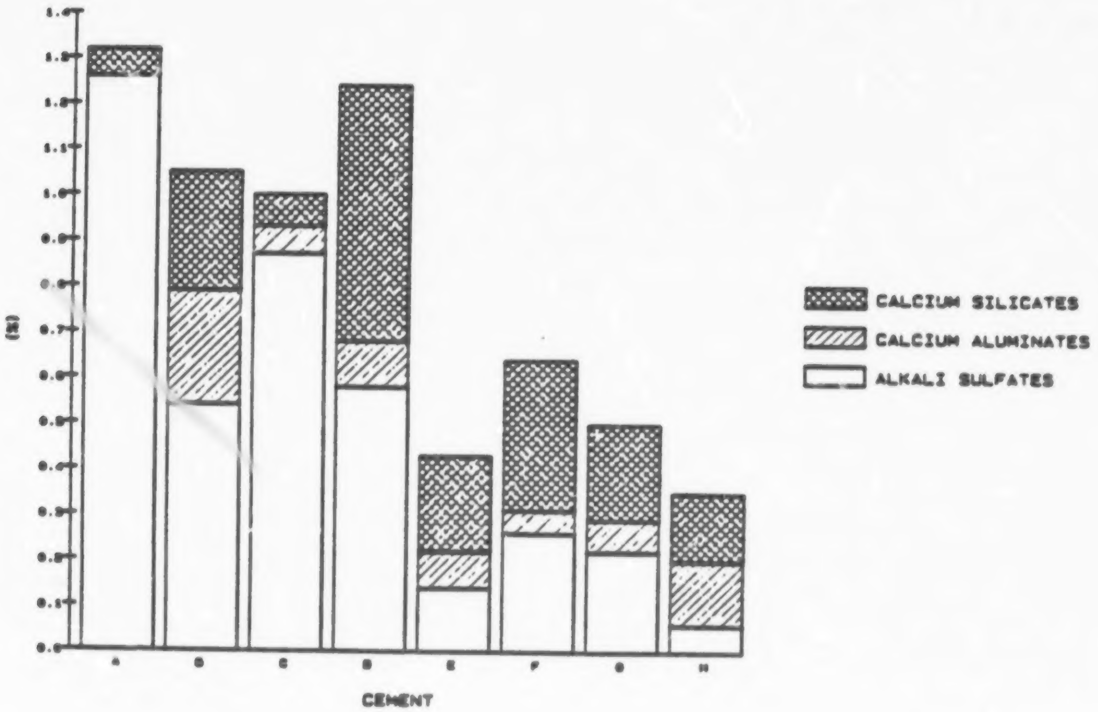

Figure 8. Results of potassium distributions determined by chemical analysis of cements after various chemical extractions.

BEST COPY AVAILABLE

present. Cements B through D derive the bulk of their alkali more or less equally from the alkali sulfate and the calcium silicate phases (though no α'-C_2S was observed in the XRD pattern of Cement D). Significantly less of the alkali present is derived from alkali sulfate phases in the four lower alkali cements. Cements E, F, and G all derive alkali in approximately equal proportions from alkali sulfate phases and from C_2S. Cement H is unique in that it derives alkali principally from the calcium silicate phases (though no α'-C_2S was observed in the XRD pattern).

In some cements, the distributions of sodium among the various phases are similar to the distributions of potassium. In Cement A, both sodium and potassium are heavily concentrated in the alkali sulfates, while in Cements D, E, and F, both sodium and potassium are alike concentrated in alkali sulfates and calcium silicates. In many cements, however, sodium and potassium differ in their distributions among the cement phases. In Cement B the sodium is concentrated in the calcium aluminates, while the potassium is concentrated in the alkali sulfates. In Cement C, the sodium is split between the alkali sulfates and the calcium silicates, while the potassium is concentrated only in the alkali sulfates. In Cement G, most sodium is split between the calcium aluminates and the calcium silicates, while most potassium is split between the alkali sulfates and the calcium silicates. Finally in Cement H, sodium is concentrated in the calcium silicates, and potassium is split between the calcium aluminates and calcium silicates.

The qualitative alkali distributions determined using XRD analysis agreed reasonably well with the quantitative distributions determined using chemical analysis. Table 10 shows a comparison of these distributions. The cements were ranked according to the proportion of alkali as determined by chemical analysis, and according to the qualitative assessment for each phase or group of phases as determined by the XRD analysis. The rankings were generally the same for both categories.

Aggregates

The aggregate materials used in this study were analyzed both for bulk chemical composition and for phase composition. Bulk chemical compositions are listed in Table 14.

Two limestone pieces were analyzed separately. They were low in SiO_2, and thus are not expected to contain substantial amounts of reactive silica. Of the two pieces, one (Piece C) contains a high level of MgO, suggesting that it may contain appreciable dolomite, $CaMg(CO_3)_2$. Since dolomite may be reactive to alkali (Ramachandran et al, 1981), Piece C was rejected as a nonreactive aggregate for these studies, and Piece A/B was used for most mortars for expansion studies.

Both the opal and the quartzite aggregate materials were largely SiO_2, though the opal contained in addition a few percent of material lost during ignition, presumably water. The granite composition falls within the range typical for granite (Travis, 1955); its composition is lower in SiO_2 and higher in all other constituents than the opal and quartzite.

Phase compositions of the aggregates were determined from XRD patterns. Two pieces of limestone were analyzed, Piece K and Piece M. Piece K (Fig. 9) consists of calcite and a considerable portion of dolomite. Before its dolomite content was realized, Piece K was used in studies of reaction kinetics, in mortars prepared for expressing pore solution, and possibly in a few mortars for expansion studies. Piece M (Fig. 10), largely free of dolomite, was used in a few mortars for expansion studies. Thus most or all expansion studies were carried out using limestone that was low in dolomite, but the same cannot be said of the

Table 14. Chemical compositions of aggregate materials (percent).

	Limestone[a] A/B	Limestone[a] C	Opal[b]	Quartzite[a]	Granite[a]
Na_2O	<0.1	<0.1	0.14	<0.01	2.81
MgO	1.37	20.32	0.28	0.12	1.30
Al_2O_3	1.13	0.90	3.91	<0.01	12.59
SiO_2	2.79	1.82	87.96	98.94	70.78
SO_3	0.15	0.17	Nil	<0.1	0.04
K_2O	0.37	0.24	0.26	0.19	3.62
CaO	51.77	31.11	0.56	0.25	1.99
Fe_2O_3	0.21	0.47	0.29	0.30	4.97
LOI	nd[c]	nd	6.54	nd	0.37

[a] Determined by X-ray fluorescence analysis.

[b] From Barneyback (1983).

[c] Not determined.

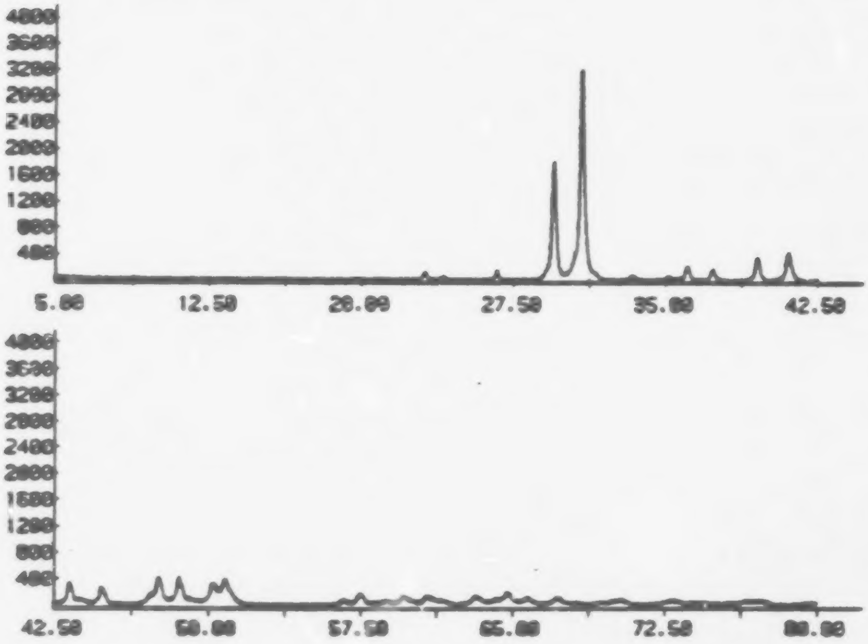

Figure 9. XRD pattern of limestone Piece K, rich in dolomite.

BEST COPY AVAILABLE

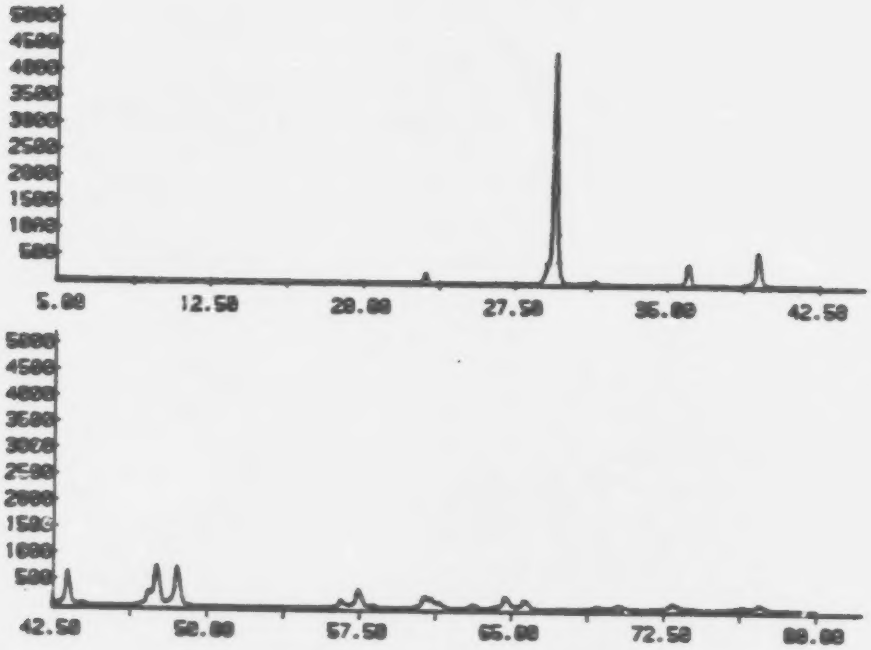

Figure 10. XRD pattern of limestone Piece M, with little dolomite.

BEST COPY AVAILABLE

studies of reaction kinetics and of pore solution composition. It is not known to what extent the dolomite affected results of these studies.

The Beltane opal rock (Fig. 11) consists of a glassy phase, cristobalite, quartz, tridymite, and kaolinite. These are the same phases reported by Gutteridge and Hobbs (1980). The quartzite (Fig. 12) contains quartz as the only crystalline constituent. The granite (Fig. 13) contains quartz, feldspars (orthoclase feldspar and plagioclase feldspar), and mica.

Quick Chemical Test for Aggregate Reactivity

The results of the quick chemical test for potential aggregate reactivity (Table 15) indicate some of the aggregates are classed as "deleterious" according to the parameters specified in this test. When results are plotted in the standard form of reduction in hydroxide ion concentration versus silica in solution (Fig. 14), the opal rock falls within the deleterious region. The quartzite and granite are inside the deleterious region, though very near the boundary as presently defined. The limestone falls within the region considered innocuous. The opal produced both a high reduction in alkalinity and a high concentration of dissolved silica, not surprising in view of its known reactivity.

The results for the opal rock (1.00 M dissolved silica and 0.28 M reduction in alkalinity) are similar to results of Gutteridge and Hobbs (1980), who reported 1.20 M dissolved silica and 0.23 M reduction in alkalinity. In contrast, the quartzite produced no significant reduction in alkalinity, but a high level of dissolved silica, 0.19 M. McConnell et al (1947) reported in the same test that novaculite produced 1.68% dissolved silica, equivalent to 0.28 M, slightly higher than the present results.

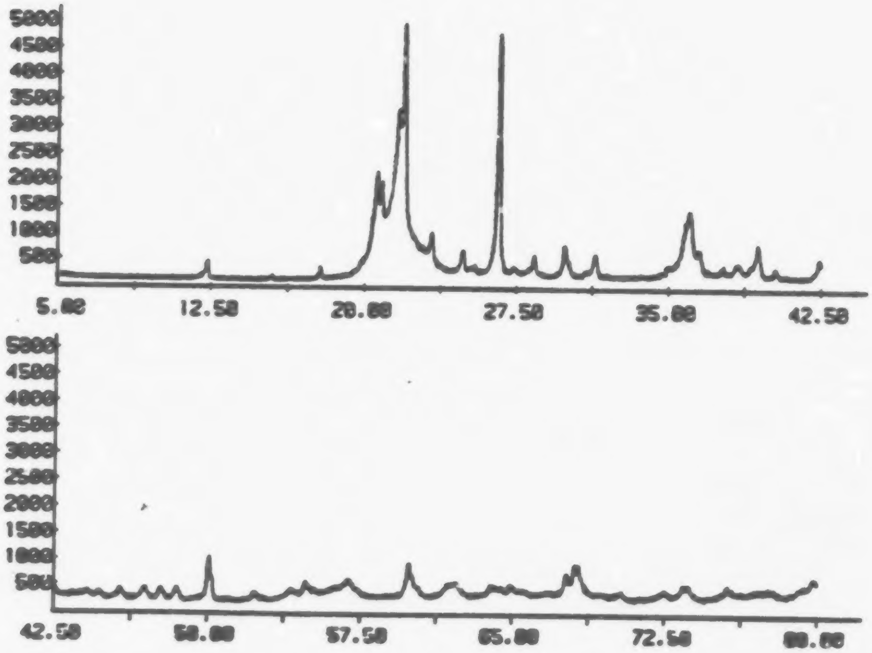

Figure 11. XRD pattern of opal.

BEST COPY AVAILABLE

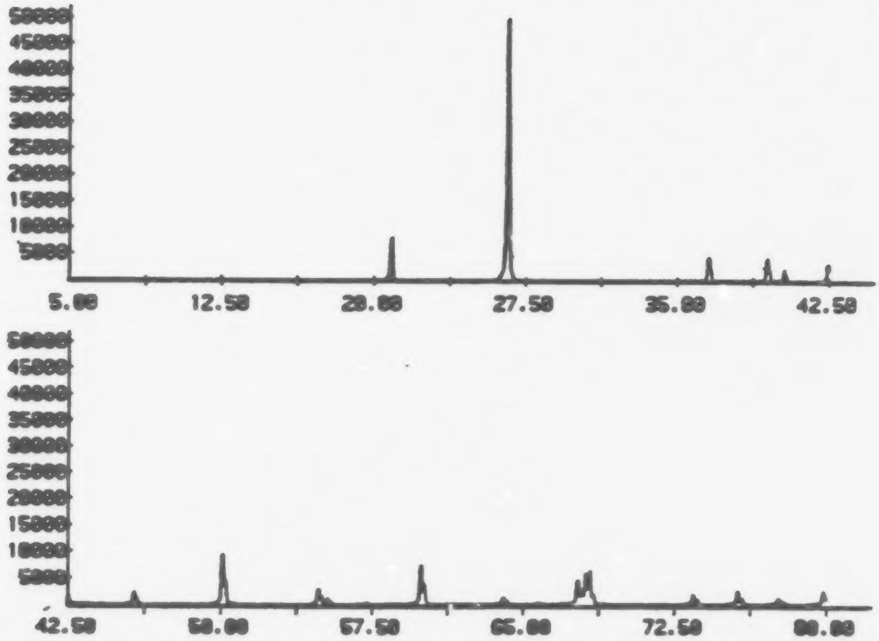

Figure 12. XRD pattern of quartzite.

BEST COPY AVAILABLE

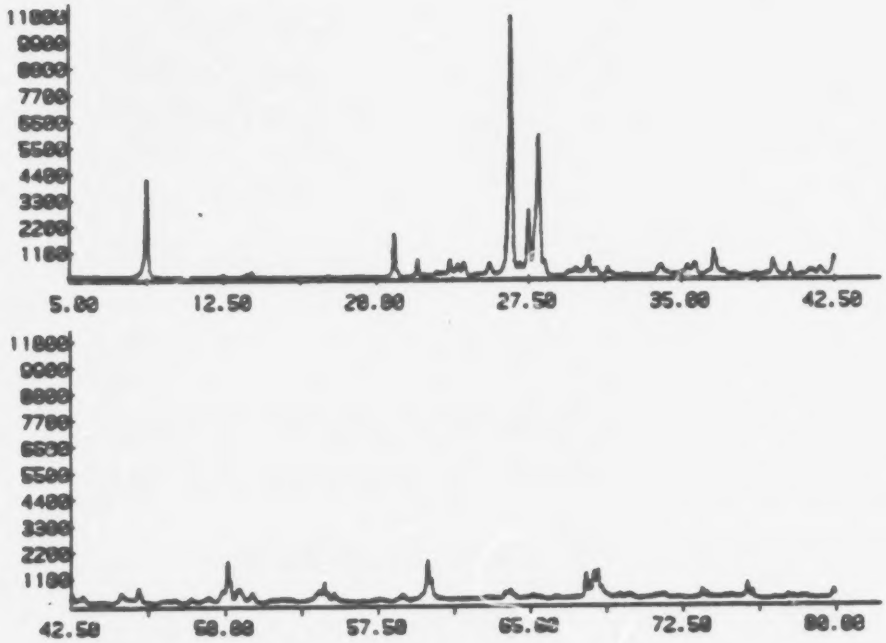

Figure 13. XRD pattern of granite.

BEST COPY AVAILABLE

Table 15. Results of quick chemical test for aggregate reactivity.

Material	Dissolved silica[a] S_c (M)	Reduction in alkalinity[a] R_c (M)
Blank	0.007	0.000
Opal	0.998	0.283
Quartzite	0.186	-0.074
Granite	0.014	-0.084
Limestone	0.008	0.336

[a] Average of three specimens.

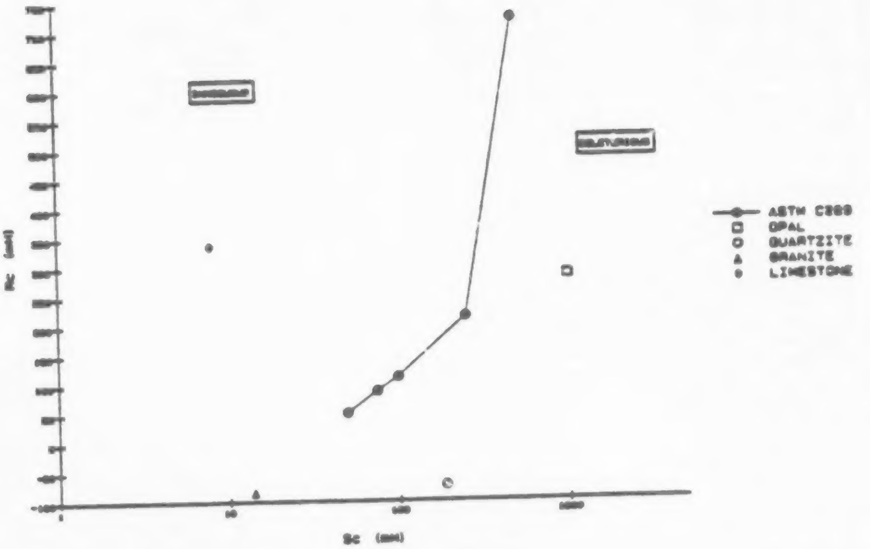

Figure 14. Results of quick chemical test, showing the curve that separates the innocuous and the deleterious regions according to ASTM C 289.

BEST COPY AVAILABLE

Although the limestone (Piece A/B) falls within the region considered innocuous, it surprisingly produced a high reduction in alkalinity, 0.3 M. A few similar cases of limestone causing reduction in alkalinity have been reported. Heck (1983) described a limestone rock that produced a reduction in alkalinity in the quick chemical test, but the level was only 16 mM, nowhere near as high as the level of 336 mM found here. He also concluded that the limestone appeared to have an inhibiting effect on alkali-silica reaction compared to a silica sand. In a review of the quick chemical test, Grattan-Bellew (1983) noted that some carbonates react with NaOH to reduce its alkalinity. Buck and Dolch (1966) reported a reaction of some non-dolomite limestones with hydrating cement, producing $Ca(OH)_2$, a reaction that might be expected to reduce the pore solution pH because it removes hydroxide ions from solution. From these references, it appears that the high reduction in alkalinity of limestone in the present study may not be an isolated phenomenon. Presumably it was caused by reaction of silica-containing phases or of dolomite with the sodium hydroxide solution, although analysis of the limestone used in the quick-chemical test (Table 14) showed only 2 to 3% SiO_2 and only 1 to 2% MgO.

Mortar Bar Expansion

Expansion data for each mortar, displayed as the average of the two bars tested, are shown here (Figs. 15 through 31) and listed in Appendix D; the final expansion levels (at ages up to 3 years) are listed in Table 16. The expansion curves seem to follow generally similar patterns for all cements and aggregates. In each case, expansion begins immediately, with no induction period apparent. The expansion rate during this initial period (the first few weeks) is the most rapid stage of expansion regardless of the aggregate type; not unexpectedly, it is much more rapid

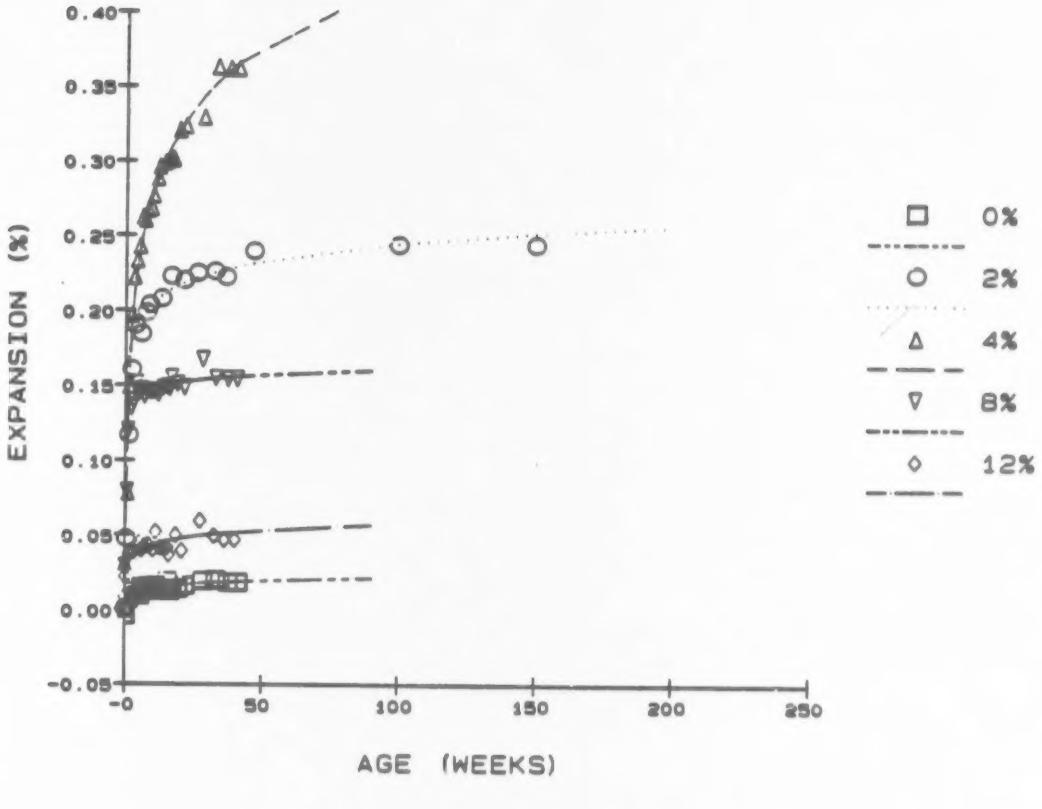

Figure 15. Expansion of mortar bars prepared with Cement A and various levels of opal.

BEST COPY AVAILABLE

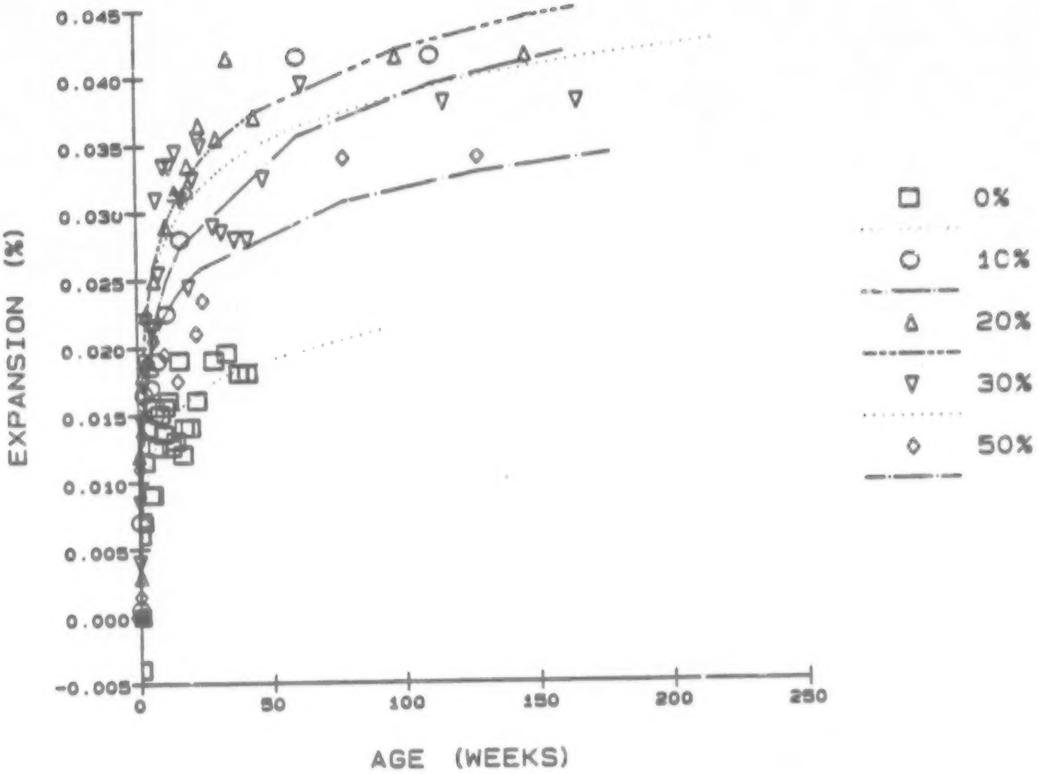

Figure 16. Expansion of mortar bars prepared with Cement A and various levels of quartzite.

BEST COPY AVAILABLE

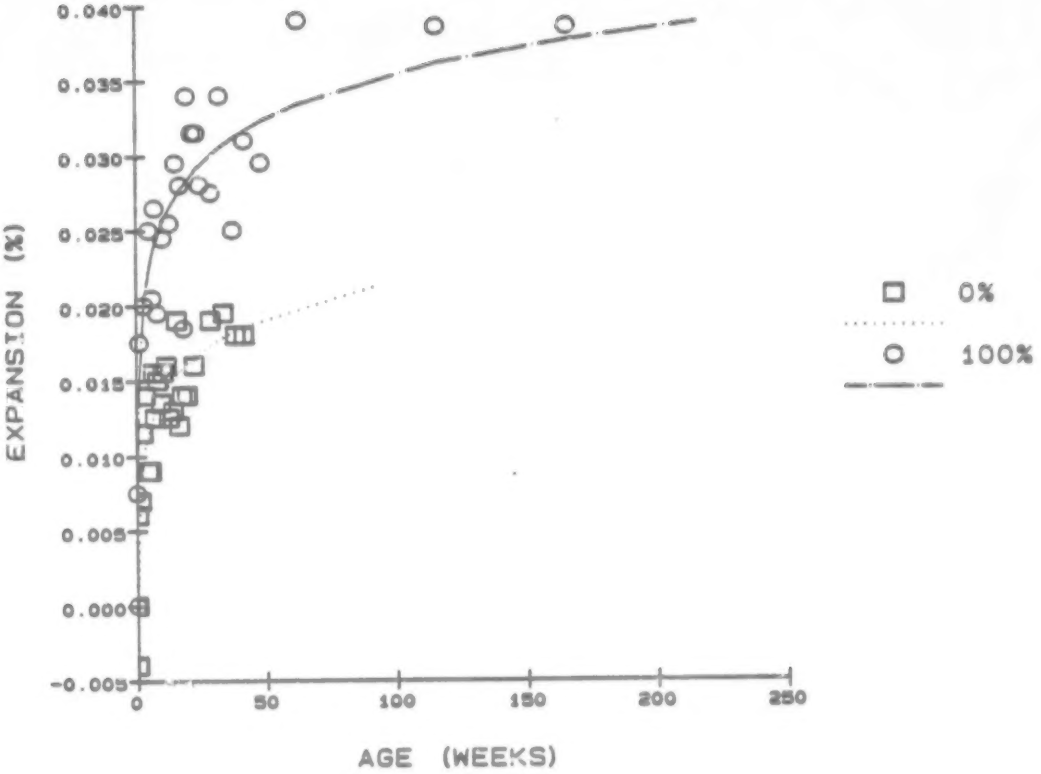

Figure 17. Expansion of mortar bars prepared with Cement A, with and without gneissic granite.

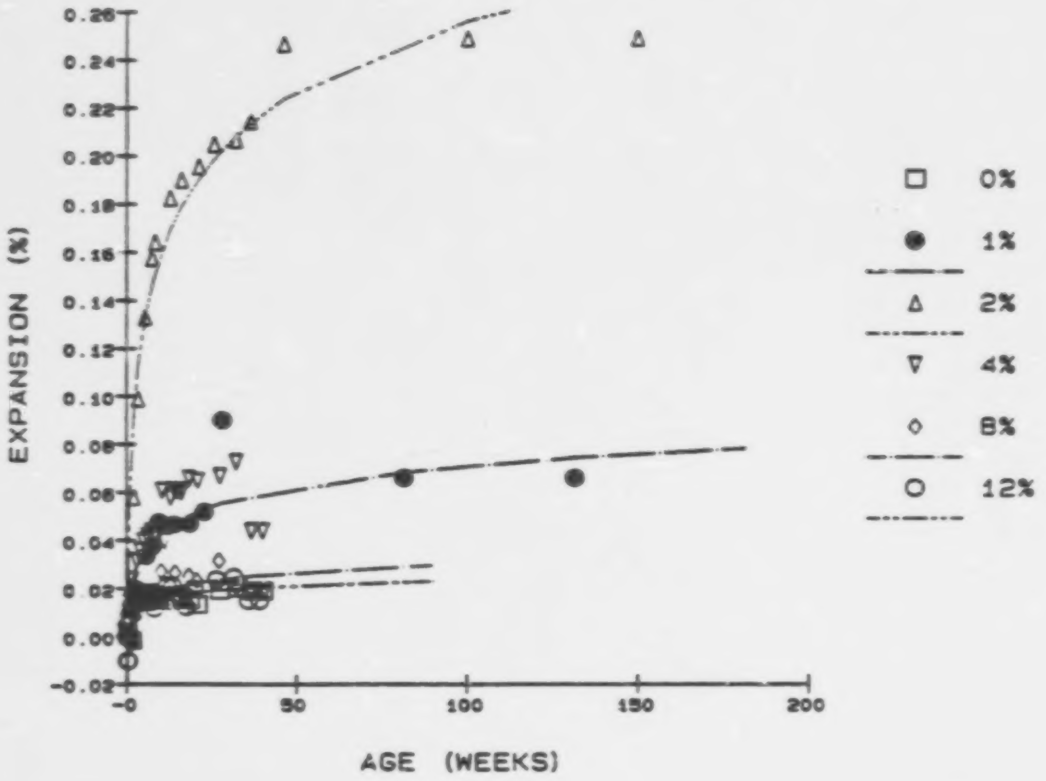

Figure 18. Expansion of mortar bars prepared with Cement B and various levels of opal.

BEST COPY AVAILABLE

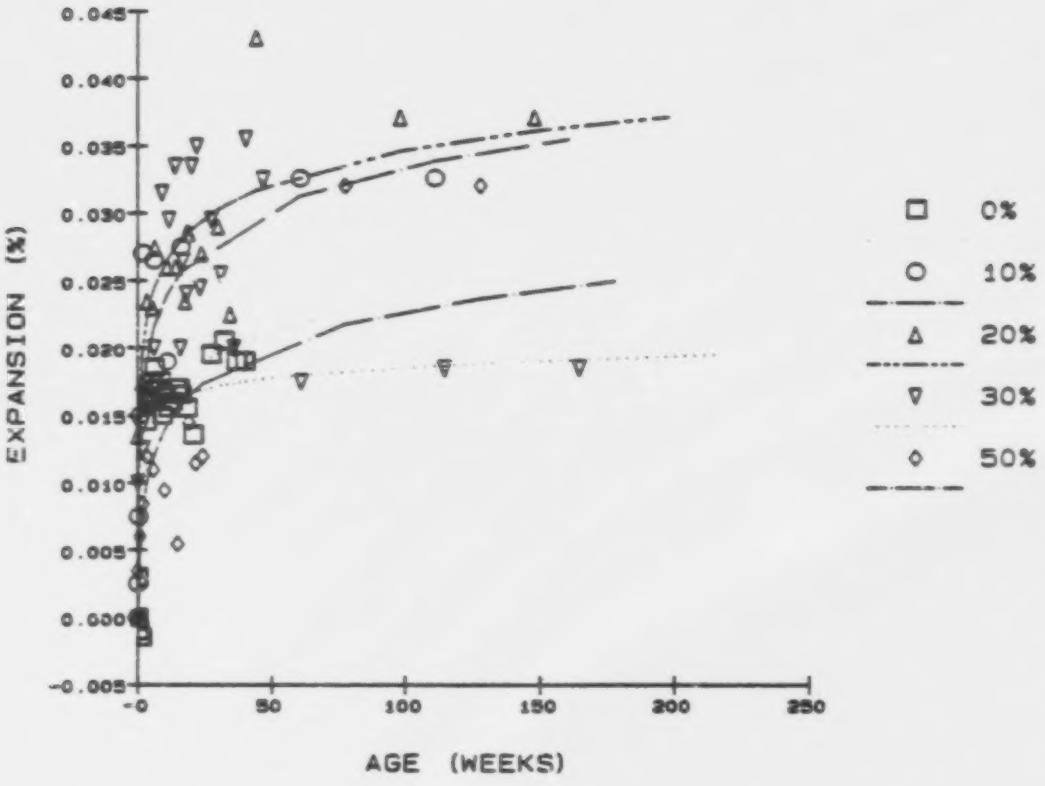

Figure 19. Expansion of mortar bars prepared with Cement B and various levels of quartzite.

BEST COPY AVAILABLE

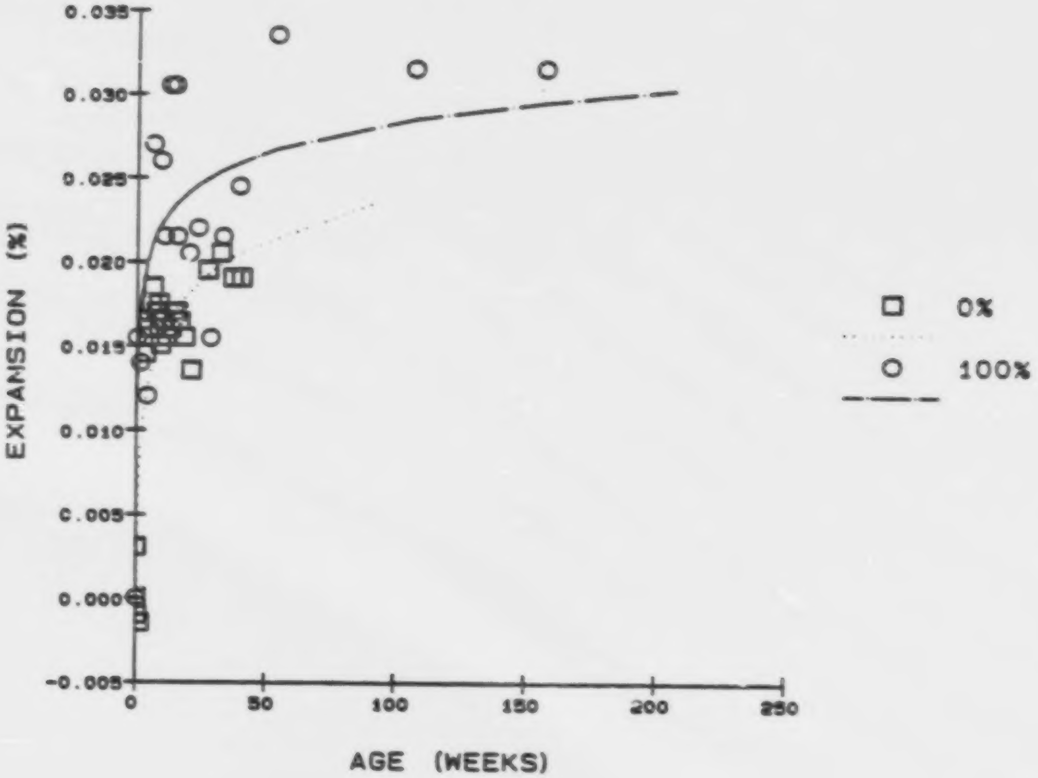

Figure 20. Expansion of mortar bars prepared with Cement B, with and without gneissic granite.

BEST COPY AVAILABLE

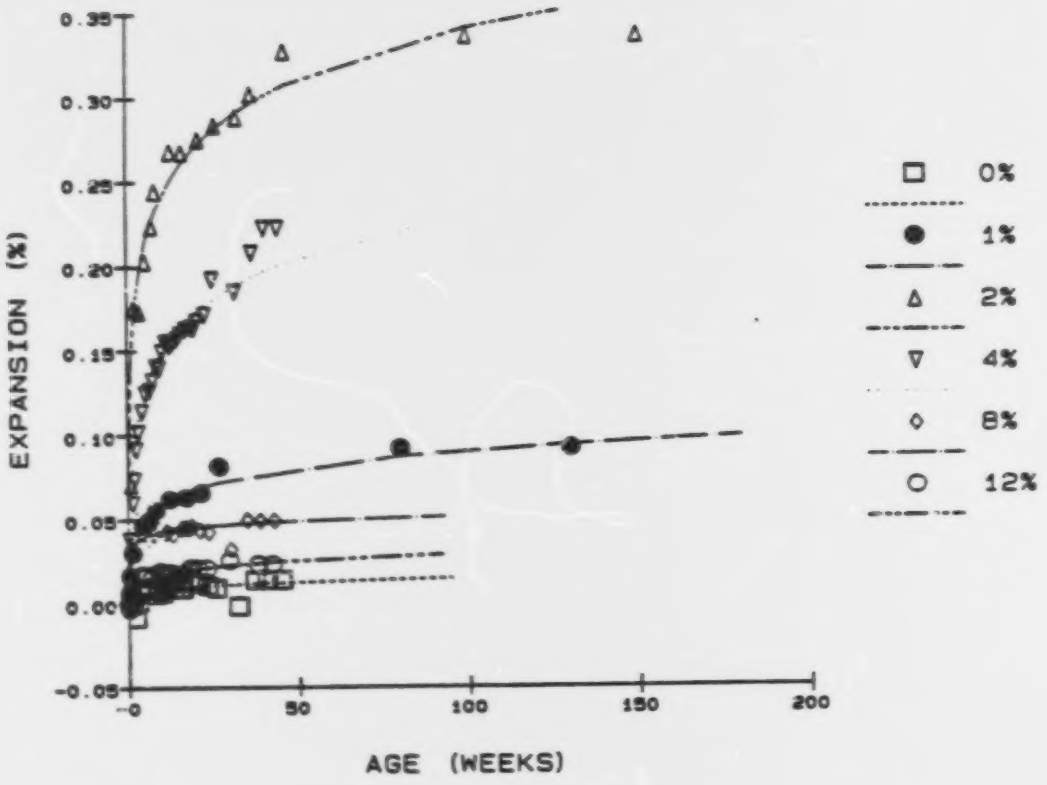

Figure 21. Expansion of mortar bars prepared with Cement C and various levels of opal.

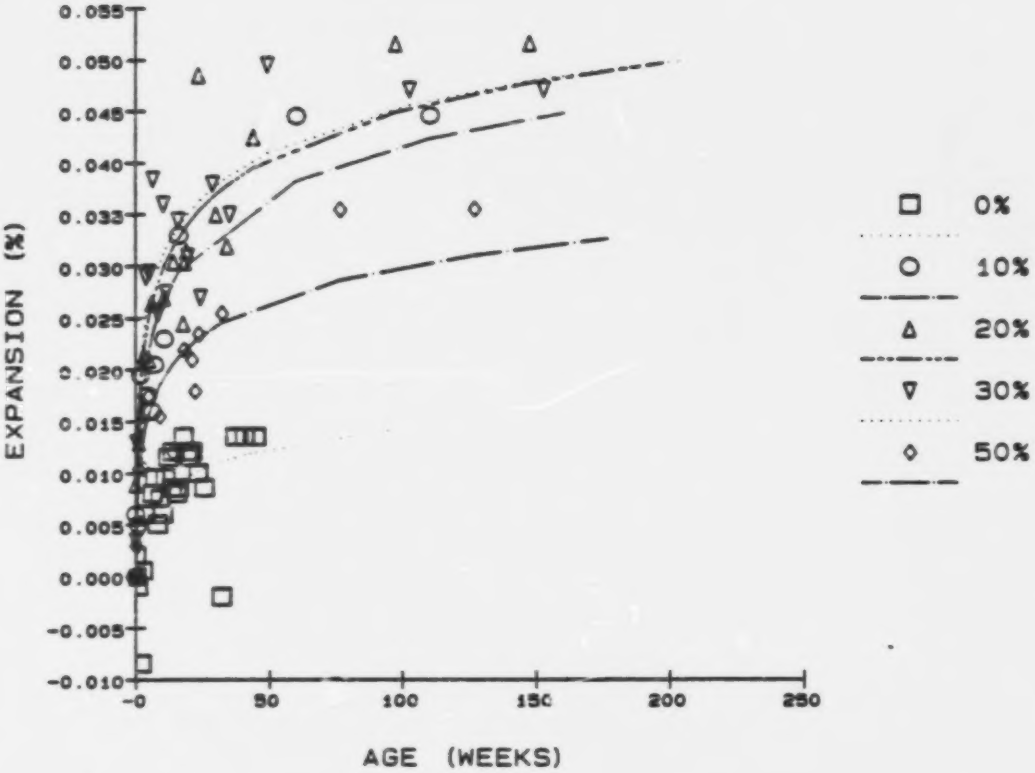

Figure 22. Expansion of mortar bars prepared with Cement C and various levels of quartzite.

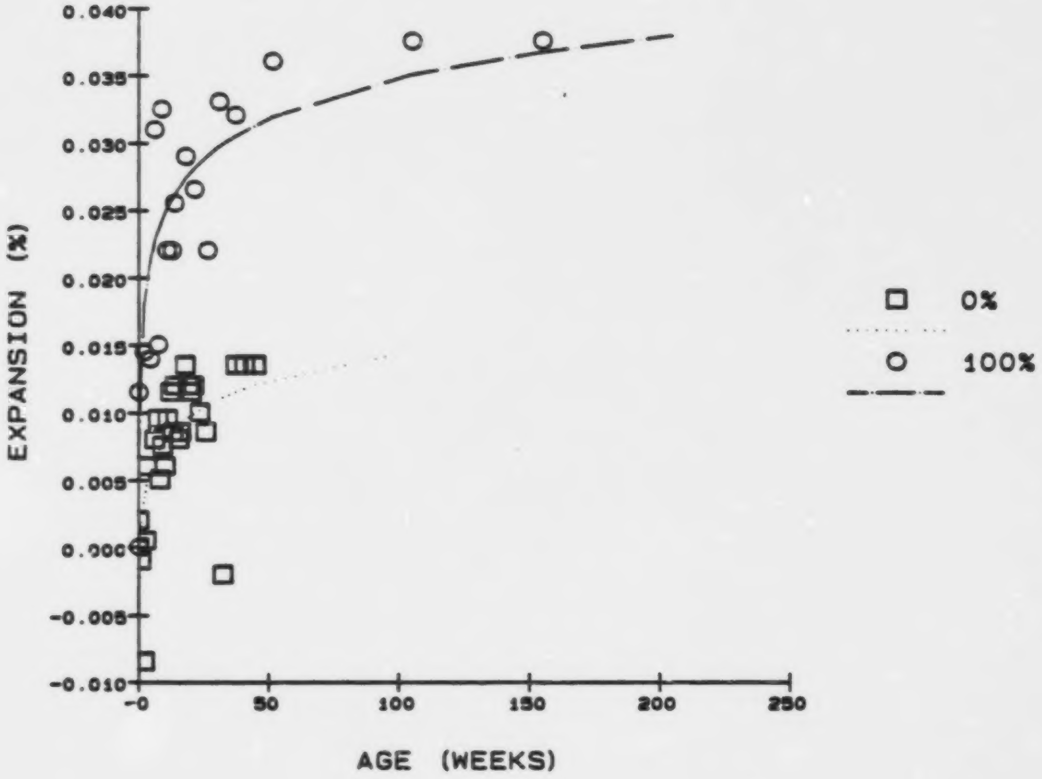

Figure 23. Expansion of mortar bars prepared with Cement C, with and without greissic granite.

BEST COPY AVAILABLE

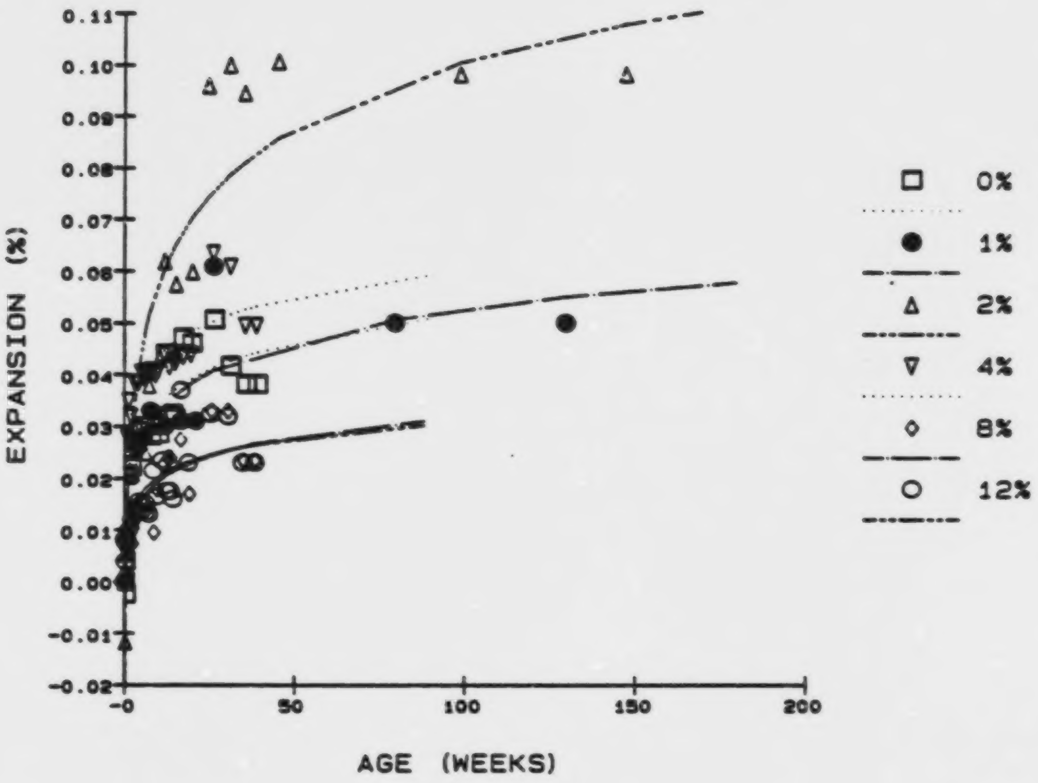

Figure 24. Expansion of mortar bars prepared with Cement D and various levels of opal.

BEST COPY AVAILABLE

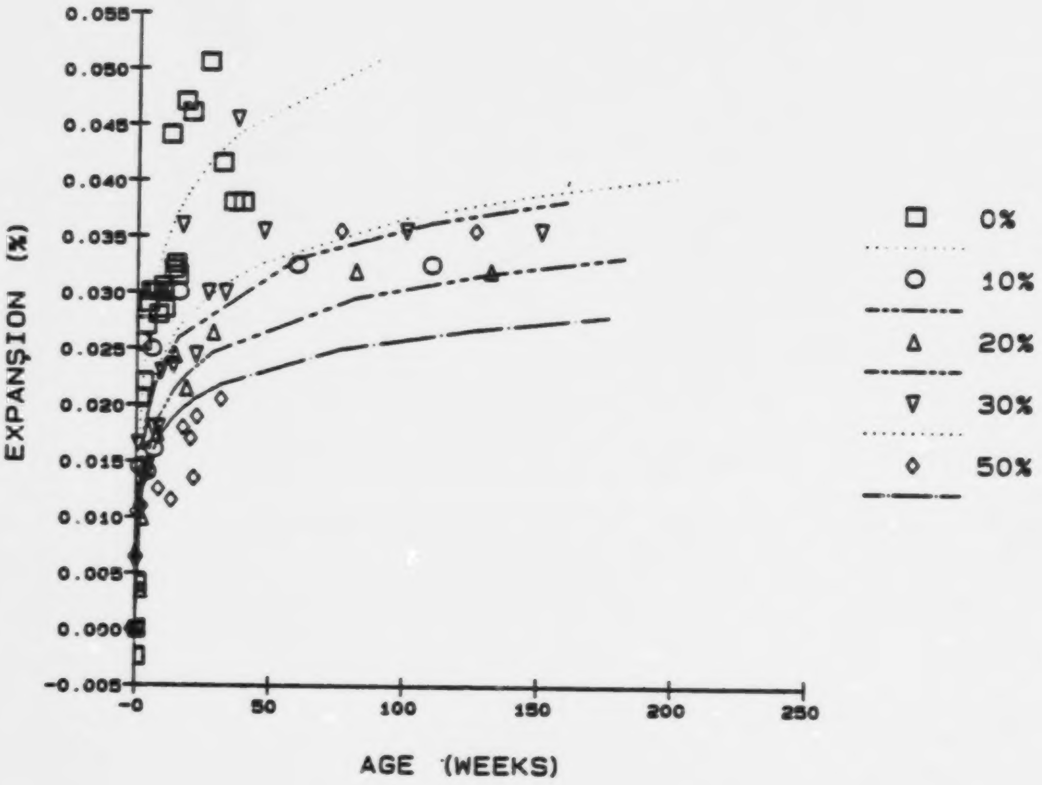

Figure 25. Expansion of mortar bars prepared with Cement D and various levels of quartzite.

BEST COPY AVAILABLE

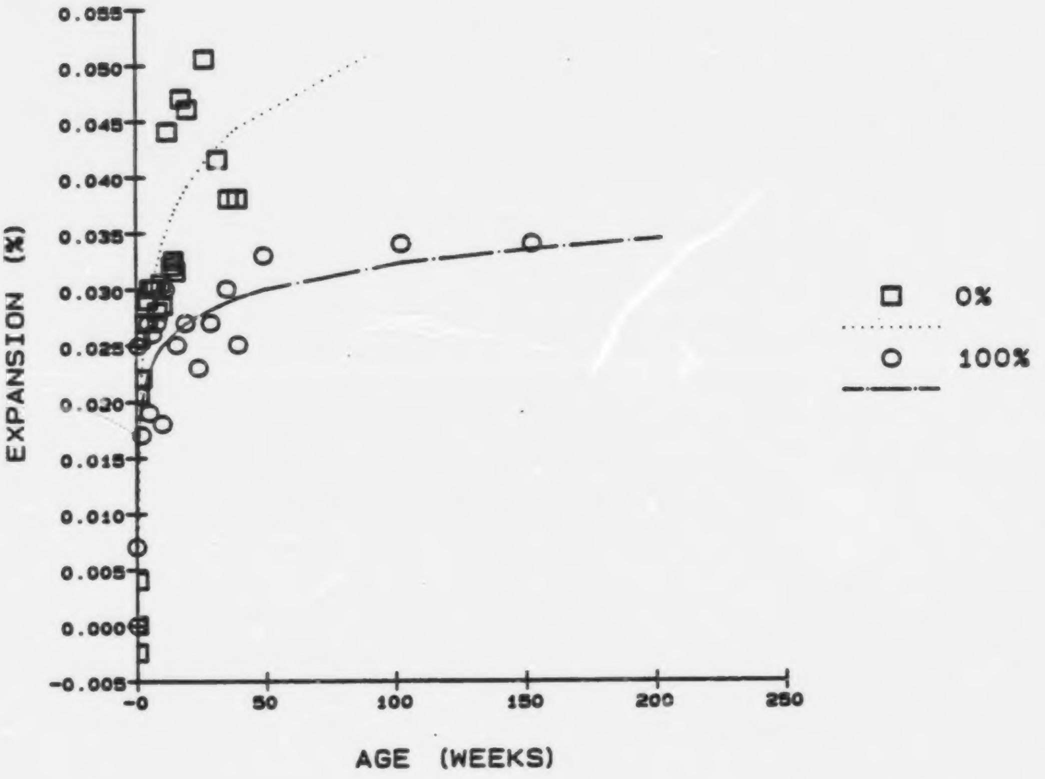

Figure 26. Expansion of mortar bars prepared with Cement D, with and without gneissic granite.

BEST COPY AVAILABLE

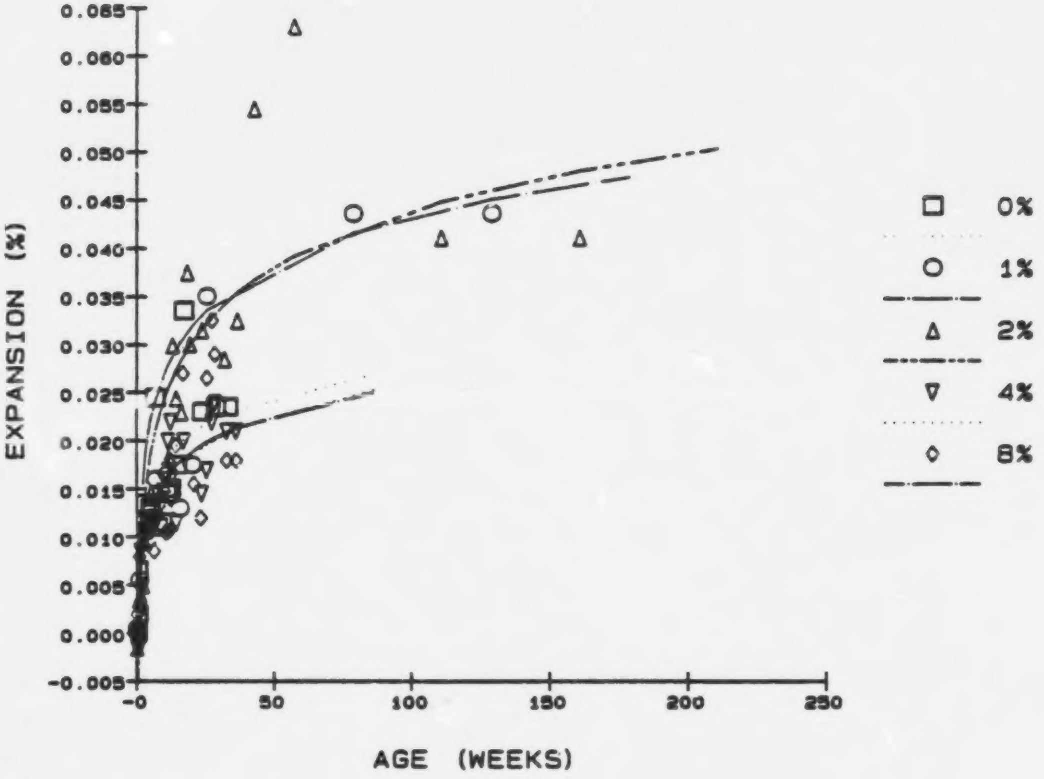

Figure 27. Expansion of mortar bars prepared with Cement E and various levels of opal.

BEST COPY AVAILABLE

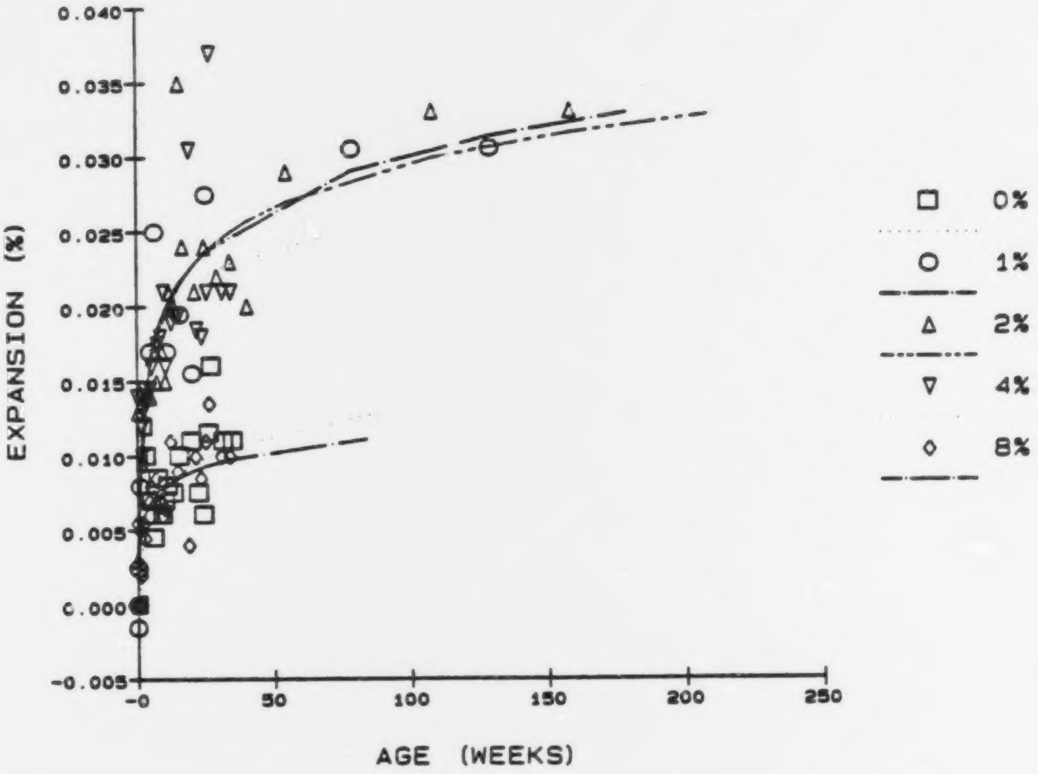

Figure 28. Expansion of mortar bars prepared with Cement F and various levels of opal.

BEST COPY AVAILABLE

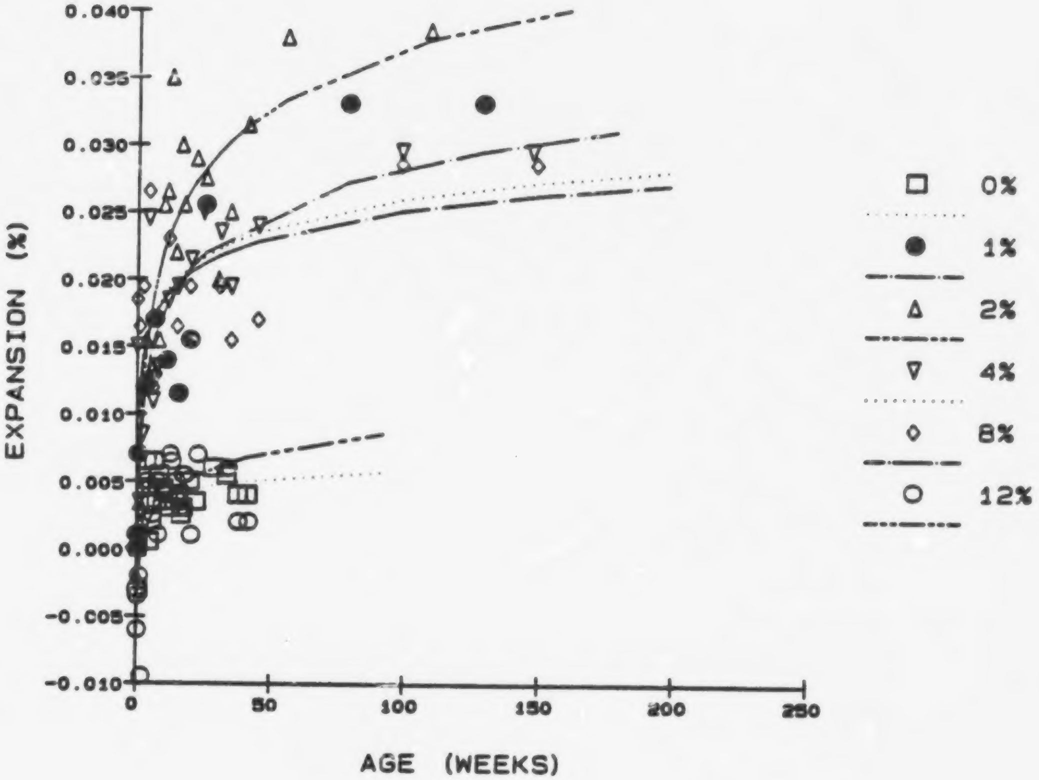

Figure 29. Expansion of mortar bars prepared with Cement G and various levels of opal.

BEST COPY AVAILABLE

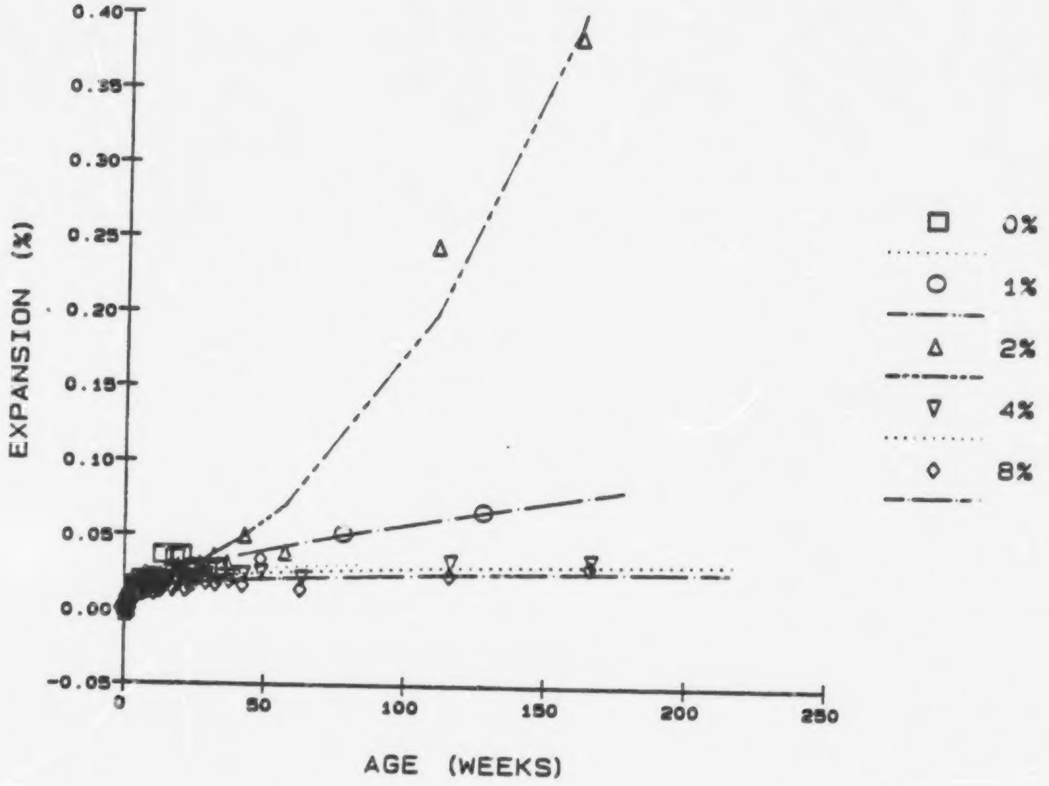

Figure 30. Expansion of mortar bars prepared with Cement H and various levels of opal.

BEST COPY AVAILABLE

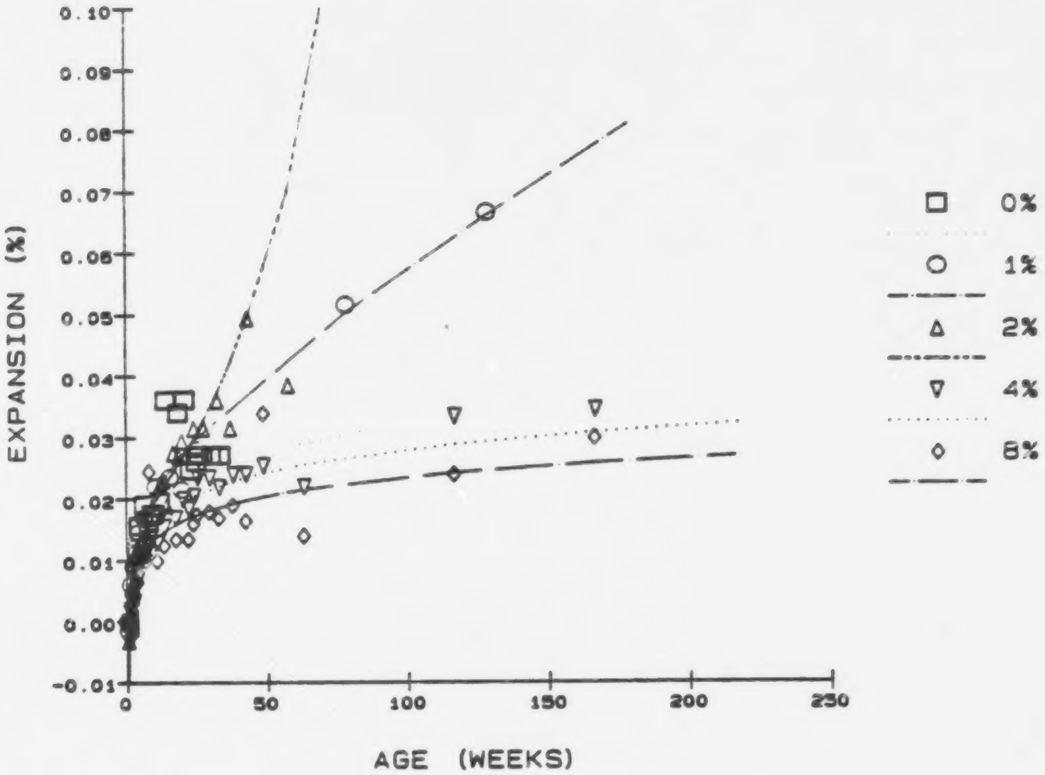

Figure 31. Expansion of mortar bars prepared with Cement H and various levels of opal, using an expanded scale for expansion.

BEST COPY AVAILABLE

Table 16. Results of mortar-bar expansion measurements.

Cement	Reactive Aggregate Material	(%)	Final Expansion[a] (%)
A	None[b]	0	0.018
	Granite	100	0.039
	Quartzite	10	0.028
		20	0.037
		30	0.040
		50	0.024
	Opal	2	0.240
		4	0.362
		8	0.154
		12	0.047
B	None	0	0.019
	Granite	100	0.034
	Quartzite	10	0.028
		20	0.043
		30	0.033
		50	0.012
	Opal	1	0.090
		2	0.247
		4	0.073
		8	0.020
		12	0.015
C	None	0	0.009
	Granite	100	0.036
	Quartzite	10	0.033
		20	0.043
		30	0.050
		50	0.026
	Opal	1	0.081
		2	0.327
		4	0.223
		8	0.005
		12	0.023

---

[a] Average measured expansion of two (in most cases) bars after expansion apparently terminated, typically after 8 months to 3 years.

[b] Only limestone aggregate.

(Table 16, continued)

Cement	Reactive Aggregate Material	(%)	Final Expansion[a] (%)
D	None	0	0.051
	Granite	100	0.033
	Quartzite	10	0.030
		20	0.027
		30	0.036
		50	0.021
	Opal	1	0.031
		2	0.101
		4	0.061
		8	0.033
		12	0.039
E	None	0	0.024
	Opal	1	0.035
		2	0.063
		4	0.021
		8	0.045
F	None	0	0.011
	Opal	1	0.028
		2	0.029
		4	0.021
		8	0.014
G	None	0	0.004
	Opal	1	0.026
		2	0.038
		4	0.024
		8	0.017
		12	0.005
H	None	0	0.027
	Opal	1	0.052
		2	0.039
		4	0.034
		8	0.024

for Beltane opal than for the other three aggregates. The expansion rates then decrease continuously from their initially high levels, and reach fairly steady values after approximately 18 to 24 weeks. At 90 weeks (22 months) the rates of expansion with quartzite, granite, and limestone, are quite low, ranging from 0 to 1.7×10^{-4} percent per week; the rates with opal are only slightly higher, ranging from 1 to 6.7×10^{-4} percent per week.

As discussed further in the following chapter, the expansion pattern described above appears to be typical, though not unique, for alkali-silica reaction (McConnell et al, 1947, and Brandt and Oberholster, 1983). There is one important difference from other studies, in that there is no evidence of an induction period. Grattan-Bellew (1981) reviewed mortar bar expansion data according to the method described in ASTM C 227, and noted that typical alkali-silica expansion curves have an induction period before the onset of the main expansive phase of the reaction; depending on the aggregate, the induction period ranged from a few days to 150 days. It is possible that the absence of an induction period is affected by the storage temperature, which was lower in the present study (~22°C) than in the ASTM method (38°C).

The expansion pattern is somewhat different for Cement D than for the other seven cements. The expansion rates of Cement D with quartzite (Fig. 25), and with granite or limestone (Fig. 26) decrease from their initial levels, such that the rates are low and steady by approximately 24 weeks, similar to behavior of Cements A, B, and C. On the other hand, the initial expansion rate for Cement D with Beltane opal (Fig. 24) appears to be no higher than it is with the other three aggregates, but it increases abruptly at approximately 30 weeks, then levels off to a low, steady value for the remainder of the test.

The expansion pattern of one mortar using Cement H and opal was also unique. As with the other three cements low in alkali, the expansion pattern of Cement H with opal level off to low values (0.01 to 0.06%) after a few weeks. In all mortars except one, these low values were maintained for the remainder of the test, typically 2 or 3 years. The mortar containing Cement H with 2% opal, however, increased substantially in expansion, to levels greater than 0.2%, sometime between 57 and 111 weeks. Because this very high expansion level was observed only for the mortar containing Cement H and 2% opal, it was not regarded as reproducible and was not included in subsequent discussions.

As discussed previously, the aggregates for this study were selected to provide a range in expansion potential, i.e. in the level and rate of expansion. In particular, the opal is known to react rapidly and to produce high levels of expansion, whereas gneissic granite is expected to react slowly and may produce expansion at a later age. However, analysis of the present expansion data do not support this concept of reactivity. All of the aggregates showed highest rates of expansion during the first 6 weeks, and reached substantial expansion levels during this early period. The principal difference in the expansion curves between Beltane opal and the less reactive aggregates lies in the actual values of expansion rate and level during this initial period. With the exception of the two mortars discussed above, one with Cement D and one with Cement H, no late or delayed expansion was observed.

Final expansion levels (at approximately 2 years) for the various mortars tested ranged from 0.01% to a high of 0.36%. In general, the highest expansion levels were produced by the high-alkali cements with opal, and these expansion levels ranged from 0.1% for Cement D to 0.2% or higher for Cements B and C, and 0.36% for Cement A. Expansion levels with opal for the four cements with lower alkali contents were much lower, below 0.06%. Expansion levels for the high alkali cements with quartzite were low, ranging between 0.01 and 0.05%; and were similarly low with granite, ranging between 0.03 and 0.04%.

Surprisingly, the high alkali cements with the limestone aggregate (Piece A/B) showed some expansion, typically around 0.01 to 0.02%, though the expansion level was even higher (0.05%) for Cement D. Thus the supposedly inert limestone showed significant expansion potential. Unreactive aggregates typically produce zero expansion or even slight shrinkage (for example, see Gaskin et al, 1955). However, Heck (1983) reported expansion levels of approximately 0.03%, similar to the present results, for limestone sand with high alkali cement (tested at 38°C). As noted previously, Heck also reported that this limestone caused some reduction in alkalinity in the quick chemical test.

Expansion levels with Beltane opal are much higher than those reported by Boswell et al (1983), in which the highest level was 0.05% at 12 months (tested at 38°C). On the other hand, levels are lower than those reported by Barneyback (1983), in which highest levels ranged between 0.5 and to 0.6% at 8 months (also tested at 38°C).

Results for both quartzite and granite were lower than have been reported elsewhere at similar replacement levels (though tested at 38°C). Expansion levels with quartzite were somewhat lower than the levels reported by McConnell et al (1947) for novaculite, which produced approximately 0.6% expansion. Expansion levels with gneissic granite were slightly lower than those reported by Buck (1983) for a similar material, which produced 0.06% at 1 year and 0.09% at 2 years. These differences are attributed to the lower temperature employed in the present studies.

For each cement, the pessimum levels of opal and quartzite may be approximated by inspecting the expansion curves. With the high alkali cements, the pessimum levels of opal appear to be near 2% with Cements B, C, and D, and 4% with Cement A. With all four low alkali cements, the pessimum levels of opal appear to be near 2%, though more difficult to estimate from the expansion curves. The pessimum levels of quartzite, tested only with high alkali cements, are less well defined and appear to be around 20% or 30% for each cement.

The pessimum levels for opal are similar to results reported by others. These comparisons are only approximate, since the proportions of cement and aggregate were not precisely the same in all cases. The pessimum proportion of Beltane opal reported by Barneyback (1983) was approximately 6% of the total aggregate, slightly higher than results here. Boswell et al (1983) reported a pessimum proportion of Beltane opal of 4%; this was the lowest level tested, so the pessimum could in fact have been lower. Brandt and Oberholster (1983) reported pessimum levels of 2, 4, or 6% for cements of various alkali levels.

The pessimum levels for quartzite differ somewhat from the level reported by McConnell et al (1947). They reported a pessimum for novaculite near 50%, somewhat higher than the 20 or 30% reported here.

Although a pessimum proportion phenomenon is observed for both opal and quartzite, the relationships observed between expansion and level of reactive aggregate is quite different for the two materials. The pessimum proportion of opal is low, occurring at approximately 2 to 4% opal for each cement tested. The pessimum of opal is also narrow, i.e. the high expansion occurs over only a narrow range of opal levels. Mortar bars prepared at levels only slightly more or less than the pessimum proportion show much less expansion. For example, Cement A produced its highest expansion level of 0.362% with 4% opal, but a moderate 0.240% expansion with 2% opal and a much lower expansion level of 0.154% with 8% opal.

For quartzite, the pessimum proportion is much higher, occurring at approximately 20% to 30% replacement. The pessimum peak of quartzite is also more broad than the pessimum of opal. Mortars with levels lower or higher than the pessimum show nearly as much expansion as mortars with the pessimum level. For example, Cement A produced an expansion level of 0.040% with 30% quartzite, and fairly similar expansion levels 0.037% and 0.024% at quartzite levels of 20% and 50%.

In practical terms, if expansion levels are to be compared between cements or aggregates in any meaningful way, such comparisons should be made at the pessimum proportion of each aggregate and cement. This is especially important for a reactive constituent such as the opal, whose pessimum is so narrow that testing at replacement levels only slightly above or below the pessimum may produce low and misleading expansion levels. The narrow pessimum of Beltane opal prompted Brandt and Oberholster (1983) to conclude that the material would not be suitable as a standard reactive aggregate.

Expansion curves for the various aggregates, shown in Figs. 32 through 35, allow comparisons of aggregates and of cements in terms of both level and rate of expansions. For all cements tested, the expansion levels fall into two groups, the extremely high level produced by opal, and the much lower level of expansion produced by the quartzite, granite, and the limestone alone. Significant differences are apparent between the cements for both the initial rate of expansion and the final expansion level. As expected, in mortars containing Beltane opal (in each case at its pessimum proportion), the high-alkali cements produced substantially greater levels and initial rates of expansion than the low-alkali cements (Fig. 32). In both respects, the high-alkali cements ranked in order (high to low): A > C > B > D. As might be expected, differences between the

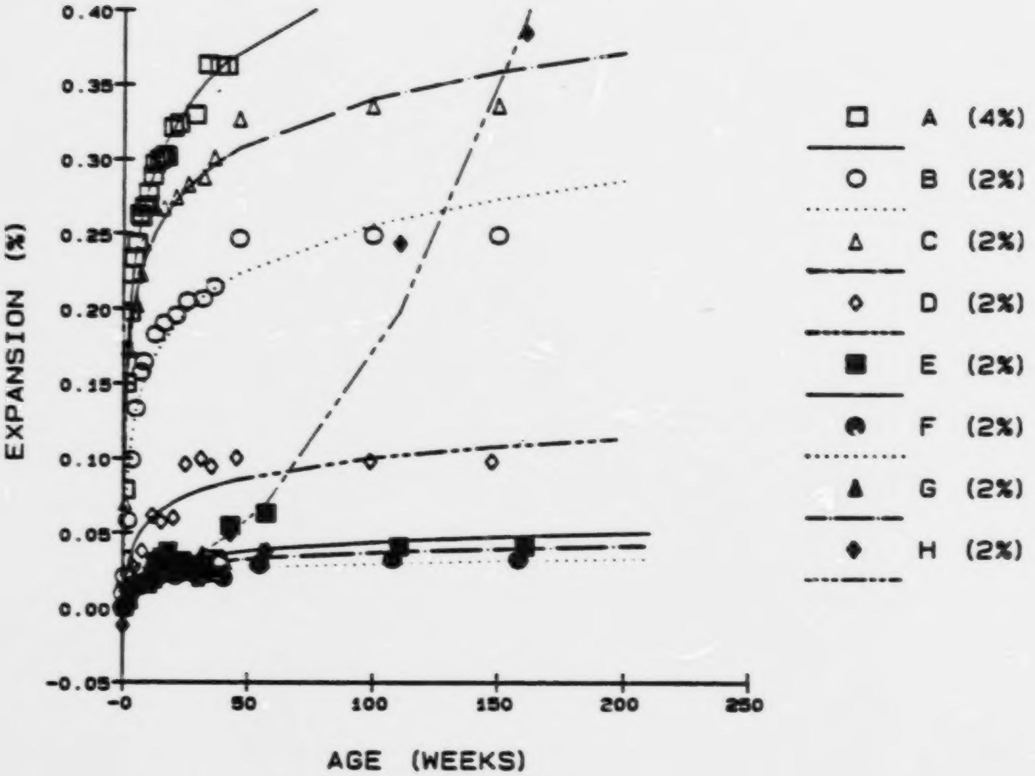

Figure 32. Expansion of mortar bars prepared with opal, at the level determined to be its pessimum for each cement (2% for all except A, which is 4%).

BEST COPY AVAILABLE

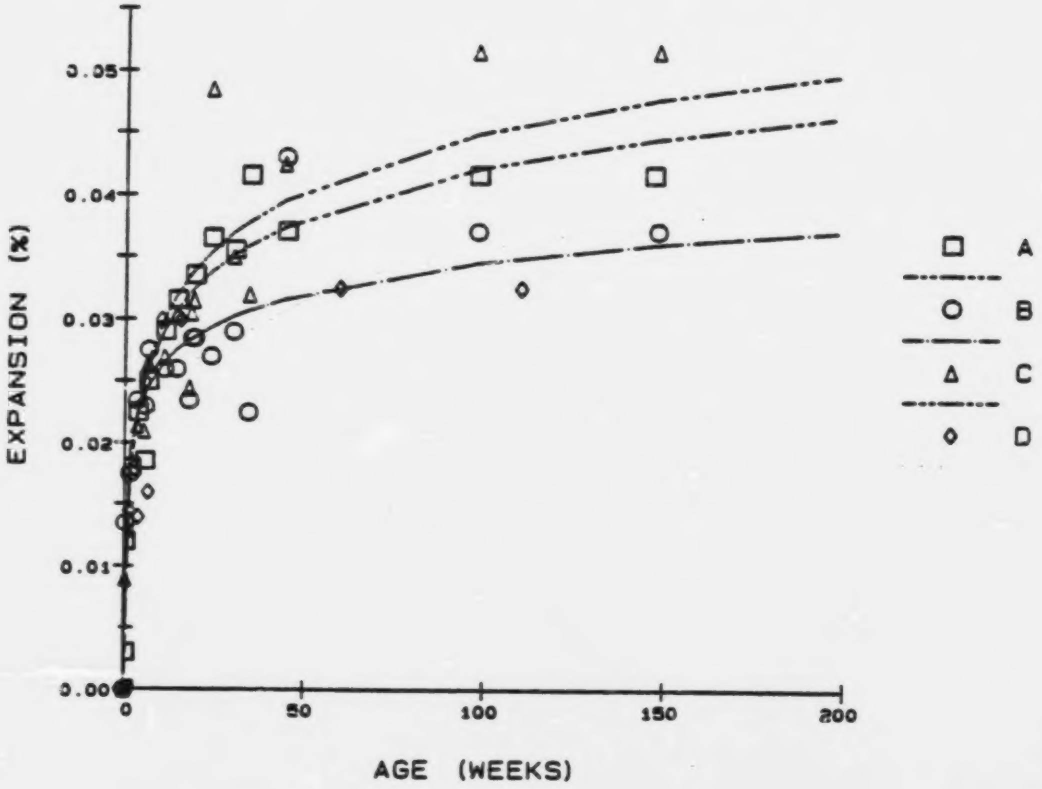

Figure 33. Expansion of mortar bars prepared with quartzite, at the level determined to be its pessimum for each cement (20% for Cements A through C, 10% for Cement D).

BEST COPY AVAILABLE

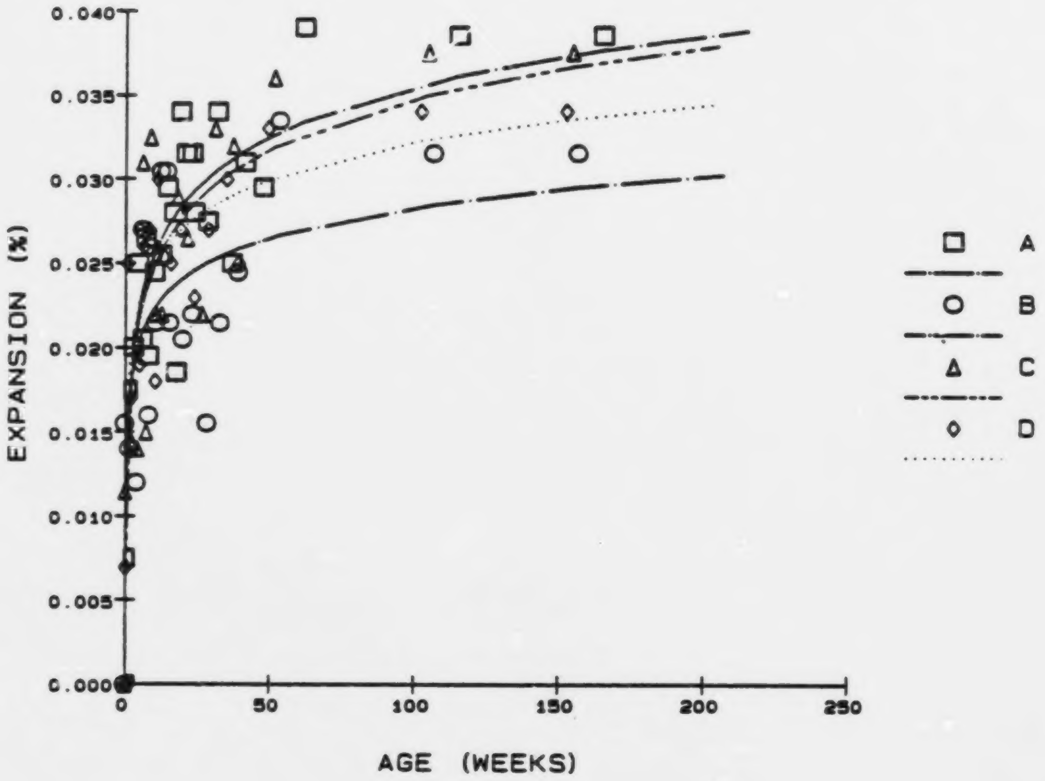

Figure 34. Expansion of mortar bars prepared with 100% gneissic granite.

BEST COPY AVAILABLE

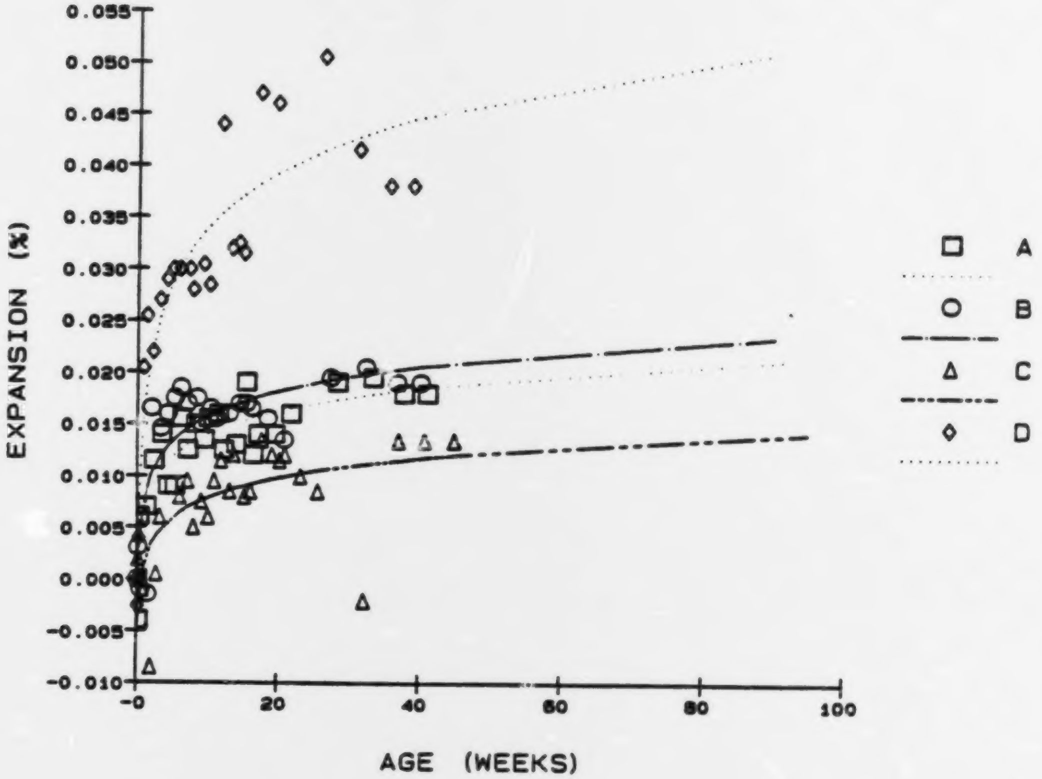

Figure 35. Expansion of mortar bars prepared with 100% limestone.

BEST COPY AVAILABLE

low-alkali cements with opal are less substantial, as are differences between the high-alkali cements with quartzite (Fig. 33) and granite (Fig. 34). Even with limestone (Fig. 35), three cements, D, E, and G, were slightly higher than the others in level and initial rate of expansion.

Reaction of Aggregates in Model Pore Solutions

The pH and dissolved silica levels produced by reaction of each aggregate in a series of model pore solutions were measured in order to determine whether the pessimum effect can be attributed to differences in the level of dissolved silica produced by differences in proportion of aggregate to solution, and whether differences in expansion produced by various cements is related to the differences in dissolution rate in each pore solution. The ratios of aggregate to solution were selected so as to duplicate the proportions of reactive constituent in the mortars used for expansion tests, and the model pore solutions approximated the alkali concentrations and pH levels of the pore solutions expressed from limestone mortars.

Solutions were mixed with specimens of sand-sized aggregate, mixtures were allowed to react for a period between 1 and 3 weeks, then filtered to collect solutions for analysis. On visual inspection, no aggregates showed any indication of dissolution or reaction. Solutions in all cases appeared clear and free of precipitated silica.

The results of these experiments are shown in Tables 17 and 18. Opal at all levels and all solutions produced extremely high concentrations of silica, in some cases greater than 2 M. Only modest concentrations of silica was produced by opal at 1 week, but silica concentrations increased substantially at 2 and 3 weeks, in what appears to be a linear manner. The concentration of silica in each solution was still increasing at 3 weeks.

Table 17. Concentrations of silica produced by reaction of aggregates in model pore solutions (mM).

Aggregate	Level (%)[a]	Solution No.[b]	Reaction Time (weeks) 0	1	2	3
Limestone	100	1	0.0	0.2	0.2	0.2
		2	0.0	0.1	0.2	0.3
		3	0.0	0.1	0.2	0.1
		4	0.0	0.1	0.1	0.1
Opal	2	1	0.0	0.1	225.6	228.2
		2	0.0	0.1	139.3	465.0
		3	0.0	0.1	334.4	923.4
		4	0.0	0.1	492.6	1177.7
Opal	4	1	0.0	0.2	257.0	500.6
		2	0.0	0.2	551.1	529.2
		3	0.0	0.2	721.7	1395.8
		4	0.0	0.2	1219.8	2396.9
Opal	8	1	0.0	0.1	214.8	530.0
		2	0.0	0.1	879.9	530.0
		3	0.0	0.1	1787.5	1198.8
		4	0.0	0.1	825.4	1689.8
Quartzite	20	1	0.0	0.2	1.6	6.7
		2	0.0	0.2	1.6	9.2
		3	0.0	0.3	1.6	11.0
		4	0.0	0.2	1.5	10.5
Quartzite	30	1	0.0	0.2	0.1	7.7
		2	0.0	0.2	0.1	9.7
		3	0.0	0.2	11.4	13.9
		4	0.0	0.2	10.8	16.2
Quartzite	50	1	0.0	0.3	0.1	8.2
		2	0.0	0.4	0.1	3.1
		3	0.0	0.3	0.1	7.3
		4	0.0	0.3	0.2	12.8
Granite	100	1	0.0	1.5	1.3	1.2
		2	0.0	nd	1.3	1.3
		3	0.0	nd	nd	nd
		4	0.0	nd	nd	1.2

[a] Equivalent replacement level by weight of total aggregate in mortars.

[b] Solution compositions in Table 6.

[c] nd, not determined.

Table 18. Level of pH produced by reaction of aggregates in model pore solutions.

Aggregate		Level	Solution	Reaction Time (weeks)		
	(%)[a]	No.[b]	0	1	2	3
Limestone	100	1	13.14	12.43	12.27	12.25
		2	13.44	12.64	12.46	12.34
		3	13.68	13.19	13.08	12.69
		4	13.85	13.54	12.79	12.79
Opal	2	1	13.14	12.03	11.82	11.75
		2	13.44	12.24	12.00	11.87
		3	13.68	13.04	12.44	12.25
		4	13.85	13.24	12.97	12.56
Opal	4	1	13.14	11.86	11.68	11.65
		2	13.44	11.98	11.76	11.75
		3	13.68	12.16	11.88	11.80
		4	13.85	12.45	12.11	12.00
Opal	8	1	13.14	11.73	11.67	11.65
		2	13.44	11.86	11.75	11.70
		3	13.68	12.01	11.81	11.75
		4	13.85	12.11	11.85	11.80
Quartzite	20	1	13.14	13.11	13.07	13.11
		2	13.44	13.37	13.42	13.43
		3	13.68	13.66	13.69	13.57
		4	13.85	13.88	13.85	13.86
Quartzite	30	1	13.14	13.11	13.12	13.08
		2	13.44	13.40	13.43	13.40
		3	13.68	13.67	13.72	13.62
		4	13.85	13.84	13.88	13.85
Quartzite	50	1	13.14	13.04	13.09	12.99
		2	13.44	13.38	13.40	13.36
		3	13.68	13.70	13.75	13.66
		4	13.85	13.84	13.87	13.87
Granite	100	1	13.14	13.04	13.07	nd[c]
		2	13.44	13.33	13.32	13.34
		3	13.68	13.62	13.54	nd
		4	13.85	13.73	13.76	13.80

---

[a] Equivalent replacement level by weight of total aggregate in mortars.

[b] Solution compositions in Table 6.

[c] nd, not determined.

Opal produced substantial reduction in pH, in excess of 1 pH unit, in all model pore solutions, but pH followed a pattern quite different than the silica. The reduction in pH occurred most rapidly during the first week, then leveled off between 2 and 3 weeks.

Quartzite at all levels and in all solutions produced moderate concentrations of silica, typically around 10 mM. As with the opal, little silica was observed with quartzite until 2 weeks. The quartzite produced no reduction in pH.

The granite in all model solutions produced low levels of silica, typically around 1 mM, and no reduction in pH. Unlike the other aggregates, however, the small increase in silica concentration occurred only during the first week.

The limestone produced only a trace of silica, generally below 0.3 mM, but a large reduction in pH, approximately 1 pH unit. Subsequent experiments were carried out using reagent-grade $CaCO_3$, to ascertain whether there might be any unexpected reaction involving $CaCO_3$ and alkali or hydroxide ion in solution. Reagent $CaCO_3$ produced no change in pH when allowed to react with the same set of model pore solutions for 1 week, in contrast to the substantial reductions in pH produced by the limestone aggregate (Table 18). Therefore, it was concluded that the measured changes in solution pH resulted from reaction with some constituent of the limestone other than $CaCO_3$.

Although it cannot be determined from these results, a possible cause for the reduction in alkalinity due to limestone is a reaction involving dolomite in the limestone. As discussed previously, the limestone used for these studies was Piece K, high in dolomite, and it is possible that the high levels of reduction in pH produced by limestone relate to its high dolomite content. However, both the levels of silica and the level of reduction in pH produced by this limestone are consistent with the results of the quick chemical test, which was carried out using

Piece A/B, which contained little dolomite. Results of the limestone reaction in model pore solutions and the quick chemical test are difficult to reconcile with the high pH levels observed in the pore solutions expressed from limestone mortars (also prepared using Piece K), as described below.

It is apparent from these data that the studies of the aggregates in model pore solutions were terminated before the reactions had gone to completion. Based on expansion data, 3 weeks had been selected as a reasonable reaction time for these studies. However, both the levels of silica in solution and the changes in pH level for many aggregates changed appreciably between 2 and 3 weeks. Thus continuing these reactions for longer reaction times would have been helpful.

Pore Solutions Expressed from Limestone Mortars

Expression

The approximate volume of solution expressed from each mortar specimen ranged from several ml for 1-week specimens to less than 2 ml per specimen at later ages. Similar volumes were reported by Barneyback (1983). In most cases, the procedure used for expressing solution, particularly the repeated cycling of load, provided at least 1 ml solution, the minimum amount required for chemical analysis.

There were clear differences in the volume of solution expressed from specimens of various ages. Several ml were expressed from mortars at an age of 1 week, with approximately 1 ml expressed by approximately 4 weeks. Differences in the volume of solution with different cements were also apparent, but did not appear to follow a clear pattern.

Although the mortar samples were not weighed and their non-evaporable water contents were not determined, one can estimate levels for these parameters and thus estimate the amount of pore solution available for expression. Mortar specimens were 47.6 mm diameter and roughly 75 mm in height, for a volume of 130 ml. Using a value of 2.3 g per ml for the density of mortar (Lea, 1971), the specimens are expected to have a mass of approximately 300 g. Based on their initial proportions, the mortars are expected to contain approximately 39 ml water. However, much of this water becomes chemically bound in hydrated phases. The amount of water not chemically bound may be estimated using data for chemically bound water reported by Barneyback (1983), though the ratios of sand-to-cement and water-to-cement (1.97 and 0.50 respectively) were slightly different than the ratios used in the present study (2.25 and 0.485 respectively). The calculated proportions of water not bound range from 0.33 g per g cement at 1 week to 0.31 g per g cement at 28 weeks. The equivalent volumes of pore water in each specimen are 27 ml at 1 week and 25 ml at 28 weeks. Therefore, the few ml of solution obtained by expression represent only a small part of the pore water that is potentially available. Furthermore, the decrease in the volume of expressed pore solution observed as the specimens age from 1 week to 28 weeks is much greater than the decrease in pore water expected due to hydration.

Chemical Compositions

Pore solutions were expressed from limestone mortars at ages between 1 and 28 weeks. These mortars were designed as "control" mortars, with no expected alkali reaction.

Of the species analyzed, the principal constituents were hydroxide and alkali ions. As summarized below, measured levels of pH ranged from 13.4 to 14.0 and hydroxide ion concentrations from 322mM to 965 mM. Concentrations of each alkali were typically several hundred mM, ranging from 6 mM to 279 mM for sodium and from 75 mM to 857 mM for potassium. Typical levels of calcium, silica, and sulfate were much lower: 0.6 mM to 2.2 mM for calcium, less than 0.05 mM for silica, and up to 77 mM for sulfate.

Total measured concentrations of cations and anions, each determined by analysis of solutions that were diluted nominally 1:100, are shown in Table 19. The average difference observed between total cations and total anions was 0.3 milliequivalents per L, and the maximum difference was 2.9 milliequivalents per L. The individual levels of precision for each calibration (standard error of estimated y) range from 0.01 milliequivalents per L for calcium to 0.10 for hydroxide (Appendix A). The sum of these precision levels is 0.35 milliequivalents per L, approximately the same level as the average difference between total cations and total anions. Thus the differences appear to be within the limits of analytical precision. Barneyback (1983) reported differences between cations and anions of a few tens of milliequivalents per L for undiluted samples, similar to the differences reported here when corrected for dilution.

The changes in concentration with age of many species varied significantly from cement to cement, as summarized below for each constituent. The concentration levels of most constituents appear to increase in a smooth, regular fashion with age, though for some constituents there is irregularity in the pattern. These variations are discussed further, both in terms of compositions of the cements and in terms of the distributions of alkalies among the cement phases, in the following chapter.

pH. The measured pH levels (Table 20) ranged from 13.4 to 14.0, higher for Cements A through D and lower for Cements E through H. The level of pH (Fig. 36) generally increased throughout the time period, most rapidly between 1 and 4 weeks, then less rapidly between 4 and 28 weeks.

Table 19. Measured ionic concentration levels in pore solutions of limestone mortars[a].

Age (weeks)	Cement	Sum Cations (meq/L[b])	Sum Anions (meq/L)	Difference (meq/L)
1	A	14.7	nd[c]	nd
	B	9.5	12.4	-2.9
	C	11.2	11.0	0.3
	D	7.5	5.5	2.0
	E	4.7	5.1	-0.4
	F	4.6	5.1	-0.5
	G	4.7	5.7	-1.0
	H	4.7	4.8	-0.1
2	A	11.7	11.7	-0.1
	B	6.9	7.0	-0.1
	C	8.9	9.6	-0.7
	D	7.6	7.6	0.0
	E	4.7	4.6	0.1
	F	4.6	5.0	-0.4
	G	4.0	4.0	0.0
	H	4.3	4.8	-0.6
4	A	11.7	11.7	0.0
	B	6.8	8.3	-1.6
	C	9.4	9.5	0.0
	D	8.3	8.1	0.2
	E	4.9	5.0	-0.1
	F	5.0	5.1	-0.1
	G	3.3	4.2	-0.8
	H	5.6	5.5	0.1

[a] Diluted approximately 1:100 for chemical analysis.

[b] Milliequivalents per liter.

[c] nd, not determined.

(Table 19, continued)

Age (weeks)	Cement	Sum Cations (meq/L)	Sum Anions (meq/L)	Difference (meq/L)
8	A	11.1	11.4	-0.3
	B	6.1	6.5	-0.3
	C	5.7	5.7	0.0
	D	8.4	8.4	0.0
	E	5.4	5.4	-0.1
	F	5.0	5.1	-0.1
	G	4.5	4.4	0.1
	H	5.0	5.0	-0.1
28	A	8.8	9.2	-0.5
	B	7.0	7.5	-0.4
	C	7.5	7.6	-0.1
	D	7.5	7.8	-0.4
	E	4.7	5.1	-0.5
	F	3.1	3.5	-0.4
	G	3.7	3.8	-0.1
	H	4.6	4.8	-0.2

Table 20. Measured pH levels in pore solutions of limestone mortars.

Cement	Age (weeks) 1	2	4	8	28
A	13.85	13.86	13.89	nd[a]	14.00
B	13.67	13.67	13.74	nd	13.83
C	13.79	nd	13.78	nd	13.88
D	13.71	13.75	13.82	nd	13.89
E	13.46	13.46	13.50	nd	13.64
F	13.42	13.50	13.56	nd	13.62
G	nd	13.43	13.53	nd	13.57
H	13.43	13.46	13.52	na	13.61

[a] nd, not determined.

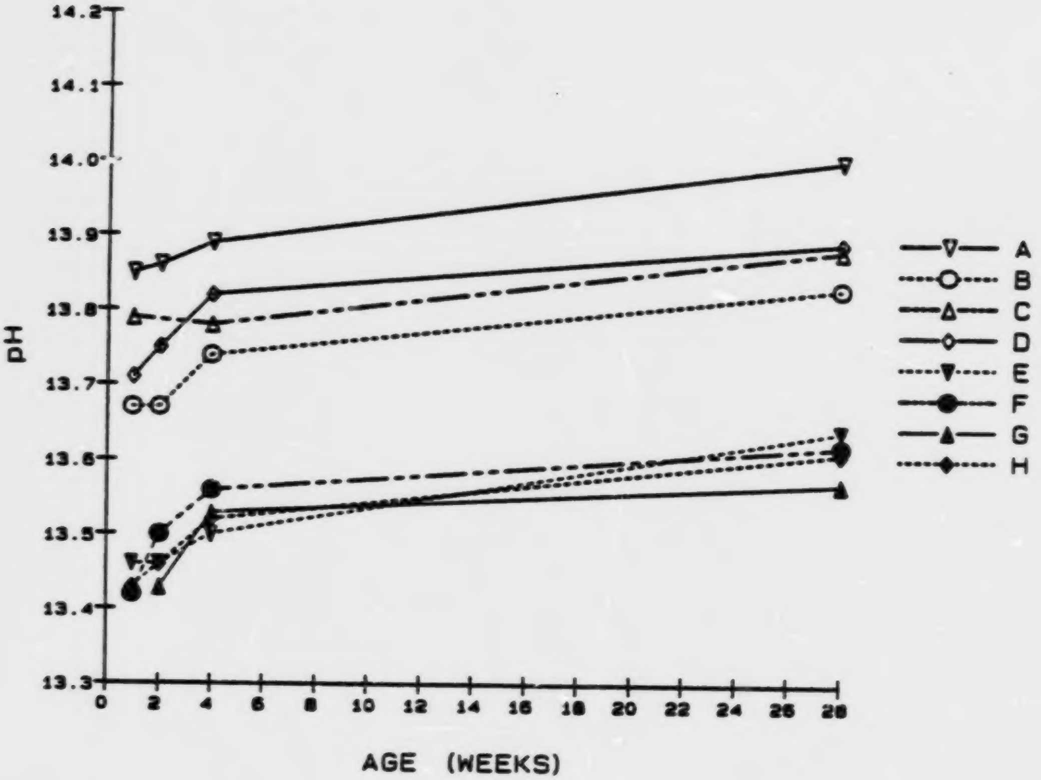

Figure 36. Levels of pH in pore solutions of limestone mortars.

BEST COPY AVAILABLE

In most cases these results are similar to those reported by earlier investigators for solution expressed either from paste or mortar. The pH levels reported elsewhere tend to fall into one of two groups, with higher pH levels produced by high-alkali cements and lower levels by low-alkali cements. Furthermore, pH levels tend to increase with age, increasing rapidly during the initial week of hydration, then more slowly, such that only a low rate of increase is observed after several weeks.

The pH levels measured for pore solutions of mortars containing the four high-alkali cements ranged from 13.65 to 14.0. Similar pH levels, 13.7 to 13.8, were reported by Luke and Glasser (1986) for a different high-alkali cement. Levels reported by Longuet et al (1973) covered a wider range, 13.3 to 13.9, with more scatter in pH from age-to-age.

The pH results for pore solutions of mortars prepared using the four low-alkali cements ranged from 13.4 to 13.6, substantially lower than those from mortars using the high-alkali cements. Both the general pH level and variation with age of pH are quite similar to data of Xue et al (1983), who examined low-alkali cement paste rather than mortar. Similarly, Luke and Glasser (1986) reported a pH at 2 weeks of 13.4, and Marr and Glasser (1983) reported a pH level at 12 weeks of 13.4, each using a different low-alkali cement paste.

Hydroxide. The relative levels of hydroxide ion concentration (Table 21) were similar to the relative pH levels; they were highest for Cements A, intermediate for Cements B, C, and D, and much lower for Cements E through H. The hydroxide concentration levels measured for pore solutions of mortars made with the four high-alkali cements increased from as low as 400 mM at 1 week to as high as 900 mM at 28 weeks. The hydroxide ion concentration levels

Table 21. Measured hydroxide levels in pore solutions of limestone mortars (mM).

	Age (weeks)				
Cement	1	2	4	8	28
A	nd[a]	965	898	890	885
B	841	609	674	601	591
C	679	724	725	408	620
D	532	639	662	623	607
E	370	381	398	403	420
F	351	385	392	385	377
G	326	360	322	344	325
H	360	426	440	407	408

[a] nd, not determined.

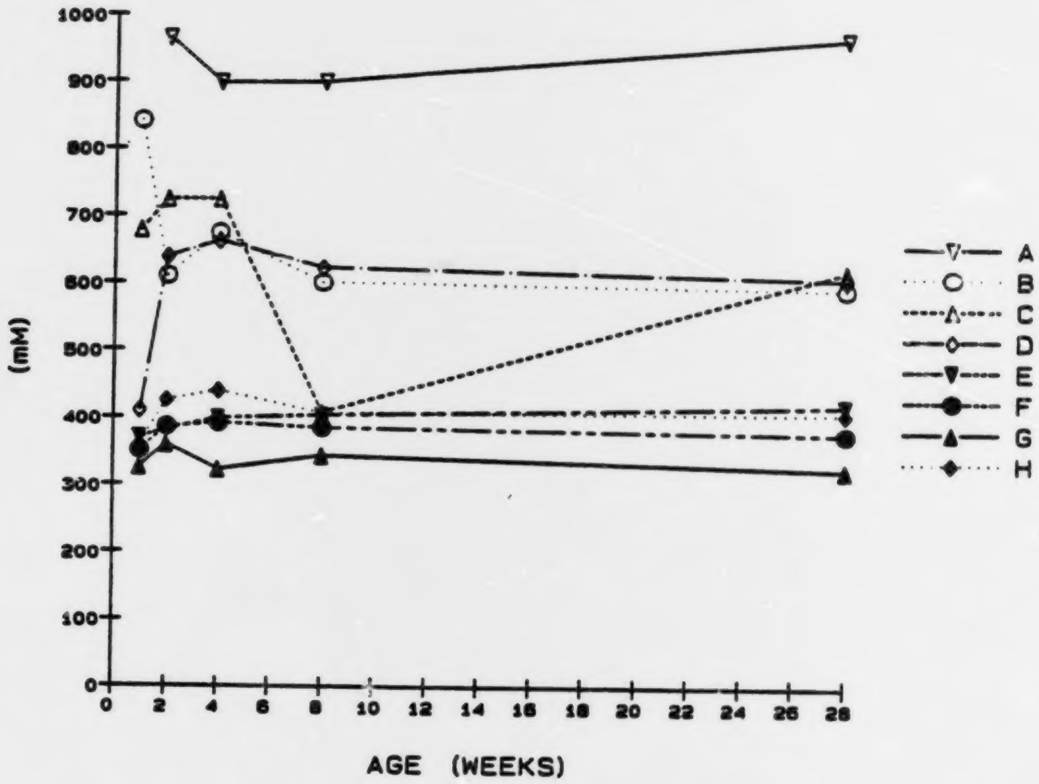

Figure 37. Levels of hydroxide ion in pore solutions of limestone mortars.

BEST COPY AVAILABLE

using the four low-alkali cements ranged from approximately 350 mM at 1 week to around 400 mM between 4 and 28 weeks. The hydroxide concentrations (Fig. 37) generally increased more rapidly between 1 and 4 weeks, then increased less rapidly or even decreased slightly between 4 and 28 weeks.

These results are similar to those reported by other investigators. Similar patterns and concentration ranges were reported by Barneyback (1983) and by Kollek and Varma (1986), each for a different high-alkali cement, and by Kollek and Varma for a different low-alkali cement.

Sodium. The sodium concentrations (Table 22) also varied between the eight cements, being highest for Cements A and H, intermediate for Cements B, C and E, and lowest for Cements D, F, and G. Sodium concentrations varied with age in a generally regular manner (Fig. 38), increasing most rapidly between 1 and 4 weeks, then increasing or decreasing slightly between 4 and 28 weeks.

The sodium concentration levels fall within the range reported by others. Reported levels after the first week vary from less than 100 mM (Silsbee et al, 1986) to approximately 300 mM (Page and Vennesland, 1983). The sodium results in the present study cover a similar range, from 6 to 279 mM.

Potassium. The potassium concentrations (Table 23) were higher for Cements A through D, generally greater than 500 mM, and lower for Cements E through H, less than 400 mM. For most cements, potassium concentration levels varied with age in the same manner as sodium concentrations (Fig. 39), increasing more rapidly between 1 and 4 weeks, and increasing more slowly or decreasing slightly between 4 and 28 weeks. Cements A and B showed a different pattern, decreasing rather than increasing between 1 and 4 weeks. The potassium concentration of the mortar with Cement C was at 8

Table 22. Measured sodium levels in pore solutions of limestone mortars (mM).

Cement	Age (weeks) 1	2	4	8	28
A	77	253	239	246	269
B	42	125	116	136	128
C	52	153	167	182	150
D	6	26	27	28	25
E	45	166	171	176	168
F	14	48	54	55	49
G	23	81	60	74	73
H	63	230	279	249	243

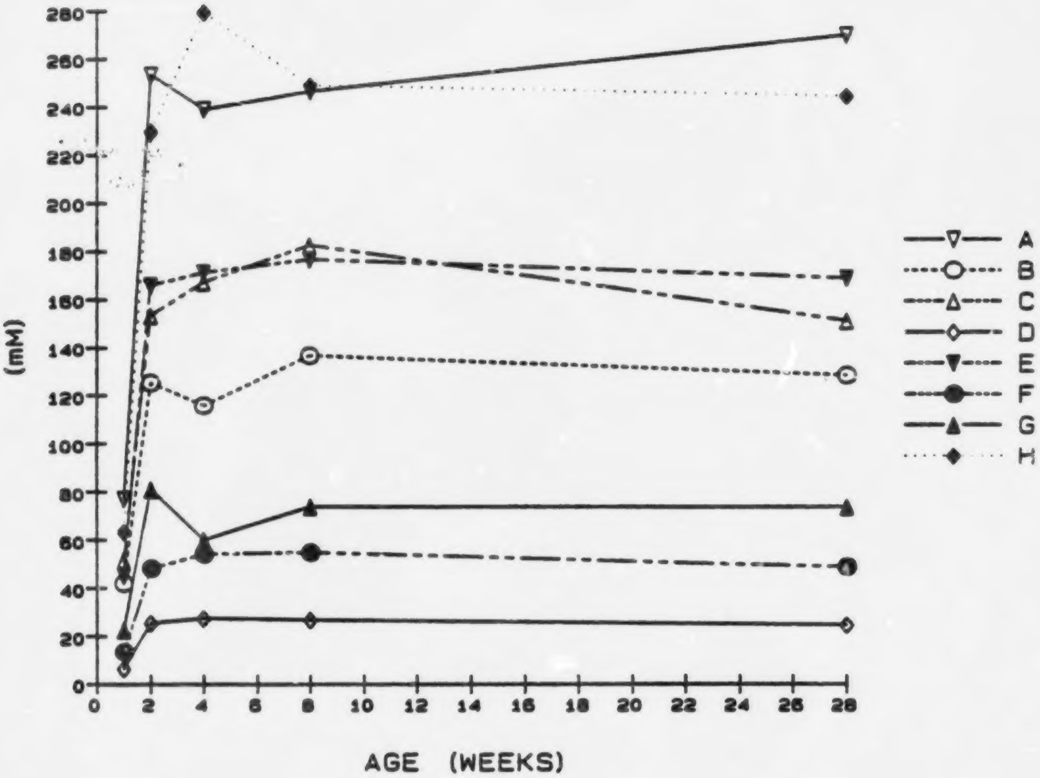

Figure 38. Levels of sodium ion in pore solutions of limestone mortars.

BEST COPY AVAILABLE

Table 23. Measured potassium levels in pore solutions of limestone mortars (mM).

	Age (weeks)				
Cement	1	2	4	8	28
A	444	834	775	781	857
B	297	515	488	601	535
C	350	610	673	264	590
D	279	649	706	669	632
E	107	239	244	252	246
F	153	328	363	366	320
G	141	295	219	304	273
H	75	159	196	179	180

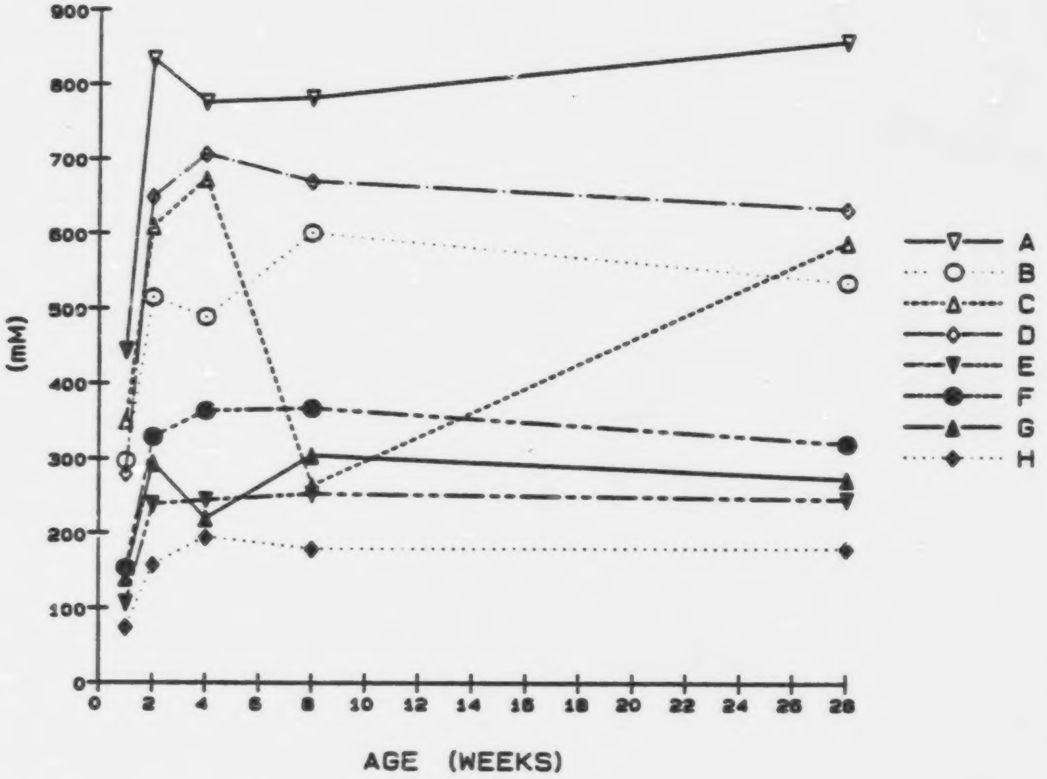

Figure 39. Levels of potassium ion in pore solutions of limestone mortars.

BEST COPY AVAILABLE

weeks only half the concentration level observed at all other ages; this result was verified by repeated analysis of the same specimen, but is considered an anomalously low value.

As with sodium, the potassium levels and patterns were similar to those reported by others. Reported levels after the first 2 weeks range from 200 mM (Silsbee et al, 1986) to 700 mM (Barneyback, 1983), and levels in the present study ranged from less than 100 mM (Cement H) to nearly 900 mM (Cement A).

Calcium. Measured levels of calcium (Table 24) were quite low, ranging between 0.6 mM and 2.5 mM. Calcium concentration levels were slightly higher for Cements E through H and slightly lower for Cements A through D, opposite to the potassium concentrations. Most samples (Fig. 40) tended to decrease in calcium level between 1 and 4 weeks, though there was considerable fluctuation from one age to the next, and then remain more constant between 4 and 28 weeks.

Reported levels during the same time period cover a considerably wider range but follow a similar pattern. When measured at much earlier ages, the concentration of calcium is initially high and then falls rapidly, reaching stable values by 1 or 2 weeks. At this time, calcium levels range from near 0 mM (Longuet et al, 1973, and Barneyback, 1983) to 4 mM (Xue et al, 1983, and Luke and Glasser, 1986). Many investigators report fluctuations of several mM in observed calcium levels at successive ages, probably because the measured levels are near the minimum level of calcium detectable by atomic absorption, the method used by most investigators.

Silica. Silica concentrations (Table 25) were considerably lower than calcium, ranging from 0 mM to 0.04 mM. Many negative measurements were obtained, which are considered

BEST COPY AVAILABLE

Table 24. Measured calcium levels in pore solutions of limestone mortars (mM).

	Age (weeks)				
Cement	1	2	4	8	28
A	0.9	2.5	0.6	0.7	1.3
B	0.6	1.8	1.0	0.3	1.3
C	1.5	0.5	1.0	0.9	1.0
D	1.4	1.4	1.1	1.1	0.8
E	1.8	2.1	1.5	1.4	1.7
F	2.2	2.0	1.3	1.5	1.5
G	1.8	1.0	1.3	1.9	1.6
H	1.8	0.6	1.6	1.4	1.2

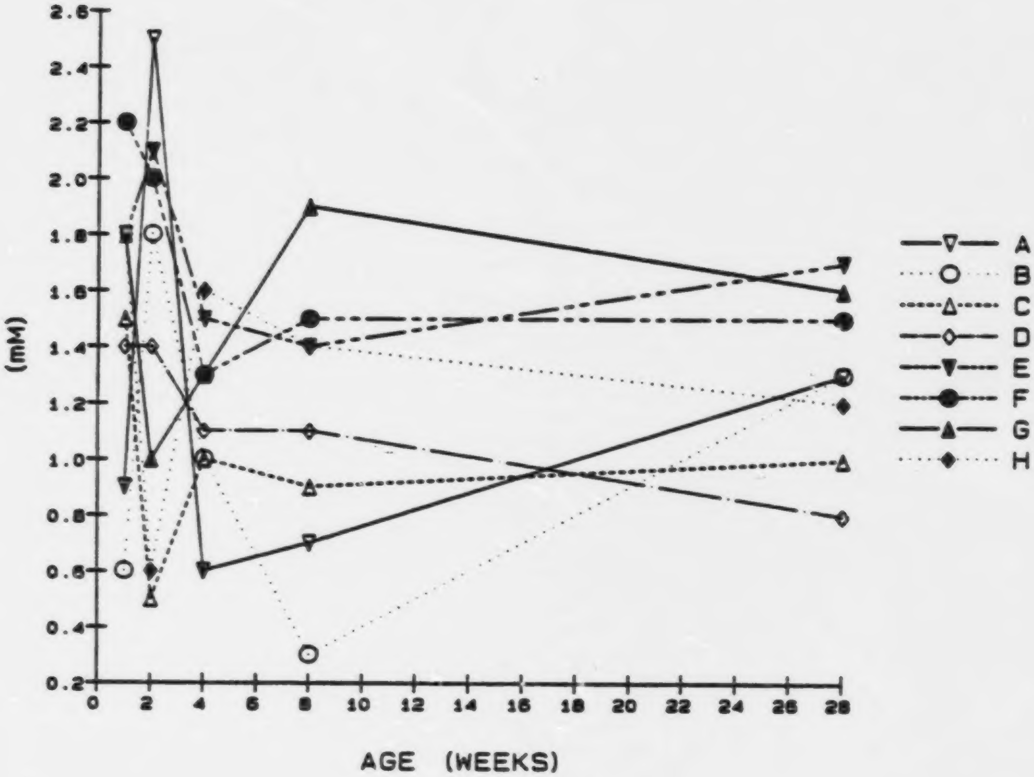

Figure 40. Levels of calcium ion in pore solutions of limestone mortars.

Table 25. Measured silica levels in pore solutions of limestone mortars (mM).

Cement	Age (weeks) 1	2	4	8	28
A	0.007	0.005	0.005	nd[a]	0.00
B	-0.006	-0.001	nd	nd	-0.003
C	-0.004	0.001	nd	nd	0.001
D	-0.018	-0.002	nd	nd	-0.002
E	0.017	0.002	nd	nd	0.014
F	0.009	-0.003	nd	nd	0.005
G	0.017	-0.001	nd	nd	0.009
H	0.044	-0.001	nd	nd	0.012

[a] nd, not determined.

equivalent to zero and indicate a practical limit to the accuracy of the colorimetric method. Silica concentration levels were slightly higher for Cements E through H and slightly lower for Cements A through D, the same relationship as shown by calcium. For those cements containing significant levels of silica (E through H), the variation with age (Fig. 41) was also similar to calcium, decreasing between 1 and 2 weeks, then remaining fairly constant between 2 and 28 weeks.

Only three other studies of pore solution composition reported values for silica, and these reported values differ considerably. Silica concentrations found in the present study are all below 0.05 mM. Xue et al (1983) reported levels of 0.1 mM at ages up to 6 months, somewhat higher than the values in the present study. Longuet et al (1973) found much higher values, ranging from 0.2 to 1.0 mM throughout 1 year. Barneyback (1983) reported silica concentration levels of up to 5 mM. Silsbee et al (1986) reported the highest silica concentration levels, up to 8 mM. It should be mentioned that contamination by silica from glassware can be difficult to avoid; such contamination can produce measured levels that are erroneously high. Furthermore, the typical analytical method for silica is atomic absorption, a method much less sensitive than the colorimetric technique used in the present study. These factors may account for the much lower levels of silica in the present study.

Sulfate. The levels of sulfate (Table 26) ranged from 3 mM to nearly 80 mM, generally higher for Cements A through D, and lower for Cements E through H. Sulfate concentration levels for Cements A through D showed considerable variation from age to age, while concentration levels for Cements E through H showed less variation (Fig. 42). Levels generally

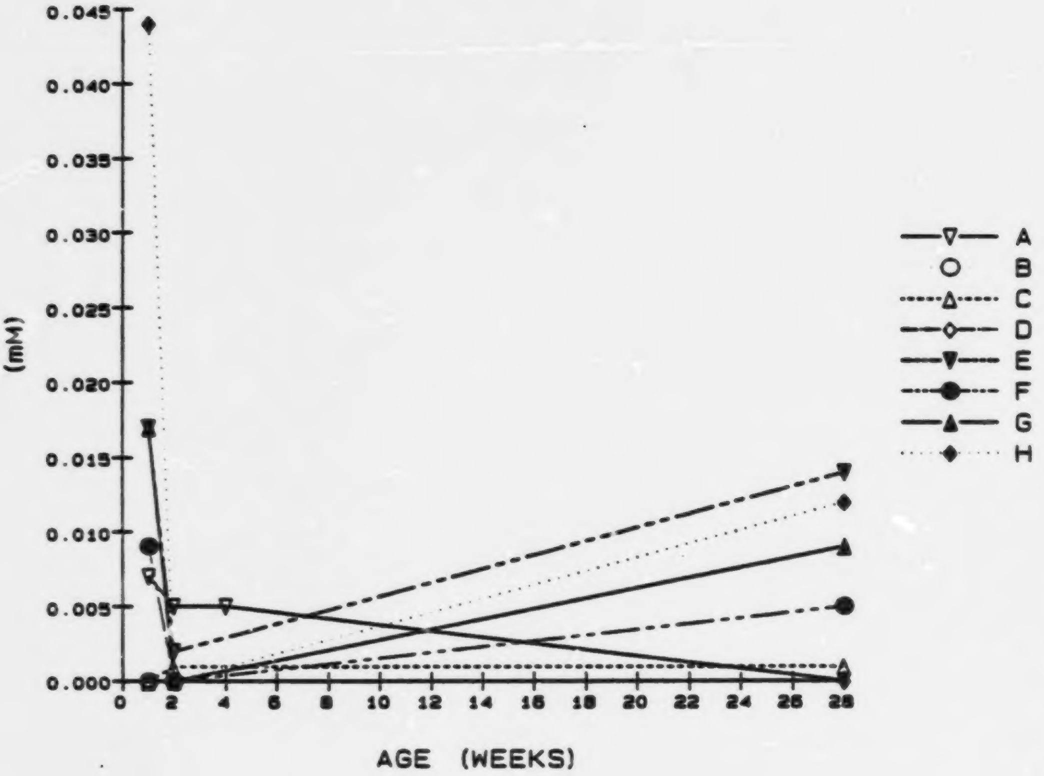

Figure 41. Levels of silica in pore solutions of limestone mortars.

BEST COPY AVAILABLE

Table 26. Measured sulfate levels in pore solutions of limestone mortars (mM).

	Age (weeks)				
Cement	1	2	4	8	28
A	30	37	40	48	77
B	18	13	15	51	30
C	18	31	7	10	46
D	5	16	14	21	21
E	3	5	6	10	14
F	5	9	8	11	17
G	3	6	8	10	12
H	4	4	6	8	12

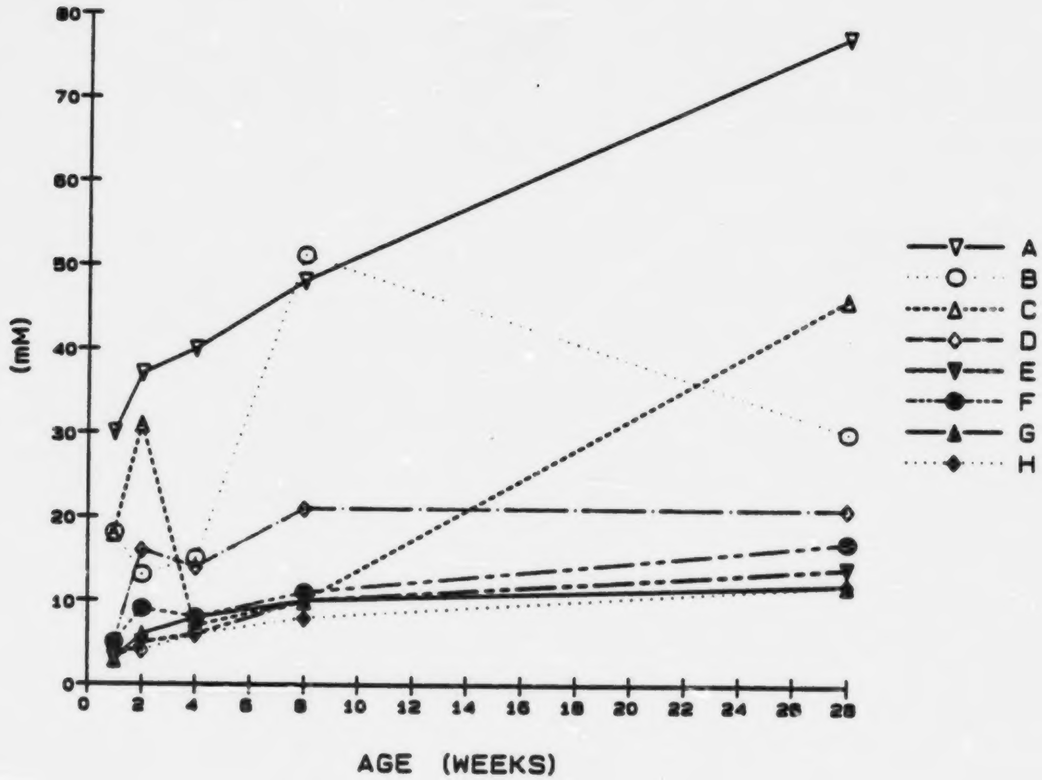

Figure 42. Levels of sulfate ion in pore solutions of limestone mortars.

BEST COPY AVAILABLE

increased throughout the time period, more rapidly from 1 to 4 weeks and less rapidly from 4 to 28 weeks.

These results differ from those reported by others. In studies where measurements were begun at lower ages, sulfate concentrations were shown to increase to a very high level, often as high as 200 mM during the first hour (Barneyback, 1983, and Penko, 1983), to maintain this level for some hours, then to decrease rapidly, reaching levels below 10 mM by 1 or 2 days (Penko, 1983, and Luke and Glasser, 1986). A second, gradual, limited increase in sulfate level has been observed between 1 week and 10 to 15 weeks, with values slowly increasing to a level between 5 and 10 mM (Longuet et al, 1973, Barneyback, 1983, and Silsbee et al, 1986), with one study reporting a level of 40 mM for this second maximum (Page and Vennesland, 1983). In no other studies were levels reported after 1 week as high as some levels in the present study. Pore solution analysis for the period before 1 week were not included in the present study, so changes in sulfate concentrations during the first week are not known. The expected gradual increase in sulfate level after 1 week was observed in solutions from all mortars in the present study. However, for two cements (A and C) the sulfate concentrations did not level off, but were still increasing at 28 weeks, a pattern not observed by other investigators.

Lithium. Weak peaks attributed to lithium were observed in the IC patterns of all pore solutions, so one calibration sample was analyzed to determine semiquantitatively the levels of lithium in pore solution samples. Lithium concentrations (Table 27) were very low; the highest level was 3 mM, and typical levels were less than 1 mM.

Table 27. Measured lithium levels in pore solutions of limestone mortars (mM)[a].

	Age (weeks)				
Cement	1	2	4	8	28
A	1	1	2	1	1
B	1	2	2	1	1
C	1	0	0	0	0
D	0	1	1	0	0
E	0	0	0	0	0
F	0	0	0	0	0
G	3	3	3	3	2
H	0	0	0	1	0

[a] Semiquantitative.

CHAPTER 4

IMPLICATIONS CONCERNING REACTION MECHANISMS

In the previous chapter, results of three separate experiments, length changes of mortar bars due to alkali-silica reaction, changes in pore solution composition with time, and reactions of aggregates in model pore solutions, were reported and compared to data of other investigators. In the present chapter, these results are discussed in greater detail, and interrelationships between various results are considered and their implications concerning alkali-silica reaction mechanisms are discussed.

Mortar Bar Expansion

In the previous discussion of the mortar-bar expansion results, it was noted that the expansion curves are similar in a number of respects. For each aggregate, expansion began immediately, the initial expansion rate was the most rapid, and expansion rates decreased continuously until low, steady values were reached after 18 to 24 weeks. The similarity of the curves, regardless of the final expansion level or the apparent reactivity of the aggregate, suggests that the curves may follow a single, general mathematical function, and that the specific parameters in such a function might provide a quantitative assessment of the tendency of each aggregate to cause expansion. As a preliminary effort, expansion data are plotted using various time scales in Figs. 43 through 46. Only data for Cement A is plotted, as this data appears typical of nearly all the

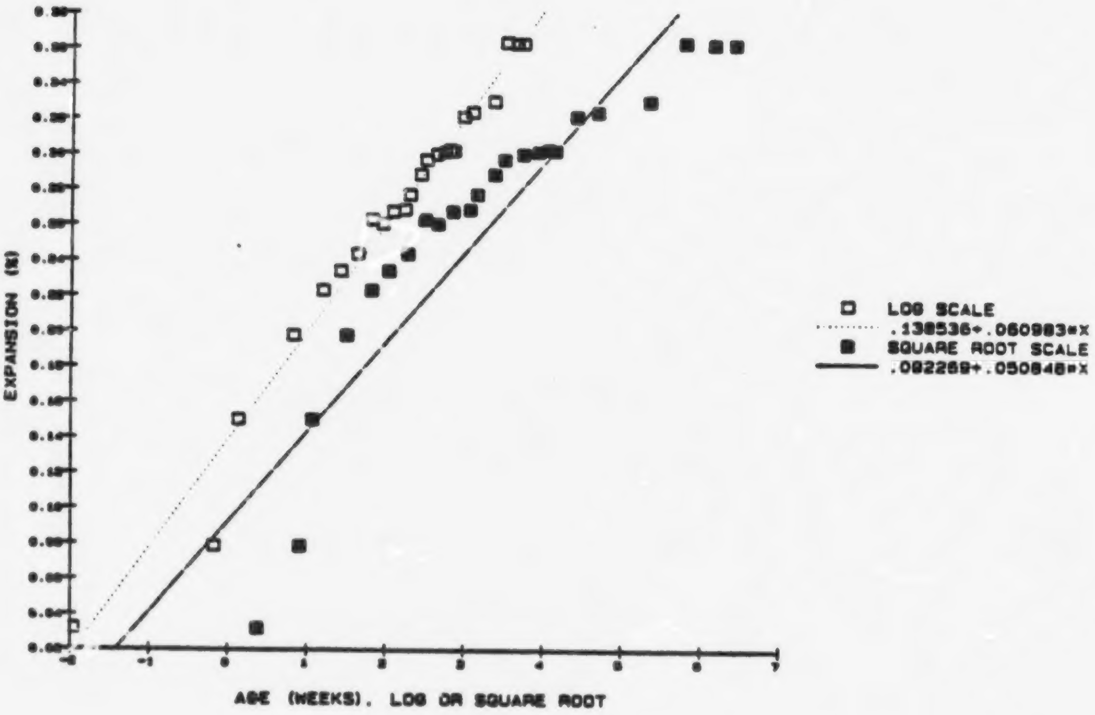

Figure 43. Expansion levels of mortar bars prepared with Cement A and 4% opal, shown on a log time scale and a square root time scale.

BEST COPY AVAILABLE

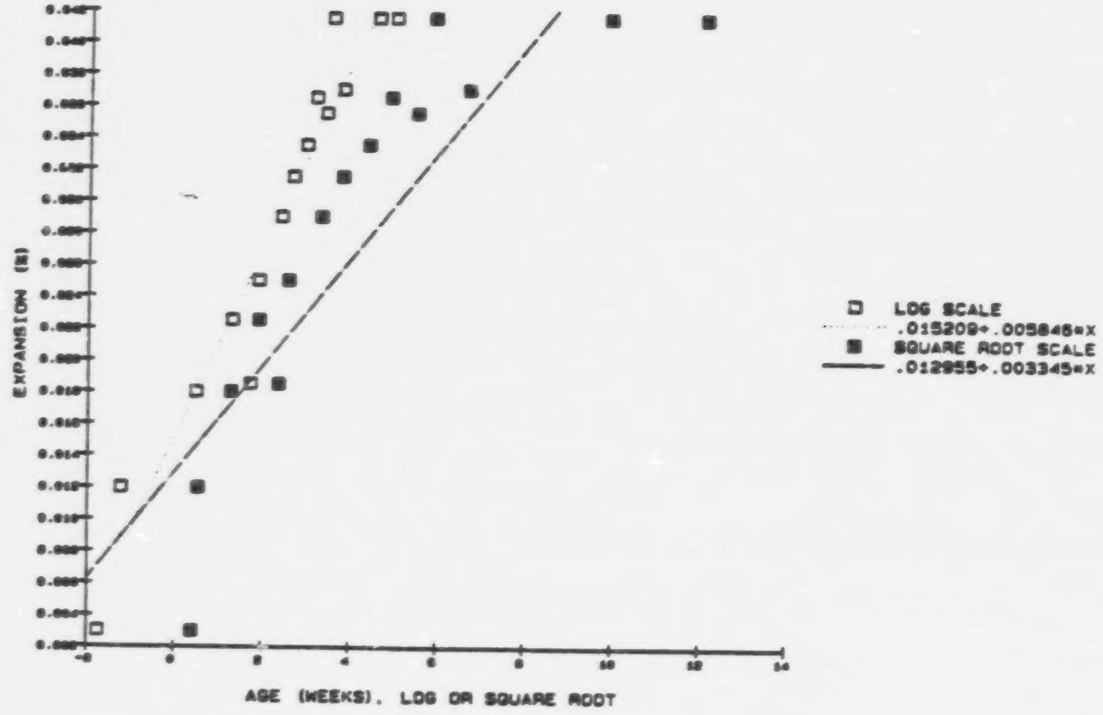

Figure 44. Expansion levels of mortar bars prepared with Cement A and 20% quartzite, shown on a log time scale and a square root time scale.

BEST COPY AVAILABLE

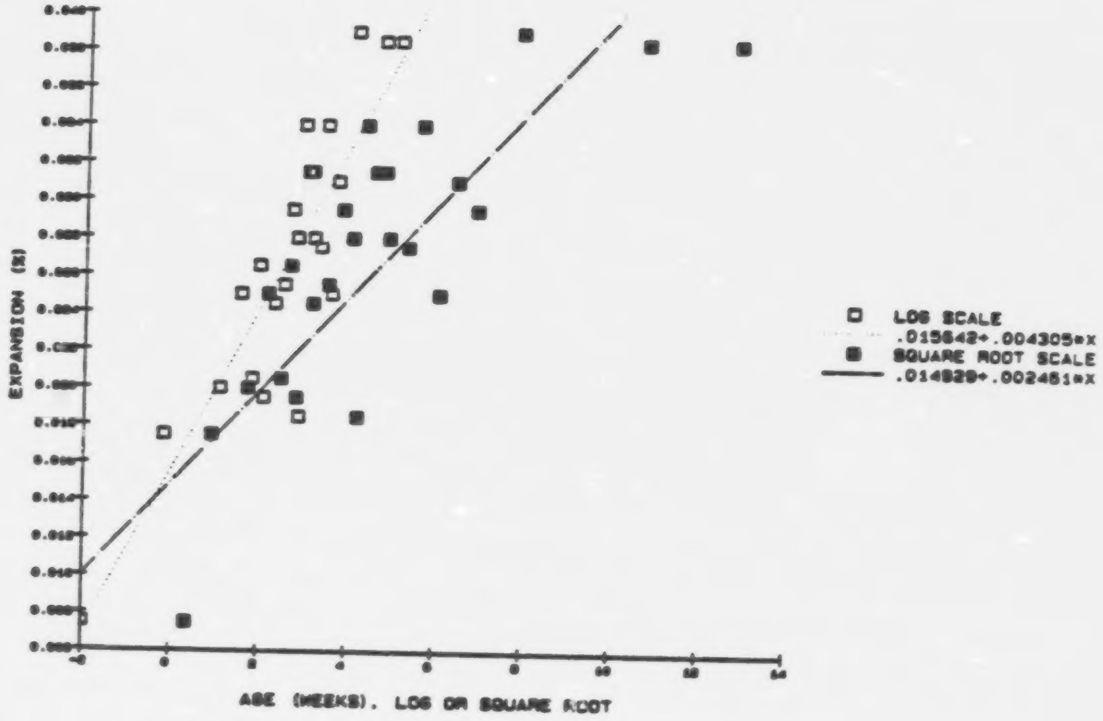

Figure 45. Expansion levels of mortar bars prepared with Cement A and granite, shown on a log time scale and a square root time scale.

BEST COPY AVAILABLE

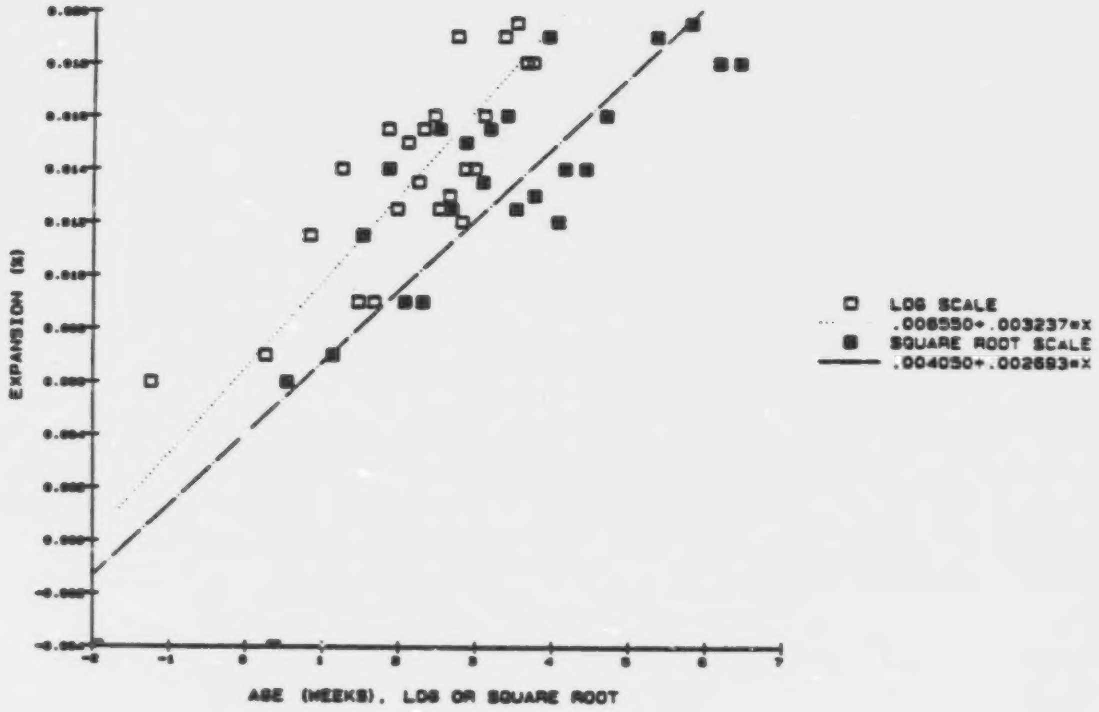

Figure 46. Expansion levels of mortar bars prepared with Cement A and limestone, shown on a log time scale and a square root time scale.

BEST COPY AVAILABLE

cements. The time scales were chosen because they have been used by other investigators.

The plots using a square root scale for time do not show a constant slope. This scale was used by Grattan-Bellew (1981) to develop quantitative relationships describing the reactivity of a large number of aggregate materials. His discussion was based on mortar-bar expansion data measured after exposure at 38°C, compared to ~22°C used in the present study. Grattan-Bellew divided the plots into three regions: an induction phase, a main expansion phase, and a late expansion phase. He noted that expansion varies linearly with the square root of time during the main expansion phase, and proposed that the slope of this line is a measure of reactivity. The present data differs from data reported by Grattan-Bellew in two respects: no induction phase was observed, and the expansion levels did not vary with the square root of time in a linear manner. However, the best straight-line fits using the square root of time provide the following slopes during the main expansion phase for Cement A (in units of percent expansion per square root day): 0.0522 for 2% opal; 0.0026 for 30% quartzite; 0.0023 for 100% granite; and 0.0016 for 100% limestone. These slopes are within the overall range reported by Grattan--Bellew. He further proposed a slope of 0.0064 as a demarcation value to distinguish expansive and non-expansive aggregates. By this measure, the opal would qualify as expansive, and the quartzite, granite, and limestone would qualify as non-expansive.

The expansion data for all aggregates used in the present study plot in a more nearly linear manner using a log scale for time. This scale has been used by others (for example Barneyback, 1983). The curves are similar for all cements used: expansion shows a single, linear relationship with log of time. These empirical efforts at fitting mortar-bar expansion data indicate that expansion tends to be linear with the log of time, but is not linear with the square root of time. Based on these results, functions were determined to describe expansion data for all mortars studied. These functions are listed in Table 28 and incorporated in the expansion plots of Figures 15 through 35. No interpretation of these results in terms of expansion mechanisms is attempted.

Cement Alkali Levels and Mortar Bar Expansion

The alkali levels and distributions in the eight cements and the mortar bar expansion results may indicate whether the alkali level and distribution in the cement influences expansion of mortar due to alkali-silica reaction. The expansion levels for each aggregate, at the level of substitution closest to the pessimum, are plotted in Figure 47 versus levels of total alkali. There appears to be a general correlation between the expansion with each aggregate and the total level of sodium plus potassium. Of the three aggregates tested, Beltane opal demonstrates the clearest relationship.

This relationship is far from perfect. Cement C has a much higher level of expansion than is expected based on this relationship, while Cement D and, to a lesser extent, Cement F have lower levels of expansion than are expected. These differences may be qualitatively related to the alkali distributions within the cements. Of the eight cements, D and F have the highest proportions of their total alkalies combined in the calcium silicate phases. Alkalies combined in the calcium silicate phases, particularly in C_2S, are expected to go into solution most slowly. Thus high concentration of alkali in C_2S, such that significant alkali does not become available for reaction until months or years of age, provides a tentative explanation for the lower than

Table 28. Functions used to describe expansion levels.

Cement	Reactive Material	Aggregate (%)	Function[a]
A	None[b]	0	y=0.007+0.003*ln(x)
	Granite	100	y=0.016+0.004*ln(x)
	Quartzite	10	y=0.010+0.006*ln(x)
		20	y=0.015+0.006*ln(x)
		30	y=0.016+0.005*ln(x)
		50	y=0.013+0.004*ln(x)
	Opal	2	y=0.166+0.017*ln(x)
		4	y=0.139+0.061*ln(x)
		8	y=0.135+0.006*ln(x)
		12	y=0.029+0.006*ln(x)
B	None	0	y=0.008+0.003*ln(x)
	Granite	100	y=0.016+0.003*ln(x)
	Quartzite	10	y=0.014+0.004*ln(x)
		20	y=0.018+0.004*ln(x)
		30	y=0.013+0.001153*ln(x)
		50	y=0.006+0.004*ln(x)
	Opal	1	y=0.015+0.012*ln(x)
		2	y=0.062+0.042*ln(x)
		4	y=0.016+0.014*ln(x)
		8	y=0.007+0.005*ln(x)
		12	y=0.009+0.003*ln(x)
C	None	0	y=0.001+0.003*ln(x)
	Granite	100	y=0.015+0.004*ln(x)
	Quartzite	10	y=0.011+0.007*ln(x)
		20	y=0.014+0.007*ln(x)
		30	y=0.017+0.006*ln(x)
		50	y=0.008+0.005*ln(x)
	Opal	1	y=0.027+0.014*ln(x)
		2	y=0.140+0.043*ln(x)
		4	y=0.067+0.035*ln(x)
		8	y=0.034+0.004*ln(x)
		12	y=0.005+0.005*ln(x)

[a] y is expansion (%) and x is age (weeks).

[b] 100% limestone aggregate.

(Table 28, continued)

Cement	Reactive Material	Aggregate (%)	Function
D	None	0	y=0.017+0.008*ln(x)
	Granite	100	y=0.018+0.003*ln(x)
	Quartzite	10	y=0.012+0.005*ln(x)
		20	y=0.009+0.005*ln(x)
		30	y=0.012+0.005*ln(x)
		50	y=0.010+0.004*ln(x)
	Opal	1	y=0.012+0.009*ln(x)
		2	y=0.014+0.019*ln(x)
		4	y=0.027+0.007*ln(x)
		8	y=0.007+0.005*ln(x)
		12	y=0.010+0.005*ln(x)
E	None	0	y=0.008+0.004*ln(x)
	Opal	1	y=0.011+0.007*ln(x)
		2	y=0.005+0.008*ln(x)
		4	y=0.005+0.005*ln(x)
		8	y=0.006+0.004*ln(x)
F	None	0	y=0.002+0.002*ln(x)
	Opal	1	y=0.009+0.005*ln(x)
		2	y=0.010+0.004*ln(x)
		4	y=0.013+0.003*ln(x)
		8	y=0.005+0.001*ln(x)
G	None	0	y=0.002+0.001*ln(x)
	Opal	1	y=0.007+0.005*ln(x)
		2	y=0.007+0.007*ln(x)
		4	y=0.012+0.003*ln(x)
		8	y=0.012+0.003*ln(x)
		12	y=-0.002+0.002*ln(x)
H	None	0	y=0.008+0.005*ln(x)
	Opal	1	y=0.005+0.006*ln(x)+0.0003*(x)
		2	y=0.002+0.008*ln(x) -0.0002*(x)+0.00002*(x^2)
		4	y=0.003+0.005*ln(x)
		8	y=0.003+0.004*ln(x)

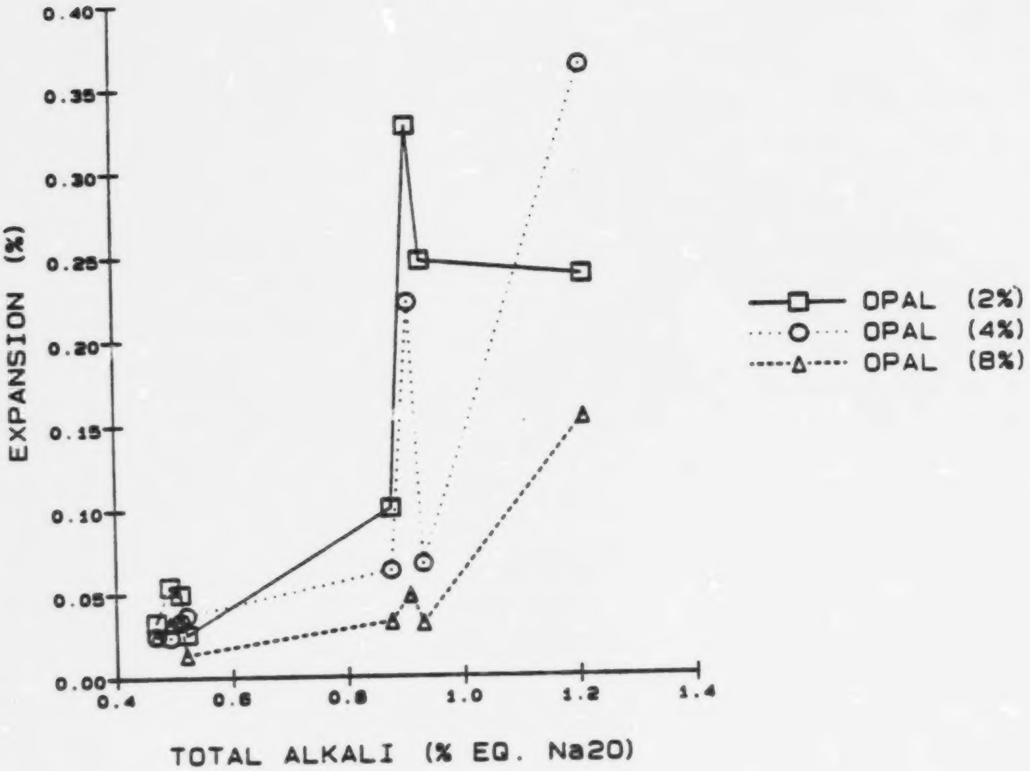

Figure 47. Final mortar bar expansion versus the total alkali level of each cement.

BEST COPY AVAILABLE

expected expansion of Cements D and F. However, it is more difficult to explain the higher than expected expansion of Cement C, whose alkali distribution is qualitatively similar to that of Cement A. The distributions of alkali provide tentative explanation in only some cases for why some cements in mortars containing opal show higher or lower expansions than expected.

As discussed previously, Davis (1951) reported that the ultimate levels of expansion were the same for two cements of the same composition, one prepared from a rapidly cooled clinker and the other from a slowly cooled clinker. He therefore concluded that the alkali distribution is not a significant factor in expansion. However, Brandt and co-workers (Brandt et al, 1981, and Brandt and Oberholster, 1983) used an available alkali test, i.e. a measure of the alkali soluble in 28 days, and found that expansion correlated more closely with the measured available alkali than with either the total alkali or the water-soluble alkali. These results suggest that there is an influence of alkali distribution on expansion. Therefore, the effects of alkali distribution on the relationship between expansion, at least for mortars containing opal, and alkali levels tend to support the relationship reported by Brandt and co-workers, and differ from Davis' interpretation.

Pore Solution Composition

The pore solution composition data presented in provide considerable information concerning steady state relationships among the various constituents in this complicated system. A major factor pertinent to alkali-aggregate reactions is the degree of alkalinity of the pore solution, more specifically its pH or hydroxide ion concentration. As discussed in Chapter 2 and Appendix A, the direct measurement of pH levels using a glass electrode and pH meter is difficult in these highly alkaline solutions. In order to assess the validity of the pH measurements made here, the pH levels obtained by direct measurements can be compared to pH levels calculated from the measured hydroxide ion concentrations. However, such comparison requires a knowledge of values for the activity coefficient of the hydroxide ion in each solution. Accurate assessment of activity coefficients in these solutions, which contain a number of ionic species in high concentrations, is difficult.

As a first approximation, the measured pH levels are compared to pH levels calculated from measured hydroxide ion concentrations using an activity coefficient of unity (Fig. 48). There is considerable scatter between the two values.

In fact, the hydroxide ion activity coefficients of these solutions are expected to be considerably less than unity, as was noted by Diamond (1975), and are expected to be variable depending on the composition of each solution. Thus it is difficult to assess the extent to which the scatter observed in Fig. 48 is due to experimental error in the pH measurement, as compared to the extent to which it is due to variation in the activity coefficient for hydroxide ions in the different solutions.

Measured pH levels would appear to provide a better indicator than measured hydroxide ion concentrations with respect to at least some aspects of chemical reactions in solution, as was suggested by Diamond (1975), if the experimental error in the pH measurement is sufficiently small. In the present work, pH levels rather than hydroxide ion concentrations are used as the primary basis for discussion, although hydroxide ion concentrations are also discussed.

Figure 49 is a plot of sulfate concentration level versus pH level for the pore solutions, which were expressed from the relatively nonreactive, limestone-bearing mortars at ages ranging from seven days to seven months. The sulfate concentration is plotted using a log scale and pH is

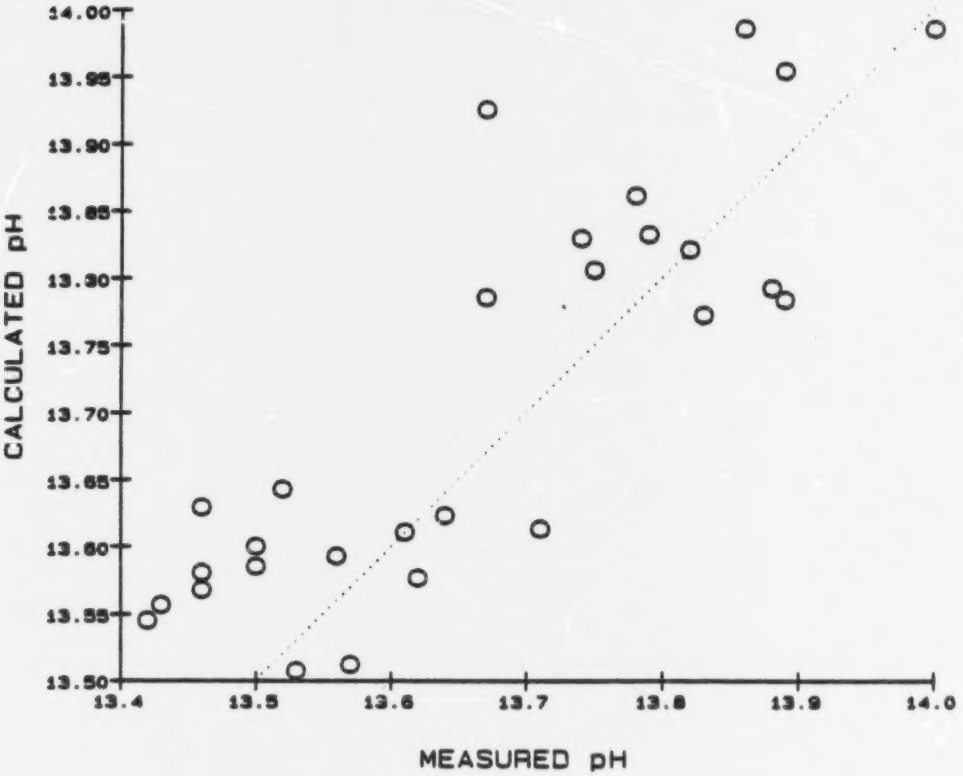

Figure 48. Calculated pH levels, from the measured hydroxide ion levels and an activity coefficient of unity, versus the measured pH levels in pore solutions of limestone mortars.

BEST COPY AVAILABLE

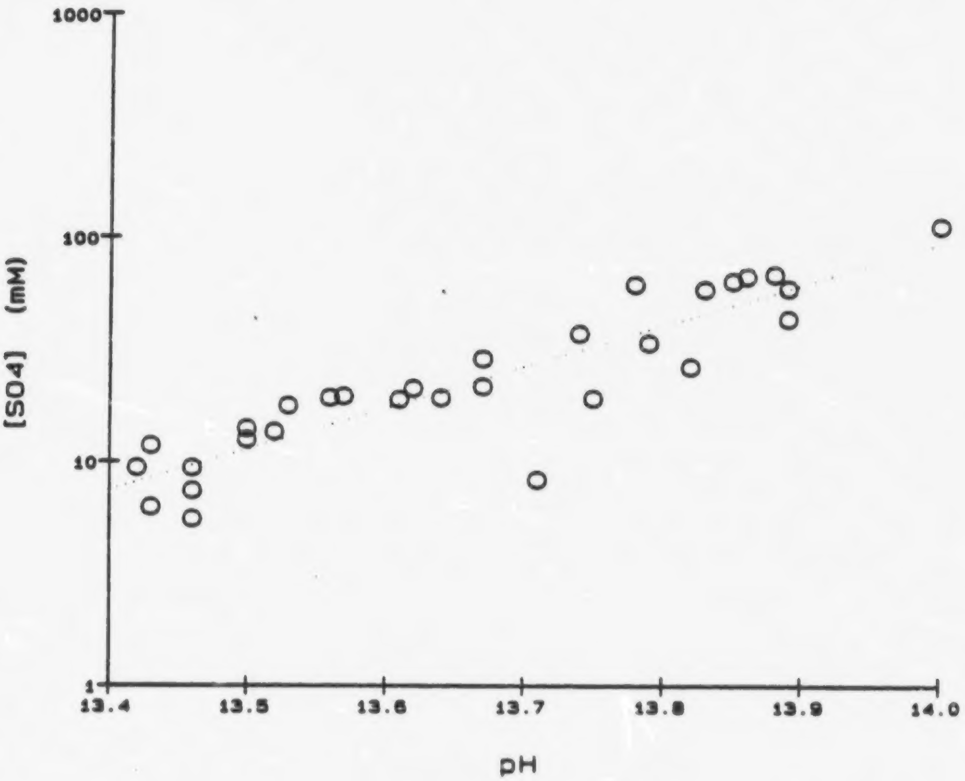

Figure 49. Measured sulfate levels versus measured pH levels in pore solutions of limestone mortars.

intrinsically a logarithmic function. For these pore solutions, a fairly close positive, linear relationship is observed between the log of sulfate concentration and the pH level (Fig. 49), i.e. high sulfate concentrations are associated with high pH levels. It should be pointed out that even the highest sulfate concentrations are small, of the order of 80 mM, as compared with hydroxide ion concentrations of nearly 1000 mM.

This is opposite to the relationship reported by Penko (1983) for pore solutions expressed from pastes at ages up to 24 hours. Penko noted an increase in hydroxide ion concentration with decreasing sulfate concentration, and attributed these changes to precipitation of a calcium sulfate phase and transformation of the pore solution from an alkali sulfate solution to an alkali hydroxide solution.

The relationship observed in the present study may similarly reflect an equilibrium response. The system is comprised principally of a solution containing calcium, sulfate, and hydroxide ions, solid calcium hydroxide, solid calcium silicate hydrate, and solid phases such as ettringite or calcium monosulfoaluminate that contain both calcium and sulfate. The sequence that Penko (1983) considered responsible for the inverse relationship between sulfate and hydroxide ion concentrations is initiated by precipitation of a calcium sulfate phase, which decreases the calcium concentration levels in solution and causes calcium hydroxide to dissolve and hydroxide ion concentration to increase. These changes occur over a few hours and at fairly constant alkali ion concentration. As hydration continues, however, potassium, sodium, and hydroxide ion concentrations continue to increase due to hydration of alkali-bearing cement phases. The increased hydroxide ion concentration level will cause calcium hydroxide to precipitate and the concentration of calcium to decrease. Decreased calcium concentration is expected to cause dissolution of calcium-containing phases, many of which also contain sulfate, causing the increase in sulfate concentration.

In contrast to the observed direct relationship between sulfate ion concentration and pH, the measured concentrations of silica show a tendency towards an inverse relationship with pH (Fig. 50). The measured levels of dissolved silica are extremely low, typically on the order of 0.01 mM. The solutions expressed from 7-day old mortars prepared with the four low-alkali cements show slightly higher silica levels, up to 0.04 mM. The same solutions also have the lowest pH levels, providing most of the basis for the apparent inverse relationship.

It was mentioned in the previous chapter that the silica concentration levels in the present study are much lower than the levels reported by Silsbee et al (1986). Additional discussion of this point is appropriate. Silsbee et al offered as explanation for their high silica concentration levels a plot of their data and earlier data of Kalousek (1944) for equilibrium concentration levels of silica in an aqueous system containing sodium, calcium, and silica. This plot shows an increase in silica concentration with increasing pH, with silica concentrations up to ~10 mM at pH ~13.6. The general relationship between silica and pH in studies of silica dissolution in alkaline solutions as discussed by Iler (1979) and reviewed in Chapter 1, is that silica concentration in ordinary alkaline solution increases with increasing pH. This tendency was indeed demonstrated in the present work in results for aggregate reactions in model pore solutions. The reactions produced very high silica concentrations, in some cases in excess of 1 M, and higher silica levels were associated with higher pH levels.

However, it is evident that the silica concentration levels observed in the pore solutions expressed from limestone mortars are very much lower than those found by Silsbee et al and several orders of magnitude lower than

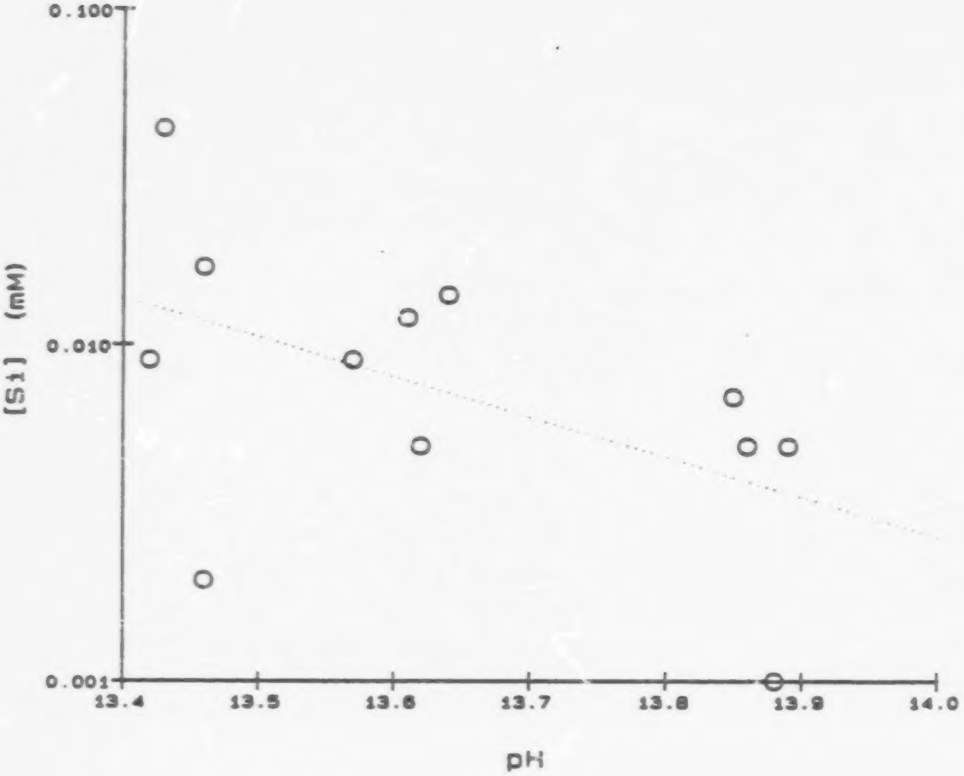

Figure 50. Measured silica levels versus measured pH levels in pore solutions of limestone mortars.

BEST COPY AVAILABLE

those produced by reactions of aggregates in model pore solutions. It is believed that the present values, and not the results of Silsbee et al, are representative generally of pore solutions in cement-based pastes and mortars. Furthermore, it appears that the silica level in such solutions is controlled not by the pH level but by some other variable, most likely the presence of calcium available for reaction.

At least to a first approximation, it is expected that the level of calcium dissolved in pore solution should decrease with increasing pH, in response to the common ion effect applied to the $Ca(OH)_2$ dissolution. This relationship was the basis for the suggestion by Powers and Steinour (1955), reviewed in Chapter 1, that the calcium content of alkali-silica reaction product affects the tendency of the gel to cause expansion, that a low-calcium, swelling gel is produced with a high-alkali cement, and a high-calcium, nonswelling gel is produced with a low-alkali cement. In examining results for the pore solutions expressed from the present mortars (Fig. 51), there does not appear to be such a relationship between calcium concentration level and pH level. The calcium levels in solutions with high-alkali cements range from 0.6 mM to 2.5 mM; those from low-alkali cements similarly range from 0.6 mM to 2.2 mM. There is very little difference in calcium concentration in the pore solutions of these eight cements. It appears unlikely that any small differences that may occur in the calcium concentration of pore solutions from high-alkali or low-alkali cement would cause a major difference in calcium level of the gel reaction product, and thus produce a swelling gel on the one hand, and a non-swelling gel on the other.

Pore Solution Composition and Alkali Distribution

Levels of alkali expected in a mortar pore solution may be estimated using the alkali distribution of the cement,

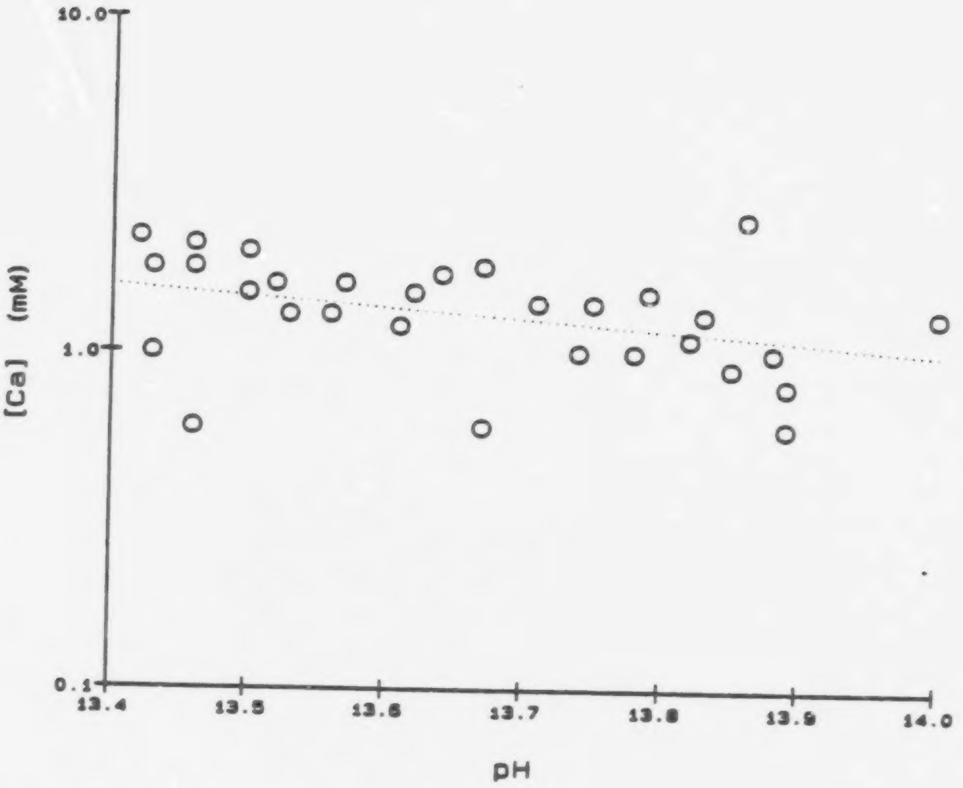

Figure 51. Measured calcium levels versus measured pH levels in pore solutions of limestone mortars.

BEST COPY AVAILABLE

the initial water-cement ratio, and the degree of hydration of the cement. These estimated alkali levels may be compared to the sodium and potassium concentration levels observed in pore solutions to demonstrate whether for each cement the observed levels are reasonable and consistent. Comparisons may also provide a test of the hypothesized relationship between the distribution of alkalies among various cement phases and the pore solution composition, a relationship based on expected differences in the rate at which the principal alkali-containing phases dissolve or hydrate.

The calculations used to estimate sodium and potassium levels in the pore solutions are presented in Appendix E. A number of simplifying assumptions were made to facilitate these comparisons. It was assumed that the alkali determined to be in the calcium silicate portion of the cements are derived solely from C_2S. Similarly, it was assumed that the alkali determined to be in the calcium aluminate and calcium aluminoferrite portion of the cements are derived solely from C_3A. The level of bound water (i.e. water chemically combined in hydrated phases) must be known to calculate the level of alkali in pore solution. Since bound water contents were not determined for the mortars in the present study, these levels were estimated using values reported by others. It was assumed that all the cements hydrate at the same rate, i.e. that the rate of reaction of each of the phases is the same for all eight cements. This assumption provides that the overall rate of increase in bound water is the same for all eight cements. Finally, the amount of the alkali bound in hydrated phases (in the absence of alkali-aggregate reaction) was disregarded. Bhatty and Greening (1978) reported that alkali are bound in synthetic C-S-H gels at a level that depends on the Ca/Si ratio of the gel, as discussed in Chapter 1. However, the Ca/Si molar ratios covered in that study ranged from 0.9 to 1.5. Extrapolating to a Ca/Si ratio of 1.8, a reasonable level for C-S-H gel that forms during cement hydration (Taylor, 1986), it appears that the level of bound alkali in such C-S-H is negligible. Based on this limited information, it seems reasonable to ignore bound alkali for the present approximation.

The objective of the present calculation is to develop models for generating curves of alkali concentration levels in pore solution between 1 and 28 weeks, and to compare the calculated curves to the measured results. Three models are used. The basis for Models 1 and 2 is that alkali levels in pore solution depend on how alkalies are combined in each cement phase and how rapidly each cement phase hydrates. The basis for Model 3 is that alkali levels in pore solution do not depend on how the alkalies are combined.

For Model 1, the hydration rates were estimated from curves of Pratt and Ghose (1983). The curves were based on quantitative analysis using a scanning electron microscope of the residual unhydrated cement phases during hydration of a single cement sample. For Model 2, hydration rates were taken, directly or by extrapolation, from data of Dalzeil and Gutteridge (1986), based on quantitative X-ray diffraction analysis of unhydrated cement phases during hydration of a different cement sample. For Model 3, the hydration rates of the various cement phases were not considered.

For all three models, the bound water contents were taken, directly or by extrapolation, from data of Dalzeil and Gutteridge (1986), which had been calculated from the ignition losses at 100°C and 750°C. The same calculations using bound water contents reported by Jons and Osbaeck (1982) and by Barneyback (1983) gave similar results, so calculations are shown using only the one set of bound water data. However, it should be noted that Taylor recently challenged the practice of using bound water determined by measuring water retained after oven-drying to represent the amount of water not in the pore solution (Taylor, 1987).

The concentration levels of sodium and potassium were calculated as follows. For each age (1, 2, 4, 8, and 28 weeks), the alkali contributions from the alkali sulfates, from C_3A, and from C_2S were added. The alkali contributions from each were estimated using the amount of alkali determined for each phase (Tables 12 and 13) and the proportion of each phase that is hydrated according to the particular model, as discussed previously. The calculated amounts of alkali were divided by the estimated amount of unbound water for that age.

The results of these calculations are shown in Figs. 52 through 59. It appears from those figures that the two models based on alkali distribution, Models 1 and 2, give quite similar levels of sodium and potassium. This similarity is particularly interesting in that the two models were based on data for proportion of each phase reacted obtained using different cements and different experimental techniques. The alkali concentration levels calculated ignoring alkali distribution, according to Model 3, are generally higher than the levels calculated according to Models 1 and 2, particularly for those cements containing appreciable levels of alkali combined in other forms than alkali sulfates.

Although the calculated values of both potassium and sodium tend to be higher than the measured values, the values calculated according to Models 1 and 2 are nearly always closer to the measured values than are the values calculated according to Model 3. For Cements A and C, the agreement between measured values and values calculated according to Models 1 and 2 is only fair, and for Cements E, F, and H, the agreement is particularly close. In some cases a decrease was observed in measured concentration levels, especially for potassium, between 8 and 28 weeks.

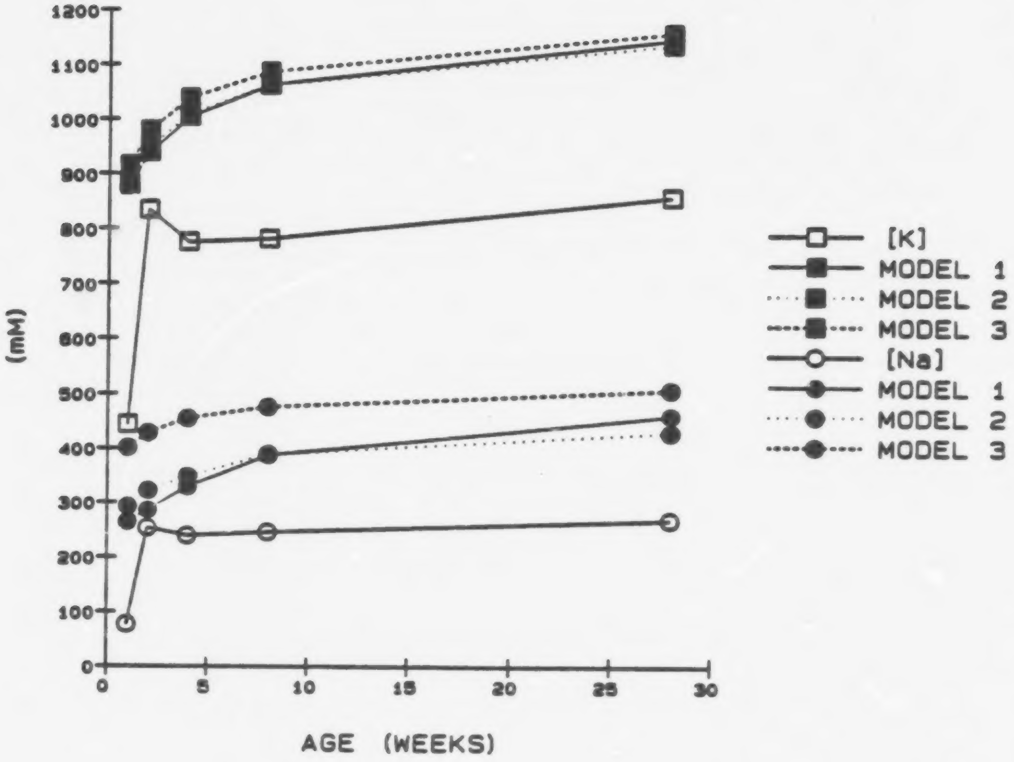

Figure 52. Alkali concentration levels in pore solutions of limestone mortars prepared using Cement A, measured and calculated according to various models.

BEST COPY AVAILABLE

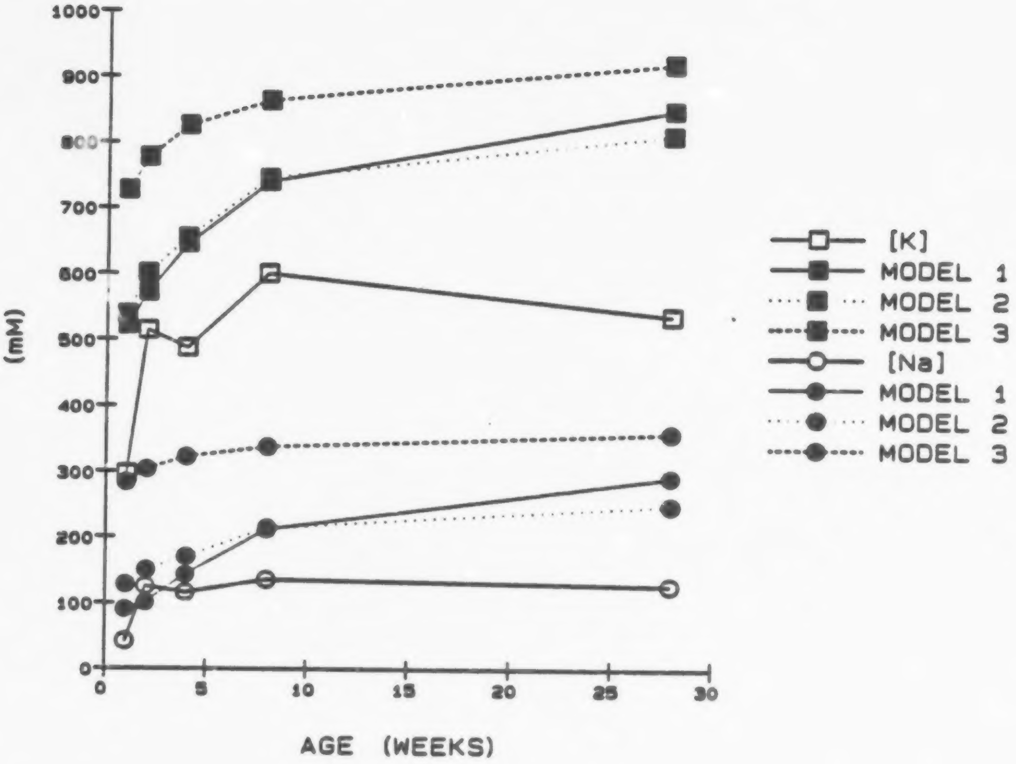

Figure 53. Alkali concentration levels in pore solutions of limestone mortars prepared using Cement B, measured and calculated according to various models.

BEST COPY AVAILABLE

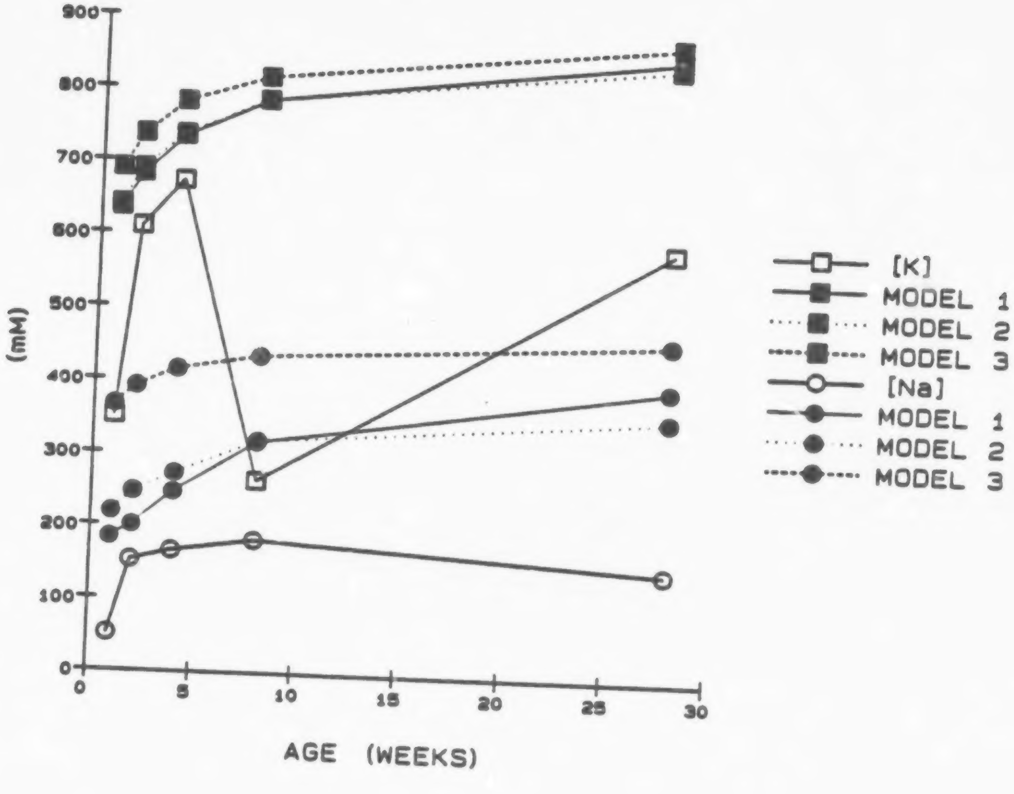

Figure 54. Alkali concentration levels in pore solutions of limestone mortars prepared using Cement C, measured and calculated according to various models.

BEST COPY AVAILABLE

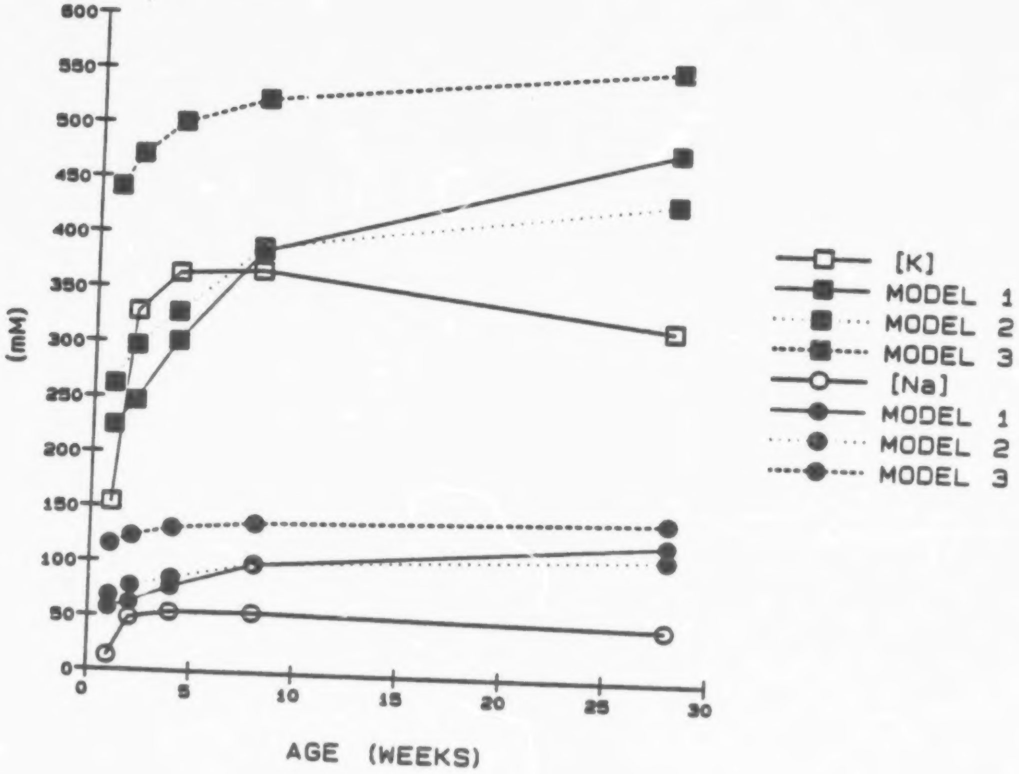

Figure 55. Alkali concentration levels in pore solutions of limestone mortars prepared using Cement D, measured and calculated according to various models.

BEST COPY AVAILABLE

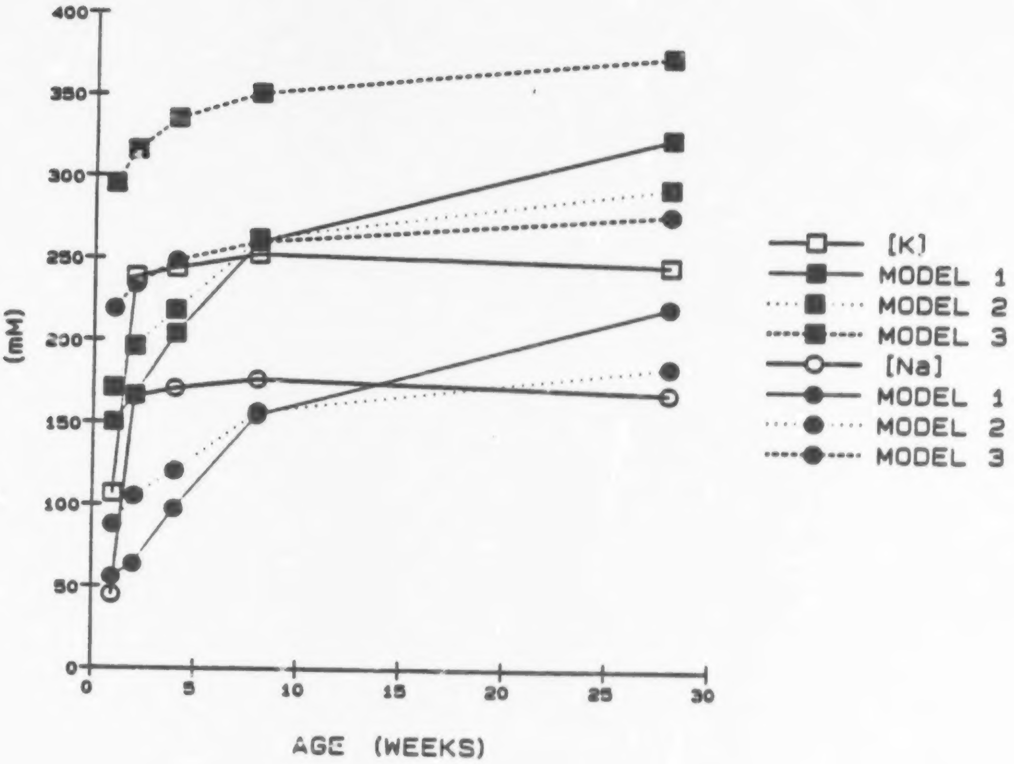

Figure 56. Alkali concentration levels in pore solutions of limestone mortars prepared using Cement E, measured and calculated according to various models.

BEST COPY AVAILABLE

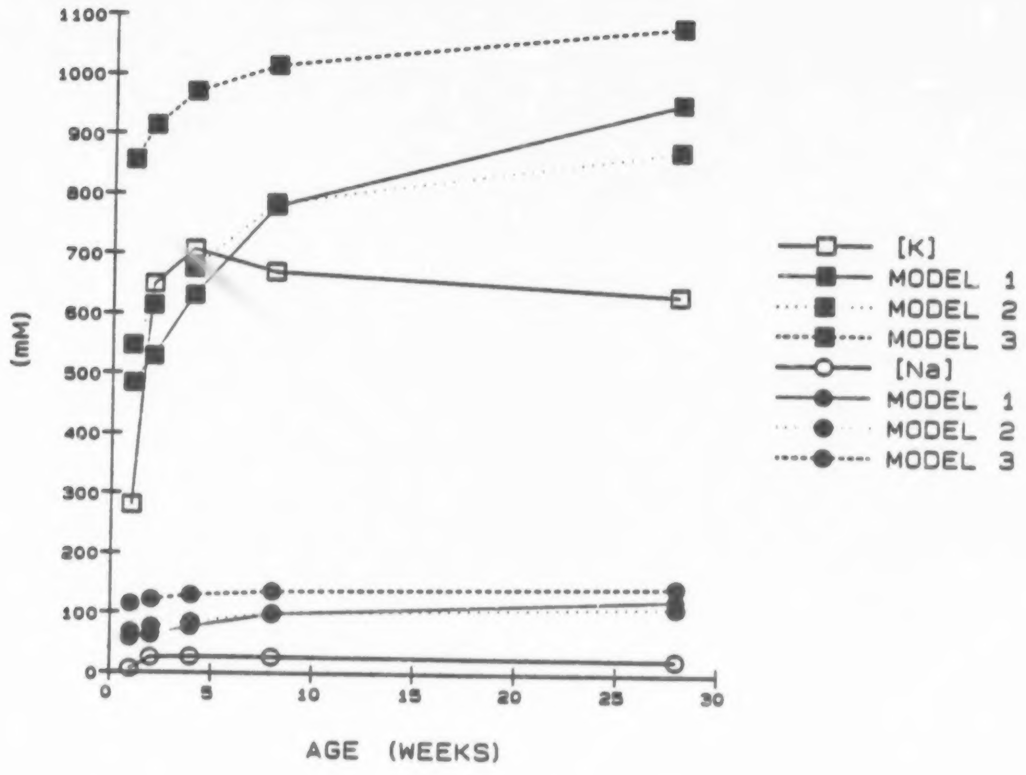

Figure 57. Alkali concentration levels in pore solutions of limestone mortars prepared using Cement F, measured and calculated according to various models.

BEST COPY AVAILABLE

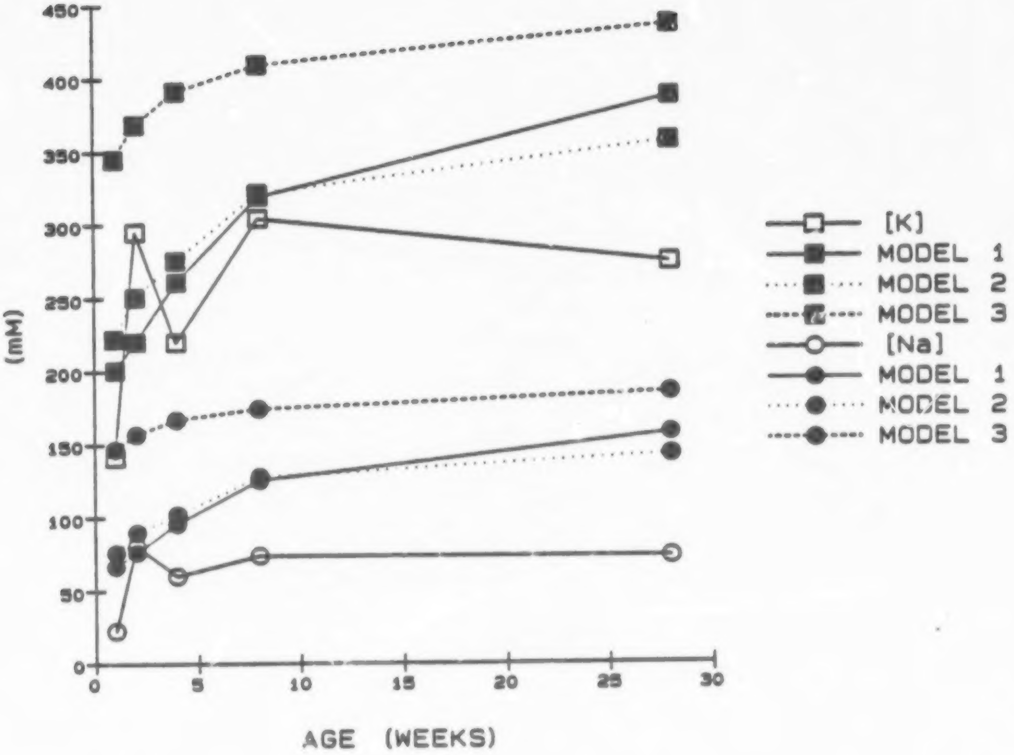

Figure 58. Alkali concentration levels in pore solutions of limestone mortars prepared using Cement G, measured and calculated according to various models.

BEST COPY AVAILABLE

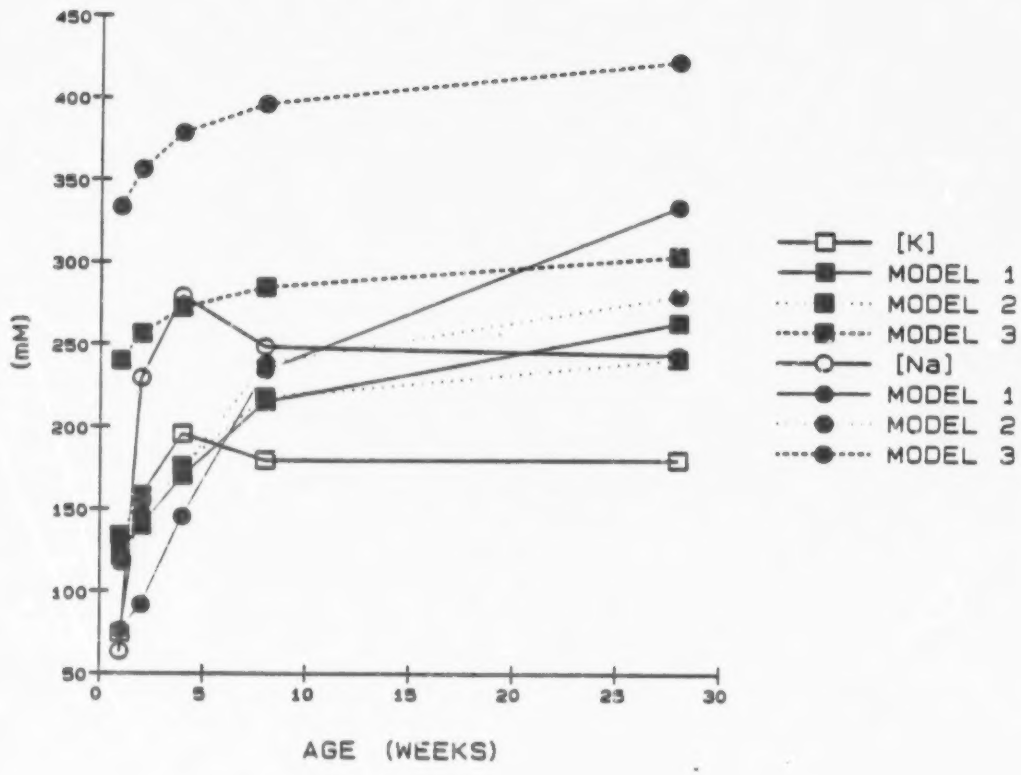

Figure 59. Alkali concentration levels in pore solutions of limestone mortars prepared using Cement H, measured and calculated according to various models.

BEST COPY AVAILABLE

None of the three models provide for such a decrease in the calculated concentration levels. The decrease is attributed to binding of alkali by calcium silicate hydrate gel. Finally, for every cement the measured concentration levels of both sodium and potassium are much lower at 1 week than at 2 weeks and beyond. Although the calculated levels follow the same pattern, no model produced as great a difference in the calculated alkali concentration levels between 1 week and 2 weeks as was measured.

The consistent difference between calculated and measured values at one week raises the possibility that not all alkalies from sulfate phases are in solution at this time. The very rapid dissolution rates observed during water-soluble alkali measurements indicate that the sulfate phases dissolve within seconds in that test, which utilizes a much greater proportion of water. In the present mortars, with restricted water contents, a tentative explanation may involve precipitation of some alkali-containing hydrate whose solubility is lower than that of the anhydrous alkali sulfate phases.

Pore Solution Composition and Mortar Bar Expansion

In order to explore relationships between expansion and pore solution composition, the expansion levels determined for mortars containing various levels of reactive aggregate are plotted versus the concentrations of certain constituents measured in pore solutions expressed from limestone mortars. These data are plotted as final expansion levels versus the concentrations in pore solutions expressed at 28 weeks.

The solutions expressed from limestone mortars represent the presumed baseline concentrations in the absence of alkali-silica reaction. Since it appears that the limestone reacted at least in terms of altering pH of model pore solutions, the baseline data itself is not completely uninfluenced by aggregate reactions. The observed data indicate the potential solution compositions, as influenced by cement composition and hydration, that are available for reaction with specific aggregates in mortars containing reactive aggregate.

There appears to be a direct relationship, though not consistent, between expansion and baseline pH (Fig. 60). There are two exceptions to the general relationship of expansion and pH. One is the low expansion observed for the cement whose baseline pore solution pH was 13.89; this is Cement D, whose anomalously low expansion potential has been noted previously. The other exception is an apparent decrease in expansion at pH levels between 13.88 and 14.0 for 2% opal. This decrease appears to be a result of the difference in pessimum proportion between the cements generating these pH levels. The opal pessimum proportion for Cement A was 4%; the opal pessimum proportion for Cements B, C, and D, which produce the lower pH levels, was only 2%. Since expansion for 2% opal decreased between pH 13.88 and 14.0, the pH levels of the pore solution do not appear to explain the pessimum effect.

Figure 60 indicates that for Beltane opal at its pessimum proportion, there is a threshold in pH, below which there is little or no expansion, and above which there is significant expansion. This threshold appears to be somewhere in the gap between 13.65 and 13.83. The threshold is consistent with earlier suggestions concerning a threshold concentration of hydroxide ion required for expansion. Diamond (1983) suggested a threshold around 0.25 M, equivalent to pH 13.4 using an hydroxide ion activity coefficient of unity. Kollek et al (1986) suggested thresholds of 0.3 M for fly ash and 0.4 M for natural pozzolan, similarly equivalent to pH 13.5 or 13.6. It appears from the present results that the measured pH threshold is higher than the

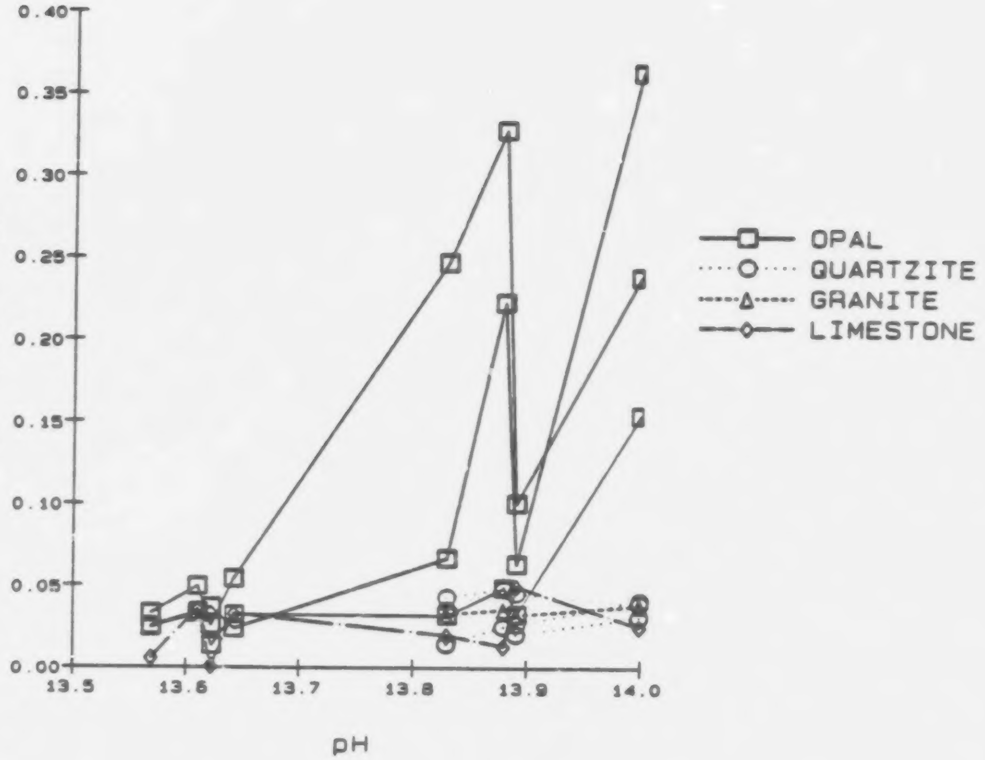

Figure 60. Final mortar bar expansion with various reactive aggregates versus pH levels of the pore solutions in limestone mortars.

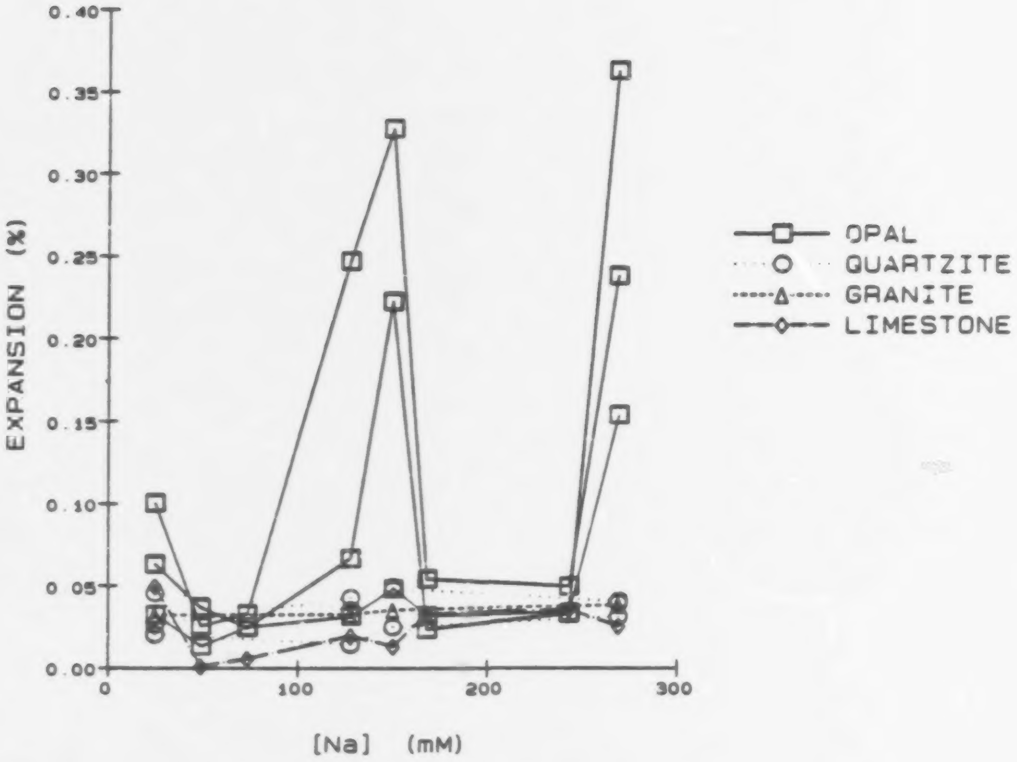

Figure 61. Final mortar bar expansion with various reactive aggregates versus sodium concentrations of the pore solutions in limestone mortars.

levels suggested by these investigators, possibly reflecting the lower activity coefficients.

Figure 61 indicates no direct relationship between expansion and sodium ion concentration in the pore solution. Highest expansion levels occur with cements producing both intermediate and high concentrations of sodium. Similarly, Figure 62 indicates only a general and somewhat inconsistent relationship between expansion and potassium concentration in the baseline pore solution. As might be expected, Fig. 63 indicates a much closer relationship between expansion and the combined level of sodium plus potassium in the baseline pore solution.

Figure 64 indicates no observable relationship between expansion and the level of calcium in the baseline pore solution. These results contradict the hypothesis of Powers and Steinour (1955), that at high concentrations of alkali, and thus low concentrations of calcium, the alkali-silica gel would be low in calcium and thus tend to swell; while at low concentrations of alkali, and thus high concentrations of calcium, the gel would incorporate appreciable calcium and not tend to swell. These hypotheses were developed long before techniques were available for expressing and analyzing pore solutions from hardened pastes and mortars. Such solutions all contain low levels of calcium. In the present study, calcium levels from both low- and high-alkali cements are 2 mM and less, while sodium and potassium levels are never lower than 150 mM, and in some cases higher than 400 mM even from low-alkali cements. Equally important, the actual levels of dissolved calcium do not show the expected inverse relationship with alkali or with pH. Finally, there is clearly no relationship between expansion and calcium level.

Another ion that is known to influence the expansion due to alkali-silica reaction is lithium. In the present study, no relationship was observed between expansion of

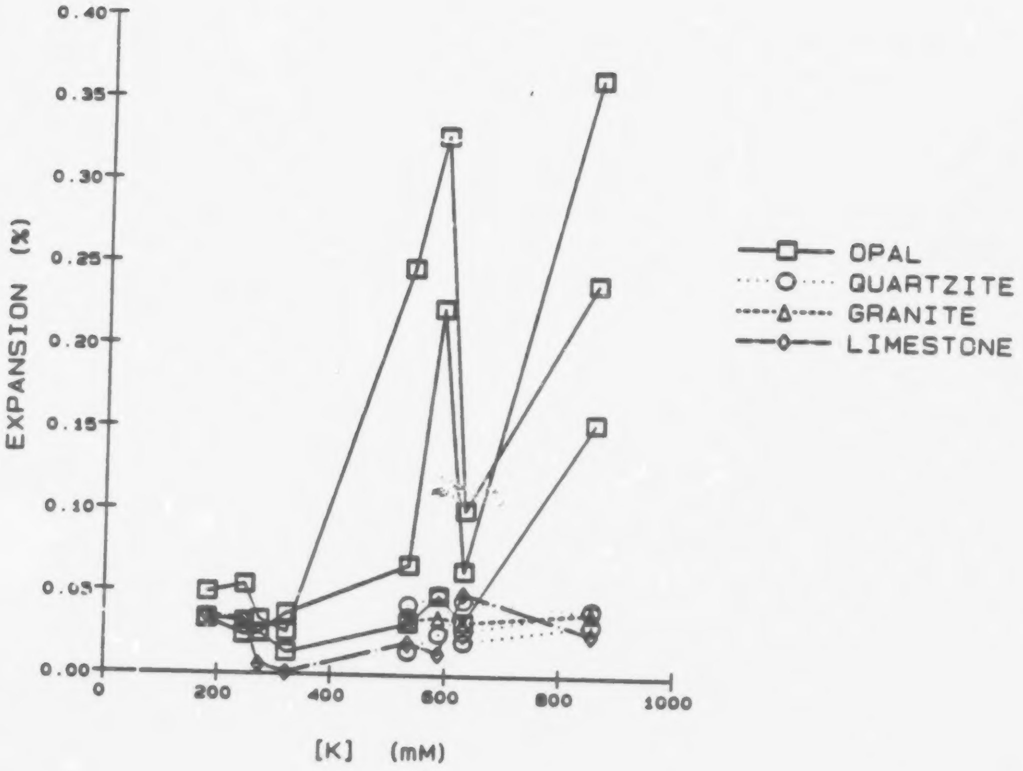

Figure 62. Final mortar bar expansion with various reactive aggregates versus potassium concentrations of the pore solutions in limestone mortars.

BEST COPY AVAILABLE

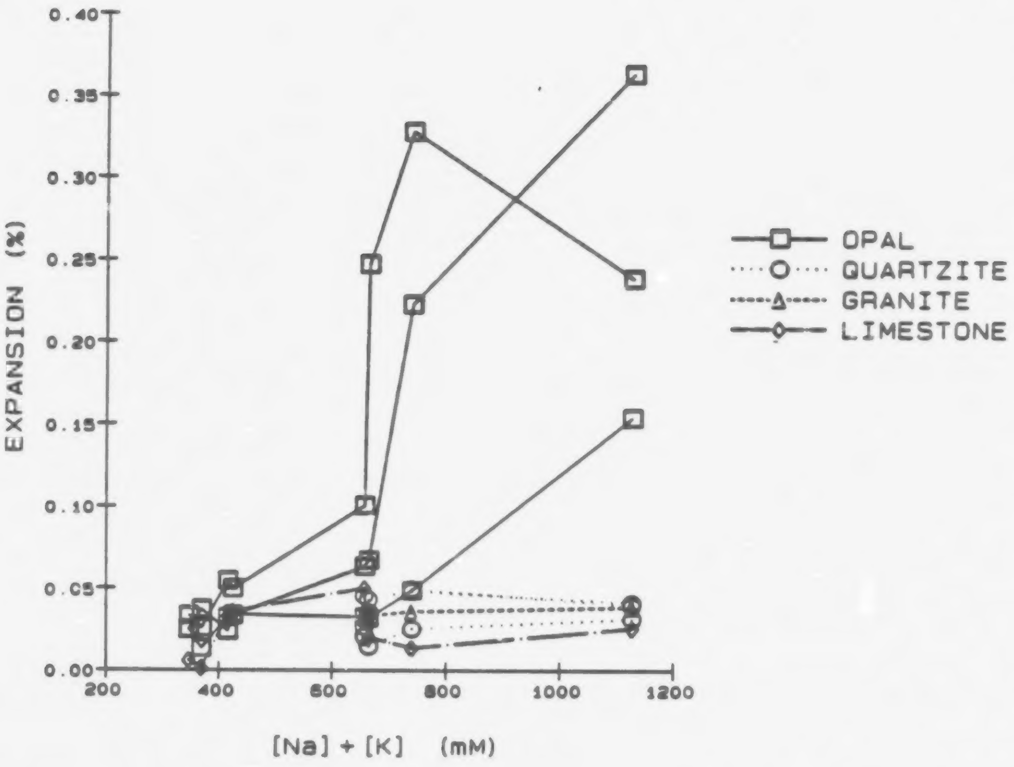

Figure 63. Final mortar bar expansion with various reactive aggregates versus total alkali (sodium plus potassium) concentrations of the pore solutions in limestone mortars.

BEST COPY AVAILABLE

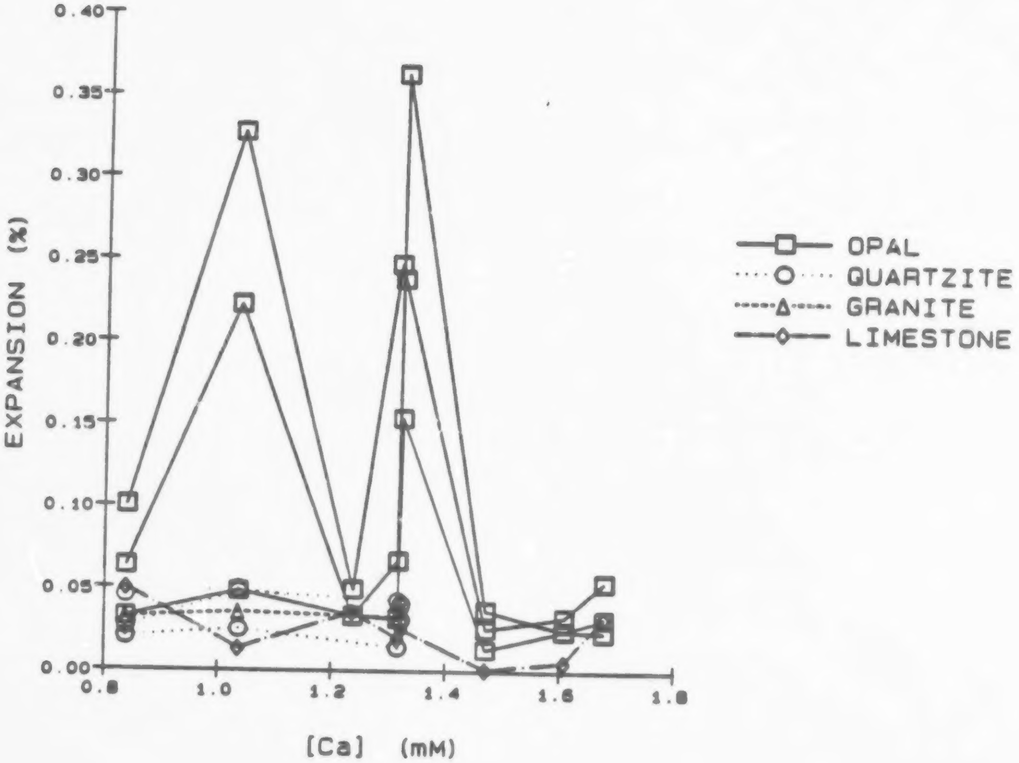

Figure 64. Final mortar bar expansion with various reactive aggregates versus calcium concentrations of the pore solutions in limestone mortars.

BEST COPY AVAILABLE

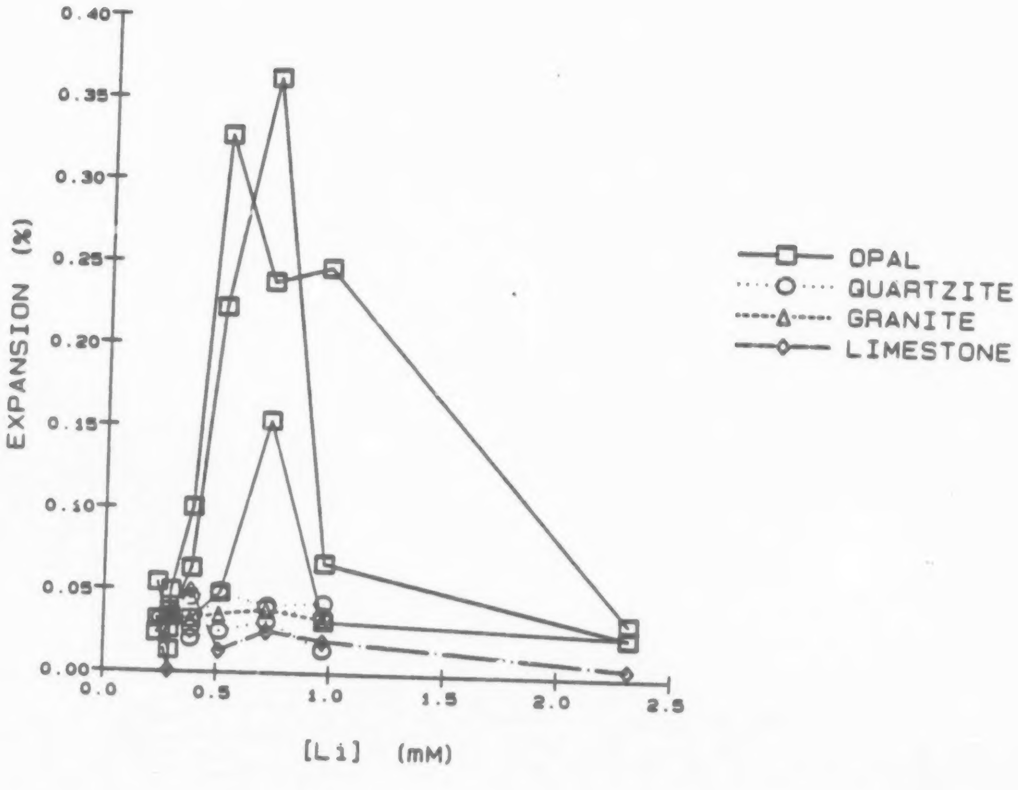

Figure 65. Final mortar bar expansion with various reactive aggregates versus lithium concentrations of the pore solutions in limestone mortars.

BEST COPY AVAILABLE

mortars containing reactive aggregate and the lithium levels measured in baseline mortar solutions (Fig. 65). This was not surprising; lithium concentrations found in the pore solutions were only a few mM, whereas concentrations reported to decrease expansion were 0.5 M and higher (McCoy and Caldwell, 1951, Lawrence and Vivian, 1961, Barneyback, 1983).

The mechanism for alkali-silica reaction and expansion developed in Chapter 1 involves first formation and then swelling of gel. Gel formation is thought to depend on the concentration of hydroxide ion in the pore solution, as well as certain features of the aggregate. Once formed, the tendency of gel to swell is thought to depend on its chemical composition, which also is expected to depend on the composition of the pore solution. Therefore, the data were examined separately for the cements whose pore solutions have higher pH levels, i.e. the four high-alkali cements, and the cements whose pore solutions have lower pH levels, i.e. the four low-alkali cements. When data of the high-alkali cements are analyzed separately (Fig. 66), there is a significant relationship between expansion and sodium concentration in the baseline pore solution, a relationship that was not observed when data of all eight cements were examined (Fig. 61). Potassium levels do not appear to influence expansion produced by the high-alkali cements (Fig. 67). The direct relationship between expansion and the combined sodium plus potassium concentrations does hold in comparisons for the high-alkali cements (Fig. 68).

Although expansion is typically discussed in terms of the sum of sodium and potassium, there is some evidence regarding possible differences in the influence of sodium and potassium. Davis (1958) concluded that sodium had more influence than potassium in the final expansion, though the opposite effect was noted in early stages of expansion. Usmanov and co-workers (Pulatov and Usmanov, 1976, and

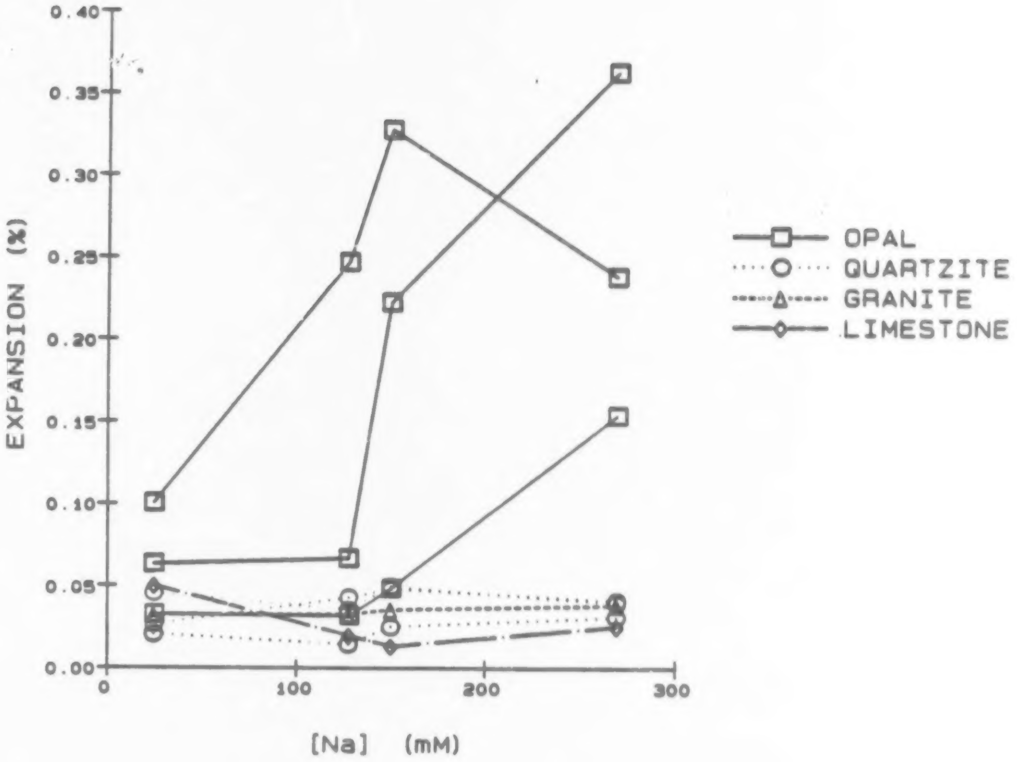

Figure 66. Final mortar bar expansion with various reactive aggregates versus the sodium concentration of the pore solutions in limestone mortars of the high-alkali cements.

BEST COPY AVAILABLE

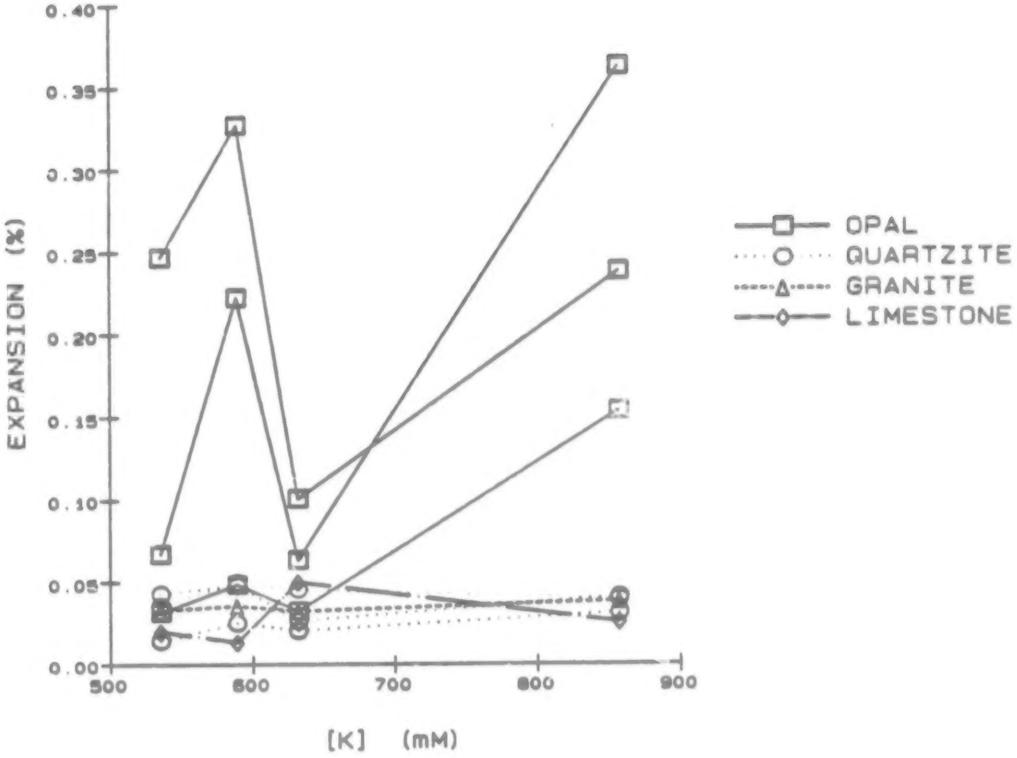

Figure 67. Final mortar bar expansion with various reactive aggregates versus the potassium concentration of the pore solutions in limestone mortars of the high-alkali cements.

BEST COPY AVAILABLE

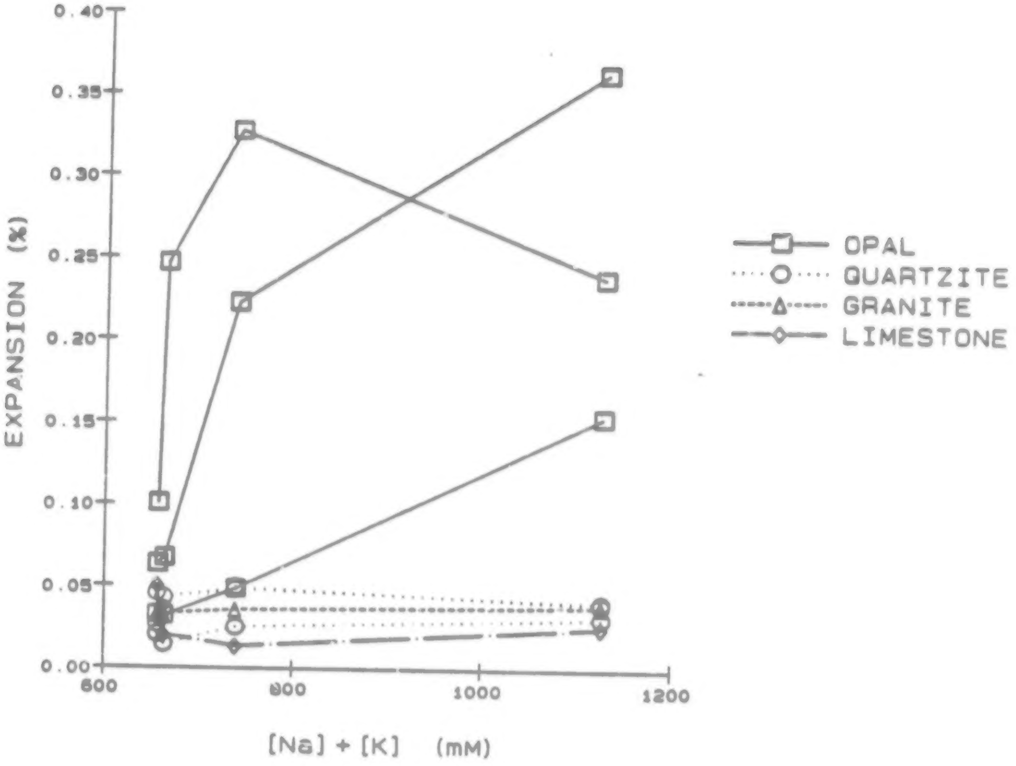

Figure 68. Final mortar bar expansion with various reactive aggregates versus the sodium plus potassium concentrations of the pore solutions in limestone mortars of the high-alkali cements.

BEST COPY AVAILABLE

Usmanov et al, 1977) also concluded that sodium has a greater effect than potassium on expansion. Results of the present study may be taken as tending to support these conclusions.

Thus the results indicate that the influence of the various cements on expansion may be explained by two separate factors: a general influence of pH (more accurately of hydroxide ion concentration) on expansion, and a specific influence of the level of alkalies in the pore solution. Results suggest a clear influence on expansion of the combined sodium plus potassium level and a possible influence of sodium level alone, but no influence of potassium level alone.

Aggregate Reactions in Model Pore Solutions

The measured changes in solution composition induced by reaction of aggregates in the model pore solutions may provide evidence concerning whether the rates and levels of dissolution of these aggregates influence their tendency to cause expansion of mortar. The results are discussed in terms of the dissolution reactions involved, then related to the expansion data.

Two important cautions should be noted at the outset of this discussion. This study was carried out only for three weeks, at which time the reactions had clearly not terminated. Therefore any interpretations are tentative in nature. Second, the level of any dissolved substance in solution is influenced by two processes, dissolution of the aggregate and precipitation of any reaction product. While no reaction product was observed by visual inspection, more rigorous evidence that no gel precipitated must be provided in order to consider that the concentration of silicon found in solution is a measure of the total amount of dissolved silica. However, the extraordinary variation in level of dissolved silica produced by reaction of the various aggregates suggests a marked variation in reaction rate. These results thus provide some understanding of the reaction of various aggregates in model solutions.

Dissolution Curve

As discussed in Chapter 1, Dent Glasser and Kataoka (1981) presented measurements of the dissolution of silica gel in sodium hydroxide solution. The data were plotted as measured levels of silica in solution versus measured pH. The final concentration of dissolved silica and pH level for each of several starting conditions formed a continuous curve, called a solubility curve because, as noted by Dent Glasser and Kataoka, it is similar to the border between stability and instability regions of silicate solutions. They also noted that the individual curves of dissolved silica and pH level for the various starting conditions form dissolution paths by which individual solutions approached this limiting curve.

The same approach was used on the results of the present study; these data (Tables 17 and 18), together with results of Dent Glasser and Kataoka, are plotted as silica in solution versus pH (Fig. 69). Data from the present study appear to show dissolution paths similar in form to the results of Dent Glasser and Kataoka. Two of the opal specimens appear to have reached a solubility curve, such that the curve formed by dissolution of opal may be an extension of the solubility curve reported by Dent Glasser and Kataoka. In that case, data obtained from quartzite and granite appear to form similar paths, but at 3 weeks are still far from the stability curve.

Dent Glasser and Kataoka (1981) differentiated between dissolution and gel formation, suggesting that while the silica in solution results from dissolution, the reduction in pH is due mainly to gel formation. Their argument that pH is not reduced through dissolution is consistent with the

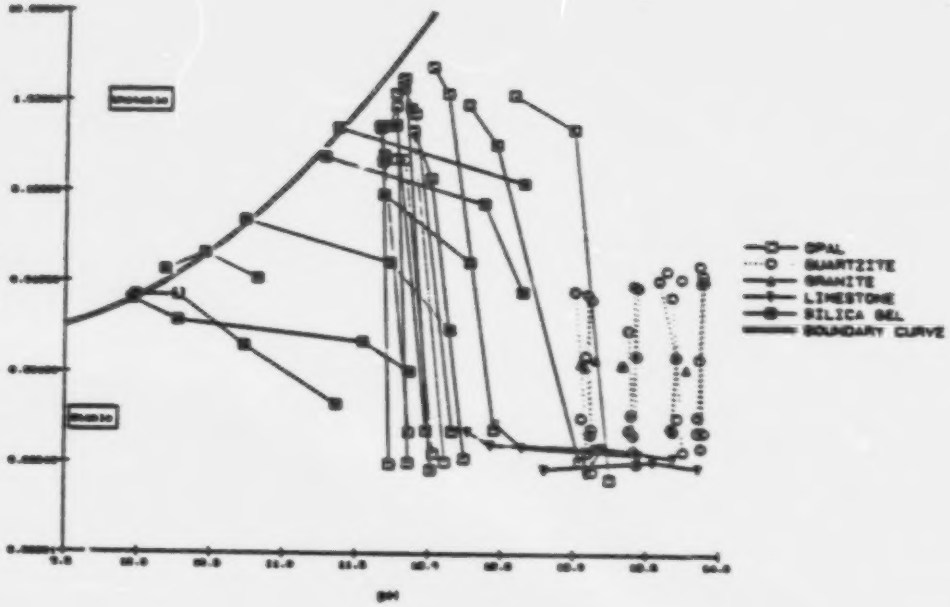

Figure 69. Silica and pH levels in alkali hydroxide solutions produced by reactions of various aggregates from the present study, and by dissolution of silica gel (Dent Glasser and Kataoka, 1981), showing the curve reported by Dent Glasser and Kataoka that separates stable and unstable silica solutions.

BEST COPY AVAILABLE

view of silica dissolution of Iler, discussed in Chapter 1. However, it is difficult to understand how silica in solution and pH reduction can be linked so closely, as shown in Fig. 69 both from results of Dent Glasser and Kataoka and from results of the present study, if the two parameters result from separate processes. This issue is discussed further below.

Reduction in pH

As reported in the previous chapter, the reactions of opal in the model pore solutions are accompanied by major reductions in pH levels, from starting levels between pH 13 and pH 14 to levels below pH 12 after 3 weeks. Similar reductions in pH were reported by Dent Glasser and Kataoka (1981) for the reactions of silica gel in sodium hydroxide solutions. As suggested by Dent Glasser and Kataoka, the reductions in pH levels may cause the silica dissolution to be self-limiting.

Implications of Pore Solution Composition

The range of alkali hydroxide concentrations in the model pore solutions was selected to duplicate the pH range in actual pore solutions, with the objective of exploring the influence of the pH level of the pore solution on the rate of reaction of each aggregate. For this discussion, it is assumed that the level of reaction may be approximated either by the level of silica in solution (bearing in mind the earlier caution) or by the reduction in pH of the solution, following the suggestion of Dent Glasser and Kataoka (1981). For convenience the calculated change in hydroxide ion concentration, rather than the measured change in pH level, is used to allow comparison on the same linear scale.

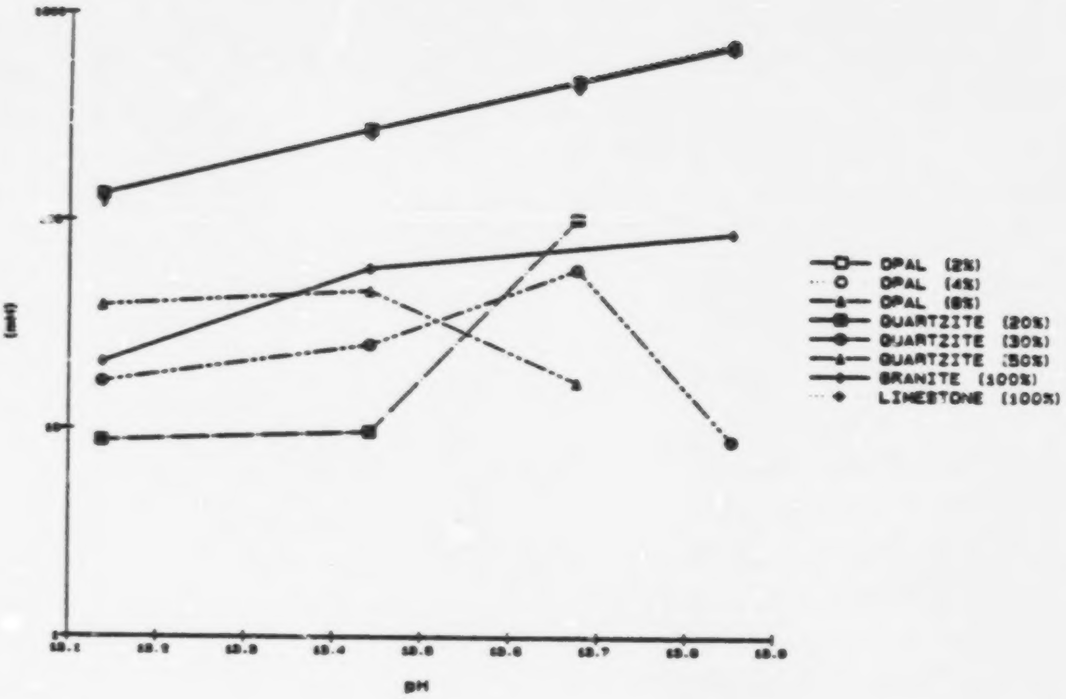

Figure 70. Reduction in hydroxide ion level produced by reaction of various aggregates in model pore solutions versus initial pH level of each solution.

The calculated reductions in hydroxide ion concentration for all aggregates at the single age of 3 weeks are plotted versus initial pH in Fig. 70, with a separate curve for each aggregate. These curves may be compared qualitatively to the levels of expansion produced by these aggregates. For opal, the reduction in hydroxide ion concentration increases steadily with increasing level of initial pH. For quartzite and granite, there is little or no reduction in hydroxide ion concentration at all pH levels. These effects are qualitatively similar to the levels of expansion produced by these aggregates in mortars containing high-alkali cement. On the other hand, for the limestone used in these studies there is substantial reduction in hydroxide ion concentration, and the level of reduction increases steadily with increasing level of initial pH. The limestone, however, produced little expansion in mortar. Thus for the limestone used the observed reduction in hydroxide ion concentration is not related to the observed level of expansion.

For all aggregates, there is no apparent threshold in initial pH level below which little reduction in hydroxide ion concentration occurs. In terms of expansion, at least for opal, there did appear to be a threshold pH level. Furthermore, there is no apparent proportion for either opal or quartzite that produces a maximum in the reduction in hydroxide ion concentration. In terms of expansion, for both opal and quartzite, there did appear to be a pessimum proportion of aggregate producing a maximum in expansion.

The silica concentration levels for all aggregates at the single age of 3 weeks are plotted versus initial pH in Fig. 71. For both opal and quartzite, the silica concentration levels increase with increasing pH, while for the granite and the limestone used the silica concentration levels are negligible and no relationships with pH are apparent. For all four aggregates, the relative silica

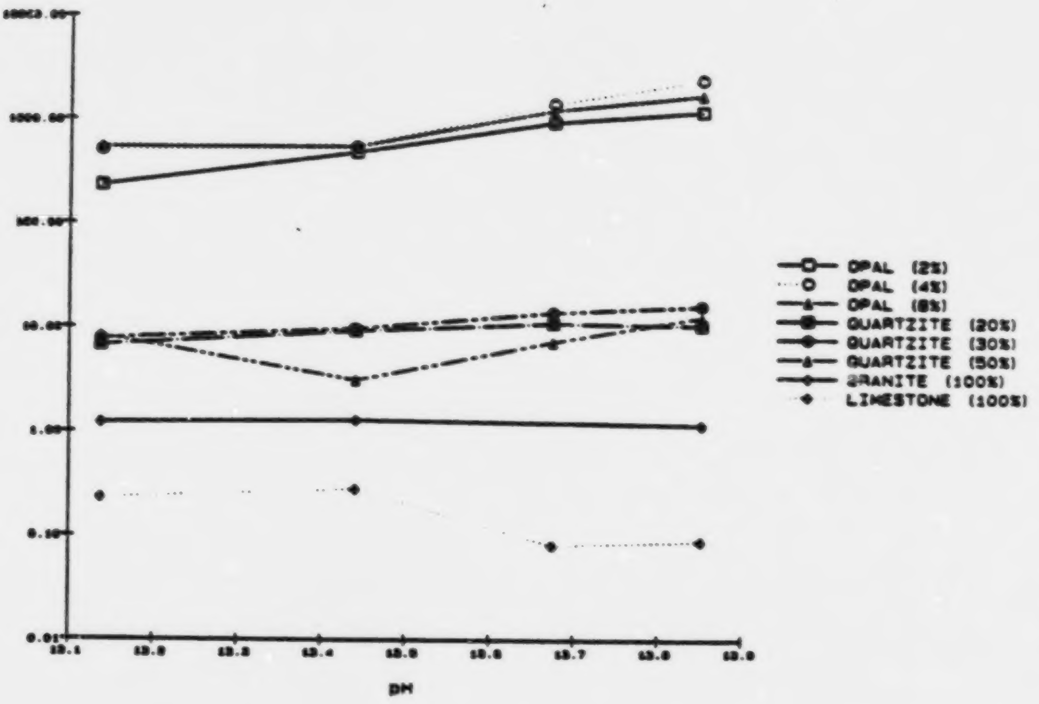

Figure 71. Silica level produced by reaction of various aggregates in model pore solutions versus initial pH level of each solution.

BEST COPY AVAILABLE

concentration levels are similar to the relative levels of expansion produced by these aggregates when combined in mortars containing high-alkali cements.

For opal, which shows the largest effects, the increase in silica concentration with increasing pH is not as regular (Fig. 71) as is the increase in the reduction in hydroxide ion concentration (Fig. 70). The silica concentration levels in solutions with initial pH levels of 13.1 and 13.5 are low, while the silica concentration levels in solution with initial pH level of 13.7 are higher and with initial pH level of 13.9 are higher yet. This jump between pH levels of 13.5 and 13.7 provides indication that there may be a threshold in pH level within that range.

The concentrations of silica in solution produced by both opal and quartzite vary with the proportions of the aggregate. In each case, the highest silica concentration is produced by the aggregate proportion equivalent to the pessimum proportion in terms of mortar bar expansion. Thus the change in concentration of silica produced by reaction of both opal and quartzite in model pore solutions varies with aggregate proportion in the same manner that expansion varies with proportion of reactive constituent in the aggregate.

Based on this preliminary qualitative discussion, it appears that the expansion produced by reaction of aggregate in mortar may be indicated by the level of silica produced in solution during reaction of aggregate in alkali hydroxide solutions. Expansion does not appear to be indicated as well by the reduction of hydroxide ion concentration produced the by reaction. This appears to be inconsistent with the conclusion of Dent Glasser and Kataoka (1981) that the reduction of hydroxide ion concentration indicates the amount of gel formed.

Correlation with Expansion

The qualitative evaluation in the preceding section may be refined using pore solution composition and expansion data to provide more quantitative relationships. In order to carry out the quantitative analysis, the two reaction parameters (reduction in hydroxide ion concentration and increase in concentration of dissolved silica) are estimated for each combination of cement and aggregate, at each level of aggregate, and at 1, 2, and 3 weeks of age. These estimates are based on pH levels, using the pH values obtained from analyses of pore solutions expressed from limestone mortars of each cement, either directly or by interpolation in Fig. 36. The pH values allow estimation of both reaction parameters, using either the curve relating reduction in hydroxide ion concentration to the pH level of the starting solution (Fig. 70) or the curve relating silica concentration (Fig. 71) to the pH level of the starting solution.

Levels of expansion, estimated by interpolating the appropriate graph, are then plotted versus each estimated reaction parameter. Expansion is plotted versus the estimated reduction in hydroxide ion concentration in Fig. 72, and versus estimated silica concentration in Fig. 73. Each plot includes all eight cements, all the aggregates, the various proportions included in reaction studies, and the three ages (1, 2, and 3 weeks).

Figure 72 shows a general relationship between expansion and reduction in hydroxide ion concentration. Expansion levels are low over much of the range of reduction in hydroxide ion concentration; and there is a general increase in expansion at the highest levels of reduction in hydroxide ion concentration. However, there is considerable variation in this overall trend. Much of this variation is attributed to the limestone, which provided a quite high estimated

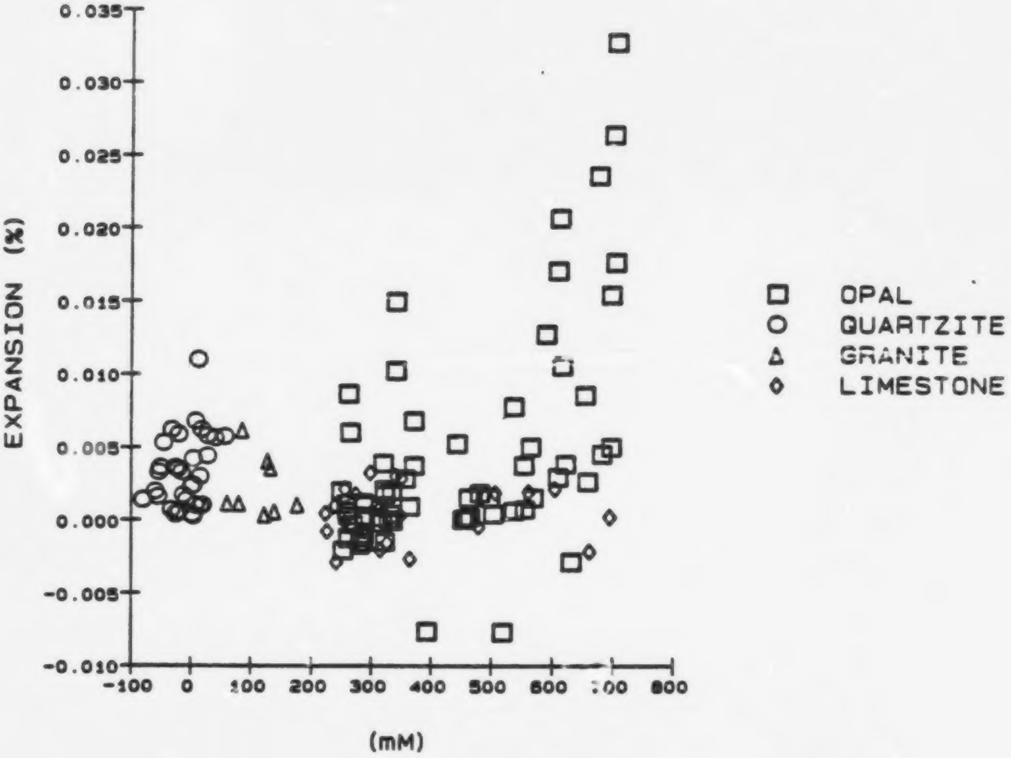

Figure 72. Measured mortar bar expansion versus estimated reduction in hydroxide ion concentration for each aggregate-pore solution reaction.

BEST COPY AVAILABLE

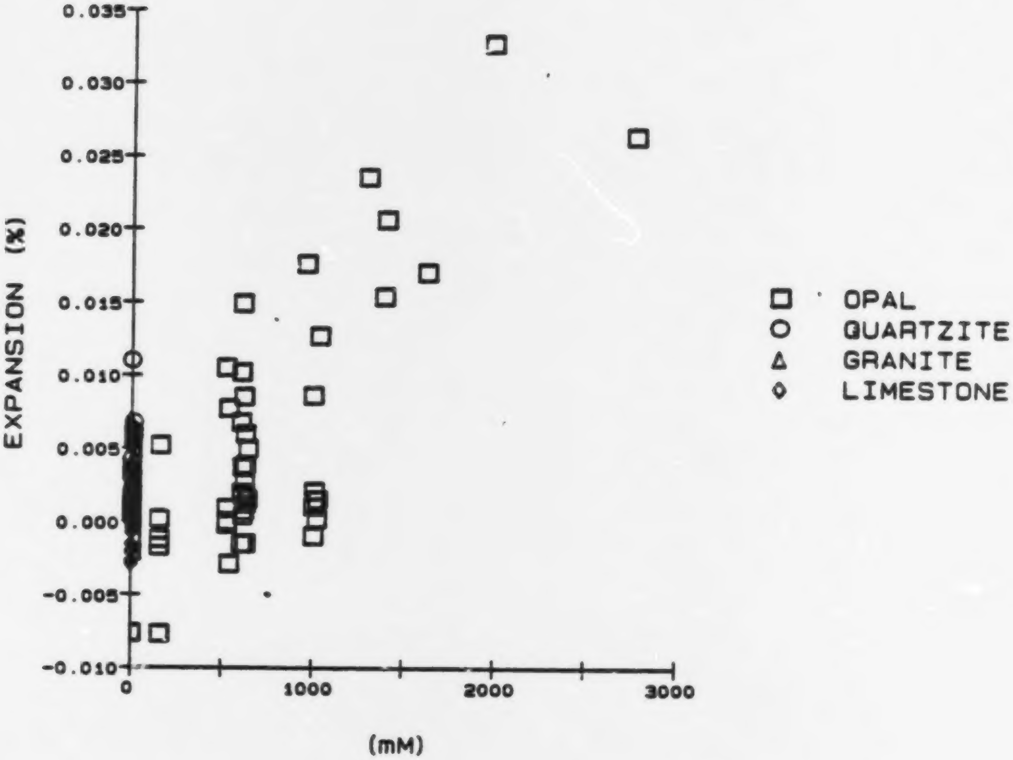

Figure 73. Measured mortar bar expansion versus estimated silica concentration for each aggregate-pore solution reaction.

BEST COPY AVAILABLE

reduction in hydroxide ion concentration, but produced very low levels of expansion.

The concept that reduction in alkali ion concentration in the pore solution provides a measure of the degree of reaction of silica in mortar was suggested previously by Diamond and Barneyback (1976). Their suggestion was based on compositions of pore solutions of reacted mortars compared to those of companion mortars produced using identical components but lacking the reactive aggregate. In that study, the measured levels of the reduction in alkali ion concentration caused by reaction of very finely ground opal (10% by weight of cement) ranged from 0.09 N at 9 days to 0.08 N at 15 days. The levels of reduction in hydroxide ion concentration provided by reaction of coarser opal in model pore solutions in the present study are much higher, approximately 0.70 N at 14 days.

The measured levels of expansion correlate even more closely with the other reaction parameter, the silica concentration in solution (Fig. 73). There are variations, discussed further below, but the overall trend is that expansion increases with increasing level of this reaction parameter.

The levels of silica produced by reaction of opal in model pore solutions, and the resulting estimated silica levels in actual pore solutions shown in Fig. 73, are approximately 3 orders of magnitude higher than levels that have been measured in pore solutions of mortars containing opal. The estimated levels are as high as 3 M, while silica concentrations measured in pore solutions expressed from mortars containing opal are only a few mM (Barneyback, 1983). Thus both the estimated silica levels and the estimated levels of reduction in hydroxide ion concentration are much higher than the corresponding measured values measured in pore solutions expressed from mortars containing opal.

The much higher estimated levels of silica concentration and reduction in hydroxide ion concentration may be a consequence of the compositions of the model pore solutions. The model solutions differed from actual pore solutions in that they contain no calcium, and possibly more important in that there is no source of calcium in the solids available to them. It is probably this lack of calcium in the model solutions that gives rise to the discrepancy in silica level. If any calcium were available in the model solutions, such high levels of silica could not develop.

It is perhaps because of this difference that the levels of silica produced in the model pore solutions appear to provide an excellent indicator of the reaction tendency of each aggregate. Alkali-silica reaction consists of a number of phenomena, of which aggregate dissolution is presumably the first stage. Thus aggregate dissolution is seen to provide a reaction parameter that is readily related to the amount of actual expansion of each aggregate when combined in mortar at an equivalent proportion.

As noted previously, there is considerable local variation in the general trend of expansion versus estimated level of silica in solution. This variation may be attributed to the differences in expansion effects produced by the different cements, which were explained previously in terms of the influence of pore solution composition on expansion. In the previous discussion of expansion versus pore solution composition, the plots of expansion versus alkali concentration of the pore solutions (Figs. 66 through 68) took the form of a separate curve for each aggregate and each proportion of reactive constituent. The relationships developed in the present discussion serve to bring these separate curves together to a single curve (Fig. 73), valid for all aggregates and all proportions tested. At least qualitatively, the local variation in Fig. 73 is explained by the variation in sodium or combined sodium plus potassium concentrations produced by each cement. For each aggregate, the cements showing lower expansions are those whose pore solution is lower in sodium and in combined sodium plus potassium.

There are major and fundamental differences between aggregate reactions in mortar and in the model pore solutions used in the present study. In mortars, the levels of silica in solution are orders of magnitude lower than the levels produced by reaction in the model solutions. In mortars, gel was observed due to the reaction, whereas there was no evidence by visual inspection or in the levels of silica in solution that gel formed in the model pore solutions. These differences indicate that the model solutions used in the present study did not model all of the effects on aggregates of pore solutions in actual mortars, but rather seem to model only the dissolution effects.

As discussed earlier, the processes of silica dissolution and of gel formation appear to be distinct. In the aggregate reactions in model pore solutions, the high levels of silica indicate that dissolution is the predominant process. In reacting mortars, this process is considered to be followed by (and perhaps altered by) gel formation. However, the correlation between expansion, which is a phenomenon of the mortars and is expected to depend primarily on gel formation, with the levels of dissolved silica in model pore solutions, presumably an indication of dissolution, suggests that dissolution and gel formation may have basic similarities in their reaction rates, or even that dissolution is the rate-controlling process.

CHAPTER 5

SUMMARY AND CONCLUSIONS

A summary of the experimental findings is listed below, followed by the conclusions.

Experimental Findings

1. A suite of portland cements was assembled whose alkali contents range up to 1.2% (equivalent Na_2O), and the allocation of alkalies among certain, specific classes of phases was quantitatively determined for each cement. These allocations provide an indication of the relative amounts of alkali expected in the pore solutions of mortars during the early hydration of these cements.

2. In these preliminary allocation studies, it was found that the alkali sulfate and calcium langbeinite levels are estimated better from measurements of alkalies dissolved during a 1-min water extraction than the conventional measurement of alkalies dissolved during a 10-min water extraction, as specified in ASTM C 114.

3. In mortar bar tests using these cements, significant differences for both the initial rates of expansion and the final expansion levels were observed between the cements, attributable at least in part to effects of the differences in distribution of alkalies among the cement phases.

4. The curves of expansion versus time for mortar bars containing reactive aggregate and exposed at room

temperature and 100% relative humidity showed a generally similar pattern for all cements and aggregates. The expansion rates were most rapid during the initial period (the first few weeks), then decreased progressively, and finally reached fairly steady values after approximately 18 to 24 weeks. Empirical efforts at fitting expansion data to mathematical functions indicate that expansion values tended to vary linearly with the log of time, but did not vary linearly with the square root of time, as had been demonstrated by others.

5. Final (approximately 2 years) expansion levels for the various mortars tested ranged from as little as 0.01% to as high as 0.36%. As expected, the highest expansion levels were produced by the high-alkali cements with opal. Expansion levels with opal for the lower alkali cements were much lower, below 0.06% for the four cements. Expansion levels with the high-alkali cements and quartzite as reactive aggregate were low (between 0.01% and 0.05%), as were levels with granite as the reactive aggregate (between 0.03% and 0.04%).

6. The pessimum level of the Beltane opal was found to be approximately 2% to 4% (of total aggregate); that of the quartzite was much higher, approximately 20% to 30%.

7. The principal dissolved ions in the pore solutions expressed from mortars containing only the relatively non-reactive limestone as aggregate, as measured between 1 week and 28 weeks of hydration, were hydroxide and alkali ions. Values of pH measured directly from the expressed solutions varied from 13.4 to 14.0. Hydroxide ion determinations yielded concentrations ranging between 322 mM and 965 mM. Concentrations of individual alkalies determined by chemical analyses ranged from 6 mM to 279 mM for sodium, and from 75

mM to 857 mM for potassium. Analytical determinations for the minor solution components yielded calcium concentrations ranging from 0.6 mM to 2.2 mM, silica concentrations less than 0.05 mM, and sulfate concentrations between 3 mM and 77 mM.

8. A number of correlations were found between measured concentrations of different components of the pore solutions from all eight cements. A positive correlation was observed between sulfate concentrations and measured pH levels, suggesting a possible redissolution of one or more sulfate-bearing phases under the high-pH conditions. Only a hint of an inverse correlation was observed between calcium concentration level and pH; indeed, the level of calcium found even in the solution derived from the cement containing the lowest level of alkali was so low that differences in calcium concentrations are not expected to influence alkali-aggregate expansions.

9. Mathematical models were developed to estimate alkali contents of the pore solutions; two models were based on a relationship between solution composition and the distribution of alkalies in the cements, and a third model was independent of any such relationship. The measured levels of sodium and potassium as a function of age were found to be more consistent with levels calculated using the models that consider how alkalies are combined in each phase and how rapidly each phase hydrates. The general agreement between measured values and calculated values suggest that the measured values are reasonably consistent with the levels expected based on the alkali distributions determined for the cements. The consistent decrease in the measured potassium levels between 8 and 28 weeks is attributed to binding of alkali by calcium silicate hydrate gel, a feature that was not included in any of the models.

10. Certain relationships were observed between expansion levels of reactive mortar bars and the base level pore solution compositions, i.e. the compositions of mortars containing the relatively non-reactive limestone. An apparent threshold in pH was observed, between 13.65 and 13.83, below which there was little or no expansion, and above which there was substantial expansion. In addition to the expected, positive relationship between expansion and pH, direct relationships were observed both between expansion and the sum of the concentrations of potassium and sodium and between expansion and the concentration of sodium.

11. Model pore solutions containing various levels of dissolved alkali hydroxides were prepared. When exposed to these solutions, aggregates were found to react extensively, producing significant reductions in pH and various levels of dissolved silica. In the three-week exposure period, the opal aggregate was found to produce very high concentrations of dissolved silica, in some cases greater than 2 M. This aggregate also produced substantial reductions in pH, in excess of 1 full pH unit. The quartzite aggregate produced a moderate concentration of dissolved silica, typically around 10 mM, and no observable reduction in pH. The granite aggregate produced still lower levels of dissolved silica, typically around 1 mM, and no observable reduction in pH. The limestone aggregate produced only a trace of silica, generally below 0.3 mM, but produced a large reduction in pH, approximately 1 pH unit.

12. The levels of silica produced in the model pore solution experiments correlated directly with the mortar-bar expansion levels produced by each aggregate and at each proportion.

Conclusions

On the basis of the experimental findings, the following conclusions have been drawn:

1. The specific distribution of the alkalies present in a particular cement influences both the level and the rate of alkali concentration in the pore solution of cement mortars. However, the differences observed do not directly cause major differences in expansion due to alkali-silica reaction.

2. Room temperature expansions of mortar bars and, by implication, of concretes appear to increase as a function of the log of time, rather than as a function of the square root of time as found by Grattan-Bellew (1981).

3. Pore solutions of mortars using a wide range of cements contain primarily alkali hydroxides, with concentration levels ranging from as low as 0.3 M to nearly 1 M. The minor components include sulfate at concentration levels ranging from quite low (3 mM) to substantial (over 75 mM), and varying directly with pH; calcium at concentration levels ranging from approximately 0.6 mM to only 2 mM, more or less independently of pH; and silica levels less than 0.05 mM. Because the cements included in these studies were deliberately chosen to cover the wide range of alkali distributions found in portland cements (though not to cover very low alkali levels), it is believed that these results are reasonably representative for cements in general, at least for the water-to-cement ratio employed (0.5).

4. Results of reactions of the aggregates in model pore solutions suggest that alkali-silica reaction must involve at least two steps, dissolution of silica from the aggregate, and subsequent precipitation of a silica-bearing

reaction product (hydrous alkali-silica gel). Only the former process occurs in the absence of calcium, producing high concentrations of dissolved silica and at the same time reducing the pH of the solution. In real cement systems, despite the presence of only low levels of dissolved calcium (ca. 1 to 2 mM), precipitation of the gel reaction product appears to prevent accumulation of dissolved silica in the pore solution, causing the silica levels to remain low. The reductions in pH level may cause the dissolution process to be self-limiting, as suggested by Dent Glasser and Kataoka (1981).

5. The reaction of aggregate on exposure to pore solution (real or model) is shown to depend on the following parameters: the specific aggregate material, its proportion relative to the amount of solution, and the pH level of the specific pore solution. The level of silica dissolved during exposure of aggregate to a model pore solution is a measure the extent of this reaction in the model solution, and appears to provide an index of the extent of reaction in a real pore solution. In a mortar, the resulting expansion level developed if water is freely available (as in the present experiments) appears to be a function of the extent of this reaction.

6. The expansion is further influenced to some degree by the specific composition of the pore solution, in particular by the sodium and potassium levels.

REFERENCES

Barneyback, R.S., Jr. 1983. Alkali-silica reaction in portland cement concrete. PhD thesis, Purdue University, 352 pages, May 1983.

Barneyback, R.S., Jr., and Diamond, S. 1981. Expression and analysis of pore fluids from hardened cement pastes and mortars. Cement and Concrete Research, 11(2), 279-285.

Bates, R.G. 1973. Determination of pH, Theory and Practice. 2nd Edition, 479 pages. New York: John Wiley & Sons.

Bhatty, M.S.Y., and Greening, N.R. 1978. Interaction of alkalies with hydrating and hydrated calcium silicates. In: Effects of Alkalies in Cement and Concrete, Proceedings of a conference held at Purdue University, June 1978, 87-111. West Lafayette: Purdue University.

Boswell, L., Robert, E.C., Buttler, F.G., and Morgan, S.R. 1983. Alkali content and expansion of mortars containing pulverised fuel ash. In: Alkalis in Concrete, edited by G.M. Idorn and S. Rostam, Proceedings of the Sixth International Conference, Copenhagen, June 22-25, 1983, 231-238. Copenhagen: Danish Concrete Association.

Brandt, M.P., and Oberholster, R.E. 1983. Investigation of Tygerberg formation aggregate for potential alkali reactivity, implications of test methods and application of the findings in practice. CSIR Research Report 580, 96 pages. Pretoria: National Building Research Institute of the Council for Scientific and Industrial Research.

Brandt, M.P., Oberholster, R.E., and Westra, W.B. 1981. The alkali-aggregate reaction: a contribution concerning the determination of the reactivity of portland cements. In: Alkali-Aggregate Reaction, edited by R.E. Oberholster, Proceedings of the Fifth International Conference on Alkali-Aggregate Reaction in Concrete, paper S252/10, pages 1-5. Pretoria: National Building Research Institute of the Council for Scientific and Industrial Research.

Bretschi, J., and Mehta, P.K. 1978. Test methods for determining potential alkali-silica reactivity in cements. Cement and Concrete Research, 8(2), 191-200.

Buck, A.D. 1983. Alkali reactivity of strained quartz as a constituent of concrete aggregate. Cement, Concrete, and Aggregates, 5(2), 131-133.

Buck, A.D., and Dolch, W.L. 1966. Investigation of a reaction involving nondolomitic limestone aggregate in concrete. Journal of the American Concrete Institute, 755-763.

Calleja, J. 1980. Durability. In: Proceedings of the Seventh International Congress on the Chemistry of Cement, Paris, Vol. I, pp. VII-2/1 through VII-2/48. Paris: General Secretariat.

Chatterji, S. 1979. The role of $Ca(OH)_2$ in the breakdown of portland cement concrete due to alkali-silica reaction. Cement and Concrete Research, 9(2), 185-188.

Dalziel, J.A., and Gutteridge, W.A. 1986. The influence of pulverized-fuel ash upon the hydration characteristics and certain physical properties of a portland cement paste. Technical Report 560, 28 pages. Wexham Springs: Cement and Concrete Association.

Davis, C.E.S. 1951. Studies in cement-aggregate reaction. XVIII. The effect of soda content and of cooling rate of portland cement clinker on its reaction with opal in mortar. Australian Journal of Applied Science, 2(1), 123-131.

Davis, C.E.S. 1958. Comparison of the effect of soda and potash on expansion. Australian Journal of Applied Science, 9(1), 52-62.

Dent Glasser, L.S. 1979. Osmotic pressure and the swelling of gels. Cement and Concrete Research, 9(4), 515-517.

Dent Glasser, L.S., and Kataoka, N. 1981. The chemistry of 'alkali-aggregate' reaction. Cement and Concrete Research, 11(1), 1-9.

Dent Glasser, L.S., and Kataoka, N. 1982. On the role of calcium in the alkali-aggregate reaction. Cement and Concrete Research, 12(3), 321-331.

Diamond, S. 1975. A review of alkali-silica reaction and expansion mechanisms 1. Alkalies in cements and in concrete pore solutions. Cement and Concrete Research, 5(4), 329-346.

Diamond, S. 1975. Long-term status of calcium hydroxide saturation of pore solutions in hardened cements. Cement and Concrete Research, 5(6), 607-616.

Diamond, S. 1976. A review of alkali-silica reaction and expansion mechanisms 2. Reactive aggregates. Cement and Concrete Research, 6(4), 549-560.

Diamond, S. 1978. Beltane opal, its alkali reaction product, and some synthetic alkali-silica gels -- a brief look at micromorphology. In: Effects of Alkalies in Cement and Concrete, Proceedings of a conference held at Purdue University, June 1978, 181-197. West Lafayette: Purdue University.

Diamond, S. 1981. Effects of two Danish flyashes on alkali contents of pore solutions of cement-flyash pastes. Cement and Concrete Research, 11(3), 383-394.

Diamond, S. 1983. Alkali reactions in concrete -- pore solution effects. In: Alkalis in Concrete, edited by G.M. Idorn and S. Rostam, Proceedings of the Sixth International Conference, held at the Technical University of Denmark, June 22-25, 1983, 155-166. Copenhagen: Danish Concrete Association.

Diamond, S., and Barneyback, R.S., Jr. 1976. A prospective measure for the extent of alkali-silica reaction. In: The Effect of Alkalis on the Properties of Concrete, edited by A.B. Poole, Proceedings of a Symposium held in London, September, 1976, 149-162. Wexham Springs: Cement and Concrete Association.

Diamond, S., and Barneyback, R.S., Jr. 1976. "Standard" alkali-reactive silica available. Cement and Concrete Research, 6(5), 726.

Diamond, S., Barneyback, R.S., Jr., and Struble, L.J. 1981. On the physics and chemistry of alkali-silica reactions. In: Alkali-Aggregate Reaction, edited by R.E. Oberholster, Proceedings of the Fifth International Conference on Alkali-Aggregate Reaction in Concrete, paper S252/22, pages 1-10. Pretoria: National Building Research Institute of the Council for Scientific and Industrial Research.

Figg, J.W. 1981. Reaction between cement and artificial glass in concrete. In: Proceedings of the Fifth International Conference on Alkali-Aggregate Reaction in Concrete, edited by R.E. Oberholster, paper S252/7, pages 1-18. Pretoria: National Building Research Institute of the Council for Scientific and Industrial Research.

Figg, J.W. 1983. An attempt to provide an explanation for engineers of the expansive reaction between alkalies and siliceous aggregates in concrete. In: Alkalis in Concrete, edited by G.M. Idorn and S. Rostam, Proceedings of the Sixth International Conference, Copenhagen, June 22-25, 1983, 137-144. Copenhagen: Danish Concrete Association.

Frondel, C. 1962. The System of Mineralogy of James Dwight Dana and Edward Salisbury Dana. Vol. III, Silica Minerals. 7th edition, 334 pages. New York: John Wiley and Sons, Inc.

Gaskin, A.J., Jones, R.H., and Vivian, H.E. 1955. The reactivity of various forms of silica in relation to the expansion of mortar bars. Australian Journal of Applied Science, 6(1), 78-87.

Gebhardt, R.F. Personal communication from R.F. Gebhardt, Lehigh Portland Cement Company, to L.J. Struble, National Bureau of Standards, June 24, 1986.

Gies, A., and Knöfel, D. 1986. Influence of alkalies on the composition of belite-rich cement clinkers and the technological properties of the resulting cements. Cement and Concrete Research, 16(3), 411-422.

Gilliland, J.L., and Bartley, T.R. 1950. Water-solubility of alkalies in portland cement. Journal of the American Concrete Institute, 22(2), 153-159.

Glasser, F.P., Angus, M.J., McCulloch, C.E., MacPhee, D., and Rahman, A.A. 1985. The chemical environment in cements. In: Materials Research Society Symposia Proceedings, 44, Scientific Basis for Nuclear Waste Management, 849-856.

Glasser, F.P., and Marr, J. 1984. The effect of mineral additives on the composition of cement pore fluids. Proceedings of the British Ceramic Society, 35, 419-429.

Glasser, F.P., and Marr, J. 1985. The alkali binding potential of OPC and blended cements. Il Cemento, (2), 85-94.

Goldberg, R.N., Manley, J.L., and Nuttall, R.L. 1985. GAMPHI -- A Database of Activity and Osmotic Coefficients for Aqueous Electrolyte Solutions. NBS Technical Note 1206, 23 pages. Washington: U.S. Department of Commerce.

Golkowska, A., and Pszonick, L. 1973. A study of the composition and properties of the ion-association complex of rhodamine B with silicomolybdic acid, with a view to its analytical application. Talanta, 20, pp. 749-754.

Grattan-Bellew, P.E. 1978. Study of expansivity of a suite of quartzwackes, argillites and quartz arenites. In: Effects of Alkalies in Cement and Concrete, Proceedings of a conference held at Purdue University, June 1978, 113-140. West Lafayette: Purdue University.

Grattan-Bellew, P.E. 1981. A review of test methods for alkali-expansivity of concrete aggregates. In: Alkali-Aggregate Reaction, edited by R.E. Oberholster, Proceedings of the Fifth International Conference on Alkali-Aggregate Reaction in Concrete, Capetown, March 30-April 3, 1981, S252/9, 1-13. Pretoria: National Building Research Institute of the Council for Scientific and Industrial Research.

Grattan-Bellew, P.E. 1983. Evaluation of test methods for alkali-aggregate reactivity. In: Alkalis in Concrete, edited by G.M. Idorn and S. Rostam, Proceedings of the Sixth International Conference, held at the Technical University of Denmark, June 22-25, 1983, 303-314. Copenhagen: Danish Concrete Association.

Gutteridge, W.A. 1979. On the dissolution of the interstitial phases in portland cement. Cement and Concrete Research, 9(3), 319-324.

Gutteridge, W.A., and Hobbs, D.W. 1980. Some chemical and physical properties of Beltane opal rock and its gelatinous alkali silica reaction product. Cement and Concrete Research, 10(2), 183-193.

Hansen, W.C. 1944. Studies relating to the mechanisms by which the alkali-aggregate reaction produces expansion in concrete. Journal of the American Concrete Institute, 40, 213-227.

Heck, W.J. 1983. Study of alkali-silica reactivity tests to improve correlation and predictability for aggregates. Cement, Concrete, and Aggregates, 5(1), 47-53.

Hester, J.A., and Smith, O.F. 1953. Alkali-aggregate phase of chemical reactivity in concrete. National Research Council Highway Research Board Proceedings, 32, 306-316.

Hobbs, D.W. 1978. Expansion of concrete due to alkali-silica reaction -- an explanation. Magazine of Concrete Research, 30(105), 215-220.

Hobbs, D.W. 1980. Influence of mix proportions and cement alkali content upon expansion due to the alkali-silica reaction. Technical Report 534, 31 pages. Wexham Springs: Cement and Concrete Association, UK.

Idorn, G.M. 1961. Studies of Disintegrated Concrete, Part 1. 77 pages. Copenhagen: The Danish National Institute of Building Research and the Academy of Technical Sciences, Committee on Alkali Reactions in Concrete.

Iler, R.K. 1979. The Chemistry of Silica. 866 pages. New York: John Wiley & Sons.

Jackson, K.B. 1984. Personnel Communication from K.B. Jackson, Orion Research Incorporated, to L.J. Struble, NBS, November 26.

Jawed, I., and Skalny, J. 1977. Alkalies in cement: a review. I. Forms of alkalies and their effect on clinker formation. Cement and Concrete Research, 7(6), 719-730.

Jawed, I., and Skalny, J. 1978. Alkalies in cement: a review. II. Effects of alkalies on hydration and performance of portland cement. Cement and Concrete Research, 8(1), 37-52.

Jawed, I., Struble, L., and Epp, J. 1983. Dissolution and hydration of C_3A-Na_2O solid solutions. In: Alkalis in Concrete, edited by G.M. Idorn and S. Rostam, Proceedings of the Sixth International Conference, held at the Technical University of Denmark, June 22-25, 1983, 209-215. Copenhagen: Danish Concrete Association.

Jons, E.S., and Osbaeck, B. 1982. The effect of cement composition on strength described by a strength-porosity model. Cement and Concrete Research, 12(2), 167-178.

Kalousek, G.L. 1944. Studies of portions of the quaternary system soda-lime-silica-water at 25C. Journal of Research of the National Bureau of Standards, 32, 285-302, 1944.

Kollek, J.J., Varma, S.P., and Zaris, C. 1986. Measurement of OH^- ion concentrations of pore fluids and expansion due to alkali-silica reaction in composite cement mortars. In: Proceedings of the Eighth International Congress on the Chemistry of Cement, Rio, Vol. IV, pp. 183-189. Rio: General Secretariat.

Lambert, P., Page, C.L., and Short, N.R. 1985. Pore solution chemistry of the hydrated system tricalcium silicate/sodium chloride/water. Cement and Concrete Research, 15(4), 675-680.

Lashchenko, V.A., and Loganina, V.I. 1972. Liquid phase of hydrated portland cement. Zhurnal Prikladnoi Khimii, 47(3), 645-647.

Lawrence, C.D. 1966. Changes in composition of the aqueous phase during hydration of cement pastes and suspensions. In: Symposium on Structure of Portland Cement Paste and Concrete, Special Report 90, pages 378-391. Washington: Highway Research Board.

Lawrence, M., and Vivian, H.E. 1961. The reactions of various alkalis with silica. Australian Journal of Applied Science, 12(1), 96-103.

Lea, F.M. 1971. The Chemistry of Cement and Concrete. 3rd Edition, 727 pages. New York: Chemical Publishing Company, Inc..

Lerch, W., and Ford, C.L. 1948. Chemical and physical tests of the cements. Chapter 3 in Long-Time Study of Cement Performance in Concrete, Bulletin 26, pages 743-795. Chicago: Portland Cement Association.

Longuet, P., Burglen, L., and Zelwer, A. 1973. La phase liquide du ciment hydrate. Revue des Materiaux de Construction et de Travaux Publics, No. 676, 35-41.

Luke, K., and Glasser, F.P. 1986. Chemical changes occurring during the early hydration of PFA-OPC mixtures. In: Materials Research Society Symposia Proceedings, 65, Fly Ash and Coal Conversion By-Products: Characterization, Utilization and Disposal II, ed. G.J. McCarthy and R.J. Lauf.

Marr, J., and Glasser, F.P. 1983. Effect of silica, PFA and slag additives on the composition of cement pore fluids. In: Alkalis in Concrete, edited by G.M. Idorn and S. Rostam, Proceedings of the Sixth International Conference, held at the Technical University of Denmark, June 22-25, 1983, 239-242. Copenhagen: Danish Concrete Association.

Mather, B. 1983. Personal communication from B. Mather, U.S. Army Corps of Engineers, to L. Struble, Martin Marietta Laboratories, July 26, 1983.

McConnell, D., Meilenz, R.C., Holland, W.Y., and Greene, K.T. 1947. Cement-aggregate reaction in concrete. Proceedings, American Concrete Institute, 44, 93-128.

McCoy, W.J., and Caldwell, A.G. 1951. New approach to inhibiting alkali-aggregate expansion. Journal of the American Concrete Institute, 22(9), 693-706.

Mindess, S., and Struble, L. 1982. Preliminary data on the cement-aggregate bond. Presented at the 84th Annual Meeting of the American Ceramic Society, Cincinatti OH.

Mindess, S., and Young, J.F. 1981. Concrete. 671 pages. Englewood Cliffs: Prentice-Hall, Inc..

Osbaeck, B. 1984. Calculation of water-soluble alkali content in portland cement clinker. Zement-Kalk-Gips, 37(9), 486-493.

Ozol, M.A. 1975. The pessimum proportion as a reference point in modulating alkali-silica reaction. In: Symposium on Alkali-Aggregate Reaction, Preventative Measures, Proceedings of a symposium held in Reykjavik, Iceland, August 1975, 113-129. Reykjavik: Icelandic Building Research Institute.

Page, C.L., and Vennesland, O. 1983. Pore solution composition and chloride binding capacity of silica--fume cement pastes. Materiaux et Constructions, 16(91), 19-25.

Penko, M. 1983. Some Early Hydration Processes in Cement Paste as Monitored by Liquid Phase Composition Measurements. PhD Thesis, Purdue University, 124 pages, 1983.

Pielert, J.H., Haverfield, J.W., and Spellerberg, P.A. 1985. Application of CCRL data in the formulation of precision estimates for selected cement standards. Cement, Concrete, and Aggregates, 7(1), 37-42.

Pike, G., Hubbard, D., and Insley, H. 1955. Mechanisms of alkali-aggregate Reaction. Journal of the American Concrete Institute, 52, 13-34.

Pollitt, H.W.W., and Brown, A.W. 1969. The distribution of alkalies in portland cement clinker. In: Proceedings of the Fifth International Symposium on the Chemistry of Cement, Tokyo, 1968, Vol. I, pp. 322-333. Tokyo: The Cement Association of Japan.

Powers, T.C., and Steinour, H.H. 1955. An interpretation of some published researches on the alkali-aggregate reaction, Part 2 -- A hypothesis concerning safe and unsafe reactions with reactive silica in concrete. Journal of the American Concrete Institute, 51, 785-812.

Pratt, P.L., and Ghose, A. 1983. Electron microscope studies of portland cement microstructures during setting and hardening. Philosophical Transactions of the Royal Society of London, A: Mathematical and Physical Sciences, 310, 93-103.

Pulatov, Z., and Usmanov, Kh. 1976. Effect of the type of alkali metal oxides on linear deformations of cement-sand mortars. Uzbekskii Khimicheskii, Zhurnal, (5), 59-61; Chemical Abstracts, 86, 160116, 1977.

Ramachandran, V.S., Feldman, R.F., and Beaudoin, J.J. 1981. Concrete Science. 427 pages. Philadelphia: Heyden & Son, Inc.

Regourd, M. 1983. Crystal chemistry of portland cement phases. In: Structure and Performance of Cements, Ed. by P. Barnes, pp. 109-138. London: Applied Science Publishers.

Regourd, M., and Mortureux, B. 1977. Tricalcium aluminate in synthetic solid solutions and in cements. In: Reaction of Aluminates During the Setting of Cements, Summaries of Contributions to a Seminar at the University of Technology, Eindhoven, The Netherlands, April 13-14, 1977, edited by H.N. Stein, pp. 1-5. Paris: CEMBUREAU.

Roy, D.M., Malek, R.I.A., Rattanussorn, M., and Grutzeck, M.W. 1985. Trapping of chloride ions in cement pastes containing fly ash. In: Materials Research Society Symposia Proceedings, 65, Fly Ash and Coal Conversion By-Products: Characterization, Utilization and Disposal II, ed. G.J. McCarthy and R.J. Lauf.

Shin, G.Y., and Glasser, F.P. 1983. Chemistry of cement pore fluids. I. Suspension reactions of $Ca_{3-x}Na_{2x}Al_2O_6$ solid solutions with and without gypsum additions. Cement and Concrete Research, 13(3), 366-376.

Silsbee, M., Malek, R.I.A., and Roy, D.M. 1986. Composition of pore fluids extruded from slag-cement pastes. In: Proceedings of the Eighth International Congress on the Chemistry of Cement, Rio, Vol. IV, pp. 263-269. Rio: General Secretariat.

Skalny, J., and Klemm, W.A. 1981. Alkalies in clinker: origin, chemistry, effects. In: Alkali-Aggregate Reaction, edited by R.E. Oberholster, Proceedings of the Fifth International Conference on Alkali-Aggregate Reaction in Concrete, paper S252/1, pages 1-7. Pretoria: National Building Research Institute of the Council for Scientific and Industrial Research.

Stanton, T.E.. 1940. Expansion of concrete through reaction between cement and aggregate. American Society of Civil Engineers Proceedings 66, 1781-1810.

Struble, L. 1979. Swell and other properties of synthetic alkali-silica gels. M.S. thesis, Purdue University, 1979.

Struble, L.J. 1985. The effect of water on maleic acid and salicylic acid extractions. Cement and Concrete Research, 15(4), 631-636.

Struble, L., and Diamond, S. 1981. Unstable swelling behavior of alkali silica gels. Cement and Concrete Research, 11(4), 611-617.

Struble, L., and Diamond, S. 1981. Swell properties of synthetic alkali silica gels. Journal of the American Ceramic Society, 64(11), 652-655.

Struble, L., and Diamond, S. 1986. Influence of cement alkali distribution on expansion due to alkali-silica reaction. Accepted for publication in ASTM STP 930, Alkalies in Concrete.

Strunge, J., Knöfel, D., and Dreizler, I. 1985. Influence of alkalies and sulfur on the properties of cement. Part II: Influence of alkalies and sulphate on the properties of cement, taking account of the silica ratio. Zement-Kalk-Gips, 38(8), 441-450, 266-271.

Takashima, S. 1958. Systematic dissolution of calcium silicate in commercial portland cement by organic acid solution. Review of General Meeting, Technical Session - Cement Association of Japan, 12, 12-13.

Taleb, H. 1985. Analytical and Mechanistic Aspects of the Action of Selected Retarders on the Hydration of "Tricalcium Silicate", the Major Component of Portland Cement. PhD thesis, Georgetown University, 159 pages, November 1985.

Tang, Ming-shu, Ye, Yu-feng, Yuan, Mei-qi, and Zhen, Shi-hua. 1983. The preventive effect of mineral admixtures on alkali-silica reaction and its mechanisms. Cement and Concrete Research, 13(2), 171-176.

Taylor, H.F.W. 1986. Chemistry of cement hydration. In: Proceedings of the Eighth International Congress on the Chemistry of Cement, Rio, Vol. I, pp. 82-112. Rio: General Secretariat.

Taylor, H.F.W. 1987. Bound water in cement pastes and its significance for pore solution compositions. To be published in: Materials Research Society Symposia Proceedings, 85, Microstructural Development during Hydration of Cement, ed. L.J. Struble and P.W. Brown.

Thaulow, N., and Knudsen, T. 1975. Quantitative microanalyses of alkali-silica gel in concrete. Cement and Concrete Research, 5(5), 443-454.

Travis, R.B. 1955. Classification of rocks. Quarterly of the Colorado School of Mines, 50(1), 1-98.

Uhlig, H.H. 1948. The Corrosion Handbook. 1188 pages. New York: John Wiley and Sons.

Usmanov, Kh., Chernysheva, G., and Pulatov, Z. 1977. Corrosion of cement-sand mortars containing active silica in alkali solutions. Uzbekskii Khimicheskii, Zhurnal, [illegible](1), 54-57, 1977; Chemical Abstracts, 87, 43276, 1977.

van Aardt, J.H.P., and Visser, S. 1982. Reactions between rocks and the hydroxides of calcium, sodium and potassium: Progress Report No. 2, Identification of reaction products and a study of the dimensional changes of cement-bonded mortar specimens immersed in alkali solutions at 40°C and 80°C. CSIR Research Report 577, 34 pages. Pretoria: National Building Research Institute of the Council for Scientific and Industrial Research.

Vivian, H.E. 1950. The effect of amount of added alkalis on mortar expansion. Part XII In: Studies in Cement-Aggregate Reaction, Bulletin No. 256, 31-47. Melbourne: Commonwealth Scientific and Industrial Research Organization.

Vivian, H.E. 1951. The effect on mortar expansion of the particle size of the reactive component in the aggregate. Australian Journal of Applied Science, 2(4), 488-494.

Xue, Jun-gan, Xu, Wen-xia, and Ye, Ming-xun. 1983. A study of the liquid phase separated from the pores of hardened cement paste. Guisuanyan Xuebao, 11(3), 276-289.

Appendix A. Analytical Procedures

Three specimens were analyzed, one undiluted specimen for pH measurement, one specimen diluted ~1:100 for hydroxyl ion titration and for analysis by ion chromatograph (IC), and the third specimen diluted for silica determination. For dilutions, the sealed plastic bag containing the pore solution was pierced by the needle of an 1-ml capacity, plastic syringe. Once it was filled with pore solution, each syringe was removed from the glove box and its mass measured, the solution expelled into a volumetric flask, and the mass of the empty syringe again measured.

pH

Pore solutions were analyzed for pH level using a meter[21] and a combination electrode[22]. Solutions were not diluted for these measurements.

Prior to each group of measurements, the pH meter was standardized using two buffer solutions, one at pH 7.00 and one at pH 11.00. These solutions were prepared by dissolving the capsule of a pre-packaged buffer compound[23] in deionized, freshly boiled (CO_2-free) water. When prepared according to directions, the buffer compound has a specified precision of ±0.02 pH units. Solutions were prepared and pH measurements were carried out in a glove box in an atmosphere of dry nitrogen, to avoid error due to carbonation of solutions. Whenever possible, solutions were stirred using a magnetic stir plate while being measured, though the small volume of the expressed pore solutions prevented their being stirred in this manner.

---

[21] Orion pH meter, Model 801A.

[22] Orion Ross combination electrode.

[23] Hydrion buffer compound.

Once the meter had been standardized, the electrode was immersed in the solution for analysis, allowed to stabilize, than a reading taken. If the electrode had not stabilized after 60 sec, a reading was taken at that time. In the high pH pore solutions, it was common that the electrode did not stabilize within 60 sec and the pH reading was still increasing. However, allowing longer time for the electrode to stabilize in these high pH solutions was considered to be potentially harmful to the electrode itself.

After each reading, one of the two calibration solutions was rechecked. If the pH of the standard had drifted by more than 0.01 pH units, the process of standardization and analysis was repeated. Typically, however, the system was free of drift within 0.005 pH units.

Preliminary studies were carried out to assess precision and accuracy of the pH electrode and meter. For the precision studies, a solution was prepared using reagent-grade potassium and sodium hydroxide, 3 mols K per mol Na, at a nominal pH of 13.3. The pH of this solution was measured at times between 30 sec and 120 sec following the procedure described above. The electrode was then recalibrated and the measurement repeated to assess precision of the procedure. Results (Fig. 74 and Table 29) show a precision (1σ) of 0.01 pH unit.

For the accuracy studies, four solutions were prepared using reagent-grade potassium and sodium hydroxide. Their measured pH levels ranged from 13.0 to 13.5 (Table 30). The hydroxyl ion concentration of each solution was determined by titration using ~0.1 M HCl, which had been standardized against a solution prepared from reagent-grade Na_2CO_3.

In order to calculate pH levels from the measured hydroxyl ion concentration levels, the activity coefficients for hydroxyl must be estimated. The activity coefficient depends on the specific cation, and becomes difficult to estimate in solutions containing more than one cation. For

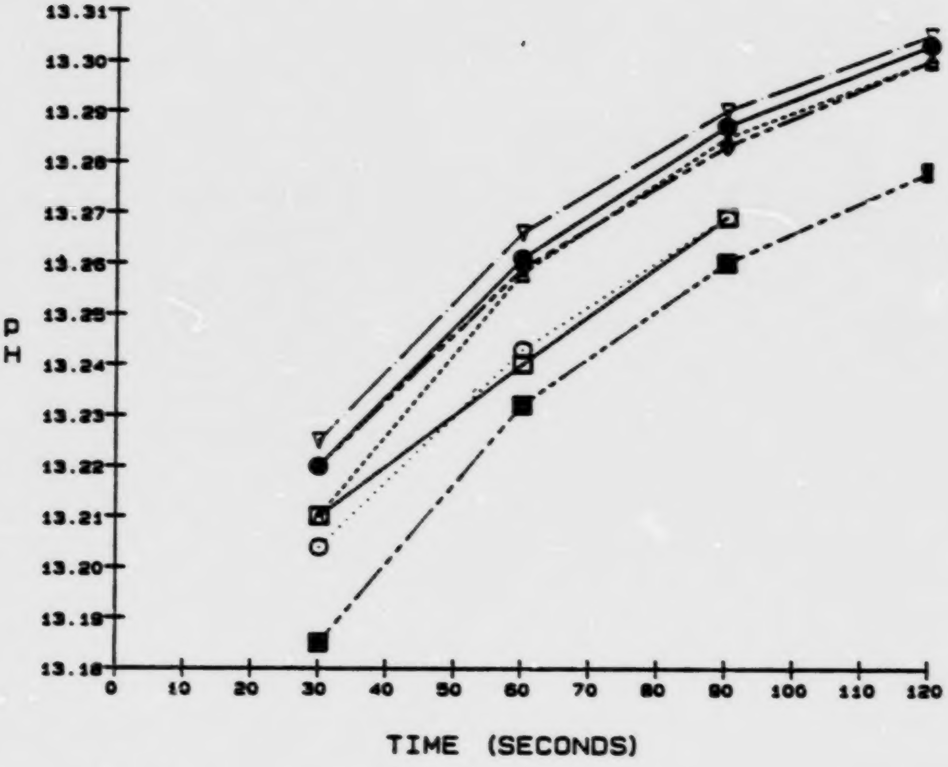

Figure 74. Replicates of measured pH levels at various times.

BEST COPY AVAILABLE

Table 29. Replicate pH measurements.

	30 sec	60 sec	90 sec	120 sec
1	13.210	13.240	13.269	nd[a]
2	13.204	13.243	13.269	nd
3	13.210	13.258	13.285	13.300
4	13.225	13.266	13.290	13.305
5	13.220	13.259	13.283	13.300
6	13.185	13.232	13.260	13.278
7	13.220	13.261	13.287	13.303
Mean	13.210	13.258	13.283	13.300
σ	0.013	0.013	0.011	0.011

[a] Not determined.

Table 30. Calculated and measured pH levels.

Solution	[OH] (mM)	γ^{a}	Calculated pH	Measured pH	Difference
KOH + NaOH	138	0.76	13.26	13.39	-0.13
KOH	136	0.76	13.25	13.29	-0.04
NaOH	155	0.75	13.32	13.29	0.02
KOH + NaOH	184	0.74	13.39	13.58	-0.19

[a] Activity coefficients estimated from Goldberg et al (1985).

the present calculations, values of activity coefficients were estimated using GAMPHI, a database with activity coefficients for aqueous solutions (Goldberg et al, 1985). The database does not include solutions of more than one cation. For the solutions containing both potassium and sodium, the effect of the combination was ignored, and the calculation made using the total cation concentration as if it were potassium. The values of activity coefficient ranged from 0.74 to 0.79 (Table 30), and thus significantly affected the calculated pH values.

The agreement between measured and calculated pH levels (Table 30) is fair. For most solutions, the measured values are higher than the calculated values, in some cases by 0.1 or 0.2 pH units. It is possible that the difference could increase for even higher pH solutions, but such solutions were not tested.

Hydroxyl

Hydroxyl ion concentrations were determined by titrating solutions that were first diluted ~1:100, the same solutions used for IC analysis (below).

Hydroxyl ion concentration levels of the diluted specimens were expected to range from 3 to 12 mM. Therefore, solutions were titrated using 10 mM HCl, which had been standardized using a 10 mM NaOH solution, itself standardized using a 25 mM solution of potassium hydrogen phthalate ($KHC_8H_4O_4$). Both the NaOH and $KHC_8H_4O_4$ solutions were prepared using reagent-grade chemicals.

Replicate titrations were carried out to assess precision and accuracy. A solution of sodium hydroxide and a solution of potassium hydroxide, each ~10 mM, were titrated using a solution of reagent-grade potassium hydrogen phthalate, ~25 mM (Table 31). These two solutions were mixed in 3/1 molar proportions, for a calculated hydroxyl ion concentration level of 8.63 mM Results of

Table 31. Hydroxyl ion titrations to assess accuracy and precision.

Solution	measured [OH] (mM)	average [OH] (mM)	σ (mM)
NaOH	9.21	9.14[a]	0.18
	9.21		
	9.47		
	8.95		
	8.99		
	8.99		
KOH	8.38	8.46[a]	0.35
	8.31		
	8.24		
	8.27		
	8.34		
	9.24		
KOH + NaOH	8.50	8.62[b]	0.09
	8.71		
	8.71		
	8.56		

[a] Titrated using 25 mM potassium hydrogen phthalate.

[b] Titrated using 10 mM hydrochloric acid that had been standardized using 10 mM sodium carbonate.

replicate titrations of this mixed solution using the standardized HCl are shown in Table 31. The average measured hydroxyl ion concentration was 8.62, agreeing closely with the calculated level, and the precision (one standard deviation) was 0.1 mM.

Calcium, Potassium, Sodium, and Sulfate Ions

Concentration levels of calcium, potassium, sodium, and sulfate ions, both of solutions first diluted ~1:100, and of standard solutions of similar concentration levels, were measured by IC[24]. Prior to analysis for each ion, the response of the instrument was assessed by analysis of a series of calibration samples. Standard solutions and the calibration solutions were prepared by diluting reagent-grade stock solutions[25]. The calibrations demonstrated that the instrument response was linear throughout the range covered, thus the solutions need not be diluted further for any analysis. Results were analyzed by a linear regression method to assess the precision for each ion.

Specimens for analysis were injected manually, using an approximate volume of 0.5 ml. Because the efficiency of each column may vary throughout its life, a standard specimen was run between every two or three unknown samples.

Most of the various cations were measured using separate analytical systems, though sodium and potassium analyses were carried out simultaneously. Both the monovalent and the divalent cations were collected using the same type of column[26]. The eluent solution for calcium analysis consisted of 0.002 M HCl and 0.002 M meta-phenylenediamine, and for sodium and potassium analysis, 0.005 M HCl. Anions were collected using a different type of column[27], and an eluent solution consisting of 0.003 M $NaHCO_3$ and 0.0024 M Na_2CO_3. The same suppression system, a cation column[28] and a 0.5 N $Ba(OH)_2$ regenerant solution, was used for both monovalent and divalent cations. The suppression system for anion determinations consisted of a column[29] and a regenerant solution of 0.025 M H_2SO_4.

---

[24] Dionex System 12 Analyzer.

[25] Fisher standard solutions, 1000 mg/L.

[26] Dionex, HPIC-CS1 column.

The calcium calibration (Fig. 75) covered a concentration range up to 0.25 mM, and the analytical precision (standard error of estimated Y) was ±0.005 mM. The sodium and potassium calibrations (Figs. 76 and 77) covered concentration ranges up to 22 mM and 13 mM, respectively. The analytical precision levels were ±0.06 mM for sodium, and ±0.08 mM for potassium. The sulfate calibration (Fig. 78) covered a concentration range up to 1 mM, and its analytical precision was ±0.05 mM.

Silica

Silica concentration levels were measured using a colorimetric method and a series of calibration specimens were initially analyzed to assess the relationship between absorbance and silica content. Typical absorbance spectra are shown in Fig. 79, and calibration results in Fig. 80. The results are linear throughout the calibration range (0 μM to 2 μM), and the analytical precision was ±0.02 μM.

Samples were diluted approximately 1:25 during their preparation for analysis. Each unknown solution and the standard solutions (0 and 2 μM Si) were prepared as follows:

---

[27] Dionex, HPIC-AS3 column.

[28] Dionex, CSC-1 column.

[29] Dionex, AFS column.

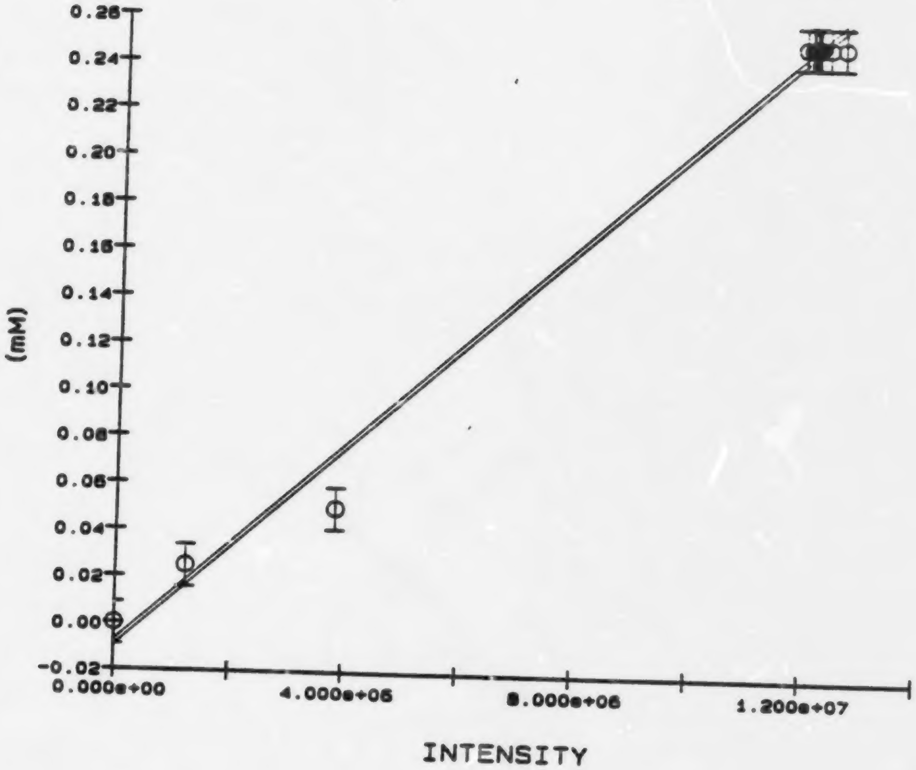

Figure 75. Calibration curve for calcium.

BEST COPY AVAILABLE

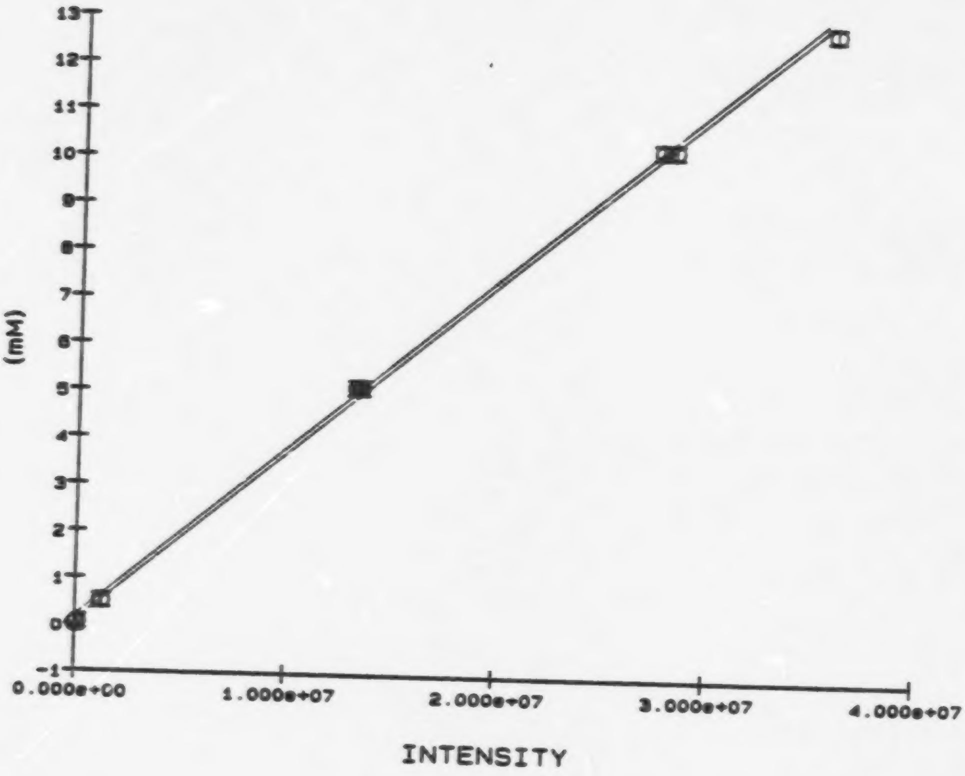

Figure 76. Calibration curve for sodium.

BEST COPY AVAILABLE

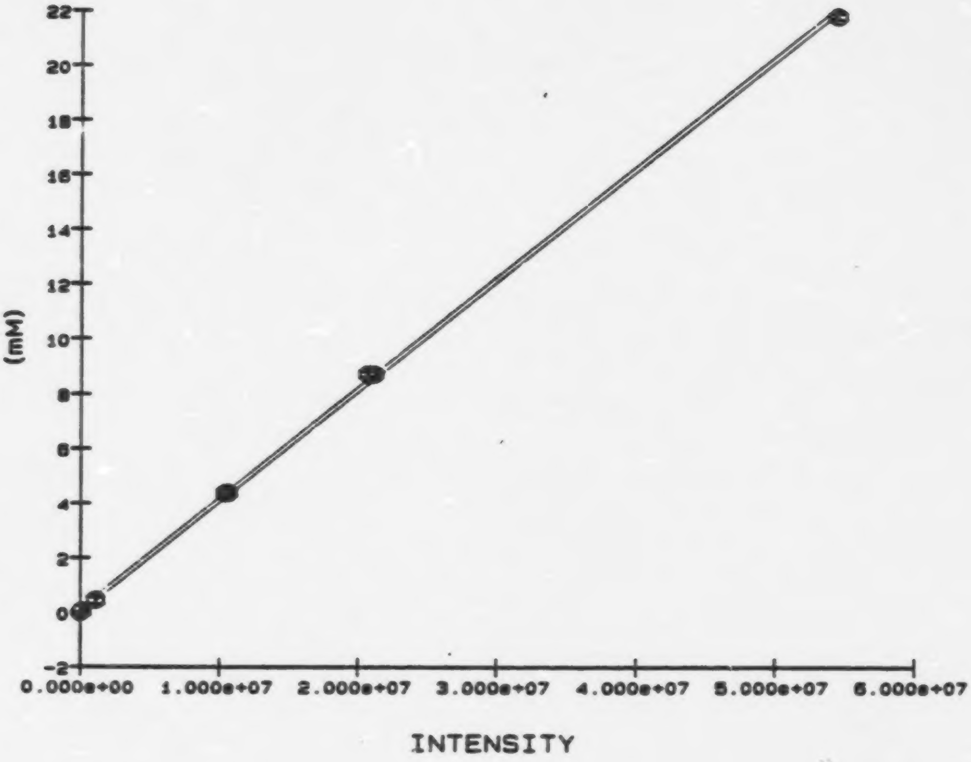

Figure 77. Calibration curve for potassium.

BEST COPY AVAILABLE

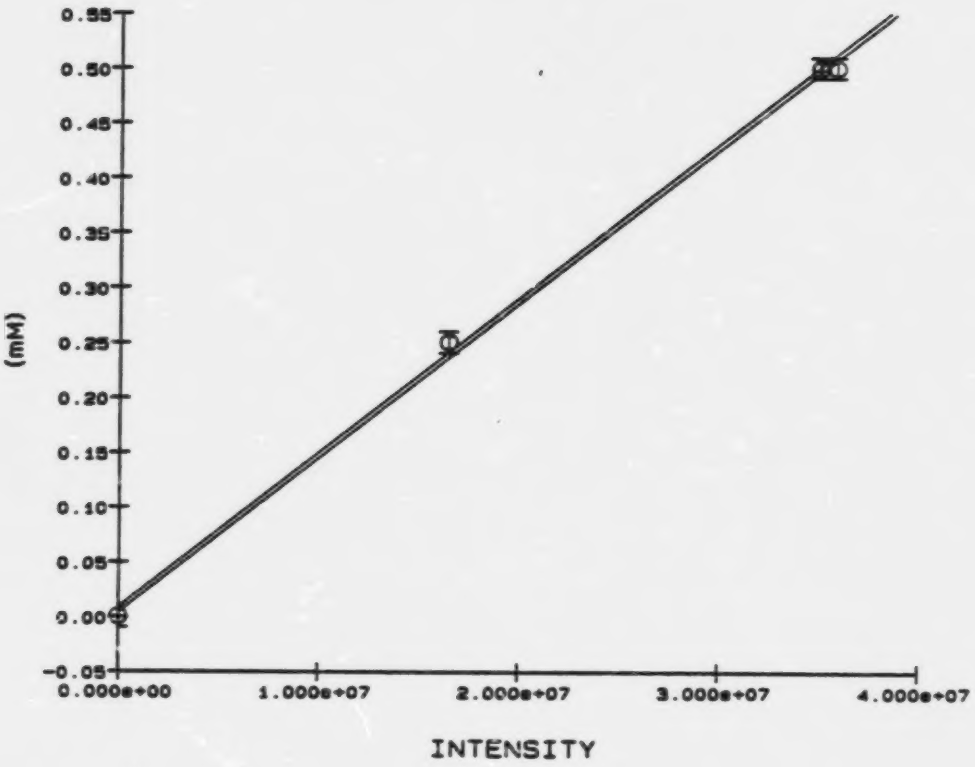

Figure 78. Calibration curve for sulfate.

BEST COPY AVAILABLE

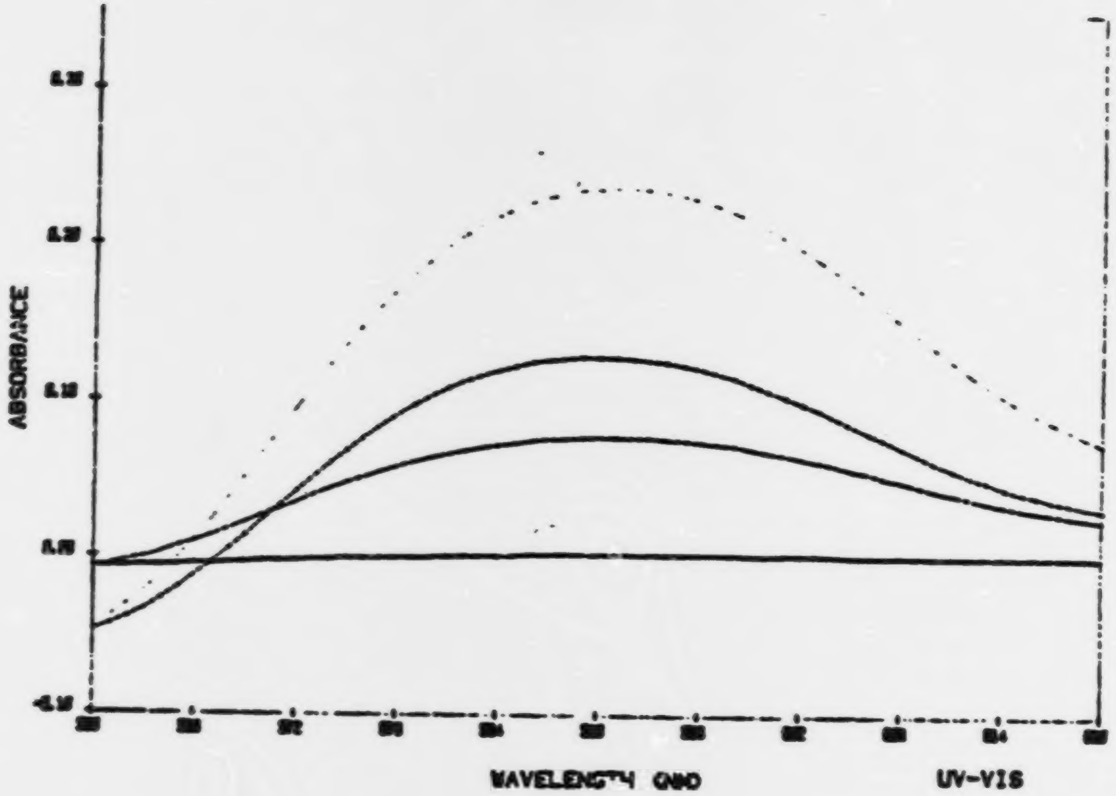

Figure 79. Typical UV absorbance spectra for silica specimens, showing reagent blank (bottom-most curve), 1.0 µM silica standard (second curve), 2.0 µM silica standard (third curve), and an unknown specimen (topmost curve).

BEST COPY AVAILABLE

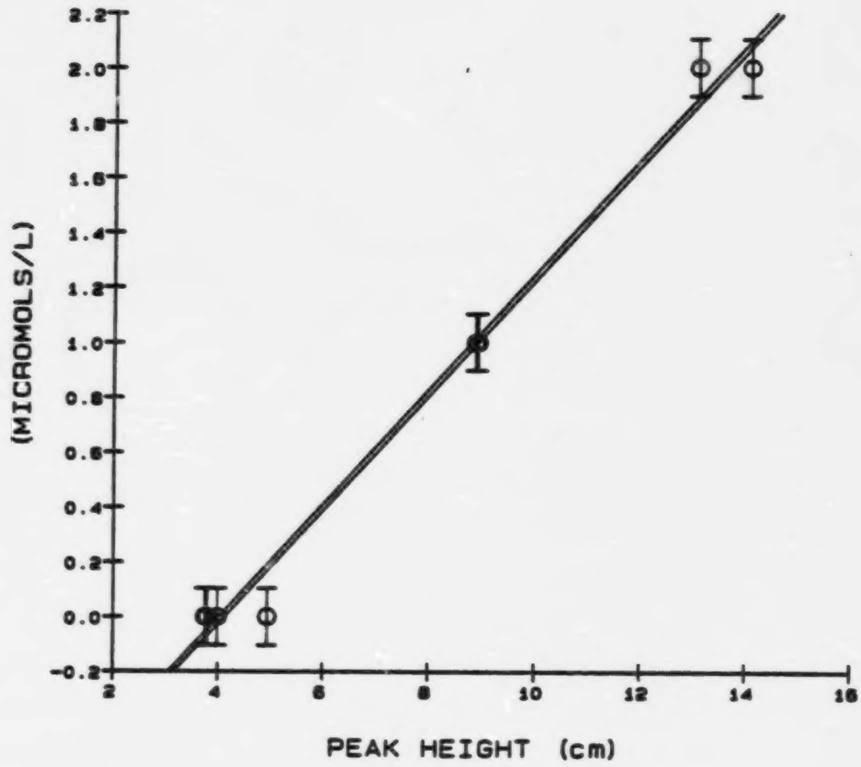

Figure 80. Calibration curve for silica.

BEST COPY AVAILABLE

1. In a 10-ml volumetric flask, 2 ml of 6 mM Na_2MoO_4 solution were mixed with 2 ml 0.06 M HNO_3 solution.

2. For the unknown specimen, ~0.4 ml sample and 1 ml water were added. The samples were removed from the sealed bag using a microsyringe; the microsyringe was weighed while containing solution and weighed again after the solution was expelled into the volumetric flask to determine the precise sample weight. For the 0 μM standard, 2.0 ml water were added; for the 1.0 μM or the 2.0 μM standard, 1.0 ml or 2.0 ml of a 10 μM silica stock solution (prepared using reagent-grade $Na_2SiO_3 \cdot 9H_2O$) were added. Solutions were agitated to mix, then allowed to react for 10 min.

3. 1 ml of 5 M HNO_3, then 2 ml of the 100 μM Rhodamine B solution were added.

4. Specimens were diluted to 10 ml with water, mixed, and allowed to react for 10 min.

Absorbance values were determined immediately, using a computer-controlled ultraviolet-visible spectrophotometer[30], which measures the difference in absorbance between specimen and blank. For this measurement, specimens were scanned over a range between 560 nm and 620 nm, at 60 nm per min. The differences in absorbance between specimen or standard and blank were collected by computer, and plots of absorbance versus wavelength generated for each specimen. The absorbance peak for the silico-molybdate-rhodamine complex occurs at approximately 590 nm; this is a broad peak, extending over approximately 60 nm (Fig. 79). Using the plots, the difference for each specimen or standard between the maximum absorbance of the silico-molybdate-rhodamine B complex and the blank at the same wavelength was measured as the height of this broad peak. The silica concentration in each specimen was calculated using the absorbance values measured for the standard solutions. The concentration in the sample was calculated from the known sample weight used for the specimen.

---

[30] Perkin-Elmer 552 Spectrophotometer.

Appendix B. Bags for Storage of Pore Solutions

Prior to expression and analysis of pore solutions, bags for storing solutions were evaluated to assess their permeability. In particular, experiments were carried out to determine whether water vapor (H_2O) or carbon dioxide gas (CO_2) would diffuse through the plastic, since significant diffusion of H_2O or CO_2 would modify the pore solution composition. For these preliminary experiments, solutions saturated in $Ca(OH)_2$ were sealed in the bags. The sealed bags were weighed during storage in laboratory air to detect any outward diffusion of water, and examined visually for cloudiness that would indicate precipitation of $CaCO_3$ due to diffusion of CO_2 into the bag.

Throughout the 24 days of observation, no precipitation was observed in the sealed bags. The reduction in mass (Table 32) was -0.07% per day, indicating that the sealed bags were slowly permeable to water. Based on these results, pore solutions were removed from the bags and diluted for analysis within 3 days.

Appendix C. X-Ray Diffraction Patterns of Cements

The existence of specific alkali-bearing phases in the cements was determined by qualitative analysis of the XRD patterns of each cement, of the residue after extraction of each ignited cement in a salicylic acid methanol solution, and of the residue after extraction of each cement in an

Table 32. Changes in mass of water-filled, sealed, plastic bags used to store pore solution.

Time (days)	Mass (grams)	Change (%)
0.00	1.68218	0.00
10.00	1.67045	0.70
16.00	1.66334	1.12
24.00	1.65447	1.65

aqueous KOH-sugar solution, shown in Figs. 81 through 96. Using the peaks in Table 33, these patterns were analyzed to identify the principal alkali-bearing phases in each cement.

Appendix D. Expansion Results

Expansion results for each mortar are presented (Table 34); data are the average expansion level measured for two bars. Length changes of the two individual bars were generally found to agree well, typically within 0.001% (expansion), though data for a few pairs differ by as much as 0.07%. When length changes of individual bars were plotted versus age, the resulting curves were generally smooth, with relatively small changes between consecutive measurements. There are a few spikes in the expansion curves, which are probably caused by fluctuations in the storage temperature.

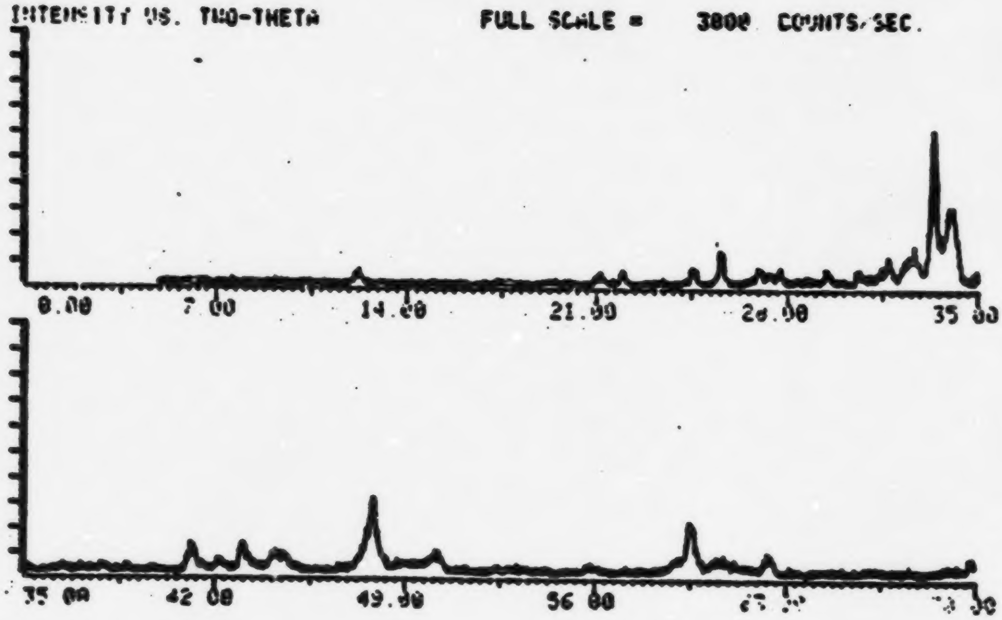

Figure 81. XRD pattern of Cement A ignited at 500°C and extracted in salicylic acid/methanol solution.

BEST COPY AVAILABLE

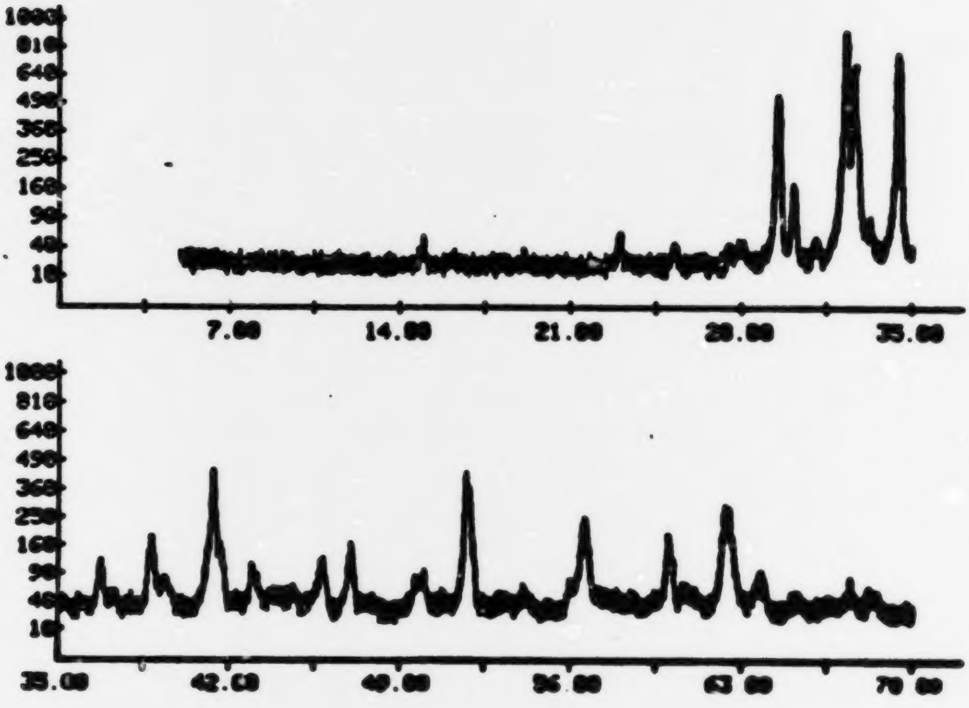

Figure 82. XRD pattern of Cement A ignited at 500°C and extracted in aqueous KOH-sugar solution.

BEST COPY AVAILABLE

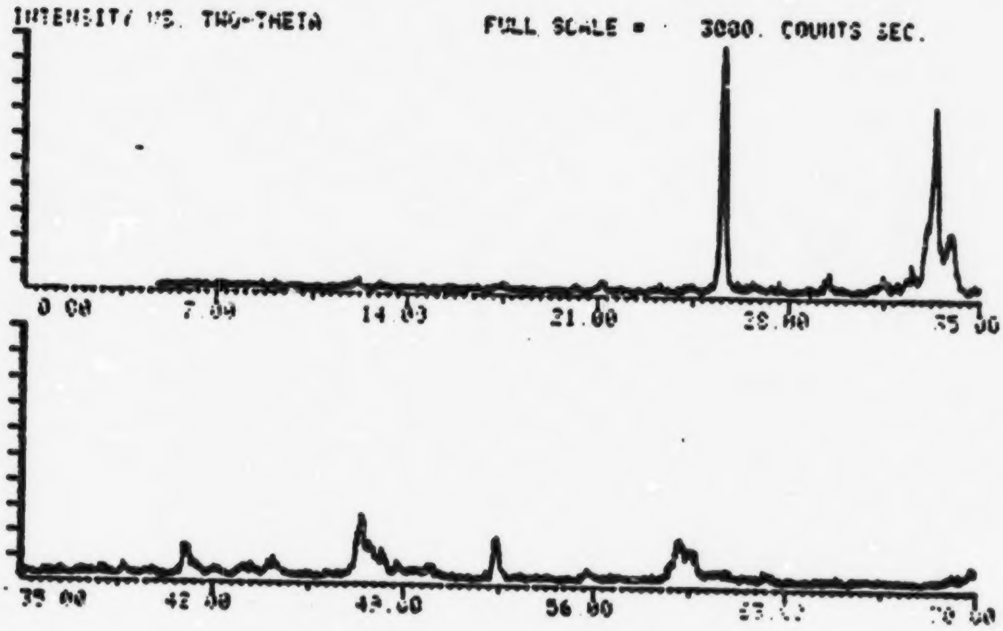

Figure 83. XRD pattern of Cement B ignited at 500°C and extracted in salicylic acid/methanol solution.

BEST COPY AVAILABLE

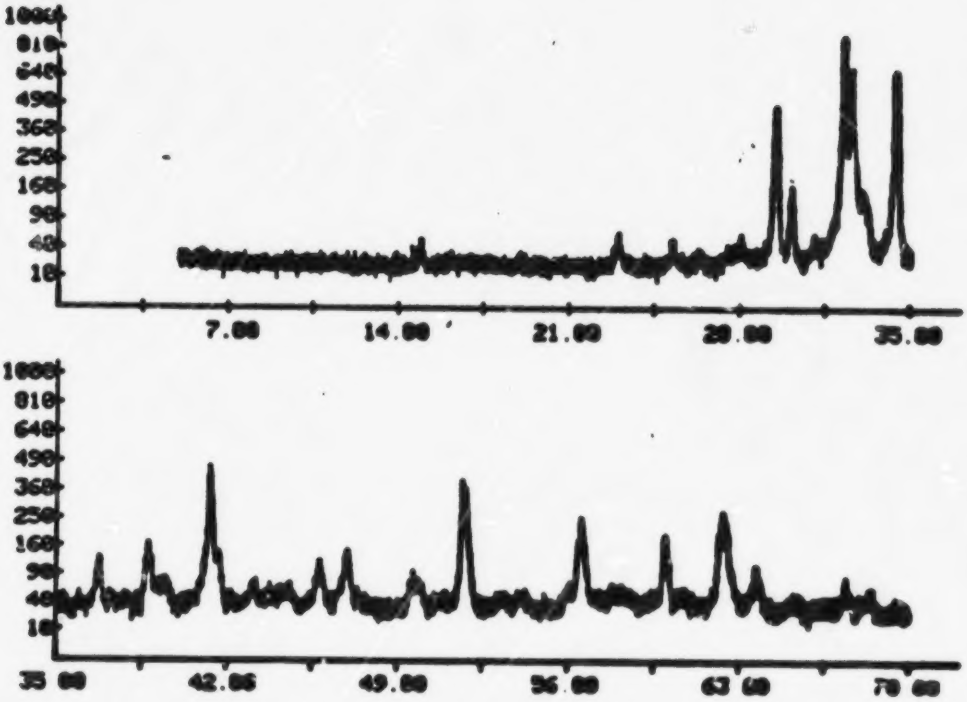

Figure 84. XRD pattern of Cement B ignited at 500°C and extracted in aqueous KOH-sugar solution.

BEST COPY AVAILABLE

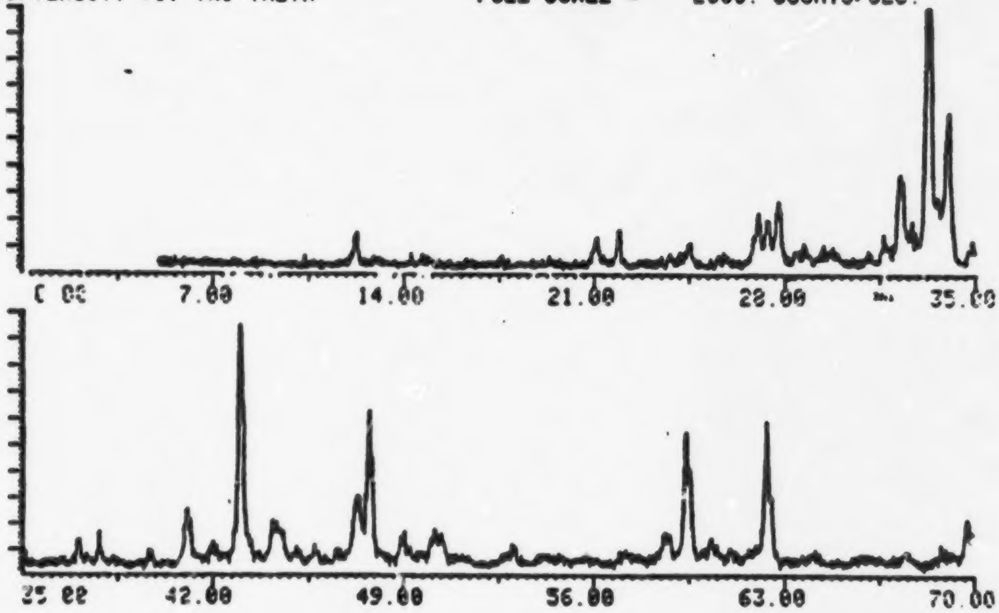

Figure 85. XRD pattern of Cement C ignited at 500°C and extracted in salicylic acid/methanol solution.

BEST COPY AVAILABLE

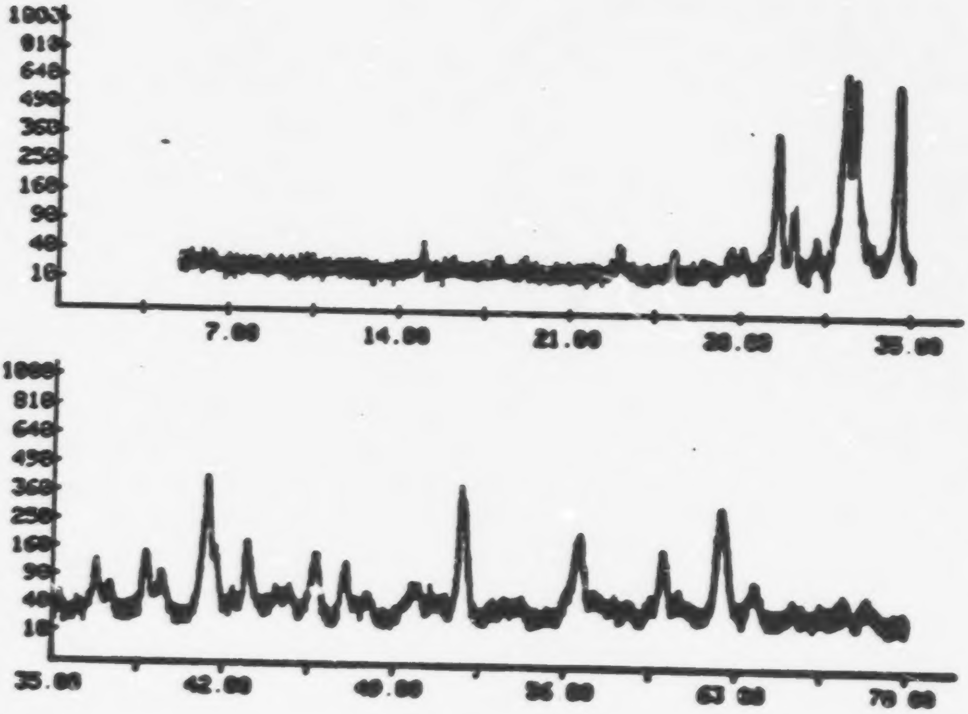

Figure 86. XRD pattern of Cement C ignited at 500°C and extracted in aqueous KOH-sugar solution.

BEST COPY AVAILABLE

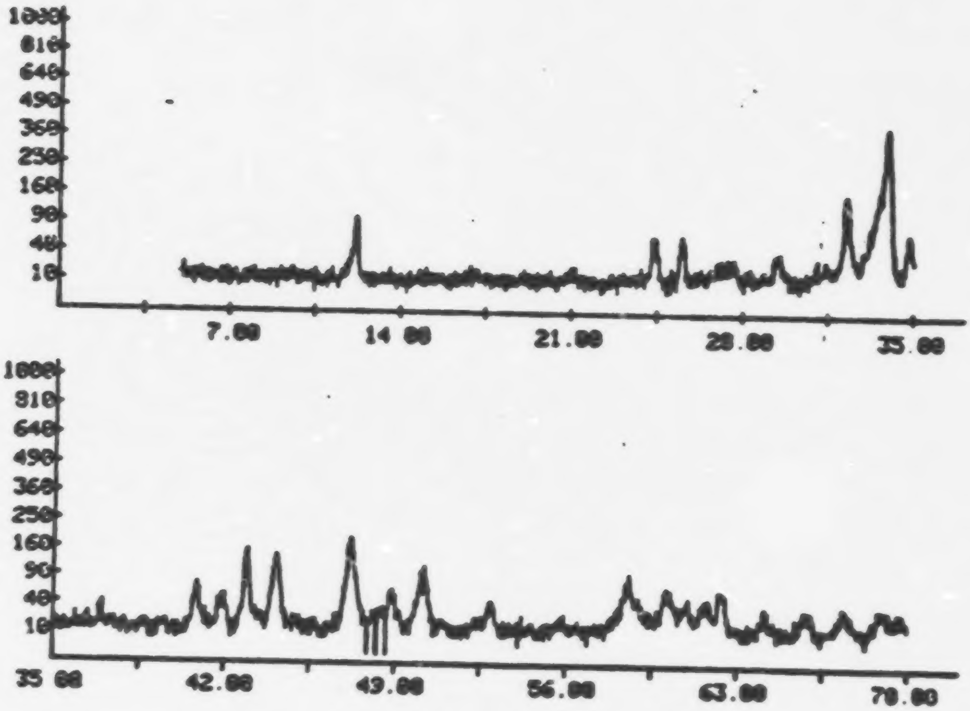

Figure 87. XRD pattern of Cement D ignited at 500°C and extracted in salicylic acid/methanol solution.

BEST COPY AVAILABLE

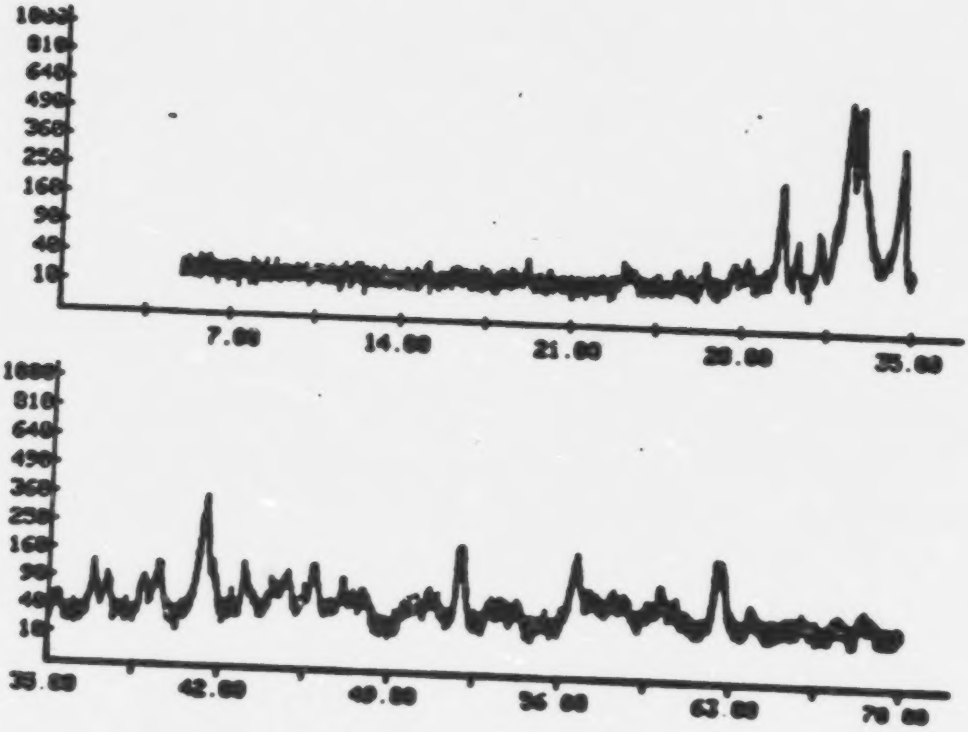

Figure 88. XRD pattern of Cement D ignited at 500°C and extracted in aqueous KOH-sugar solution.

BEST COPY AVAILABLE

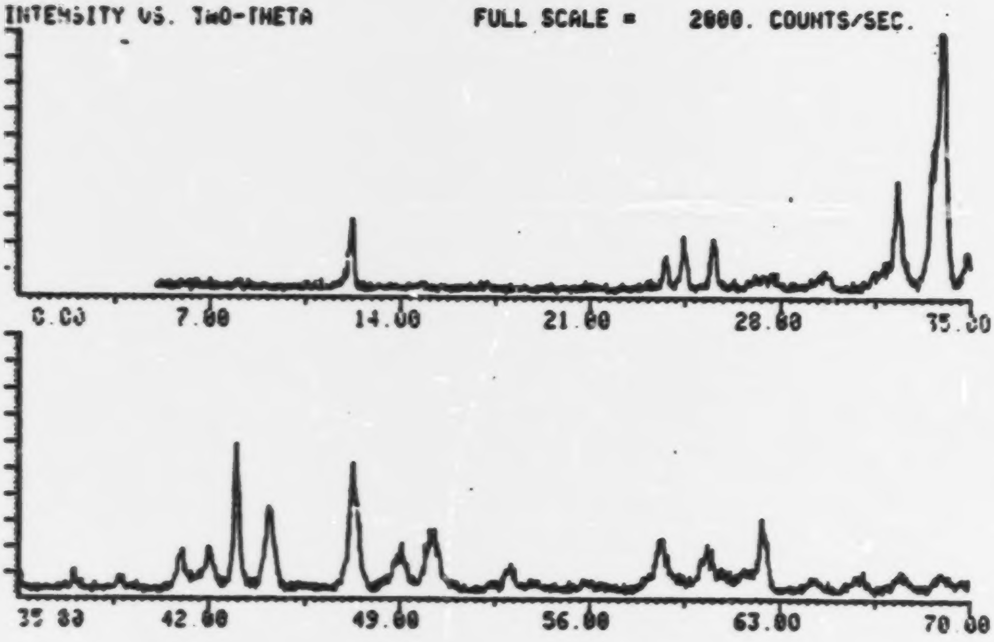

Figure 89. XRD pattern of Cement E ignited at 500°C and extracted in salicylic acid/methanol solution.

BEST COPY AVAILABLE

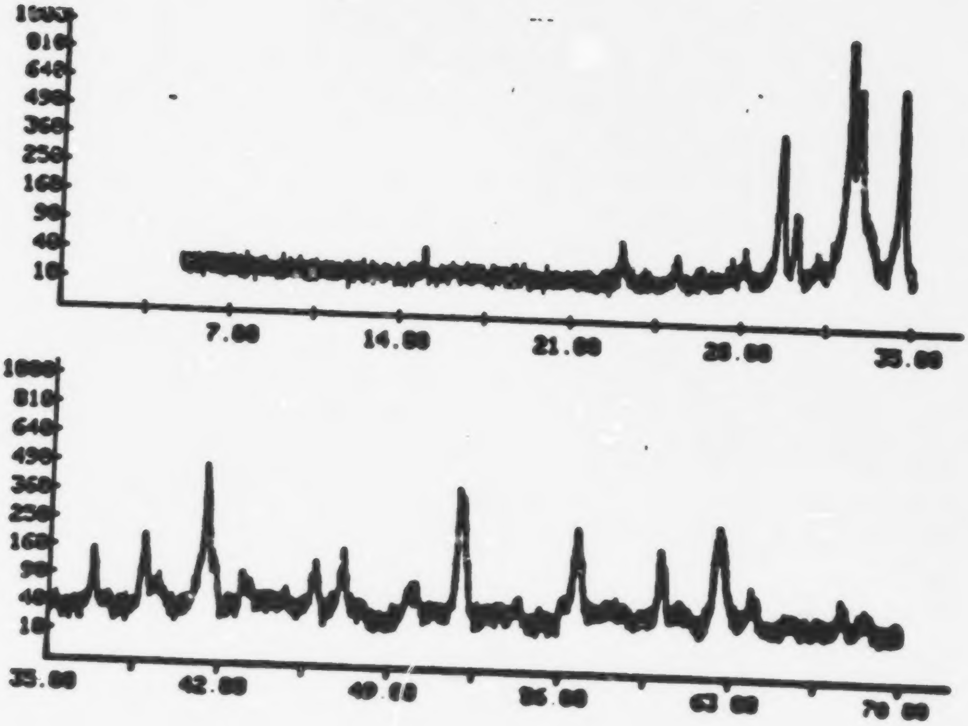

Figure 90. XRD pattern of Cement E ignited at 500°C and extracted in aqueous KOH-sugar solution.

BEST COPY AVAILABLE

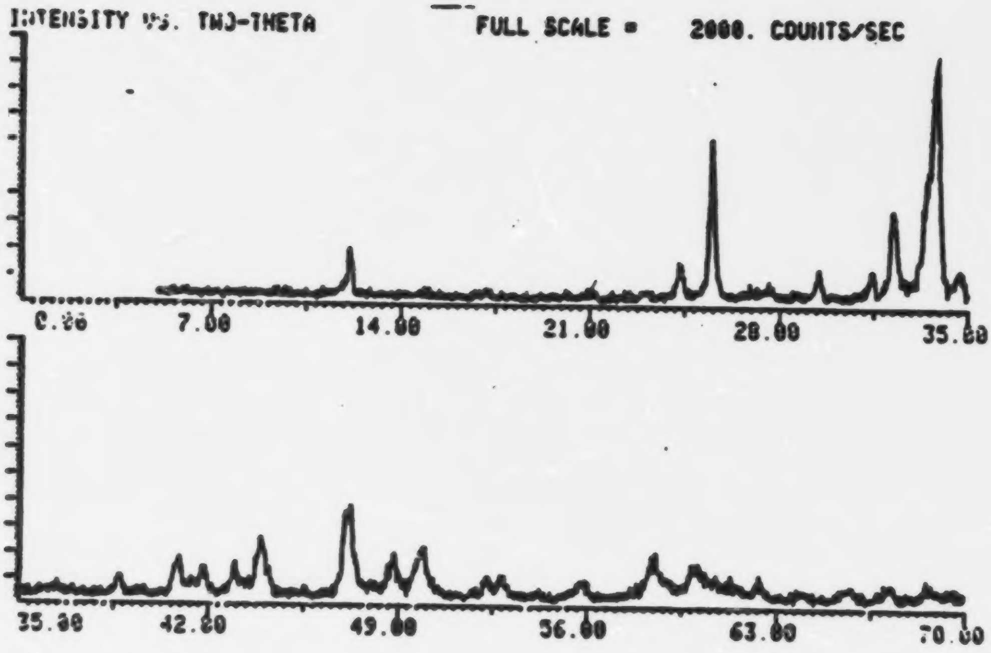

Figure 91. XRD pattern of Cement F ignited at 500°C and extracted in salicylic acid/methanol solution.

BEST COPY AVAILABLE

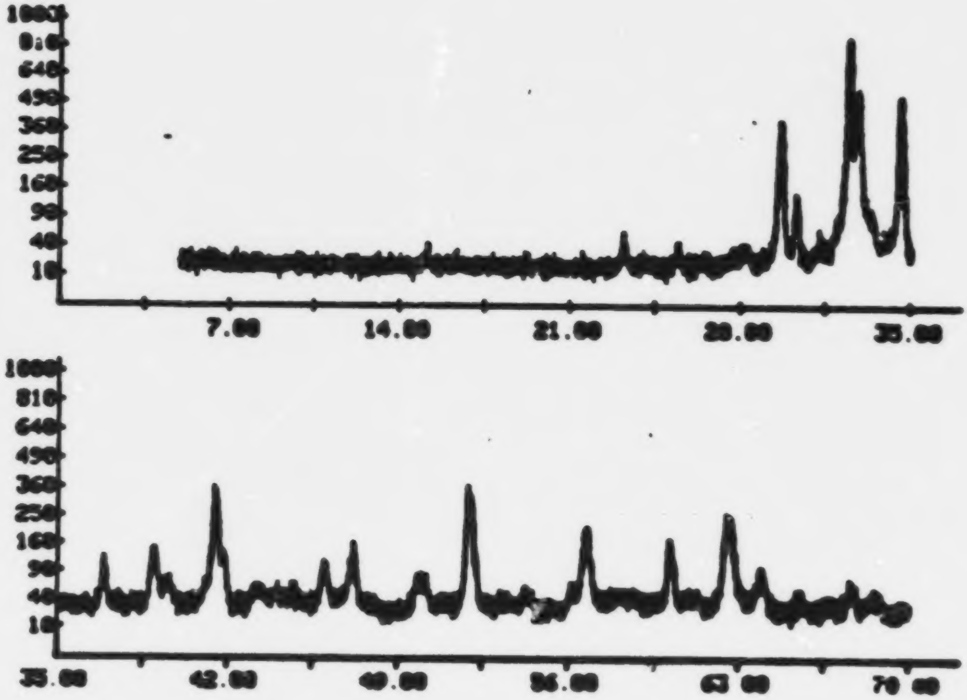

Figure 92. XRD pattern of Cement F ignited at 500°C and extracted in aqueous KOH-sugar solution.

BEST COPY AVAILABLE

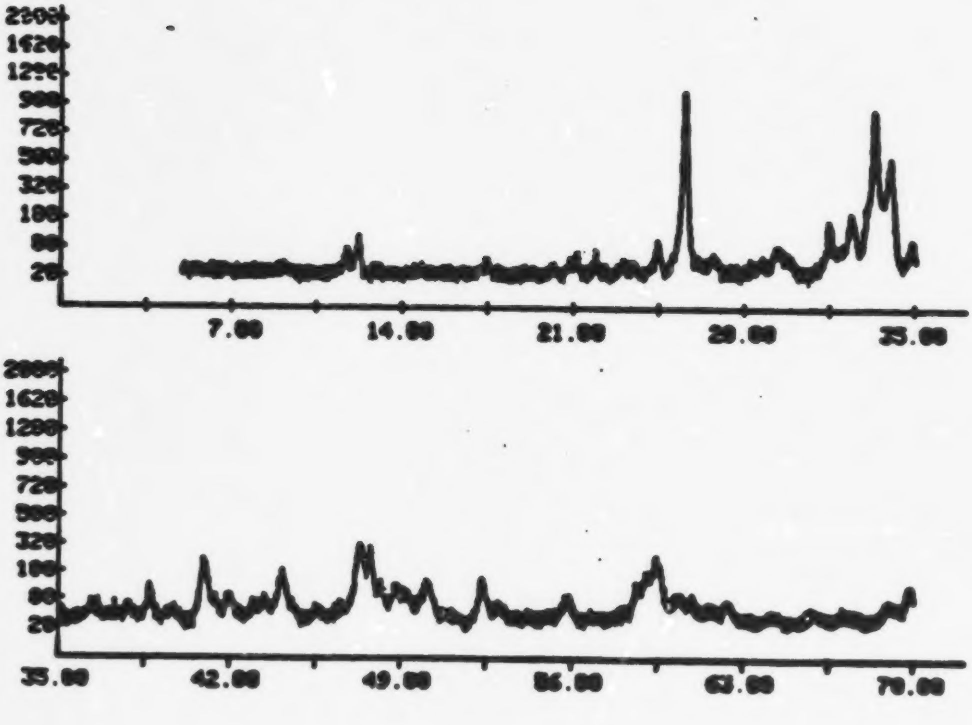

Figure 93. XRD pattern of Cement G ignited at 500°C and extracted in salicylic acid/methanol solution.

BEST COPY AVAILABLE

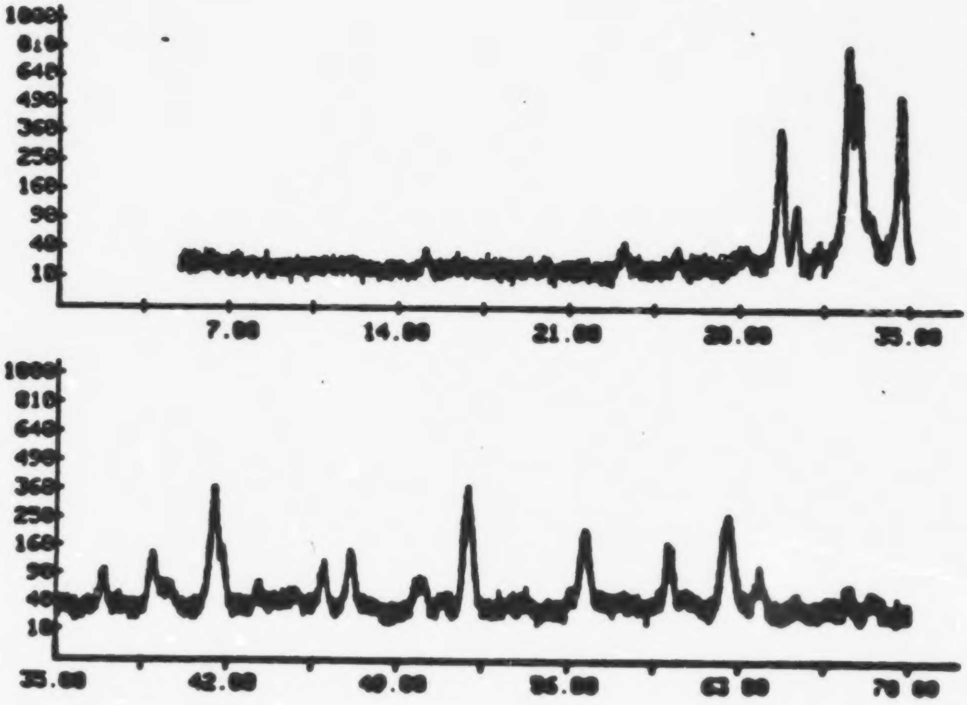

Figure 94. XRD pattern of Cement G ignited at 500°C and extracted in aqueous KOH-sugar solution.

BEST COPY AVAILABLE

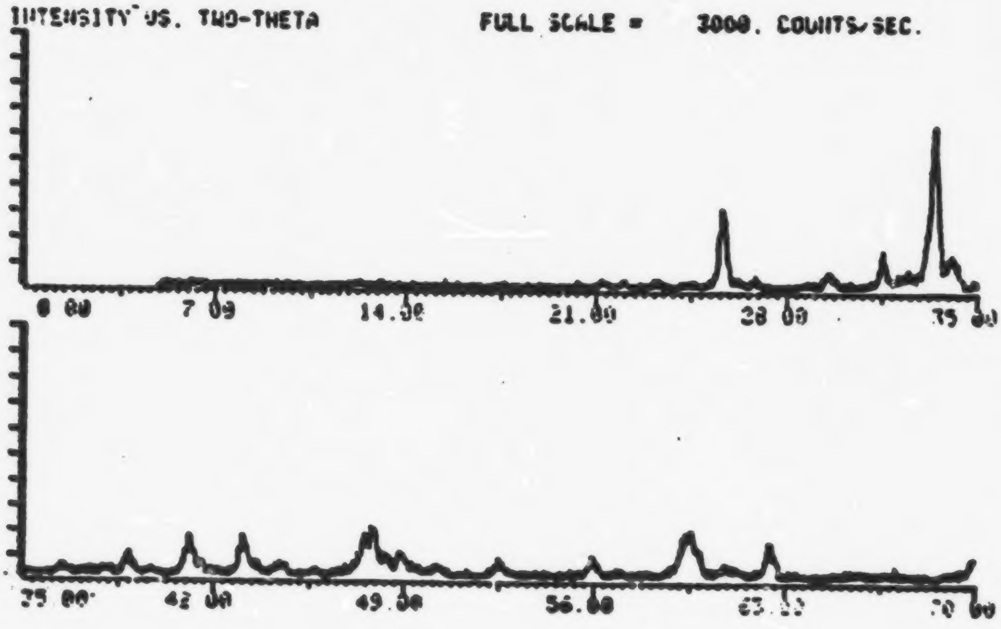

Figure 95. XRD pattern of Cement H ignited at 500°C and extracted in salicylic acid/methanol solution.

BEST COPY AVAILABLE

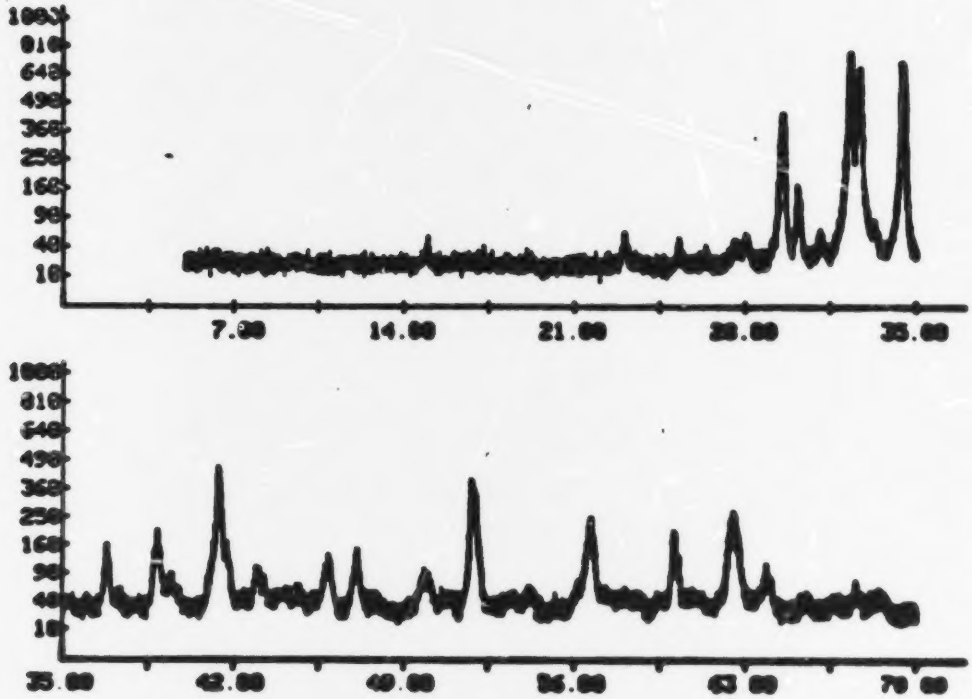

Figure 96. XRD pattern of Cement H ignited at 500°C and extracted in aqueous KOH-sugar solution.

BEST COPY AVAILABLE

Table 33. XRD peaks used to identify alkali phases.

Phase	Peak positions (nm)	(°2θ)	h,k,l	Reference
K_2SO_4[a]	0.2902	30.79	013	24-703[b]
$K_2Ca_2(SO_4)_3$[a]	0.3315	26.88	130,031	20-867[b]
	0.3267	27.27	310,301	
	0.3225	27.64	013,103	
Orthorhombic C_3A[a]	0.441	20.12	202	33-251[b]
α'-C_2S[c]	0.2717	32.96	110	d

[a] Identified in salicylic acid/methanol extraction residue.

[b] JCPDS Card Number.

[c] Identified in KOH-sugar extraction residue.

[d] Reference: Gies and Knöfel (1986).

Table 34. Average measured expansion for each mortar[a].

Cement A 100% limestone		Cement A 2% opal		Cement A 4% opal		Cement A 8% opal	
Age (weeks)	Exp. (%)	Age (weeks)	Exp. (%)	Age (weeks)	Exp. (%)	Age (weeks)	Exp. (%)
0.00	0.00	0.00	0.00	-0.00	0.00	0.00	0.00
0.14	0.00	0.14	0.00	0.14	0.00	0.14	0.00
0.29	-0.00	0.30	0.00	0.84	0.03	0.69	0.03
1.28	0.01	1.15	0.05	1.13	0.08	0.99	0.08
2.28	0.01	2.29	0.12	2.27	0.15	2.12	0.12
3.45	0.01	3.61	0.16	3.30	0.20	3.16	0.13
4.28	0.01	5.60	0.19	4.14	0.22	3.99	0.14
5.29	0.01	7.57	0.18	5.14	0.23	5.00	0.15
6.30	0.01	8.60	0.20	6.15	0.24	6.01	0.15
7.14	0.02	13.01	0.20	7.00	0.26	6.85	0.15
8.14	0.01	16.41	0.21	8.00	0.26	7.85	0.14
9.43	0.02	21.32	0.22	9.28	0.27	9.13	0.15
10.00	0.01	26.00	0.22	9.85	0.27	9.71	0.15
11.45	0.02	32.31	0.22	11.30	0.28	11.15	0.15
12.28	0.02	36.60	0.23	12.13	0.29	11.98	0.15
13.98	0.01	46.61	0.22	13.83	0.30	13.69	0.14
15.42	0.01	100.02	0.24	15.27	0.30	15.13	0.15
16.43	0.02	150.16	0.24	16.28	0.30	16.14	0.15
17.16	0.01			17.01	0.30	16.87	0.15
19.44	0.01			19.29	0.30	19.14	0.15
21.83	0.01			21.69	0.32	21.54	0.15
28.44	0.02			28.30	0.32	28.15	0.15
33.42	0.02			33.28	0.33	33.14	0.17
37.85	0.02			37.70	0.36	37.55	0.15
41.16	0.02			41.01	0.36	40.87	0.15

---

[a] In most cases the average of two bars, otherwise the results of one bar.

(Table 34, continued)

Cement A 12% opal		Cement A 10% quartzite		Cement A 20% quartzite		Cement A 30% quartzite	
Age (weeks)	Exp. (%)	Age (weeks)	Exp. (%)	Age (weeks)	Exp. (%)	Age (weeks)	Exp. (%)
0.00	0.00	0.00	0.00	0.00	0.00	0.00	0.00
0.15	0.00	0.14	0.00	0.17	0.00	0.14	0.00
0.44	0.01	0.44	0.00	0.30	0.00	0.27	0.00
1.57	0.02	2.15	0.01	1.61	0.01	0.98	0.01
2.61	0.04	4.87	0.02	3.60	0.02	2.29	0.01
3.44	0.04	6.41	0.02	5.58	0.02	3.12	0.02
4.45	0.04	7.45	0.01	6.61	0.02	4.83	0.02
5.46	0.04	11.01	0.02	11.02	0.02	6.27	0.02
6.30	0.05	16.43	0.02	14.42	0.03	7.28	0.02
7.31	0.04	60.87	0.03	19.32	0.03	8.11	0.03
8.59	0.04	111.00	0.04	24.00	0.03	10.29	0.03
9.16	0.04			30.31	0.04	12.68	0.03
10.61	0.04			34.61	0.04	14.98	0.03
11.44	0.04			44.61	0.04	16.84	0.03
13.13	0.05			98.03	0.04	17.97	0.03
14.58	0.04			146.56	0.04	19.29	0.05
15.59	0.04					21.28	0.02
16.32	0.04					23.26	0.03
18.60	0.04					24.28	0.04
20.99	0.05					28.70	0.04
27.61	0.04					32.10	0.03
32.59	0.06					37.00	0.03
36.58	0.05					41.67	0.03
40.32	0.05					47.99	0.03
						62.29	0.03
						115.71	0.04
						165.70	0.04

(Table 34, continued)

Cement A 50% quartzite		Cement A 100% granite		Cement B 100% limestone		Cement B 1% opal	
Age (weeks)	Exp. (%)	Age (weeks)	Exp. (%)	Age (weeks)	Exp. (%)	Age (weeks)	Exp. (%)
0.00	0.00	0.00	0.00	0.00	0.00	0.00	0.00
0.14	0.00	0.14	0.00	0.15	0.00	0.15	0.00
0.29	0.00	0.84	0.01	0.46	0.00	1.54	0.00
1.14	0.01	2.98	0.02	1.43	-0.00	2.14	0.01
2.13	0.01	4.69	0.02	2.01	-0.00	2.88	0.01
3.85	0.02	6.13	0.03	3.30	0.02	5.83	0.02
5.87	0.02	7.14	0.02	4.30	0.01	7.56	0.03
10.16	0.02	7.97	0.03	5.31	0.02	9.58	0.04
14.86	0.02	10.15	0.02	6.16	0.02	13.86	0.05
19.16	0.02	12.54	0.02	7.16	0.02	18.57	0.05
21.88	0.03	14.84	0.03	8.44	0.02	22.87	0.05
24.46	0.02	16.70	0.03	9.01	0.02	28.16	0.05
77.87	0.02	17.84	0.03	10.46	0.02	81.58	0.09
127.99	0.03	19.15	0.02	11.29	0.02	131.59	0.07
		21.14	0.03	12.99	0.02		
		23.12	0.03	14.44	0.02		
		24.15	0.03	15.44	0.02		
		28.56	0.03	16.17	0.02		
		31.96	0.03	16.45	0.02		
		36.86	0.03	20.85	0.02		
		41.53	0.03	27.46	0.01		
		47.85	0.03	32.44	0.02		
		62.15	0.03	36.86	0.02		
		115.57	0.04	40.17	0.02		

(Table 34, continued)

Cement B 2% opal		Cement B 4% opal		Cement B 8% opal		Cement B 12% opal	
Age (weeks)	Exp. (%)	Age (weeks)	Exp. (%)	Age (weeks)	Exp. (%)	Age (weeks)	Exp. (%)
0.00	0.00	0.00	0.00	-0.00	0.00	-0.00	0.00
0.14	0.00	0.14	0.00	0.16	0.00	0.14	0.00
0.85	0.01	0.31	0.00	0.83	0.00	0.30	0.00
1.99	0.02	0.98	0.01	1.13	0.00	0.44	-0.01
3.30	0.06	1.27	-0.00	1.72	-0.00	1.02	-0.01
5.29	0.10	1.86	-0.00	3.01	0.02	1.46	0.01
7.27	0.13	3.15	0.02	4.00	0.01	2.30	0.01
8.30	0.16	4.15	0.03	5.01	0.02	3.30	0.01
12.71	0.16	5.16	0.04	5.86	0.02	4.31	0.01
16.11	0.18	6.00	0.04	6.86	0.02	5.16	0.01
21.01	0.19	7.01	0.04	8.14	0.02	6.16	0.02
25.69	0.20	8.29	0.04	8.71	0.02	7.44	0.01
32.00	0.21	8.86	0.04	10.16	0.02	8.01	0.01
36.30	0.21	10.31	0.04	10.99	0.03	9.46	0.01
46.30	0.21	11.14	0.06	12.69	0.02	10.29	0.02
99.72	0.25	12.84	0.04	14.14	0.01	11.99	0.02
149.83	0.25	14.28	0.06	15.14	0.03	13.44	0.02
		15.29	0.06	15.88	0.02	14.44	0.02
		16.02	0.06	18.15	0.02	15.18	0.01
		18.30	0.06	20.55	0.03	17.45	0.02
		20.69	0.07	27.16	0.02	19.85	0.01
		27.31	0.07	32.14	0.03	26.46	0.02
		32.29	0.07	36.56	0.02	31.44	0.02
		36.71	0.07	39.88	0.02	35.86	0.02
		40.02	0.04			39.18	0.02

(Table 34, continued)

Cement B		Cement B		Cement B		Cement B	
10% quartzite		20% quartzite		30% quartzite		50% quartzite	
Age (weeks)	Exp. (%)	Age (weeks)	Exp. (%)	Age (weeks)	Exp. (%)	Age (weeks)	Exp. (%)
0.00	0.00	0.00	0.00	0.00	0.00	0.00	0.00
0.14	0.00	0.15	0.00	0.14	0.00	0.14	0.00
0.29	0.00	1.47	0.01	1.17	0.01	1.00	0.00
0.98	0.01	3.46	0.02	2.00	0.01	1.98	0.01
2.01	0.02	5.43	0.02	3.70	0.01	3.71	0.01
4.73	0.03	6.46	0.02	5.15	0.02	5.73	0.01
6.26	0.02	10.88	0.03	6.16	0.02	10.01	0.01
7.31	0.03	14.27	0.03	6.99	0.02	14.72	0.01
10.87	0.02	17.85	0.03	9.16	0.02	19.02	0.01
16.29	0.02	18.45	0.02	11.56	0.03	21.74	0.01
60.73	0.03	19.18	0.03	13.86	0.03	24.31	0.01
110.86	0.03	23.86	0.03	15.72	0.03	77.73	0.01
		30.17	0.03	16.85	0.02	127.85	0.03
		34.46	0.03	18.17	0.03		
		44.47	0.02	20.16	0.02		
		97.89	0.04	22.13	0.03		
		147.89	0.04	23.16	0.04		
				27.58	0.02		
				30.98	0.03		
				35.88	0.03		
				40.55	0.02		
				46.87	0.04		
				61.17	0.03		
				114.59	0.02		
				164.58	0.02		

(Table 34, continued)

Cement B 100% granite		Cement C 100% limestone		Cement C 1% opal		Cement C 2% opal	
Age (weeks)	Exp. (%)	Age (weeks)	Exp. (%)	Age (weeks)	Exp. (%)	Age (weeks)	Exp. (%)
0.00	0.00	0.00	0.00	0.00	0.00	0.00	0.00
0.14	0.00	0.14	0.00	0.14	0.00	0.16	0.00
1.44	0.02	0.71	0.00	0.59	0.01	1.01	0.02
3.84	0.01	2.00	0.00	1.32	0.02	2.15	0.07
6.13	0.01	2.69	-0.01	4.28	0.03	3.47	0.18
7.99	0.03	3.12	0.00	6.00	0.05	5.46	0.17
9.13	0.02	6.00	0.01	8.02	0.05	7.43	0.20
10.45	0.03	7.16	0.01	12.31	0.05	8.46	0.22
12.44	0.02	8.00	0.01	17.01	0.06	12.87	0.24
14.44	0.03	9.00	0.01	21.31	0.06	16.27	0.27
15.44	0.03	10.00	0.01	26.61	0.07	21.18	0.27
19.85	0.02	10.85	0.01	80.02	0.08	25.86	0.27
23.25	0.02	11.85	0.01	130.03	0.09	32.16	0.28
28.16	0.02	13.14	0.01			36.46	0.29
32.83	0.02	13.71	0.01			46.47	0.30
39.15	0.02	15.16	0.01			99.88	0.33
53.45	0.02	15.99	0.01			150.00	0.34
106.86	0.03	17.69	0.01			157.00	0.03
		19.13	0.01				
		20.14	0.01				
		20.87	0.01				
		23.14	0.01				
		25.54	0.01				
		32.15	0.01				
		37.13	-0.00				
		40.72	0.01				
		44.87	0.01				

(Table 34, continued)

Cement C		Cement C		Cement C		Cement C	
4% opal		8% opal		12% opal		10% quartzite	
Age (weeks)	Exp. (%)	Age (weeks)	Exp. (%)	Age (weeks)	Exp. (%)	Age (weeks)	Exp. (%)
0.00	0.00	0.00	0.00	0.00	0.00	0.00	0.00
0.14	0.00	0.13	0.00	0.14	0.00	0.15	0.00
1.42	0.04	0.68	0.02	0.29	0.00	0.84	0.01
2.11	0.06	1.12	0.03	0.44	0.00	1.86	0.01
2.54	0.07	1.85	0.03	0.58	0.00	4.58	0.02
3.27	0.09	2.84	0.04	2.15	0.01	6.12	0.02
4.27	0.10	3.99	0.05	4.17	0.00	7.16	0.02
5.42	0.11	5.15	0.04	5.46	0.02	10.72	0.02
6.58	0.13	6.00	0.04	6.45	0.02	16.14	0.02
7.42	0.13	6.99	0.04	7.46	0.01	60.58	0.03
8.42	0.13	7.99	0.04	8.31	0.02	110.71	0.04
9.42	0.14	8.85	0.04	9.31	0.01		
10.27	0.14	9.85	0.04	10.59	0.02		
11.27	0.15	11.13	0.05	11.16	0.02		
12.56	0.16	11.70	0.04	12.61	0.02		
13.13	0.15	13.15	0.04	13.44	0.02		
14.58	0.16	15.68	0.04	15.14	0.02		
15.41	0.16	17.12	0.04	16.58	0.02		
17.11	0.16	18.13	0.04	17.59	0.02		
18.55	0.16	18.86	0.04	18.32	0.02		
19.56	0.16	21.14	0.05	20.60	0.02		
20.29	0.16	23.53	0.04	23.00	0.02		
22.56	0.17	30.15	0.04	29.61	0.02		
24.96	0.17	35.12	0.03	38.17	0.03		
31.57	0.19	38.71	0.05	42.32	0.02		
36.55	0.19	42.86	0.05				
40.14	0.21						
44.29	0.22						

(Table 34, continued)

Cement C 20% quartzite		Cement C 30% quartzite		Cement C 50% quartzite		Cement C 100% granite	
Age (weeks)	Exp. (%)	Age (weeks)	Exp. (%)	Age (weeks)	Exp. (%)	Age (weeks)	Exp. (%)
0.00	0.00	0.00	0.00	0.00	0.00	0.00	0.00
0.14	0.00	0.15	0.00	0.14	0.00	0.14	0.00
1.31	0.01	0.44	0.00	1.12	0.00	2.00	0.01
3.30	0.01	2.14	0.01	2.85	0.01	4.30	0.01
5.27	0.02	4.00	0.01	4.87	0.01	6.16	0.01
6.30	0.02	5.14	0.03	9.15	0.02	7.29	0.03
10.72	0.03	6.46	0.03	13.86	0.02	8.61	0.02
14.11	0.03	8.44	0.04	18.16	0.01	10.60	0.03
17.69	0.03	10.42	0.03	20.88	0.02	12.58	0.02
18.29	0.02	11.45	0.04	22.41	0.02	13.60	0.02
19.02	0.03	15.86	0.03	23.45	0.02	18.02	0.03
23.70	0.03	19.26	0.03	32.44	0.02	21.42	0.03
30.01	0.05	24.17	0.03	76.87	0.03	26.32	0.03
34.30	0.04	28.84	0.03	127.01	0.04	30.99	0.02
44.31	0.03	35.15	0.04			37.31	0.03
97.73	0.04	49.46	0.04			51.61	0.03
147.73	0.05	102.87	0.05			105.03	0.04
		153.01	0.05			155.16	0.04

(Table 34, continued)

Cement D		Cement D		Cement D		Cement D	
100% limestone		1% opal		2% opal		4% opal	
Age (weeks)	Exp. (%)	Age (weeks)	Exp. (%)	Age (weeks)	Exp. (%)	Age (weeks)	Exp. (%)
0.00	0.00	0.00	0.00	0.00	0.00	0.00	0.00
0.15	0.00	0.88	0.01	0.15	0.00	0.14	0.00
0.29	0.00	3.84	0.01	0.29	-0.01	0.71	0.01
0.87	0.00	5.56	0.03	1.13	0.01	1.16	0.03
1.32	0.02	7.58	0.03	2.45	0.01	2.00	0.04
2.15	0.03	11.87	0.03	4.44	0.02	3.00	0.03
3.16	0.02	16.57	0.03	6.42	0.03	4.01	0.04
4.17	0.03	20.87	0.03	7.45	0.02	4.86	0.04
5.01	0.03	26.17	0.03	11.86	0.04	5.86	0.04
6.01	0.03	79.58	0.06	15.26	0.06	7.14	0.04
7.29	0.03	129.59	0.05	20.16	0.06	7.71	0.04
7.87	0.03			24.84	0.06	9.16	0.04
9.31	0.03			31.15	0.10	9.99	0.04
10.14	0.03			35.45	0.10	11.69	0.04
11.85	0.03			45.45	0.09	13.14	0.04
13.29	0.04			98.87	0.10	14.14	0.04
14.30	0.03			147.40	0.10	14.87	0.04
15.03	0.03					17.15	0.04
17.31	0.03					19.55	0.04
19.70	0.05					26.16	0.04
26.31	0.05					31.14	0.06
31.30	0.05					35.56	0.06
35.71	0.04					38.87	0.05
39.03	0.04						

(Table 34, continued)

Cement D 8% opal		Cement D 12% opal		Cement D 10% quartzite		Cement D 20% quartzite	
Age (weeks)	Exp. (%)	Age (weeks)	Exp. (%)	Age (weeks)	Exp. (%)	Age (weeks)	Exp. (%)
0.00	0.00	0.00	0.00	0.00	0.00	0.00	0.00
0.14	0.00	0.14	0.00	0.15	0.00	0.14	0.00
0.59	0.00	0.44	0.00	1.18	0.00	1.82	0.01
1.42	0.01	1.28	0.01	3.89	0.01	2.42	0.00
2.29	0.01	2.15	0.01	5.43	0.01	3.16	0.01
2.43	0.01	3.29	0.01	6.47	0.02	7.83	0.01
3.44	0.01	4.14	0.01	10.03	0.02	14.14	0.02
4.28	0.01	5.14	0.02	15.46	0.03	18.44	0.02
5.29	0.01	6.42	0.01	59.89	0.03	28.44	0.02
6.57	0.02	6.99	0.02	110.03	0.03	81.86	0.03
7.14	0.01	8.44	0.01			131.87	0.03
8.58	0.01	9.27	0.02				
9.42	0.01	10.97	0.02				
11.12	0.02	12.42	0.02				
12.56	0.02	13.42	0.02				
13.57	0.02	14.16	0.02				
14.30	0.02	16.43	0.02				
16.58	0.02	18.83	0.04				
18.97	0.03	25.44	0.02				
25.59	0.02	30.43	0.03				
30.57	0.03	34.84	0.03				
34.99	0.03	38.24	0.02				
38.39	0.02						

(Table 34, continued)

Cement D		Cement D		Cement D		Cement E	
30% quartzite		50% quartzite		100% granite		100% limestone	
Age (weeks)	Exp. (%)	Age (weeks)	Exp. (%)	Age (weeks)	Exp. (%)	Age (weeks)	Exp. (%)
0.00	0.00	0.00	0.00	0.00	0.00	0.00	0.00
0.14	0.00	0.15	0.00	0.14	0.00	0.14	0.00
0.69	0.01	1.87	0.01	0.71	0.01	0.29	0.00
1.71	0.02	3.90	0.01	1.85	0.02	0.43	0.00
2.85	0.01	8.18	0.01	4.73	0.02	1.44	0.01
4.17	0.01	12.88	0.01	4.85	0.03	2.28	0.01
6.15	0.01	17.18	0.01	6.17	0.02	3.28	0.01
8.13	0.02	19.90	0.02	8.15	0.03	4.57	0.01
9.16	0.02	21.44	0.02	10.13	0.03	5.14	0.01
13.57	0.02	22.48	0.01	11.16	0.02	6.58	0.01
16.97	0.02	31.46	0.02	15.57	0.03	7.42	0.02
21.88	0.04	75.90	0.02	18.97	0.03	9.12	0.01
26.55	0.02	126.03	0.04	23.88	0.03	10.56	0.01
32.86	0.03			28.55	0.02	11.57	0.01
37.16	0.03			34.86	0.03	12.30	0.01
47.17	0.05			39.16	0.03	14.58	0.01
100.58	0.04			49.17	0.03	16.97	0.02
150.72	0.04			102.58	0.03	23.58	0.03
				152.72	0.03	28.57	0.02
						32.99	0.02

(Table 34, continued)

Cement E 1% opal		Cement E 2% opal		Cement E 4% opal		Cement E 8% opal	
Age (weeks)	Exp. (%)	Age (weeks)	Exp. (%)	Age (weeks)	Exp. (%)	Age (weeks)	Exp. (%)
0.00	0.00	0.00	0.00	0.00	0.00	0.00	0.00
0.15	0.00	0.14	0.00	0.14	0.00	0.13	0.00
0.98	0.00	0.57	0.00	0.28	0.00	0.82	0.00
3.11	0.01	1.14	0.00	0.96	0.00	0.96	0.00
4.83	0.01	2.15	0.00	1.10	0.00	1.14	0.01
6.86	0.01	2.98	0.01	1.29	0.00	1.99	0.01
11.14	0.02	5.16	0.01	2.13	0.01	2.99	0.01
15.85	0.02	7.55	0.01	3.14	0.01	4.27	0.01
20.15	0.01	9.85	0.02	4.42	0.01	4.85	0.01
25.44	0.02	11.71	0.02	4.99	0.01	6.29	0.01
78.86	0.03	12.85	0.02	6.43	0.01	7.12	0.01
128.98	0.04	14.16	0.03	7.27	0.01	8.82	0.01
		16.15	0.02	8.97	0.01	10.27	0.01
		18.13	0.02	10.41	0.01	11.28	0.01
		19.16	0.04	11.42	0.02	12.01	0.01
		23.57	0.03	12.15	0.02	14.28	0.01
		31.87	0.03	14.43	0.02	16.68	0.02
		36.55	0.03	16.83	0.01	20.84	0.03
		42.86	0.03	23.44	0.02	23.29	0.02
		57.16	0.05	25.43	0.01	25.47	0.01
		110.58	0.06	27.40	0.02	27.25	0.03
		160.70	0.04	28.42	0.02	28.28	0.03
				32.84	0.02	32.69	0.03
				36.24	0.02	36.10	0.02

(Table 34, continued)

Cement F		Cement F		Cement F		Cement F	
100% limestone		1% opal		2% opal		4% opal	
Age (weeks)	Exp. (%)	Age (weeks)	Exp. (%)	Age (weeks)	Exp. (%)	Age (weeks)	Exp. (%)
0.00	0.00	0.00	0.00	0.00	0.00	0.00	0.00
0.15	0.00	0.14	0.00	0.14	0.00	0.14	0.00
1.87	0.01	0.29	0.00	0.29	0.00	1.32	0.01
3.15	0.01	0.83	0.00	0.41	0.00	1.46	0.01
3.72	0.01	2.96	0.01	4.98	0.01	1.60	0.01
5.17	0.01	4.69	0.01	7.28	0.01	2.60	0.01
6.00	0.01	6.71	0.02	9.14	0.02	3.17	0.01
7.70	0.00	10.99	0.03	10.28	0.02	4.62	0.01
9.15	0.01	15.70	0.02	11.59	0.01	5.45	0.01
10.16	0.01	20.00	0.02	13.58	0.02	7.15	0.02
10.99	0.01	25.29	0.02	15.56	0.02	8.60	0.02
13.16	0.01	78.71	0.03	16.59	0.04	9.61	0.02
15.56	0.01	128.83	0.03	21.00	0.02	10.44	0.02
19.71	0.01			24.40	0.02	12.61	0.02
22.17	0.01			29.30	0.02	15.01	0.02
24.15	0.01			33.98	0.02	19.16	0.02
26.13	0.01			40.29	0.02	21.62	0.03
27.16	0.01			54.59	0.02	23.61	0.02
31.57	0.02			108.01	0.03	25.58	0.02
34.97	0.01			158.13	0.03	26.61	0.02
						31.02	0.04
						34.42	0.02

(Table 34, continued)

Cement F 8% opal		Cement G 100% limestone		Cement G 1% opal		Cement G 2% opal	
Age (weeks)	Exp. (%)	Age (weeks)	Exp. (%)	Age (weeks)	Exp. (%)	Age (weeks)	Exp. (%)
0.00	0.00	0.00	0.00	0.00	0.00	0.00	0.00
0.14	0.00	0.14	0.00	0.14	0.00	0.15	0.00
1.01	0.01	0.28	0.00	0.68	0.00	0.30	0.00
1.14	0.01	0.42	0.00	2.82	0.01	0.85	0.00
1.29	0.00	1.42	0.00	4.54	0.01	1.00	0.00
2.29	0.00	3.59	0.00	6.56	0.01	1.13	0.00
2.86	0.01	4.42	0.01	10.85	0.02	3.30	0.01
4.30	0.00	5.43	0.00	15.55	0.01	5.70	0.02
5.14	0.01	6.44	0.00	19.85	0.01	7.99	0.01
6.84	0.01	7.28	0.01	25.15	0.02	9.85	0.02
8.28	0.01	8.28	0.00	78.56	0.03	10.99	0.03
9.29	0.01	9.56	0.01	128.68	0.03	12.31	0.03
10.12	0.01	10.14	0.00			14.30	0.03
12.30	0.01	11.58	0.00			16.27	0.02
14.69	0.01	12.41	0.00			17.30	0.03
18.85	0.01	14.11	0.00			21.71	0.03
21.31	0.00	15.56	0.00			25.11	0.03
23.29	0.01	16.57	0.00			30.02	0.03
25.27	0.01	17.30	0.00			34.70	0.02
26.29	0.01	19.57	0.00			41.00	0.02
30.71	0.01	21.97	0.00			55.31	0.03
34.11	0.01	28.58	0.00			108.72	0.04
		33.56	0.01			158.84	0.04
		37.98	0.01				
		41.30	0.00				

(Table 34, continued)

Cement G 4% opal		Cement G 8% opal		Cement G 12% opal		Cement H 100% limestone	
Age (weeks)	Exp. (%)	Age (weeks)	Exp. (%)	Age (weeks)	Exp. (%)	Age (weeks)	Exp. (%)
0.00	0.00	0.00	0.00	0.00	0.00	0.00	0.00
0.13	0.00	0.15	0.00	0.14	0.00	0.14	0.00
0.99	0.02	0.85	0.02	0.29	0.00	0.29	0.00
2.30	0.00	2.17	0.02	0.43	-0.01	1.29	0.00
4.29	0.01	4.15	0.02	1.02	0.00	1.86	0.01
6.27	0.02	6.13	0.03	2.00	0.00	3.30	0.01
7.29	0.01	7.16	0.01	4.02	-0.01	4.14	0.01
11.71	0.01	11.57	0.01	5.31	0.01	5.84	0.02
15.11	0.02	14.97	0.02	6.30	0.00	7.29	0.02
20.01	0.02	19.88	0.02	7.31	0.00	8.29	0.02
24.69	0.02	24.55	0.02	8.16	0.01	9.13	0.02
31.00	0.02	30.86	0.03	9.16	0.00	11.30	0.02
35.30	0.02	35.16	0.02	10.44	0.01	13.70	0.02
45.30	0.02	45.17	0.02	11.01	0.00	17.85	0.04
98.72	0.02	98.58	0.02	12.46	0.00	20.31	0.03
147.25	0.03	148.70	0.03	13.29	0.01	22.30	0.04
				14.99	0.01	24.27	0.02
				16.44	0.01	25.30	0.03
				17.44	0.00	29.71	0.03
				18.17	0.01	33.11	0.03
				20.45	0.01		
				22.85	0.00		
				29.46	0.01		
				34.43	0.01		
				38.03	0.01		
				42.17	0.00		

(Table 34, continued)

Cement H 1% opal		Cement H 2% opal		Cement H 4% opal		Cement H 8% opal	
Age (weeks)	Exp. (%)	Age (weeks)	Exp. (%)	Age (weeks)	Exp. (%)	Age (weeks)	Exp. (%)
0.00	0.00	0.00	0.00	0.00	0.00	0.00	0.00
0.14	0.00	0.14	0.00	0.14	0.00	0.15	0.00
0.28	0.00	0.28	0.00	0.70	0.00	0.31	0.00
0.28	0.00	1.29	0.00	1.14	0.00	0.59	0.00
0.43	0.00	2.30	0.00	1.72	0.01	1.17	0.00
1.29	0.01	3.13	0.01	3.16	0.01	2.61	0.00
2.27	0.01	5.30	0.01	3.99	0.01	3.44	0.01
3.99	0.01	7.70	0.02	5.70	0.01	5.14	0.01
6.02	0.02	9.99	0.02	7.14	0.01	6.59	0.01
10.30	0.02	11.85	0.02	8.15	0.01	7.60	0.02
15.00	0.02	12.99	0.02	8.98	0.01	8.43	0.01
19.30	0.02	14.31	0.02	11.16	0.01	10.60	0.01
24.60	0.03	16.30	0.03	13.55	0.02	13.00	0.01
78.02	0.05	18.27	0.03	17.71	0.02	17.16	0.01
128.13	0.07	19.30	0.03	20.16	0.02	21.60	0.01
		23.71	0.03	22.15	0.02	23.57	0.02
		27.11	0.03	24.13	0.02	24.60	0.02
		32.02	0.04	25.16	0.02	29.02	0.02
		36.69	0.03	29.57	0.02	32.42	0.02
		43.00	0.05	32.97	0.02	37.32	0.02
		57.31	0.04	37.87	0.02	41.99	0.02
		110.72	0.24	42.54	0.02	48.31	0.03
		160.72	0.38	48.86	0.03	62.61	0.01
				63.16	0.02	116.03	0.02
				116.58	0.03	166.02	0.03
				166.57	0.03		

Appendix E.

Calculations of Alkali Levels in Pore Solutions

The levels of sodium and potassium expected in the mortar pore solutions were estimated based on the alkali distribution of the cement (Tables 12 and 13), the initial water-cement ratio (0.485), the proportion of bound water (Table 35), and the degree of hydration of the cement phases (Tables 36, 37, or 38). For each cement and each age, the level of sodium or potassium ion in the pore solution is calculated as follows:

$$[Na^{+}] = [NAS + NCS*HCS + NCA*HCA)*NF*IC]/ [WC*(1 - BW)] \tag{1}$$

or

$$[K^{+}] = [KAS + KCS*HCS + KCA*HCA)*KF*IC]/ [WC*(1 - BW)] \tag{2}$$

where NAS and KAS are the Na_2O and K_2O present in alkali sulfate phases (%), NCS and KCS are the Na_2O and K_2O present in calcium silicate phases (%), HCS is the proportion of C_2S hydrated at that age, NCA and KCA are the Na_2O and K_2O present in calcium aluminate phases (%), HCA is the proportion of C_3A hydrated at that age, NF and KF are the factors to convert % Na_2O and % K_2O to millimoles Na and K per gram cement, IC is the grams ignited cement per gram cement, WC is the liters of water per gram cement, and BW is the proportion of bound water at that age.

Table 35. Bound water (estimated using data reported by Dalzeil and Gutteridge, 1986).

Age (weeks)	Bound water (%)
1	37
2	41
4	45
8	47
28	50

Table 36. Degree of hydration of cement phases for Model 1 (estimated from curves reported by Pratt and Ghose, 1983).

Age (weeks)	C_2S (%)	C_3A (%)
1	8	77
2	10	83
4	25	87
8	50	92
28	75	94

Table 37. Hydration rates of cement phases for Model 2 (estimated from data reported by Dalzeil and Gutteridge, 1986).

Age (weeks)	C_2S (%)	C_3A (%)
1	26	69
2	32	76
4	36	80
8	51	94
28	59	93

Table 38. Hydration rates of cement phases for Model 3.

Age (weeks)	C_2S (%)	C_3A (%)
1	100	100
2	100	100
4	100	100
8	100	100
28	100	100

VITA

Leslie Jeanne Struble was born May 30, 1947, in Olympia, Washington. She attended University of Puget Sound in Tacoma, Washington, for two years, then received a BA degree in chemistry from Pitzer College, Claremont California, in 1970. For the next six years, she was employed by California Portland Cement Company as a Research Chemist. She received an MS degree in Civil Engineering from Purdue University in 1979. During the next four years she was employed by Martin Marietta Laboratories as a Scientist. She began PhD studies at Purdue University while employed at Martin Marietta Laboratories, and the studies were continued while she was employed at the National Bureau of Standards as a Materials Research Engineer.

NBS-114A (REV. 2-80)

U.S. DEPT. OF COMM. **BIBLIOGRAPHIC DATA SHEET** *(See instructions)*	1. PUBLICATION OR REPORT NO. NBSIR 87-3632	2. Performing Organ. Report No.	3. Publication Date SEPTEMBER 1987

4. TITLE AND SUBTITLE

The Influence of Cement Pore Solution on Alkali-Silica Reaction

5. AUTHOR(S)

L.J. Struble

6. PERFORMING ORGANIZATION *(If joint or other than NBS, see instructions)*

NATIONAL BUREAU OF STANDARDS
U.S. DEPARTMENT OF COMMERCE
GAITHERSBURG, MD 20899

7. Contract/Grant No.

8. Type of Report & Period Covered

9. SPONSORING ORGANIZATION NAME AND COMPLETE ADDRESS *(Street, City, State, ZIP)*

National Bureau of Standards

10. SUPPLEMENTARY NOTES

☐ Document describes a computer program; SF-185, FIPS Software Summary, is attached.

11. ABSTRACT *(A 200-word or less factual summary of most significant information. If document includes a significant bibliography or literature survey, mention it here)*

To improve our understanding of certain details of alkali-silica reaction mechanisms, expansion studies were carried out using cements with various alkali contents and distributions and certain reactive aggregates. These studies indicated an influence of the cement alkali distribution on expansion due to alkali-silica reaction. Pore solutions expressed form limestone mortars prepared from the same cements were shown to consist primarily of hydroxyl and alkali ions, with pH levels ranging from 13.4 to 14.0. When composition results were compared with the expansion results of mortars containing opal, the levels of hydroxyl and alkali ions were shown to influence the expansion. Reactions of the aggregates in model pore solutions produced various levels of silica correlated directly with the mortar-bar expansion levels produced by each aggregate and proportion. Thus expansion appears to be a function of the extent of the reaction of aggregate in pore solution, which depends on the material, its proportion, and the solution pH level, and is further influenced by the amount of sodium or sodium plus potassium in the pore solution.

12. KEY WORDS *(Six to twelve entries; alphabetical order; capitalize only proper names; and separate key words by semicolons)*

aggregate; alkali; alkali-silica; cement; concrete; expansion; expression; pore solution; reactive aggregate; silica

13. AVAILABILITY

☐ Unlimited
☒ For Official Distribution. Do Not Release to NTIS
☐ Order From Superintendent of Documents, U.S. Government Printing Office, Washington, D.C. 20402.
☐ Order From National Technical Information Service (NTIS), Springfield, VA. 22161

14. NO. OF PRINTED PAGES

15. Price

USCOMM-DC 6043-P80